

### Subsection 2.5.2 Table of Contents

<u>Section</u>	<u>Title</u>	<u>Page</u>
2.5.2	Vibratory Ground Motion .....	2.5.2-1
2.5.2.1	Seismicity .....	2.5.2-2
2.5.2.2	Geologic and Tectonic Characteristics of the Site and Region .....	2.5.2-8
2.5.2.3	Correlation of Earthquake Activity with Seismic Sources .....	2.5.2-25
2.5.2.4	Probabilistic Seismic Hazard Analysis and Controlling Earthquakes .....	2.5.2-27
2.5.2.5	Seismic Wave Transmission Characteristics of the Site .....	2.5.2-52
2.5.2.6	Ground Motion Response Spectra .....	2.5.2-60
2.5.2.7	References .....	2.5.2-62
2.5.2-A	Computer Program: P-SHAKE .....	2.5.2-A-2
2.5.2-A-1	Description .....	2.5.2-A-2
2.5.2-A-2	Validation .....	2.5.2-A-2
2.5.2-A-3	Extent of Application .....	2.5.2-A-2

### Subsection 2.5.2 List of Tables

<u>Number</u>	<u>Title</u>
2.5.2-1	Conversion Between Body-Wave ( $m_b$ ) and Moment ( $M_w$ ) Magnitudes
2.5.2-2	Seismicity Catalog for Pre-1985 for the Gulf of Mexico Investigation Region [24°N to 32°N, 100°W to 83°W] for which the Events are Rmb Magnitude Greater than or Equal to 3.0 or Intensity Greater than or Equal to IV
2.5.2-3	Seismicity Catalog from 1985 to Present for the Project Investigation Region [24°N to 40°N, 107°W to 83°W] for which the Events are Rmb Magnitude Greater than or Equal to 3.0 or Intensity Greater than or Equal to IV
2.5.2-4	Seismicity Events Recommended for Recurrence Analysis within the Gulf of Mexico
2.5.2-5	Region 2 Matrix of Detection Probabilities; Modified to Extend the Matrix to Year 2007
2.5.2-6	Matrix of Detection Probabilities for the Gulf of Mexico
2.5.2-7	Summary of Bechtel Group Seismic Source Zones
2.5.2-8	Summary of Dames & Moore Seismic Source Zones
2.5.2-9	Summary of Law Engineering Seismic Source Zones
2.5.2-10	Summary of Rondout Associates Seismic Source Zones
2.5.2-11	Summary of Weston Geophysical Corporation Seismic Source Zones
2.5.2-12	Summary of Woodward-Clyde Consultants Seismic Source Zones
2.5.2-13	Comparison of 1989 EPRI (Reference 2.5.2-1) Hazard Results for STPEGS Site and Current Hazard Results for VCS Site for Bechtel Team Using 1989 EPRI (Reference 2.5.2-1) Assumptions
2.5.2-14	Comparison of 1989 EPRI (Reference 2.5.2-1) Hazard Results for STPEGS Site and Current Hazard Results for VCS Site for Dames & Moore Team Using 1989 EPRI (Reference 2.5.2-1) Assumptions
2.5.2-15	Comparison of 1989 EPRI (Reference 2.5.2-1) Hazard Results for STPEGS Site and Current Hazard Results for VCS Site For Law Engineering Inc. Team Using 1989 EPRI (Reference 2.5.2-1) Assumptions
2.5.2-16	Comparison of 1989 EPRI (Reference 2.5.2-1) Hazard Results for STPEGS Site and Current Hazard Results for VCS Site for Rondout Using 1989 EPRI (Reference 2.5.2-1) Assumptions
2.5.2-17	Comparison of 1989 EPRI (Reference 2.5.2-1) Hazard Results for STPEGS Site and Current Hazard Results for VCS Site for Weston Geophysical Team Using 1989 EPRI (Reference 2.5.2-1) Assumptions
2.5.2-18	Comparison of 1989 EPRI (Reference 2.5.2-1) Hazard Results for STPEGS Site and Current Hazard Results for VCS Site for Woodward-Clyde Team Using 1989 EPRI (Reference 2.5.2-1) Assumptions

**List of Tables (Cont.)**

<u>Number</u>	<u>Title</u>
2.5.2-19	Comparison of Original EPRI-SOG Gulf Coastal Source Zones Characterizations and Modifications Made for the VCS Site
2.5.2-20	Seismic Source Characterization of the Meers Fault
2.5.2-21	Rio Grande Rift Faults Modeled as Discrete Fault Sources
2.5.2-22	Summary of Rio Grande Rift Fault Source Characterization
2.5.2-23	Rio Grande Rift Southern Extension Characterization
2.5.2-24	Mean and Median Rock UHRS Accelerations (g)
2.5.2-25	Controlling Magnitudes and Distances From Deaggregation
2.5.2-26	Assigned Strong Motion Durations in P-SHAKE
2.5.2-27	Horizontal $10^{-4}$ and $10^{-5}$ UHRS and GMRS, and Vertical GMRS

### Subsection 2.5.2 List of Figures

<u>Number</u>	<u>Title</u>
2.5.2-1	The VCS Site, Large Project Seismicity Investigation Window (24° to 40° N, 107° to 83° W), the 200 Mile Radius Site Region, and both EPRI Catalog and Supplemental Earthquakes
2.5.2-2	VCS Site Region Seismicity
2.5.2-3	Gulf of Mexico Seismicity Recurrence Area
2.5.2-4	Bechtel Group Source Zones Contributing Most Significantly to Seismic Hazard at the VCS Site
2.5.2-5	Dames and Moore Source Zones Contributing Most Significantly to Seismic Hazard at the VCS Site
2.5.2-6	Law Engineering Source Zones Contributing Most Significantly to Seismic Hazard at the VCS Site
2.5.2-7	Rondout Source Zones Contributing Most Significantly to Seismic Hazard at the VCS Site
2.5.2-8	Weston Geophysical Source Zones Contributing Most Significantly to Seismic Hazard at the VCS Site
2.5.2-9	Woodward-Clyde Source Zones Contributing Most Significantly to Seismic Hazard at the VCS Site
2.5.2-10	Location of the Meers Fault, Simplified Fault Segments to Model the Rio Grande Rift (RGR) Faults, and Fault of the New Madrid Seismic Zone (NMSZ)
2.5.2-11	Pattern of Concentrate Seismicity in the New Madrid Seismic Zone (NMSZ)
2.5.2-12	Historical Seismicity in the Vicinity of the VCS Site and Test Area Used to Test the Effects of Additional Seismicity
2.5.2-13	Earthquake Occurrence Rates for EPRI (1989) Catalog and for Catalog Extended Through 2007 for Test Area
2.5.2-14	Mean Peak Ground Acceleration (PGA) Rock Hazard from Original EPRI Analysis Compared to Mean PGA Hazard Using the Updated Catalog and Extended Seismic Sources
2.5.2-15	Clinton Source Characterization Logic Tree for the NMSZ (Reference 2.5.2-70)
2.5.2-16	NMSZ Source Model (source geometry from Reference 2.5.2-29)
2.5.2-17	Logic Tree of Return Period and Characteristic Magnitude for the Meers Fault
2.5.2-18	10 Hz Mean Rock Seismic Hazard Curves for EPRI-SOG Teams Plus New Madrid, for New Madrid Alone, for Rio Grande Rift Faults Alone, and for Meers Fault Alone
2.5.2-19	1 Hz Mean Rock Seismic Hazard Curves For EPRI-SOG Teams Plus New Madrid, for New Madrid Alone, for Rio Grande Rift Faults Alone, and for Meers Fault Alone

**List of Figures (Cont.)**

<u>Number</u>	<u>Title</u>
2.5.2-20	10 Hz Mean Rock Seismic Hazard Curves for EPRI Teams (Each Team Curve Includes the New Madrid Source)
2.5.2-21	5 Hz Mean Rock Seismic Hazard Curves for EPRI Teams (Each Team Curve Includes the New Madrid Source)
2.5.2-22	2.5 Hz Mean Rock Seismic Hazard Curves for EPRI Teams (Each Team Curve Includes the New Madrid Source)
2.5.2-23	1 Hz Mean Rock Seismic Hazard Curves for EPRI Teams (Each Team Curve Includes the New Madrid Source)
2.5.2-24	10 Hz Mean Rock Seismic Hazard Curves by Source for Each EPRI Team and for The New Madrid Source
2.5.2-25	5 Hz Mean Rock Seismic Hazard Curves by Source for Each EPRI Team and for The New Madrid Source
2.5.2-26	2.5 Hz Mean Rock Seismic Hazard Curves by Source for Each EPRI Team and for the New Madrid Source
2.5.2-27	1 Hz Mean Rock Seismic Hazard Curves by Source for Each EPRI Team and for the New Madrid Source
2.5.2-28	10 Hz Median Rock Seismic Hazard Curves by Source for each EPRI Team and for the New Madrid Source
2.5.2-29	5 Hz Median Rock Seismic Hazard Curves by Source for each EPRI Team and for the New Madrid Source
2.5.2-30	2.5 Hz Median Rock Seismic Hazard Curves by Source for each EPRI Team and for the New Madrid Source
2.5.2-31	1 Hz Median Rock Seismic Hazard Curves by Source for each EPRI Team and for the New Madrid Source
2.5.2-32	Mean and Fractile PGA Rock Hazard Curves
2.5.2-33	Mean and Fractile 25 Hz Rock Hazard Curves
2.5.2-34	Mean and Fractile 10 Hz Rock Hazard Curves
2.5.2-35	Mean and Fractile 5 Hz Rock Hazard Curves
2.5.2-36	Mean and Fractile 2.5 Hz Rock Hazard Curves
2.5.2-37	Mean and Fractile 1 Hz Rock Hazard Curves
2.5.2-38	Mean and Fractile 0.5 Hz Rock Hazard Curves
2.5.2-39	Sensitivity of 1 Hz Mean Hazard to Ground Motion Equation for the New Madrid Source
2.5.2-40	Mean Rock UHRS for $10^{-4}$ , $10^{-5}$ , and $10^{-6}$
2.5.2-41	Median Rock UHRS for $10^{-4}$ , $10^{-5}$ , and $10^{-6}$
2.5.2-42	1 and 2.5 Hz Deaggregation of Mean Hazard for $10^{-4}$

**List of Figures (Cont.)**

<u>Number</u>	<u>Title</u>
2.5.2-43	5 and 10 Hz Deaggregation of Mean Hazard for $10^{-4}$
2.5.2-44	1 and 2.5 Hz Deaggregation of Mean Hazard for $10^{-5}$
2.5.2-45	5 and 10 Hz Deaggregation of Mean Hazard for $10^{-5}$
2.5.2-46	1 and 2.5 Hz Deaggregation of Mean Hazard for $10^{-6}$
2.5.2-47	5 and 10 Hz Deaggregation of Mean Hazard for $10^{-6}$
2.5.2-48	Mean HF and LF Rock Spectra for $10^{-4}$
2.5.2-49	Mean HF and LF Rock Spectra for $10^{-5}$
2.5.2-50	Input Log-Mean Shear Wave Velocity Profile (Plus/Minus One Standard Deviation) for Randomization Process — Unit 1
2.5.2-51	Input Log-Mean Shear Wave Velocity Profile (Plus/Minus One Standard Deviation) for Randomization Process — Unit 2
2.5.2-52	Strain Dependent Degradation Curves for Sand 4
2.5.2-53	Strain Dependent Damping Ratio Properties for Sand 4
2.5.2-54	Randomized Shear Wave Velocity Profiles, Log-Mean Shear Wave Velocity Profile and the Base Profile Used for Randomization — Unit 1
2.5.2-55	Randomized Shear Wave Velocity Profiles, Log-Mean Shear Wave Velocity Profile and the Base Profile Used for Randomization — Unit 2
2.5.2-56	Log-Mean of Site Amplification Factor at the GMRS Horizon (99 ft Depth) from Analysis of the 60 Modified Random Profiles with the $10^{-4}$ LF Input Motion — Unit 1
2.5.2-57	Log-Mean of Site Amplification Factor at the GMRS Horizon (102 ft Depth) from Analysis of the 60 Modified Random Profiles with the $10^{-4}$ LF Input Motion — Unit 2
2.5.2-58	Log-Mean of Site Amplification Factor at the GMRS Horizons (Unit 1 at 99 ft Depth and Unit 2 at 102 ft Depth) with the $10^{-4}$ LF Input Motion
2.5.2-59	Maximum Strain Versus Depth Calculated for the 60 Profiles and their Log-Mean (Thick Red Line) with the $10^{-4}$ LF Input Motion — Unit 1
2.5.2-60	Maximum Strain Versus Depth Calculated for the 60 Profiles and their Log-Mean (Thick Red Line) with the $10^{-4}$ LF Input Motion — Unit 2
2.5.2-61	Log-Mean of Site Amplification Factor at the GMRS Horizon (99 ft Depth) from Analyses of the 60 Modified Random Profiles with the $10^{-4}$ HF Input Motion — Unit 1
2.5.2-62	Log-Mean of Site Amplification Factor at the GMRS Horizon (102 ft Depth) from Analysis of the 60 Modified Random Profiles with the $10^{-4}$ HF Input Motion — Unit 2
2.5.2-63	Log-Mean of Site Amplification Factor at the GMRS Horizons (Unit 1 at 99 ft Depth and Unit 2 at 102 ft Depth) with the $10^{-4}$ HF Input Motion

**List of Figures (Cont.)**

<u>Number</u>	<u>Title</u>
2.5.2-64	Maximum Strain Versus Depth Calculated for the 60 Profiles and their Log-Mean (Thick Red Line) with the $10^{-4}$ HF Input Motion — Unit 1
2.5.2-65	Maximum Strain Versus Depth Calculated for the 60 Profiles and their Log-Mean (Thick Red Line) with the $10^{-4}$ HF Input Motion — Unit 2
2.5.2-66	Log-Mean of Site Amplification Factor at the GMRS Horizon (99 ft Depth) from Analysis of the 60 Modified Random Profiles with the $10^{-5}$ LF Input Motion — Unit 1
2.5.2-67	Log-Mean of Site Amplification Factor at the GMRS Horizon (102 ft Depth) from Analysis of the 60 Modified Random Profiles with the $10^{-5}$ LF Input Motion — Unit 2
2.5.2-68	Log-Mean of Site Amplification Factor at the GMRS Horizons (Unit 1 at 99 ft Depth and Unit 2 at 102 ft Depth) with the $10^{-5}$ LF Input Motion
2.5.2-69	Maximum Strain Versus Depth Calculated for the 60 Profiles and their Log-Mean (Thick Red Line) with the $10^{-5}$ LF Input Motion — Unit 1
2.5.2-70	Maximum Strain Versus Depth Calculated for the 60 Profiles and their Log-Mean (Thick Red Line) with the $10^{-5}$ LF Input Motion — Unit 2
2.5.2-71	Log-Mean of Site Amplification Factor at the GMRS Horizon (99 ft Depth) from Analysis of the 60 Modified Random Profiles with the $10^{-5}$ HF Input Motion — Unit 1
2.5.2-72	Log-Mean of Site Amplification Factor at the GMRS Horizon (102 ft Depth) from Analysis of the 60 Modified Random Profiles with the $10^{-5}$ HF Input Motion — Unit 2
2.5.2-73	Log-Mean of Site Amplification Factor at the GMRS Horizons (Unit 1 at 99 ft Depth and Unit 2 at 102 ft Depth) with the $10^{-5}$ HF Input Motion
2.5.2-74	Maximum Strain Versus Depth Calculated for the 60 Profiles and their Log-Mean (Thick Red Line) with the $10^{-5}$ HF Input Motion — Unit 1
2.5.2-75	Maximum Strain Versus Depth Calculated for the 60 Profiles and their Log-Mean (Thick Red Line) with the $10^{-5}$ HF Input Motion — Unit 2
2.5.2-76	Log-Mean Maximum Strain Profiles — Unit 1
2.5.2-77	Log-Mean Maximum Strain Profiles — Unit 2
2.5.2-78	Log-Mean Profiles of Strain-Compatible Soil Damping — Unit 1
2.5.2-79	Log-Mean Profiles of Strain-Compatible Soil Damping — Unit 2
2.5.2-80	Comparison of the Envelopes of the Unit 1 and Unit 2 Log-Mean Soil Amplification Factors at the GMRS Horizon 1 for LF and HF, $10^{-4}$ and $10^{-5}$ Input Motion
2.5.2-81	Smooth Horizontal $10^{-4}$ and $10^{-5}$ UHRS and GMRS

**List of Figures (Cont.)**

<u>Number</u>	<u>Title</u>
2.5.2-82	WUS Soil V/H Ratios (Reference 2.5.2-113) for Magnitudes 5.9, 6.6, and 7.7 at Distances of 36, 190, and 200 Kilometers, Respectively, with Frequencies Shifted by a Factor of 62.5/16.7 to Approximate a WUS-to-CEUS Transformation
2.5.2-83	Smooth Horizontal and Vertical GMRS

## 2.5.2 Vibratory Ground Motion

This subsection provides a detailed description of the vibratory ground motion assessment for the VCS site. This assessment uses the guidance in RG 1.208. RG 1.208 incorporates developments in ground motion estimation models, updated models for seismic sources, methods for determining site response, and new methods for defining a site-specific, performance-based earthquake ground motion that satisfy the requirements of 10 CFR 100.23. Identification and characterization of seismic sources lead to the determination of safe shutdown earthquake (SSE) ground motion. This subsection develops the site-specific ground motion response spectrum (GMRS) characterized by horizontal and vertical response spectra determined as free-field motions on the ground surface using performance-based procedures.

The GMRS represents the first part in development of an SSE for a site as a characterization of the regional and local seismic hazard. The certified seismic design response spectra (CSDRS) is the ground motion for the site, the vibratory ground motion for which certain structures, systems, and components are designed to remain functional, pursuant to Appendix S to 10 CFR Part 50.

The starting point for the GMRS assessment is the probabilistic seismic hazard analysis (PSHA) conducted by the Electric Power Research Institute (EPRI) for the seismicity owners group (SOG). The EPRI-SOG seismic hazard study is based on the evaluation of seismicity, seismic source models and ground motion attenuation relationships ([Reference 2.5.2-1](#)).

[Subsections 2.5.2.1](#) through [2.5.2.4](#) document the review and update of the available EPRI earthquake catalog, seismic source models, and ground motion characterizations. [Subsection 2.5.2.5](#) summarizes information about the seismic wave transmission characteristics of the site with reference to a more detailed description of all engineering aspects of the subsurface in [Subsection 2.5.4](#).

[Subsection 2.5.2.6](#) describes development of the horizontal GMRS ground motion for the site. Following RG 1.208, the selected ground motion is based on the risk-consistent/performance-based approach. Site-specific horizontal ground motion amplification factors are developed using site-specific estimates of subsurface soil and rock properties. These amplification factors are then used to scale the hard rock spectra to develop uniform hazard response spectra (UHRS) accounting for site-specific conditions using Approach 2A of NUREG/CR-6728 ([Reference 2.5.2-2](#)).

[Subsection 2.5.2.6](#) also describes vertical GMRS, developed by scaling the horizontal GMRS by a frequency-dependent vertical-to-horizontal (V:H) factor.

### 2.5.2.1 Seismicity

The seismic hazard analysis conducted by EPRI ([Reference 2.5.2-1](#)) relied on an analysis of historical seismicity in the central and eastern United States (CEUS) to estimate seismicity parameters (rates of seismic activity, Richter b-values and maximum magnitude) for individual seismic sources. The historical earthquake catalog used in the EPRI seismic hazard analysis was complete through 1984. The earthquake data for the site region since 1984 through 2007 was reviewed and used to update the EPRI catalog (see [Subsection 2.5.2.1.2](#)). The EPRI seismic hazard methodology did not originally incorporate contributions to hazard from seismic sources in the Gulf of Mexico except along its immediate coast. Therefore, special attention in the update of the EPRI catalog was given to earthquakes throughout the Gulf of Mexico (see [Subsection 2.5.2.1.3](#)).

#### 2.5.2.1.1 1988 EPRI Regional Earthquake Catalog

Many seismic networks record earthquakes in the CEUS. An effort was made during the EPRI seismic hazard study to combine available data on historical earthquakes and to develop a homogeneous earthquake catalog that contained all recorded earthquakes for the region. “Homogeneous” means that estimates of body-wave magnitude ( $m_b$ ) for all earthquakes are consistent, duplicate earthquakes have been removed, non-earthquakes (e.g., mine blasts and sonic booms) have been eliminated, and significant events in the historical record have not been missed. The EPRI earthquake catalog ([Reference 2.5.2-3](#)) forms a strong basis on which to estimate seismicity parameters such as earthquake recurrence rates and maximum magnitude.

#### 2.5.2.1.2 Updated Seismicity Data

The earthquake catalog used in the study region was updated to determine whether regional earthquake patterns and seismicity parameters developed from the EPRI catalog ([Reference 2.5.2-3](#)) remained unchanged. RG 1.206 specifies that earthquakes of modified Mercalli intensity (MMI) greater than or equal to IV or magnitude greater than or equal to 3.0 should be listed “that have been reported within 200 miles (320 km) of the site.” In updating the EPRI earthquake catalog, a latitude-longitude window of 24° to 40° N, 107° to 83° W was used. This large window, called the project seismicity investigation window, incorporates the 200 miles (320 km) radius “site region” and all seismic sources contributing significantly to earthquake hazard at the site. [Figure 2.5.2-1](#) shows the site and its associated site region, the defined latitude-longitude window, both the original EPRI catalog earthquakes and updated seismicity data. [Figure 2.5.2-2](#) shows that there are no cataloged earthquakes within 50 miles (80 km) of the site.

Given the general completeness of the EPRI catalog through 1984, an initial update of the catalog within the project seismicity investigation window was performed for the period 1985 through 2007. The earthquake catalogs used for this initial update are:

- Frohlich and Davis (DPC, FDNC, PDEf) ([Reference 2.5.2-4](#))
- Engdahl et al. (EHB98) ([Reference 2.5.2-5](#))
- Perez (PEREZ) ([Reference 2.5.2-6](#))
- Advanced National Seismic System ([Reference 2.5.2-7](#))
- International Seismological Centre ([Reference 2.5.2-8](#))
- Significant U.S. Earthquakes (USHIS) ([Reference 2.5.2-9](#))
- Mexico, Central America and Caribbean, 1900–1979 (MCAC) ([Reference 2.5.2-10](#))
- Eastern, Central, and Mountain States of the United States (SRA) ([Reference 2.5.2-11](#))
- NEIC Preliminary Determination of Epicenters (PDE, PDE-W, PDE-Q) ([Reference 2.5.2-12](#))

No events were found in either the PEREZ or MCAC catalogs. In the event of duplicate entries in the remaining seven catalogs, the preference order chosen was: DPC, FDNC, PDEf, EHB98, ANSS, ISC, USHIS, SRA, PDE, PDE-W and PDE-Q. Non-preferred duplicate entries were deleted.

#### 2.5.2.1.2.1 Assessment of Best Estimate and Uniform Magnitude

For the EPRI-SOG methodology, two types of magnitudes are required for each event in the catalog: 1) best, or expected, estimate of body-wave magnitude ( $E[m_b]$ ), also referred to as  $E_{mb}$  in the 1988 EPRI study; ([Reference 2.5.2-3](#)); and 2) uniform magnitude  $m_b^*$  (referred to as  $R_{mb}$  in the 1988 EPRI study).

#### **Best Estimate Magnitude $E_{mb}$**

Various magnitude types may be available for a given event. Each available magnitude was considered in the evaluation of  $E_{mb}$  for that event. If a body-wave magnitude ( $m_b$ ) was available, it was adopted directly. Other magnitudes were converted to additional estimates of  $E_{mb}$  using the Equation 4-1 and Table 4-1 in the 1988 EPRI study:

$$E_{mb} = 0.253 + 0.907 \cdot M_d \quad (2.4.13-1)$$

$$E_{mb} = 0.655 + 0.812 \cdot M_L \quad \text{Equation 2.5.2-2}$$

$$E_{mb} = 2.302 + 0.618 \cdot M_s \quad (2.4.13-3)$$

where  $M_d$  is duration (or coda) magnitude,  $M_L$  is “local” magnitude, and  $M_s$  is surface-wave magnitude.

The EPRI PSHA study expressed maximum magnitude ( $M_{\max}$ ) values in terms of body-wave magnitude ( $m_b$ ), whereas most modern seismic hazard analyses describe  $M_{\max}$  in terms of moment magnitude ( $M_w$ ). To provide a consistent comparison between magnitude scales, body-wave magnitude was related to moment magnitude using the arithmetic average of three equations, or their inversions, presented by Atkinson and Boore (Reference 2.5.2-13), Frankel et al. (Reference 2.5.2-14), and EPRI (Reference 2.5.2-15). Throughout the description in Subsections 2.5.2.2 and 2.5.2.3, the largest values of  $M_{\max}$  distributions assigned by the Earth Science Teams (EST) (Reference 2.5.2-16) to seismic sources are presented for both magnitude scales ( $m_b$  and  $M_w$ ). For example, EPRI  $m_b$  values of  $M_{\max}$  are followed by the equivalent  $M_w$  value. Conversion values from  $m_b$  to  $M_w$  and  $M_w$  to  $m_b$  are provided in Table 2.5.2-1.  $m_b$  magnitudes converted from moment magnitudes in this fashion were considered estimates of Emb.

For each event the final Emb was taken as the largest estimate of Emb.

### Uniform Magnitude Rmb

The EPRI-SOG seismic hazard methodology modifies the Emb values to develop a uniform magnitude,  $m_b^*$ , to assess an unbiased estimate of seismicity recurrence parameters. EPRI Equation 4-2 (Reference 2.5.2-3) indicates that the equation from which  $m_b^*$  is estimated from  $E[m_b]$  and the standard deviation of  $m_b$ ,  $\sigma_{mb}$ , (referred to as Smb in the 1988 EPRI study) is:

$$m_b^* = E[m_b] + (1/2) \cdot \ln(10) \cdot b \cdot \sigma_{mb}^2 \quad (2.4.13-4)$$

where,  $b = 1.0$

Values for  $\sigma_{mb}$  [Smb] were estimated for each earthquake in the updated catalog, and  $m_b^*$  [Rmb] values were calculated for each event added to the updated earthquake catalog.

The result of the above process was an initial homogeneous earthquake update of the EPRI earthquake catalog (Reference 2.5.2-3) for earthquakes occurring after 1984 within the project seismicity investigation window. For the purpose of earthquake recurrence analysis, all events added for the update are assumed to be independent events.

#### 2.5.2.1.3 Gulf of Mexico Seismicity

Two observations suggested that additional examination of earthquakes in the Gulf of Mexico was needed. First, earthquakes commonly cataloged as located within the Gulf of Mexico are often reported by so few nearby stations that determination of their epicenters may not be considered reliable (Reference 2.5.2-17). This indicated that evaluation of locations of Gulf of Mexico seismicity was needed. Second, an examination of the original EPRI analysis (Reference 2.5.2-18, Table 5.1) indicated that earthquake recurrence parameters had not been evaluated for much of the Gulf of Mexico Figure 2.5.2-3. The occurrence of two recent moderate earthquakes in the Gulf of Mexico

(see [Subsection 2.5.2.1.4](#)) indicated the potential for a significant contribution to seismic hazard at the site from this area. This required a careful evaluation of Gulf of Mexico seismicity, both before and after the development of the EPRI earthquake catalog.

The seismicity was re-evaluated with specific emphasis on the southeast portion (24°N to 32°N, 100°W to 83°W) of the project seismicity investigation region (24°N to 40°N, 107°W to 83°W). This southeast portion is referred to as the “Gulf of Mexico investigation region.” The objective was to develop an improved characterization of seismicity for all time within the Gulf of Mexico investigation region for events of EPRI recurrence magnitude  $R_{mb} \geq 3.0$  or intensity  $\geq IV$ . When combined with the seismicity catalog described in [Subsection 2.5.2.1.2](#), this allows an improved characterization of the seismicity within the project seismicity investigation window.

The nine catalogs described above, but for their complete temporal coverage, plus the EPRI catalog were considered in the development of the reevaluated earthquake catalog for the Gulf of Mexico.

The preference order chosen among the catalogs was: EPRI, DPC, FDNC, PDEf, EHB98, ISC, ANSS, USHIS, SRA, PDE, PDE-W, and PDE-Q.

In this compilation, the ISC entries were given preference over ANSS entries if event-specific ISC evaluations had been made. This was because a few ANSS locations for events in the Gulf of Mexico were found to have few recordings from nearby stations and to have unacceptably large travel time residuals for these few nearby stations.

A detailed review of all duplicate information (more than one record per event) was made for the Gulf of Mexico investigation region. The review included examining phase data for events. Events that were reported only at distant networks and not reevaluated by ISC were scrutinized and removed if warranted. Man-made and spurious events, such as those listed in the 2002 Frohlich and Davis ([Reference 2.5.2-4](#)) earthquake catalog, were also removed.

For the purpose of developing earthquake recurrence statistics in the Gulf of Mexico investigation region, it was necessary to eliminate dependent events (e.g., foreshocks, aftershocks, and secondary events of an apparent seismicity cluster). As described earlier, the EPRI earthquake catalog has MAIN (independent) events distinguished from dependent events. Guided by the EPRI characterization of MAIN vs. non-MAIN, as well as by apparent spatial and temporal similarity between events, dependent events were identified and removed. The remaining events in the Gulf of Mexico investigation region were assessed to be equivalent to EPRI MAIN events.

In the development of the revised composite project earthquake catalog, the magnitudes given in all catalogs were converted to best, or expected, estimates of  $m_b$  ( $E_{mb}$ ), using the same conversion equations described above.

If no explicit magnitudes are available for an event, an available maximum intensity value [ $I_0$ ] was converted to Emb, using a relationship from Table 4-1 in the 1988 EPRI study ([Reference 2.5.2-3](#)):

$$\text{Emb} = 0.709 + 0.599 \cdot I_0 \quad (2.4.13-5)$$

#### 2.5.2.1.4 Final Earthquake Catalog

The final earthquake catalog for the project seismicity investigation region (24°N to 40°N, 107°W to 83°W) is the composite of the earthquakes in the EPRI catalog supplemented by the earthquakes in [Tables 2.5.2-2](#) and [2.5.2-3](#).

Within the updated earthquake catalog (1985 through 2007) there are two new moderate seismic events in the Gulf of Mexico that are significant for an updated characterization of the regional seismicity. These are: (1) a  $M_w$  5.1 ( $m_b$  5.5) earthquake that occurred on February 10, 2006, offshore of the Louisiana coast within the Gulf of Mexico, and (2) a  $M_w$  5.8 ( $m_b$  6.1) earthquake that occurred on September 10, 2006 off the Florida coast within the Gulf of Mexico.

A moment-tensor source can be used to model the surface waves generated by the February 10, 2006 earthquake if the earthquake centroid is placed within a few miles of the earth's surface in a medium with a very low shear modulus. The explanation for the February 10th earthquake that is currently in best agreement with the observed seismic data is a gravity-driven displacement surface within a thick shallow sedimentary wedge ([Reference 2.5.2-50](#)).

The focal mechanism for the September 10, 2006 earthquake indicates a reverse sense of motion, and the earthquake depth is reported as 13 to 19 miles (22 to 31 km) ([Reference 2.5.2-19](#)). This mechanism is that of an earthquake caused by tectonically driven stresses within the earth's crust.

The implications of these earthquakes for the characterization of earthquake potential in the Gulf of Mexico are described in [Subsection 2.5.2.3](#).

#### 2.5.2.1.5 Periods of Completeness for the Gulf of Mexico Earthquakes

The EPRI seismic hazard methodology ([Reference 2.5.2-3](#)) uses estimates of periods of completeness for the reporting of earthquakes as a function of magnitude. This methodology employs a matrix of probability of detection of earthquakes for an area for selected ranges of time-before-present and magnitude. The purpose of this section is to develop a matrix of detection probability for the Gulf of Mexico seismicity recurrence area (see [Figure 2.5.2-3](#)) where such information is not available in the original EPRI parameterization ([Reference 2.5.2-18](#)). This matrix is used later in [Subsection 2.5.2.4](#) to develop EPRI-consistent earthquake recurrence parameters for the Gulf of Mexico for use in the PSHA of the site.

[Table 2.5.2-4](#) lists the 22 earthquakes within the Gulf of Mexico seismicity recurrence area, considered EPRI MAIN or independent events that were used to develop the matrix of detection probability for this area. This matrix was prepared to be consistent with the 1988 EPRI seismic hazard methodology. Generation of the matrix of detection probability used, as a conservative guideline, the adjacent EPRI matrices of detection probability available onshore. The 1988 EPRI seismic hazard study used a detailed analysis of U.S. demographics and history, number, and quality and distribution of seismographic instruments to develop matrices of probability of completeness as a function of time period, gridded area, and magnitude interval. Given uneven population distributions over time and uneven deployment of seismographic networks, these completeness probability matrices also vary by location. EPRI “Incompleteness Regions” 2 and 3 are closest to the part of the Gulf of Mexico that is nearest the site ([Reference 2.5.2-18](#), Table 5-1).

It was assumed that the probabilities of earthquake detection for the Gulf of Mexico are less than those given for onshore coastal locations for comparable time periods. The procedure followed for estimating detection probabilities for the Gulf of Mexico was, therefore, to start with the available EPRI matrix, suggesting the lowest probabilities along the shoreline (EPRI Incompleteness Region 2) and to assume lower probabilities of detection within the Gulf of Mexico.

[Table 2.5.2-5](#) is a version of the EPRI Incompleteness Region 2 matrix, modified to add additional years since 1984 (the last complete year in the 1988 EPRI earthquake catalog). The latest bin time of the Incompleteness Region 2 matrix (1975–1983) has detection probabilities of 1.00 for all magnitude bins. Therefore, given that detection probability would not be expected to decrease with time, additional time bins with detection probabilities of 1.00 for all magnitudes were appended to the Incompleteness Region 2.

The matrix of detection probability shown in [Table 2.5.2-5](#) is appropriate for onshore sites of seismic activity near the project site. This matrix may be used for seismicity occurring through the year 2007.

In developing a matrix of detection probability appropriate for the Gulf of Mexico region, [Table 2.5.2-5](#) was qualitatively modified in consideration of the following constraints:

- For a given magnitude bin, detection probability for a given time bin would be expected to be the same or more than the detection probability of an adjacent earlier time bin. That is, the overall trend is for detection probabilities for a given magnitude interval to increase with time.
- For a given time bin, the probability of earthquake detection for a given magnitude bin would be the same or more than the detection probability an adjacent smaller magnitude bin. That is, the overall trend is for detection probabilities for a given time interval to increase with magnitude.

- Given the lack of regional seismographic stations in the Gulf of Mexico, as well as the obvious lack of felt or damage reports in the Gulf, detection probabilities for the Gulf of Mexico are expected to be no higher for any magnitude and time bin than that corresponding to the nearest onshore location of lowest detection probabilities.
- It was assumed that after the advent of the World-Wide Standardized Seismograph Network in the mid-1960s, most earthquakes of magnitude 5.5 and greater would be detectable and recorded ([Reference 2.5.2-20](#)).
- In general, global “b-values” tend to average about 0.8 to 1.2 (see Table 2 of the 2002 Engdahl and Villasenor study [[Reference 2.5.2-20](#)] and Table 4-7 of the 1994 Johnston et al. study for stable continental regions [[Reference 2.5.2-21](#)]). It was assumed that a value within this range is reasonable for the Gulf of Mexico.

Following these elements of expert judgment, the EPRI Incompleteness Region 2 matrix of detection probability was modified for the Gulf of Mexico as given in [Table 2.5.2-6](#). The time intervals of the original matrix of detection probabilities were subdivided to allow for refinement of the probabilities of detection for the Gulf of Mexico. Using the detection probability matrix with the seismicity of the Gulf of Mexico results in a b-value of 1.05.

#### 2.5.2.2 Geologic and Tectonic Characteristics of the Site and Region

Guidance from the NRC regarding seismic source characterizations used for PSHA is presented in RG 1.208. This guidance states that,

“. . . PSHA is conducted with up-to-date interpretations of earthquake sources, earthquake recurrence, and strong ground motion estimation” (page 3).

The issued guidance also states that,

“. . . seismic sources and data accepted by the NRC in past licensing decisions may be used as a starting point (for the PSHA)” (page 14).

Acceptable starting-point source zone characterizations identified within RG 1.208 include the Lawrence Livermore National Lab study presented in NUREG/CR-5250 ([Reference 2.5.2-23](#)) and the Electric Power Research Institute Seismicity Owners Group (EPRI-SOG) study ([References 2.5.2-1](#), [2.5.2-3](#), [2.5.2-16](#), [2.5.2-18](#), [2.5.2-24](#), [2.5.2-25](#), and [2.5.2-26](#)). As part of the acceptance of these studies, RG 1.208 states that site-specific geological, geophysical, and seismological studies should be performed to determine if these accepted source models adequately describe the seismic hazard for the site of interest given any new data developed since acceptance of the original models. The regulatory guidance explicitly states that:

“The results of these investigations will also be used to assess whether new data and their interpretation are consistent with the information used in recent probabilistic seismic hazard studies accepted by NRC staff. If new data, such as new seismic sources and new ground motion attenuation relationships, are consistent with the existing earth science database, then updating or modifying the information used in the site-specific hazard analysis is not required. It will be necessary to update seismic sources and ground motion attenuation relationships for sites where there is significant new information provided by the site investigation” (page C-1).

For the case of new information requiring updated source characterizations, RG 1.208 states that the development of updated source characterizations should follow the guidance presented in NUREG/CR-6372 ([Reference 2.5.2-27](#)).

NUREG/CR-6372, prepared by a Senior Seismic Hazard Analysis Committee (SSHAC), provides recommendations on the development of PSHA studies for nuclear facilities. A primary recommendation of the SSHAC is that for a given technical issue (e.g., source zone characterization),

“The following should be sought . . . (1) a representation of the legitimate range of technically supportable interpretations among the entire informed technical community . . .” (page xv of [Reference 2.5.2-27](#)).

The SSHAC outlines four levels of study for developing the range of interpretations with the choice of level depending on the complexity of the issue to be addressed. The four levels, level 1 through 4, are distinguished by the increasing levels of sophistication, resources, and participation by technical experts.

For the VCS ESP application, the EPRI-SOG source characterizations are used as the base source model in the PSHA. The EPRI-SOG model is chosen based on: (1) explicit statements within RG 1.208 that identify the EPRI-SOG source characterizations as an acceptable base model and (2) the availability of detailed documentation describing the EPRI-SOG model ([References 2.5.2-1](#), [2.5.2-3](#), [2.5.2-16](#), [2.5.2-18](#), [2.5.2-24](#), [2.5.2-25](#), and [2.5.2-26](#)). However, another supporting reason for using the EPRI-SOG model is that the EPRI-SOG methodology and resultant source characterizations ([Reference 2.5.2-16](#)) are largely consistent with a high level SSHAC study (e.g., level 3 to 4), and the final aggregate source characterizations were developed to:

“. . . reflect the range of current thinking on the causes of earthquakes in the eastern United States” (report summary page 1 of [Reference 2.5.2-16](#)).

As recommended by RG 1.208, site and regional data collected for the VCS site presented in Subsections 2.5.1 and [2.5.2.1](#) have been reviewed to:

“ . . . determine whether there are any new data or interpretations that are not adequately incorporated into the existing PSHA databases” (page 11).

For many nuclear power plants in existence in the 1980s, the EPRI-SOG study determined a database of source zones that contributed to the hazard at each site ([Reference 2.5.2-1](#)). The VCS site is a greenfield site, so such a database does not exist for the VCS site. The base EPRI-SOG model used for the VCS site is described in [Subsection 2.5.2.2.1](#), but in brief, the source model includes all EPRI-SOG source zones within the site region and is consistent with the source model generated for South Texas Project (STPEGS) Units 1 and 2 site in the EPRI-SOG study ([References 2.5.2-1 and 2.5.2-28](#)).

Under the guidance of RG 1.208, any inadequacies found in the existing EPRI-SOG source characterizations should be addressed through an update of the source model. Particular attention was paid to this review of new data collected for the VCS site because of the time elapsed since development of the EPRI-SOG source characterizations. The source characterizations of the Weston Geophysical and Law Engineering ESTs were subject to additional scrutiny because their respective source models generally contribute the greatest and least to hazard estimates for the VCS site, respectively. From this review it has been determined that no new data exists requiring alteration of the EPRI-SOG source characterizations for the VCS site with the exception of those updates presented in [Subsection 2.5.2.4](#). Included in these updates are two source model modifications that contribute to the hazard calculated at the VCS site:

- An updated characterization of the New Madrid Seismic Zone
- Updated  $M_{\max}$  values for some EPRI-SOG source zones within the Gulf of Mexico.

Both of these updates were adopted from previous COL and ESP applications submitted to NRC, and both were developed following the SSHAC process ([References 2.5.2-28 and 2.5.2-29](#)).

The following subsections present the seismic source characterizations from the EPRI-SOG model ([References 2.5.2-16 and 2.5.2-18](#)) used in the PSHA for the VCS site. Following those descriptions, a summary of seismic sources used in more recent seismic hazard studies relevant to VCS site is presented.

#### 2.5.2.2.1 Summary of EPRI-SOG Seismic Source Model

The EPRI-SOG study completed during the 1980s ([References 2.5.2-1, 2.5.2-3, 2.5.2-16, 2.5.2-18, 2.5.2-24, 2.5.2-25, and 2.5.2-26](#)) captured epistemic uncertainty in seismic source characterizations for the CEUS through the elicitation of source characterizations from six independent ESTs for the CEUS. The six teams (Bechtel Group, Dames & Moore, Law Engineering, Rondout Associates, Weston Geophysical Corporation, and Woodward-Clyde Consultants) independently evaluated the

same database of geologic, geophysical, and seismological observations to develop seismic source characterizations for the CEUS. The ESTs began by developing criteria for assessing the seismogenic activity of a tectonic feature (e.g., spatial association with large- or small-magnitude earthquakes, evidence of geologically recent slip, and orientation relative to the regional stress regime). The ESTs then used the common database to identify potentially seismogenic tectonic features and used their individual and unique criteria to evaluate the probability of seismogenic activity for these features. Each EST then defined seismic sources associated with the tectonic features and characterized the sources using the EPRI-SOG PSHA methodology (References 2.5.2-1, 2.5.2-3, 2.5.2-16, 2.5.2-18, 2.5.2-24, 2.5.2-25, and 2.5.2-26). Within this methodology, each source is characterized by a probability of activity, a maximum earthquake magnitude ( $M_{max}$ ) distribution, alternative source geometries, source interdependencies, and smoothing parameters for use in determining seismicity recurrence parameters.

Each EST provided detailed documentation of their seismic hazard assessments and source characterizations in separate volumes of the EPRI-SOG study (Reference 2.5.2-16). During the implementation of the EST source zones into the EPRI-SOG PSHA model, some simplifications were made to the original source characterizations as documented in the EQHAZARD Primer (Reference 2.5.2-1). These simplifications primarily reduced unneeded complexity in  $M_{max}$  distributions. The EQHAZARD Primer (Reference 2.5.2-18) is the primary source of the source zone parameters presented below, and the ESTs' individual volumes are the source of the descriptive characterization of the source zones.

As part of the EPRI-SOG study, databases of source zones were constructed for many of the nuclear power plants in the CEUS at the time of the study (Reference 2.5.2-1). These databases included all of the source zones that were determined in the EPRI-SOG study to contribute most significantly to the seismic hazard at the site being considered (Reference 2.5.2-1). The VCS site is a greenfield site, so there is no existing database of EPRI-SOG sources for the site. Therefore, an original set of EPRI-SOG source zones was compiled to create the base EPRI-SOG source model for the VCS site. The base model includes all of the EPRI-SOG source zones that approach within the 200-mile (322-km) radius site region.

The one exception to the inclusion of all sources within the site region in the base source model is with the Woodward-Clyde EST. For Woodward-Clyde, the only source zones within the site region are source zones designed specifically for and centered on other nuclear power plants that were considered in the EPRI-SOG study (e.g., STPEGS Units 1 and 2) (Reference 2.5.2-1). These large aerial source zones represent the Woodward-Clyde Central U.S. Background source zone that was defined individually for each nuclear power plant (Reference 2.5.2-18). The individual zones are specific to the particular plants, and it would be inappropriate to use these representations of the Woodward-Clyde Central U.S. Background source zone for the VCS site. Therefore, a new source

zone representing the Woodward-Clyde Central U.S. Background source zone is constructed for the VCS site. This new source zone is described in [Subsection 2.5.2.4.5.2](#) and shown in [Figure 2.5.2-9](#).

[Tables 2.5.2-7](#) through [2.5.2-12](#) summarize the source zone characterizations of the EPRI-SOG base model used for the VCS site ([References 2.5.2-16](#) and [2.5.2-18](#)). The source zone geometries are shown in [Figures 2.5.2-4](#) through [2.5.2-9](#). Also shown in these figures are earthquakes from the updated seismicity catalog for the VCS site (see [Subsection 2.5.2.1](#)) and earthquakes in the original EPRI-SOG catalog ([Reference 2.5.2-3](#)) both for earthquakes with  $Emb \geq 3.0$ . The database of EPRI-SOG sources used for the VCS site, including the new representation of the Woodward Clyde background zone, is consistent with the database of sources determined during the EPRI-SOG study for STPEGS Units 1 and 2, an existing nuclear power plant which is located approximately 60 miles (97 km) east-northeast of the VCS site ([Reference 2.5.2-1](#)).

In [Subsections 2.5.2.2.1.1](#) through [2.5.2.2.1.6](#), the contributing source zones for each EST are briefly described. More detailed information on each source zone is provided in the EST volumes of the EPRI-SOG documentation ([Reference 2.5.2-16](#)).

#### 2.5.2.2.1.1 Sources Identified by Bechtel Group

The Bechtel Group EST defined two source zones within the VCS site region ([Table 2.5.2-7](#) and [Figure 2.5.2-4](#)): Gulf Coast (BZ1) and Texas Platform (BZ2). Following is a brief description of these seismic source zones.

##### **Gulf Coast (Zone BZ1)**

The Gulf Coast source zone is a large background source zone encompassing the Texas Gulf Coast and extending through Louisiana and continuing eastward to the offshore region east of Florida ([Figure 2.5.2-4](#)). The zone is characterized by an upper-bound  $M_{max}$  of  $m_b$  6.6 ([Table 2.5.2-7](#)). The VCS site is contained within the zone.

##### **Texas Platform (Zone BZ2)**

The Texas Platform source zone is a large background source zone extending from eastern New Mexico into Texas ([Figure 2.5.2-4](#)). The zone is characterized by an upper-bound  $M_{max}$  of  $m_b$  6.6 ([Table 2.5.2-7](#)). The closest approach of the zone to the VCS site is 9.3 miles (15 km).

#### 2.5.2.2.1.2 Sources Identified by Dames & Moore

The Dames & Moore Group EST defined four source zones within the VCS site region: South Coastal Margin (zone 20), Ouachitas Fold Belt (zone 25), New Mexico (zone 67), and combination zone C08 ([Figure 2.5.2-5](#) and [Table 2.5.2-8](#)). Following is a brief description of these seismic source zones.

### **Southern Coastal Margin (Zone 20)**

The South Coastal Margin source zone is a large aerial zone that extends from the continental shelf off eastern Florida, along the Texas coastal plain, and into Mexico (Figure 2.5.2-5). Dames & Moore designed the zone to largely parallel the southern-rifted margin of North America. The zone is characterized by an upper-bound  $M_{\max}$  of  $m_b$  7.2 (Table 2.5.2-8). The VCS site is contained within the zone.

### **Ouachitas Fold Belt (Zone 25)**

The Ouachitas Fold Belt source zone encompasses the Ouachita orogenic front extending from Arkansas through Oklahoma, Texas, and into eastern Mexico (Figure 2.5.2-5). The zone is characterized by an upper-bound  $M_{\max}$  of  $m_b$  7.2 (Table 2.5.2-8). The closest approach of the zone to the VCS site is 68 miles (110 km).

### **New Mexico (Zone 67)**

The New Mexico source zone extends from Texas into New Mexico and part of northern Mexico (Figure 2.5.2-5). Dames & Moore describe the boundaries of the zone as being defined largely on the basis of the extent of arches and basins formed during the Paleozoic (Reference 2.5.2-6). The zone is characterized by an upper-bound  $M_{\max}$  of  $m_b$  7.2 (Table 2.5.2-8). The closest approach of the zone to the site is 140 miles (225 km).

### **Combination Zone C08**

Combination zone C08 is spatially equivalent to the Ouachitas Fold Belt source zone (25) with the exclusion of the kink in the Ouachita fold belt (zone 25A) at the Texas-Oklahoma border (Figure 2.5.2-5). The zone is characterized by an upper-bound  $M_{\max}$  of  $m_b$  7.2 (Table 2.5.2-8). The closest approach of the zone to the site is 68 miles (110 km).

#### **2.5.2.2.1.3 Sources Identified by Law Engineering**

The Law Engineering EST defined two source zones within the VCS site region (Figure 2.5.2-6 and Table 2.5.2-9): New Mexico-Texas Block (zone 124) and South Coastal Block (zone 126). Following is a brief description of these seismic source zones.

### **New Mexico-Texas Block (Zone 124)**

The New Mexico-Texas Block source zone is a large aerial source defined by the boundaries of the Southern Oklahoma Aulacogen, the Ouachita gravity high, and the magnetic trend of the Rio Grande Rift-Colorado Front Ranges (Reference 2.5.2-16). This zone encompasses the majority of Texas, excluding the Gulf Coastal Plain, and extends into eastern New Mexico (Figure 2.5.2-6). The zone is

characterized by an upper-bound  $M_{\max}$  of  $m_b$  5.8 (Table 2.5.2-9). The closest approach of the zone to the site is 44 miles (70 km).

### **South Coastal Block (Zone 126)**

The South Coastal Block source zone is a large aerial source that extends from the continental shelf off eastern Florida westward into Texas and Mexico (Figure 2.5.2-6). The northern edge of the zone was defined to coincide with the Paleozoic edge of the North American craton. The zone is characterized by an upper-bound  $M_{\max}$  of  $m_b$  4.9 (Table 2.5.2-9). The VCS site is contained within the zone.

#### **2.5.2.2.1.4 Sources Identified by Rondout Associates**

The Rondout Associates EST defined two source zones within the VCS site region (Table 2.5.2-10 and Figure 2.5.2-7): Gulf Coast to Bahamas fracture zone (zone 51) and Background 50/Grenville Crust (zone C02). Following is a brief description of these seismic source zones.

### **Gulf Coast to Bahamas Fracture Zone (Zone 51)**

The Gulf Coast to Bahamas fracture zone (zone 51) is a large areal source defined by the presence of Paleozoic crust along the Gulf coastal region and a maximum horizontal tensile stress directed at a high angle to the coast (Reference 2.5.2-16). The zone extends from southern Florida eastward to Texas and Mexico (Figure 2.5.2-7). The zone is characterized by an upper-bound  $M_{\max}$  of  $m_b$  5.8 (Table 2.5.2-10). The VCS site is contained within the zone.

### **Grenville Crust (Zone C02)**

The Grenville Crust source zone is a set of discrete source zones that extend across the eastern and southern margin of the U.S. The portion of the source zone within the VCS site region encompasses central and eastern Texas. The source zone is a background source representing all of the Grenville age crust that is not contained within a source zone that was defined based on the presence of tectonic features (Reference 2.5.2-16). The zone is characterized by an upper-bound  $M_{\max}$  of  $m_b$  5.8 (Table 2.5.2-10). The closest approach of the zone to the VCS site is 93 miles (150 km).

#### **2.5.2.2.1.5 Sources Identified by Weston Geophysical**

The Weston Geophysical Corporation EST defined three source zones within the VCS site region (Table 2.5.2-11 and Figure 2.5.2-8): Gulf Coast (zone 107), Southwest (zone 109), and Combination C31. Following is a brief description of these seismic source zones.

### **Gulf Coast (Zone 107)**

The Gulf Coast source zone is a large aerial source that extends from Florida through Texas and into eastern Mexico (Figure 2.5.2-8). The majority of the site region occurs within this source zone. The upper-bound  $M_{\max}$  for the zone is  $m_b$  6.0 (Table 2.5.2-11). The VCS site is contained within this zone.

### **Southwest (Zone 109)**

The Southwest source zone is a large background source that extends over much of Texas, New Mexico, Colorado, and Wyoming (Figure 2.5.2-8). The zone is characterized by an upper-bound  $M_{\max}$  of  $m_b$  6.6 (Table 2.5.2-11). The closest approach of the zone to the VCS site is 97 miles (156 km).

### **Combination C31**

The Combination zone C31 is an alternative geometry for the Southwest (zone 109) background zone that excludes the Delaware basin in west Texas (Figure 2.5.2-8). The zone is characterized by an upper-bound  $M_{\max}$  of  $m_b$  6.6 (Table 2.5.2-11). The closest approach of the zone to the VCS site is 97 miles (156 km).

#### **2.5.2.2.1.6 Sources Identified by Woodward-Clyde Consultants**

As described in the introduction to Subsection 2.5.2.2.1, the Woodward-Clyde Consultants EST defined the Central U.S. Background for the central U.S. individually for each nuclear power plant in the EPRI-SOG study all with the same source characterization (Table 2.5.2-12 and Figure 2.5.2-9) but with geometries unique to the specific location (e.g., centered on the particular site). Because the VCS site is a greenfield site, there is no existing Central U.S. Background source zone geometry for the site. Therefore, a new background source geometry was constructed for the VCS site based on the geometry of the zone defined for STPEGS Units 1 and 2 which are located approximately 60 miles (100 km) east-northeast of the VCS site. This minor modification to the EPRI-SOG model is described in Subsection 2.5.2.4.5.2.

#### **2.5.2.2.2 Post-EPRI-SOG Source Characterization Studies**

Since publication of the EPRI-SOG seismic source characterizations for the CEUS (Reference 2.5.2-16), there have been several regional-scale source characterization studies within the greater VCS site region that are potentially relevant to the VCS site. These studies include:

- A Lawrence Livermore National Laboratory (LLNL) report on the seismic hazard characterization of nuclear power plants in the CEUS (References 2.5.2-23 and 2.5.2-30)

- A draft report prepared by Geomatrix Consultants for the NRC on the Quaternary activity of the Meers fault ([Reference 2.5.2-31](#))
- A LLNL PSHA study for the Pantex nuclear weapon support facility outside Amarillo, Texas ([Reference 2.5.2-32](#))
- The United States Geological Survey (USGS) National Seismic Hazard Map program source characterizations used in developing the national seismic hazard maps ([References 2.5.2-14](#), [2.5.2-33](#), and [2.5.2-34](#))
- The PSHA as part of the COLA for STPEGS Units 3 and 4 ([Reference 2.5.2-28](#))
- The Johnston et al. (1994) ([Reference 2.5.2-21](#)) study that attempted to characterize earthquakes within stable continental regions

The source characterizations used within these studies relevant to the VCS site are briefly summarized below. Source characterizations from these studies that were developed using post-EPRI-SOG research were evaluated as possible revisions or additions to the EPRI-SOG model following the guidance of RG 1.208.

#### 2.5.2.2.2.1 Lawrence Livermore National Laboratory 1989 Study

In 1989, LLNL completed a PSHA study under the direction of the NRC for nuclear power plants within the CEUS ([Reference 2.5.2-23](#)). The LLNL study was similar to the EPRI-SOG study in that the PSHA included source characterizations and ground motion attenuation equations for the CEUS that were developed independently by a group of experts. Hazard at a particular site was calculated from the source model defined by each expert using each of the ground motion relationships, and the final hazard at the site was the aggregate of all source models and ground motion relationships. As stated in RG 1.208, the resultant PSHA model is accepted by the NRC for use in PSHA studies supporting ESP and COL applications if modifications are made to account for new information and data on ground motion equations and source characterizations.

The source characterizations of the 1989 LLNL study were developed by 11 independent experts resulting in 11 different source models ([Reference 2.5.2-23](#)). The source models were developed by the experts using geologic and geophysical data the experts compiled themselves; though at later stages of the study, a uniform seismicity catalog was provided to all of the experts. The source models were revised through a series of feedback loops with the project organizers at LLNL that provided clarification of the project methodology and preliminary results for the source models. The final source models presented in the 1989 report volume ([Reference 2.5.2-23](#)) are defined by their source zone geometry, type of recurrence relationship,  $M_{\max}$ , and seismicity recurrence parameters—all of which are provided by the individual experts.

As part of the 1989 LLNL study ([Reference 2.5.2-23](#)), seismic hazard curves were calculated for many existing nuclear power plants in the CEUS. The VCS site was not included in this analysis because it is a greenfield site. However, hazard was calculated at STPEGS Units 1 and 2, located approximately 60 miles (100 km) east-northeast of the VCS site ([Reference 2.5.2-30](#)). For the STPEGS site, the study identified what they considered the most significant source zones based on their contribution to hazard at the STPEGS site ([Reference 2.5.2-30](#)). In general, within each expert's source models, the largest contribution to hazard comes from large background source zones that either contain the site or are near the site. These zones have mean  $M_{\max}$  values ranging from  $m_b$  5.5 to 6.5. For two of the experts, the New Madrid seismic zone (mean  $M_{\max}$  of  $m_b$  7.5 to 7.8) is a primary contributing source. For one expert the Oklahoma aulacogen, characterized by a  $M_{\max}$  of  $m_b$  7.2, is a primary contributing source. Full descriptions of the source zones are presented within the documentation for the study ([References 2.5.2-23](#) and [2.5.2-30](#)).

An update to the 1989 LLNL study was completed in 1994 with the publication of NUREG-1488 ([Reference 2.5.2-35](#)). The focus of this study was to reduce the uncertainty in ground motion estimates, and this was accomplished in part by having the experts reevaluate the uncertainty they assigned to seismicity parameters. There were no significant changes to the source model characterizations described above.

The geometry,  $M_{\max}$  values, and seismicity parameters of source zones identified as being significant to the hazard at the STPEGS Units 1 and 2 site are broadly consistent with the EPRI-SOG source zones used as the basis for the PSHA at the VCS site ([Tables 2.5.2-7](#) through [2.5.2-12](#); [Figures 2.5.2-4](#) through [2.5.2-9](#)). As such, the source zones of the LLNL study do not present new information that requires modification of the EPRI-SOG model for the VCS site.

#### 2.5.2.2.2.2 Draft Report to the NRC on the Quaternary Faulting of the Meers Fault

Swan et al. ([Reference 2.5.2-31](#)) provided the NRC with a draft report describing the results of a study investigating Quaternary faulting in southern Oklahoma. In the report, the Meers and Criner faults, approximately 400 miles (640 km) from the VCS site, are identified as the only potentially capable faults in the region. A seismic source characterization of the Meers fault based largely on this report is used in a screening study for the VCS site. This source characterization and the results of the screening study are described in [Subsection 2.5.2.4](#).

The Swan et al. study ([Reference 2.5.2-31](#)) did not find conclusive evidence supporting the capability or lack of capability of the Criner fault. They conservatively characterized the Criner fault as capable of  $m_b$  6.3 to 6.6 earthquakes with return periods on the order of 2000 to 3000 years. Studies post-dating that of Swan et al. ([Reference 2.5.2-31](#)) have shown that the Criner fault is not a capable tectonic source ([References 2.5.2-36](#), [2.5.2-37](#), [2.5.2-38](#), [2.5.2-39](#), and [2.5.2-40](#)). Therefore, the Criner fault was not considered a capable fault for the VCS site ESP application.

#### 2.5.2.2.2.3 LLNL PSHA for Pantex Nuclear Weapons Support Facility

In 1998, Savy et al. (Reference 2.5.2-32) with LLNL conducted a PSHA for the Pantex nuclear weapons support facility in Amarillo, Texas, over 500 miles (800 km) from the VCS site. The study region was a 10 degree x 10 degree quadrilateral centered on the Pantex site that includes eastern Colorado and New Mexico, Oklahoma, Kansas, and the majority of Texas; thus, part of this study region overlaps the VCS site region. Within the study region Savy et al. (Reference 2.5.2-32) defined five aerial source zones and 14 faults largely based on the results of previous seismic source characterization studies. Of these different sources, only the extended margin and craton background source zones of Savy et al. (Reference 2.5.2-32) extend into the VCS site region.

The source characterization of these two zones (i.e., activity rates,  $M_{max}$ , geometry) is based on zones of the same name used in the 1996 USGS National Seismic Hazard Maps (Reference 2.5.2-14). For these maps the extended margin zone encompasses all of the CEUS seaward of the limit of Precambrian crustal rifting associated with opening of the Iapetus ocean, and the craton zone includes the rest of the crust within the VCS site region. Seismicity rates for the zones are spatially uniform and were developed primarily using rates from the 1996 USGS model (Reference 2.5.2-14). Upper- and lower-bound  $M_{max}$  values for the zones were also defined based on the USGS values (Reference 2.5.2-14): craton  $M_w$  6.0 and 6.75 ( $m_b$  6.3 and 6.76), and extended margin  $M_w$  6.75 and 7.8 ( $m_b$  6.76 and 7.4).

The aerial source zones defined by Savy et al. (Reference 2.5.2-32) are broadly consistent with the EPRI-SOG source zones used as the basis for the PSHA at the VCS site. The craton source zone of Savy et al. (Reference 2.5.2-32) is spatially correlated to similar zones of the EPRI-SOG ESTs that represent non-extended crust, and the extended margin zone is spatially correlated with similar zones of the EPRI-SOG ESTs that represent the extended margin along the Gulf of Mexico (see Subsection 2.5.2.2.1.1). However, the  $M_{max}$  values of the Savy et al. (Reference 2.5.2-32) zones are generally higher than the  $M_{max}$  values defined by the EPRI-SOG ESTs for corresponding source zones (Tables 2.5.2-7 through 2.5.2-12; Figures 2.5.2-4 through 2.5.2-9). This contrast is typically greatest between the upper-bound  $M_{max}$  values of the extended margin zone of Savy et al. (Reference 2.5.2-32) ( $m_b$  7.4) to upper-bound  $M_{max}$  values for correlative EPRI-SOG zones (e.g., Bechtel Group Gulf Coast zone with  $m_b$  6.6, Dames & Moore South Coastal Margin with  $m_b$  7.2, Law Engineering South Coastal Block with  $m_b$  4.9, Rondout Associates Gulf Coast to Bahamas Fracture Zone with  $m_b$  5.8, Weston Geophysical Corporation Gulf Coast with  $m_b$  6.0).

As previously mentioned, the  $M_{max}$  values used by Savy et al. (Reference 2.5.2-32) are based on the 1996 USGS National Seismic Hazard Maps evaluation of  $M_{max}$ . As described in Subsection 2.5.2.2.2.4, the USGS  $M_{max}$  characterization of CEUS seismic sources is based on assuming that stable continental regions (SCRs) worldwide are analogous, and the characteristics of seismicity (i.e.,  $M_{max}$ ) are the same for all SCRs (Reference 2.5.2-34). The USGS largely bases its

use of this interpretation on the Johnston et al. study ([Reference 2.5.2-21](#)). The Johnston et al. study and the USGS models are described in [Subsections 2.5.2.2.2.6](#) and [2.5.2.2.2.4](#), respectively. The implications of these studies, and thus also the Savy et al. study ([Reference 2.5.2-32](#)), on  $M_{\max}$  values for source zones used in the VCS PSHA are described in [Subsection 2.5.2.2.3](#) where it is concluded that these studies do not motivate a modification to the  $M_{\max}$  values for the EPRI-SOG source zones.

#### 2.5.2.2.2.4 USGS National Seismic Hazard Maps

As part of the USGS National Seismic Hazard Mapping program, seismic hazard maps for the conterminous United States were produced in 1996 ([Reference 2.5.2-14](#)), 2002 ([Reference 2.5.2-33](#)), and 2008 ([Reference 2.5.2-34](#)) using source characterizations developed by the USGS. The USGS does not follow a SSHAC process ([Reference 2.5.2-27](#)) in developing their source characterizations (e.g., they do not use a formal expert elicitation process and do not attempt to represent the full range of uncertainty within the informed technical community). However, the source models are developed from published literature, and working groups are held to discuss source characterizations. Therefore, the USGS source characterizations can be viewed as informed representations of the seismic sources they represent. Aspects of the USGS source characterizations based on the 2008 model ([Reference 2.5.2-34](#)) relevant to the VCS site are described below.

The USGS source model does not have any discrete fault sources within the VCS site region, but the region is represented with four weighted aerial source zones based on historical seismicity that extend throughout the CEUS ([Reference 2.5.2-34](#)). Three of the models have gridded or smoothed seismicity rates, and one of the models has four large background zones with uniform seismicity rates within each zone ([Reference 2.5.2-34](#)). For all of these models, the USGS defines five zones with unique  $M_{\max}$  distributions ([Reference 2.5.2-34](#)). Two of these zones (the craton and extended margin  $M_{\max}$  zones) are within the site region and are thus relevant to the VCS site. The extended margin zone encompasses all of the CEUS seaward of the limit of Precambrian crustal rifting associated with opening of the Iapetus ocean and contains the VCS site. The remainder of the CEUS east of longitude 102° W is the craton zone. The extended margin zone has a mean  $M_{\max}$  of  $M_w$  7.5 ( $m_b$  7.2), and the craton zone has a mean  $M_{\max}$  of  $M_w$  7.0 ( $m_b$  6.9) ([Reference 2.5.2-34](#)). These  $M_{\max}$  values are generally higher than those defined by the EPRI-SOG ESTs for similar areas within the site region ([Tables 2.5.2-7](#) through [2.5.2-12](#); [Figures 2.5.2-4](#) through [2.5.2-9](#)).

As reported in the documentation for the 2008 maps ([Reference 2.5.2-34](#)), the  $M_{\max}$  values used for these two zones are based on: (1) a qualitative analysis by Wheeler ([Reference 2.5.2-41](#)) that concluded the two zones should have different  $M_{\max}$  values, and (2) analogies between the extended margin and craton zone and analogous SCRs worldwide ([References 2.5.2-42](#) and [2.5.2-43](#)). The basis cited for comparing the CEUS craton and extended margin zones to the other SCRs in

developing  $M_{\max}$  values for the zones is the study of Johnston et al. (References 2.5.2-21 and 2.5.2-34). The Johnston et al. study (Reference 2.5.2-21) is described in Subsection 2.5.2.2.6, but the conclusion of this study cited by the USGS to support their  $M_{\max}$  values is the observation of Johnston et al. (Reference 2.5.2-21) that the largest magnitude earthquakes in SCRs worldwide occur in extended crust. This observation, and the fundamental assumption that extended margin and craton zones worldwide have similar seismogenic behavior (e.g., the same  $M_{\max}$ ) (Reference 2.5.2-43), lead the USGS to prescribe the  $M_{\max}$  values for these zones from a qualitative analysis of the distribution of earthquakes observed in SCRs worldwide (Reference 2.5.2-34).

The USGS source zones are consistent with those of the EPRI-SOG model (Reference 2.5.2-16) in that their geometry is based on tectonic characteristics and their activity rates are based on historical seismicity. The USGS source zones are different from some of the EPRI-SOG source zones (Reference 2.5.2-16) in that the  $M_{\max}$  values used for the USGS zones are generally greater than correlative zones from the EPRI-SOG model. This difference is the most distinct for zones representing extended crust along the Gulf of Mexico (see Subsection 2.5.2.2.1.1). The difference in  $M_{\max}$  values is based on: (1) the assumption of Johnston et al. (Reference 2.5.2-21) and adopted by the USGS, that seismicity from other cratonic and extended margin regions can be used to estimate the  $M_{\max}$  for the CEUS, (2) the methodology of the USGS to define only a few  $M_{\max}$  zones for the CEUS (Reference 2.5.2-34), and (3) the observation of Johnston et al. (Reference 2.5.2-21) that the largest magnitude earthquakes occur in SCRs worldwide in extended crust. Based on these observations, the implications of the USGS  $M_{\max}$  values for the VCS site were evaluated, and it was determined that they do not motivate an update to the  $M_{\max}$  values used for the VCS site. This evaluation is presented in Subsection 2.5.2.2.3.

There are several other seismic sources within the 2008 USGS source model that occur outside of the site region yet are relevant to the VCS site due to the absence of any capable faults within the site region. These sources are considered for the VCS site because they are the closest fault sources within the USGS model with the potential for large magnitude ( $M_w > 7.0$ ) earthquakes. These sources are the Meers fault, the New Madrid Seismic Zone (NMSZ) and faults of the Rio Grande Rift (RGR).

The Meers fault is included in the 2008 USGS source model (Reference 2.5.2-34) and is based on studies post-dating the EPRI-SOG study (e.g., References 2.5.2-31, 2.5.2-44, 2.5.2-45, 2.5.2-46, 2.5.2-47, 2.5.2-48, and 2.5.2-49) that demonstrate the Meers fault is generally capable of larger magnitude earthquakes and has shorter return periods than represented in the EPRI-SOG model (Reference 2.5.2-16). As described in Subsection 2.5.2.4.4.2, this new information motivates updating the Meers fault characterization within the EPRI-SOG model, and thus the USGS characterization of the Meers fault does motivate an update to the EPRI-SOG model. This updated source characterization is described in Subsection 2.5.2.4.4.2.

The 2008 USGS source model also includes a characterization of the NMSZ ([Reference 2.5.2-34](#)) that is based on studies that post-date the EPRI-SOG study ([Reference 2.5.2-16](#)). These studies largely demonstrate a shorter return period for New Madrid events than captured in the EPRI-SOG model ([Reference 2.5.2-16](#)). As described in [Subsection 2.5.2.4.4.1](#), these more recent observations, and thus the USGS characterization of the NMSZ, motivates an update to the EPRI-SOG model. This updated source characterization is described in [Subsection 2.5.2.4.4.1](#).

The 2008 USGS model ([Reference 2.5.2-34](#)) also includes tens of faults that are part of the RGR. The characterization of these faults is largely based on post-EPRI-SOG research ([Reference 2.5.2-34](#)), and the EPRI-SOG ESTs generally did not include the RGR in their source characterizations ([Reference 2.5.2-16](#)) (see description in [Subsection 2.5.2.4.4.3](#)). Therefore, USGS characterization of the RGR motivates an update to the EPRI-SOG model. However, the characterizations of the RGR faults used for the VCS site are based on those within the 2002 USGS Seismic Hazard Maps ([Reference 2.5.2-33](#)) because the 2008 map documentation had not been released at the time the screening study for the VCS site was conducted. There were no significant changes to the characterization of the RGR faults in the 2008 maps that will affect the results of the screening study given the large distance between the site and the RGR.

#### 2.5.2.2.2.5 Source Characterizations Used in the STPEGS Units 3 & 4 COLA

Since the EPRI-SOG study ([References 2.5.2-1, 2.5.2-3, 2.5.2-16, 2.5.2-18, 2.5.2-24, 2.5.2-25, and 2.5.2-26](#)), a COLA has been submitted for STPEGS Units 3 & 4, which is approximately 60 miles (100 km) east-northeast of the VCS site ([Reference 2.5.2-28](#)). The STPEGS application was developed under the guidance of RG 1.208 and used the EPRI-SOG source model ([References 2.5.2-1, 2.5.2-3, 2.5.2-16, 2.5.2-18, 2.5.2-24, 2.5.2-25, and 2.5.2-26](#)) as a base source model. To this source model several modifications were made including:

- Updates to  $M_{\max}$  values for gulf coastal source zones (GCSZs) based on the occurrence of earthquakes within the Gulf of Mexico with magnitudes larger than the lower-bound  $M_{\max}$  values of the source zones
- Inclusion of the Mt. Enterprise-Elkhart Graben (MEEG) in a screening study as a potential seismogenic source
- Inclusion of an updated model of the NMSZ
- Revisions to the smoothing parameters for Dames & Moore South Coastal Margin source zone
- Updates to the southern extent of the EPRI-SOG model to extend seismicity parameters for sources zones that extend into the Gulf of Mexico throughout their area

Similar changes to these were made to the base EPRI-SOG source model for the VCS site with the exception of the inclusion of the MEEG as a potential seismogenic source. The MEEG was not included as a potential source because analysis of the published literature regarding the MEEG suggests that the MEEG is not a capable fault (see description in Subsection 2.5.1.1.4.3.5.1). The changes made to the EPRI-SOG base model for the VCS site are described in [Subsection 2.5.2.4](#).

#### 2.5.2.2.2.6 Johnston et al. Study of Stable Continental Region Seismicity

Johnston et al. ([Reference 2.5.2-21](#)) conducted a study from the mid-1980s to the early 1990s under the direction of EPRI to develop an earthquake database for SCRs worldwide and explore the possibility of using this database to help constrain the potential for large earthquakes within SCRs. To accomplish this goal Johnston et al. ([Reference 2.5.2-21](#)) conducted a detailed study that included:

- (1) Defining the SCRs of the world, subdividing these regions into tectonic domains, and defining descriptor variables for these domains (e.g., crust type, age, stress regime)
- (2) Compiling a global catalog of earthquakes within SCRs
- (3) Testing for significant statistical correlations between the SCRs subdivided at different levels and the maximum observed earthquake magnitude with these subdivisions to determine if a robust estimator of  $M_{\max}$  values could be developed

The fundamental assumptions of the Johnston et al. (1994) ([Reference 2.5.2-21](#)) study are: (1) that for similar tectonic domains within SCRs worldwide, space can be traded for time to allow development of a composite earthquake catalog for that particular tectonic domain that is larger than the catalog of earthquakes just within that domain, and (2) these grouped domains have the same fundamental seismicity characteristics (i.e.,  $M_{\max}$ ).

EPRI's primary motivation for initiating the Johnston et al. (1994) ([Reference 2.5.2-21](#)) study was twofold: (1) provide the EPRI-SOG ESTs ([References 2.5.2-1, 2.5.2-3, 2.5.2-16, 2.5.2-18, 2.5.2-24, 2.5.2-25, and 2.5.2-26](#)) guidance on estimating  $M_{\max}$  values for source zones within the CEUS, and (2) determine if there is a robust method for estimating  $M_{\max}$  based on historical seismicity. Given the needs of the EPRI-SOG study ([References 2.5.2-1, 2.5.2-3, 2.5.2-16, 2.5.2-18, 2.5.2-24, 2.5.2-25, and 2.5.2-26](#)) and the natural development of the Johnston et al. ([Reference 2.5.2-21](#)) study, the Johnston et al. ([Reference 2.5.2-21](#)) study was conducted in two phases.

As part of the first phase, Johnston et al. ([Reference 2.5.2-21](#)) developed an initial division of SCRs based on tectonic features and a global catalog of earthquakes within SCRs. These materials were then used to develop first-order conclusions aimed at aiding the ESTs in their development of source characterizations for the CEUS. The main conclusion of the first phase that was presented to the

ESTs was that there is an association between rifts and passive margins of Mesozoic and younger age and the largest observed earthquakes in SCRs.

The second phase of the Johnston et al. (Reference 2.5.2-21) study attempted to expand upon this conclusion and determine if there was a robust method for estimating  $M_{\max}$  based on historical earthquakes by following the three steps outlined in the beginning of this subsection. As part of this effort Johnston et al. (Reference 2.5.2-21) refined their subdivision of tectonic domains and their defining characteristics. The broadest subdivision of domains identified by Johnston et al. (Reference 2.5.2-21) is that of extended and non-extended crust where extended crust includes regions of rifting, distributed continental extension, and passive margins. Non-extended crust includes the remainder of SCR crust. With a higher level of detail than this distinction, Johnston et al. (Reference 2.5.2-21) further defined 24 different categories of non-extended crust and 720 categories of extended crust based on what they refer to as descriptor variables characterizing the crust (e.g., stress regime, crustal type, and crustal age).

These subdivisions representing different sets of descriptor variables were examined to determine if there was a statistically significant correlation between the subdivisions and the maximum observed earthquakes in the subdivisions using an updated global catalog of SCR earthquakes. The conclusion reached by Johnston et al. (Reference 2.5.2-21) from analyzing all of the different subdivisions and descriptor variables was that there is only a slight statistical difference between the mean maximum observed earthquake magnitude in extended crust and the mean maximum observed magnitude in non-extended crust. No other descriptor variable was found to have a statistically significant correlation. Johnston et al. (Reference 2.5.2-21) qualify the impact of these conclusions by stating that, “we find that there is no strong evidence that any typical extended crust domain has a larger maximum magnitude than a typical non-extended crust domain,” (page 5-17). Johnston et al. (Reference 2.5.2-21) essentially concluded that a robust estimator of  $M_{\max}$  cannot be found using the assumption of space-time equivalence for seismicity and the tectonic descriptions of SCRs defined by Johnston et al. (Reference 2.5.2-21).

Despite this lack of a robust estimator for  $M_{\max}$ , the main conclusion the first phase of the Johnston et al. (Reference 2.5.2-21) study was refined to say that the maximum observed earthquake in extended SCRs worldwide is greater than the maximum observed earthquake in non-extended SCRs. This conclusion has become one of the most widely stated observations of the Johnston et al. (Reference 2.5.2-21) study with respect to the determination of  $M_{\max}$  values for the CEUS (e.g., Reference 2.5.2-34). The relevance of this conclusion to the EPRI-SOG source characterizations used for the VCS site is described below in [Subsection 2.5.2.2.3](#).

### 2.5.2.2.3 Maximum Magnitude Evaluation

As described in [Subsection 2.5.2.2.4](#), the USGS hazard maps ([Reference 2.5.2-34](#)) have  $M_{\max}$  values that are generally higher than correlative zones within the EPRI-SOG source zones ([Reference 2.5.2-16](#)) used as the base model for the VCS site (see [Subsection 2.5.2.2.1](#)). The USGS source model was created following development of the EPRI-SOG source characterizations, so the USGS model could be interpreted as new information that should be considered under the guidance of RG 1.208 (see introduction to [Subsection 2.5.2.2](#)). To evaluate whether the  $M_{\max}$  values of the USGS model imply that the EPRI-SOG model should be updated, the actual new information used to develop the  $M_{\max}$  values needs to be identified.

As described in [Subsection 2.5.2.2.4](#), the basis for  $M_{\max}$  values used by the USGS is: (1) a qualitative analysis by Wheeler ([Reference 2.5.2-41](#)) that suggested the extended margin and craton zones should have different  $M_{\max}$  values, and (2) analogies between the extended margin and craton zone and other SCRs worldwide ([References 2.5.2-42](#) and [2.5.2-43](#)). The second basis depends on: (1) adopting the assumption of Johnston et al. ([Reference 2.5.2-21](#)) that seismicity from other cratonic and extended margin regions can be used to estimate the  $M_{\max}$  for the CEUS, and (2) the observation of Johnston et al. ([Reference 2.5.2-21](#)) that the largest magnitude earthquakes occurring globally in SCRs occur in extended crust. As described below, the only actual information or data contained within any of these points is the observation that the largest earthquakes occurring within SCRs worldwide occur within regions of extended crust. This observation was made prior to the development of the EPRI-SOG source characterizations, and was explicitly presented to the participant ESTs (see description in [Subsection 2.5.2.2.6](#)), so there is no new information within the USGS source characterizations ([Reference 2.5.2-34](#)) or the Johnston et al. study ([Reference 2.5.2-21](#)) regarding  $M_{\max}$  values for the CEUS aerial source zones that implies updating the EPRI-SOG study.

The first basis for the  $M_{\max}$  values used by the USGS is the work of Wheeler ([Reference 2.5.2-41](#)) that suggests there are differences in seismic behavior (i.e.,  $M_{\max}$  values) of the CEUS associated with the limit of lapetan faulting. Essentially, Wheeler ([Reference 2.5.2-41](#)) defines two large domains within the CEUS: the craton landward of the limit of lapetan faulting and the extended margin seaward of the same limit of faulting. Wheeler ([Reference 2.5.2-41](#)) posits that normal faults associated with lapetan rifting in the extended crust are capable of larger earthquakes. The EPRI-SOG ESTs followed the same methodology of using tectonic features and characteristics to define source zone geometry ([Reference 2.5.2-16](#)). The observations used by Wheeler ([Reference 2.5.2-41](#)) to derive his division of the CEUS are not significantly different from those available to the ESTs during their evaluations, so there is no new information contained in Wheeler's subdivisions that were not considered by the ESTs. Therefore, there is no need to update the EPRI-SOG source zones to reflect the work of Wheeler ([Reference 2.5.2-41](#)).

The second basis for the  $M_{\max}$  values used by the USGS for the CEUS depends on: (1) adopting the assumption of Johnston et al. (Reference 2.5.2-21) that seismicity from other cratonic and extended margin regions can be used to estimate the  $M_{\max}$  for the CEUS, and (2) the observation of Johnston et al. (Reference 2.5.2-21) that the largest magnitude earthquakes occurring globally in SCRs occur in extended crust. The assumption of Johnston et al. (Reference 2.5.2-21), and thus the USGS that seismicity from other SCRs can be used to estimate  $M_{\max}$  for the CEUS is stated in Johnston et al. (Reference 2.5.2-21) as an underlying philosophy, and there is no explicit effort within the study to justify this philosophy or assumption. As such, there is no new data supporting this assumption that needs to be evaluated for impact on the EPRI-SOG ESTs source characterizations (Reference 2.5.2-16). It is also important to note that the EPRI-SOG ESTs were presented with the Johnston et al. (Reference 2.5.2-21) philosophy, and they evaluated its appropriateness for use in their source characterizations.

The final part of the second basis for the  $M_{\max}$  values used by the USGS for the CEUS depends on the observation of Johnston et al. (Reference 2.5.2-21) that the largest magnitude earthquakes occurring globally in SCRs occur in extended crust. As described in Subsection 2.5.2.2.6, this basic conclusion of the Johnston et al. (Reference 2.5.2-21) was reached at the conclusion of the first phase of their work, remained essentially unchanged at the end of the second phase, and was presented to the EPRI-SOG ESTs for use in their evaluation of source zone characteristics for CEUS. As such, this basis for the USGS  $M_{\max}$  values depends on information that was available to and evaluated by the EPRI-SOG ESTs during their source characterization efforts, and this basis also does not present any new information that motivates updating the EPRI-SOG model.

For VCS, it was determined that the divergence in  $M_{\max}$  values between the USGS (Reference 2.5.2-34) and EPRI-SOG (Reference 2.5.2-16) source models is not based on the availability of new data or information that has been developed since the EPRI-SOG study. The difference in values is due to different interpretations developed by the ESTs and the USGS. Following the guidance provided in RG 1.208 and the observation that the EPRI-SOG study essentially followed a SSHAC level 3 or 4 process (see introduction to Subsection 2.5.2.2), it was further determined that the  $M_{\max}$  values defined by the EPRI-SOG ESTs do not need to be revised based on the conclusions of the Johnston et al. study (Reference 2.5.2-21) or the  $M_{\max}$  values used in the USGS hazard maps (Reference 2.5.2-34).

### 2.5.2.3 Correlation of Earthquake Activity with Seismic Sources

As described in Subsection 2.5.2.2.1, EPRI-SOG ESTs used the spatial distribution of seismicity as input to their subdivision of the CEUS into seismic source zones (Reference 2.5.2-16). The earthquake catalog used by the ESTs was the EPRI-SOG catalog described in Subsection 2.5.2.1.1. An updated catalog was developed for the VCS site (see Subsection 2.5.2.1.2), and the two catalogs can be compared to assess any changes in the patterns of seismicity or to determine if any

correlation exists between geologic structures and seismicity not identified within the EPRI-SOG study. Comparison of the catalogs yields the following conclusions:

- The updated seismicity catalog does not show any earthquakes of  $E_{mb} \geq 3.0$  within approximately 80 miles (~130 km) of the site. Accordingly, there are no earthquakes of  $E_{mb} \geq 3.0$  within 80 miles (130 km) of the site that can be associated with a known geologic structure (Figure 2.5.2-2).
- The closest cluster of seismicity to the site that is spatially correlated with a geologic structure is a west-northwest trending band of seismicity extending from Arkansas, through southern Oklahoma, and into the Texas panhandle over 350 miles (~560 km) to the north of the site (Figure 2.5.2-10). This pattern of seismicity is consistent with the pattern of seismicity observed in the EPRI-SOG earthquake catalog and was associated with the Southern Oklahoma Aulacogen by the ESTs.
- The updated catalog contains a concentration of seismicity in the New Madrid Seismic Zone (Figures 2.5.2-10 and 2.5.2-11) that has a spatial pattern consistent with seismicity patterns apparent in the EPRI-SOG earthquake catalog and observations made in the original EPRI-SOG study (Reference 2.5.2-16). In particular, the original and updated catalogs both demonstrate the presence of two northeast trending bands of seismicity in the New Madrid region offset by a third northwest-trending band of seismicity (Figure 2.5.2-11).
- The updated seismicity catalog does not show a pattern of seismicity different from that of the EPRI-SOG catalog that would suggest a new seismic source in addition to those included in the EPRI-SOG characterizations, or suggest a change to the existing geometry of the source zones (Figures 2.5.2-4 through 2.5.2-9).
- The updated catalog contains four earthquakes that have larger magnitudes than some of the lower-bound  $M_{max}$  values used by ESTs to characterize the source zones within which these earthquakes occurred. These earthquakes are the April 14, 1995 earthquake, the January 2, 1992 earthquake, the February 10, 2006 earthquake, and the September 10, 2006 earthquake (Figures 2.5.2-4 through 2.5.2-9). Three of these events require revisions to  $M_{max}$  values for some EPRI-SOG source zones, and the other earthquake partially motivates the development of a new source zone (see description in Subsection 2.5.2.4.3).
- The February 10, 2006  $E_{mb}$  5.5 earthquake reported in the updated catalog has been proposed by Nettles (Reference 2.5.2-50) to be related to gravity sliding on a low-angle normal fault at the edge of the continental shelf. This hypothesis suggests a potential association between seismicity in the Gulf of Mexico and normal growth faults at the edge of the continental shelf. However, no other events within the updated catalog have been

attributed to such mechanisms, and no additional research has been conducted to support or refute this hypothesis (e.g., [Reference 2.5.2-51](#)). The edge of the continental shelf (Figure 2.5.1-1) generally is encompassed by the various EST aerial source zones for the Gulf of Mexico region ([Figures 2.5.2-4 to 2.5.2-9](#)). As such, increases in  $M_{\max}$  to account for the February 10, 2006 Emb 5.5 earthquake, as well as the September 10, 2006 Emb 6.1 earthquake (see description in [Subsection 2.5.2.4.3](#)), adequately account for any potential association between earthquakes within the Gulf of Mexico and normal faults along the edge of the continental shelf.

#### 2.5.2.4 Probabilistic Seismic Hazard Analysis and Controlling Earthquakes

This section describes the probabilistic seismic hazard analysis (PSHA) conducted for the VCS site. Following the procedures outlined in RG 1.165 and RG 1.208, [Subsection 2.5.2.4.1](#) describes the basis for the PSHA, which is the 1989 EPRI study ([Reference 2.5.2-1](#)). [Subsection 2.5.2.4.2](#) presents sensitivity studies using an updated earthquake catalog that includes an analysis of historical earthquakes through 2007. The significance of new information on maximum magnitudes and on seismic source characterization is described in [Subsections 2.5.2.4.3 and 2.5.2.4.4](#), respectively. The effects of recent models to characterize earthquake ground motions in the CEUS are presented in [Subsections 2.5.2.4.5 and 2.5.2.4.6](#), which indicates the results of these revisions to the PSHA in the form of uniform hazard response spectra (UHRS).

##### 2.5.2.4.1 1989 EPRI Seismic Hazard Study

The 1989 EPRI study ([Reference 2.5.2-1](#)) was the starting point for probabilistic seismic hazard calculations. This follows the recommendation of RG 1.165. An underlying principle of this study was that expert opinion on alternative, competing models of earthquake occurrence (size, location, and rates of occurrence) and of ground motion amplitude and its variability should be used to weight alternative hypotheses. The result is a family of weighted seismic hazard curves from which mean and fractile seismic hazard can be derived.

The first task was to calculate seismic hazard using the assumptions on seismic sources and ground motion equations developed in the 1989 EPRI study to ensure that seismic sources were modeled correctly and that the software being used could accurately model the 1989 study assumptions. The VCS site was not modeled in the 1989 EPRI calculations, so a direct comparison of seismic hazard results cannot be made. However, results of the 1989 EPRI study are available for the STPEGS site, which lies about 60 miles (100 km) east-northeast of the VCS site. The results of this comparison depend on the EPRI team. [Table 2.5.2-13](#) compares the mean annual frequencies of exceedance calculated for the VCS site to published annual frequencies of exceedance from the 1989 EPRI project for the STPEGS site for the Bechtel team. All results are for hard rock conditions. The “% diff” row shows the percent difference of rock hazard calculated at the VCS site compared to the 1989 result for the STPEGS site. Comparisons are shown for peak ground acceleration (PGA) hazard for

the mean, 15th, median, and 85th fractile hazard curves. The current calculation indicates generally lower hazard, with up to –12 percent difference for the 15th fractile at 100 cm/sec<sup>2</sup>. The VCS site mean hazards are lower than those from the 1989 EPRI study for the STPEGS site by up to -11 percent. The lower overall hazard calculated for the VCS site is attributed to the ~60 miles (~100 km) difference in location and to the VCS site lying within a geographical degree cell that has lower seismicity than that for the STPEGS site.

A comparison of hazards for the Dames & Moore team is shown in [Table 2.5.2-14](#). In this case the current hazards are significantly lower than those obtained from the 1989 EPRI study for the STPEGS site. The seismicity files received from EPRI did not have seismicity parameters for the four geographical degree cells surrounding the site, so the current calculations indicate very low hazard; the 1989 EPRI study mean hazards for Dames & Moore are similar to those for Bechtel, so this difference is attributed to an undocumented assumption used in the 1989 EPRI study.

A comparison of hazards for the Law Engineering team is shown in [Table 2.5.2-15](#). For the Law team, the VCS site lies within source LAW-126, which has all values of  $M_{\max} < 5.0$ . The other Law source, LAW-124, has values of  $M_{\max} > 5.0$  with probability 0.7. Thus the current calculation indicates 15th fractile hazards that are effectively zero, but the 1989 EPRI results for the STPEGS site are on the order of  $10^{-10}$ . The difference in results is attributed to undocumented assumptions used in the 1989 EPRI study related either to the assumption of  $M_{\max}$  values or to assumptions on minimum hazard when no earthquakes with  $m_b > 5.0$  occur.

[Table 2.5.2-16](#) shows a comparison of hazards for the Rondout team. The mean hazards calculated for the VCS site are somewhat lower (up to –13 percent) than hazards for the STPEGS site from the 1989 EPRI study. This difference is attributed to the difference in location between the two sites. The 15th fractile hazard calculated for the VCS site is effectively zero, which is consistent with  $M_{\max} < 5.0$  assigned to source RND-51 with weight 0.2 (this is the only source used in the Rondout hazard calculation). The higher hazard reported in the 1989 EPRI study for the STPEGS site is attributed to undocumented assumptions regarding either  $M_{\max}$  values or the minimum hazard when no earthquakes with  $m_b > 5.0$  occur.

[Table 2.5.2-17](#) shows a comparison of hazards for the Weston team. For this comparison the current hazards calculated for the VCS site are generally lower than those reported for the 1989 EPRI study for the STPEGS site, by up to –12 percent. Mean hazards are lower by up to –9 percent. These differences are attributed to the difference in location between the two sites.

[Table 2.5.2-18](#) shows a comparison of hazards for the Woodward-Clyde team. For this comparison, the current hazards calculated for the VCS site are, in all cases, lower than those reported for the 1989 EPRI study for the STPEGS site by up to –17 percent, except for the 15th fractile hazard. The Woodward-Clyde team used a background source to represent hazard for the STPEGS site, and this

background source had an  $M_{\max}$  distribution that extended below 5.0 with probability 0.17. The difference in results for the 15th fractile is attributed to undocumented assumptions used in the 1989 EPRI study, related either to the assumption of  $M_{\max}$  values or to assumptions on minimum hazard when no earthquakes with  $m_b > 5.0$  occur. The difference in hazard results for other fractiles and for the mean hazard is attributed to the difference in location between the two sites.

Given that the nearest site for which comparisons can be made is about 60 miles (100 km) from the VCS site, that seismicity rates calculated for the geographical degree cell containing the VCS site is lower than calculated for the STPEGS site, and that there apparently were undocumented assumptions used to calculate the 1989 EPRI SOG seismic hazards, the comparisons shown in [Tables 2.5.2-13](#) through [2.5.2-18](#) are considered an acceptable agreement.

Several types of new information on the sources of earthquakes may require changes in inputs to PSHA, resulting in changes in the level of seismic hazard at the VCS site compared to what would be calculated based on the 1989 EPRI ([Reference 2.5.2-1](#)) evaluation. Seismic source characterization data and information that could affect the calculated level of seismic hazard include:

- Effects caused by an updated earthquake catalog and resulting changes in the characterization of the rate of earthquake occurrence as a function of magnitude for one or more seismic sources
- Changes in the characterization of the maximum magnitude for seismic sources
- Identification of possible new seismic sources that might contribute to hazard
- Additional revisions to the EPRI-SOG source model
- Changes to models used to estimate strong ground shaking and its variability in the CEUS

Possible changes to seismic hazard caused by changes in these areas are addressed in the following sections.

#### 2.5.2.4.2 **Effect of Updated Earthquake Catalog**

[Subsection 2.5.2.1](#) describes the development of an updated earthquake catalog. This updated catalog includes modifications to the EPRI evaluation by subsequent researchers, the addition of earthquakes that have occurred after completion of the EPRI evaluation development (post March 1985), and identification of additional earthquakes in the time period covered by the EPRI evaluation for the project region (1758 to 1984). In addition, the study region of the original EPRI catalog was extended to the south to include additional areas of the Gulf of Mexico that were outside the original study region. The impact of the new catalog information was assessed in two areas. First, investigation was made on the effect of the new earthquake data on earthquake recurrence

estimates within a several-hundred-kilometer region around the VCS site. Second, the new earthquake catalog was used to estimate seismicity parameters for EPRI team sources that extend into the Gulf of Mexico and adjacent on-shore regions that were not included in the original EPRI study region. This second step produced more complete estimates of seismicity parameters for coastal EPRI team sources than were previously available.

#### 2.5.2.4.2.1 Local Region

The effect of the updated earthquake catalog on earthquake occurrence rates in the local region around the VCS site was assessed by computing earthquake recurrence parameters for the test area shown in [Figure 2.5.2-12](#). This consisted of a rectangular area encompassing seismicity in the vicinity of the site, with dimensions 4 degrees latitude by 4 degrees longitude. These dimensions were chosen to encompass historical seismicity in the vicinity of the site because local events within 60 miles (100 km) of the site dominate the hazard (with the exception of the New Madrid seismic zone, which is treated separately). Note that the original EPRI study region did not extend south of latitude 28°N in the vicinity of the VCS site, as shown in [Figure 2.5.2-3](#), so the test area did not extend south of that latitude. The truncated exponential recurrence model was fit to historical seismicity data using the EPRI EQPARAM program, which uses the maximum likelihood technique. Earthquake recurrence parameters were first computed using the original EPRI catalog and periods of completeness, and then using the updated catalog and extending the periods of completeness to 2007, assuming that the probability of detection for all magnitudes is unity for the time period 1985 to 2007. The resulting earthquake recurrence rates are compared in [Figure 2.5.2-13](#) for the test area. The comparison shows that the extended earthquake catalog results in earthquake recurrence rates that are comparable to, and slightly higher than, rates from the original earthquake catalog.

On the basis of the comparison shown in [Figure 2.5.2-13](#), it is concluded that the earthquake occurrence rate parameters developed in the 1989 EPRI evaluation ([Reference 2.5.2-1](#)) in the vicinity of the VCS site and to the north are comparable to the rate parameters that would be estimated with an updated catalog. Conclusions for occurrence rate parameters to the south of the site are addressed in the following paragraph.

#### 2.5.2.4.2.2 Gulf of Mexico and Coastal Regions

The original 1989 EPRI ([Reference 2.5.2-1](#)) study region was limited to locations north of latitude 28°N (see [Figure 2.5.2-3](#)). [Subsections 2.5.2.1.3](#) and [2.5.2.1.5](#) describe how the seismicity catalog was extended for this region and how periods of complete reporting were developed. With these inputs, the EPRI EQPARAM software was run to calculate seismicity parameters (a- and b-values) for degree cells that were not available from the original analysis. As described above, this unavailability was a result of the original EPRI study region extending only as far south as latitude 28°N in the vicinity of the VCS site, as shown in [Figure 2.5.2-3](#). Therefore, no parameters were

calculated south of that line in the original study. The following EPRI team sources were recalculated in this way, to extend the availability of seismicity parameters.

Bechtel: source BZ1  
Dames & Moore: source 20  
Law Engineering: source 126  
Rondout: source 51  
Woodward-Clyde: source BG  
Weston Geophysical: source 107

The original EPRI team smoothing assumptions were used for each source. [Figure 2.5.2-14](#) compares mean seismic hazard curves for PGA calculated using the original EPRI seismicity parameters with hazard using the updated parameters for the above sources. The updated parameters indicate an increase in seismic hazard. As a result of this comparison, and because the updated sources were based on a more complete earthquake catalog (through 2007) that covered an extended region not included in the original 1989 EPRI ([Reference 2.5.2-1](#)) study, the updated parameters were used for seismic hazard calculations and are described below.

#### 2.5.2.4.2.3 New Madrid Region

As described in Subsection 2.5.1.1.4.3.5.6, paleoliquefaction studies have been conducted in the region of the 1811–1812 New Madrid, Missouri earthquakes since the EPRI-SOG study. These studies have identified several sequences of prehistoric earthquakes that allow estimation of recurrence intervals between major earthquakes in the region. These sequences have led to an estimated mean recurrence interval for large earthquakes in the NMSZ of approximately 500 years. This mean recurrence interval represents a higher activity rate than was estimated by the EPRI-SOG ESTs. Therefore, an updated NMSZ source model (see [Subsection 2.5.2.4.4.1](#)) is included in the seismic source interpretation for each EPRI-SOG EST. This updated model is consistent with that used for the COL application for STPEGS Units 3 & 4 ([Reference 2.5.2-28](#)).

#### 2.5.2.4.3 New Maximum Magnitude Information

Geologic and seismological data published since the EPRI-SOG study for the site region and more distant areas are summarized and described in Subsection 2.5.1, [2.5.2.1.2](#), and [2.5.2.2.2](#). A review of this data has shown that there is no basis for updating the  $M_{\max}$  distributions of the EPRI-SOG source zones used for the PSHA at the VCS site with the exception of ([Tables 2.5.2-7 through 2.5.2-12](#)):

- $M_{\max}$  distributions for GCSZs from five of the ESTs that are updated to reflect the occurrence of earthquakes within the Gulf of Mexico since the EPRI-SOG study ([Subsection 2.5.2.4.3.1](#)).

- The  $M_{\max}$  distribution for the Law Engineering New Mexico-Texas Block that is updated to reflect the occurrence of an earthquake since the EPRI-SOG study ([Subsection 2.5.2.4.3.2](#)).

In addition to these updates, the April 14, 1995 Emb 5.6 Alpine earthquake in west Texas ([Figures 2.5.2-4 through 2.5.2-9](#)) occurred within several source zones that have lower-bound  $M_{\max}$  values less than the magnitude of the earthquake ([Tables 2.5.2-7 through 2.5.2-12](#)). This earthquake could be interpreted as justification for updating the  $M_{\max}$  of these EPRI-SOG source zones. However, the event occurred along the eastern boundary of the RGR ([Reference 2.5.2-52](#)), an extensional tectonic province characterized by active seismicity related to normal faulting. Research has shown that the RGR influences the upper crustal state of stress well eastward of the topographically defined RGR (e.g., [References 2.5.2-53, 2.5.2-54, 2.5.2-55, 2.5.2-56, 2.5.2-57, 2.5.2-58, 2.5.2-59, and 2.5.2-60](#)). Partly based on these observations, some researchers believe that this earthquake is related to RGR tectonics ([Reference 2.5.2-61](#)).

None of the EPRI-SOG source zones that contain the Alpine earthquake were originally designed to characterize the seismotectonic behavior of the RGR ([Reference 2.5.2-16](#)), so it is not appropriate to account for the seismic hazard potential reflected by this earthquake by increasing the  $M_{\max}$  values of the host source zones. Instead, the potential effect of earthquakes similar to the Alpine event is accounted for with the development of a new source characterization of the RGR (see [Subsection 2.5.2.4.4.3](#)).

#### 2.5.2.4.3.1 $M_{\max}$ Updates for GCSZs

As described in [Subsection 2.5.2.1](#), two moderate magnitude earthquakes have occurred within the Gulf of Mexico since the EPRI-SOG study: the February 10, 2006 Emb 5.5 earthquake and the September 10, 2006 Emb 6.1 earthquake. These earthquakes occur within or very close to the GCSZs defined by five of the EPRI-SOG ESTs ([Figures 2.5.2-4 through 2.5.2-9](#)), and the lower-bound  $M_{\max}$  values of these source zones are lower than the magnitude of the earthquakes indicating a need to revise the  $M_{\max}$  distributions of the GCSZs. The updated source zone magnitudes for the VCS site are identical to those developed in the STPEGS 3 & 4 COLA in response to the same earthquakes ([Reference 2.5.2-28](#)). The methodology for the updated magnitudes is briefly summarized here.

The  $M_{\max}$  distribution for a particular GCSZ is updated when two conditions are met: (1) one or both of the 2006 moderate-magnitude earthquakes cannot be determined to have occurred outside the source zone with reasonable certainty, and (2) the observed Emb magnitude for the largest earthquake in the zone is greater than the lower-bound  $M_{\max}$  of the zone. These criteria result in updates to five of the six GCSZs  $M_{\max}$  distributions ([Table 2.5.2-19](#)). The updated distributions were developed following the original methodology used by the ESTs in the EPRI-SOG study ([References 2.5.2-1, 2.5.2-3, 2.5.2-16, 2.5.2-18, 2.5.2-24, 2.5.2-25, and 2.5.2-26](#)) as closely as

possible. Following the original EST methodology ensures consistency between the original distributions and those updated here using more recent seismicity data.

#### 2.5.2.4.3.1.1 Bechtel Group Gulf Coast Source Zone (Zone BZ1)

The Bechtel Group assigned  $M_{\max}$  values of 5.4, 5.7, 6.0, and 6.6 to the Gulf Coast source zone (zone BZ1) (Table 2.5.2-19). Because the Emb 5.5 and Emb 6.1 earthquakes from the updated catalog occur well within this zone (Figure 2.5.2-4), and because these magnitudes are greater than the lower-bound  $M_{\max}$  values for the source zone, the  $M_{\max}$  distribution for this source zone has been updated.

The updated  $M_{\max}$  values of 6.1, 6.4, and 6.6 with weightings of 0.1, 0.4, and 0.5 used here (Table 2.5.2-19) follow from Bechtel's methodology of defining  $M_{\max}$  distributions (Reference 2.5.2-19):

- The lower bound magnitude of the distribution is defined as the greater of either the largest observed earthquake magnitude within the zone, or  $m_b$  5.4.
- The next higher magnitude is 0.3 magnitude units greater than the minimum.
- The third magnitude is 0.6 magnitude units above the minimum.
- The fourth magnitude, and upper bound of the distribution, is  $m_b$  6.6.
- The weightings on the four  $M_{\max}$  values are 0.1, 0.4, 0.4, and 0.1, assigned consecutively from the minimum  $M_{\max}$  value.

If these guidelines result in an upper bound magnitude or magnitudes greater than  $m_b$  6.6, then the upper  $M_{\max}$  distribution is truncated at  $m_b$  6.6, and all weightings for magnitudes greater than or equal to 6.6 are summed and collapsed onto the magnitude 6.6 upper bound.

#### 2.5.2.4.3.1.2 Dames & Moore South Coastal Margin (Zone 20)

Dames & Moore assigned  $M_{\max}$  values of 5.3 and 7.2 to the South Coastal Margin source zone (zone 20) (Table 2.5.2-19). The Emb 5.5 earthquake from the updated catalog is inside this zone, and the Emb 6.1 earthquake is well outside the zone (Figure 2.5.2-5). Because the Emb 5.5 event is within the source zone and has a magnitude larger than the lower bound  $M_{\max}$  value, the  $M_{\max}$  distribution for this source zone has been revised.

The methodology used to determine the  $M_{\max}$  distribution for the South Coastal Margin zone in the EPRI 1989 model does not provide a means of updating the lower-bound 5.3  $M_{\max}$  value to reflect the occurrence of the Emb 5.5 earthquake (References 2.5.2-16 and 2.5.2-18). Given the lack of a

well-documented methodology to follow, the  $M_{\max}$  distribution used here results from increasing the lower-bound  $M_{\max}$  to match the magnitude of the observed Emb 5.5 earthquake while maintaining the same upper bound and weightings of the original  $M_{\max}$  distribution for the source zone. The updated  $M_{\max}$  values are  $m_b$  5.5 and 7.2 with weightings of 0.8 and 0.2, respectively (Table 2.5.2-19).

#### 2.5.2.4.3.1.3 Law Engineering South Coastal Block (Zone 126)

Law Engineering assigned  $M_{\max}$  values of 4.6 and 4.9 to the South Coastal Block source zone (zone 126) (Table 2.5.2-19). The Emb 5.5 earthquake is 22 miles (36 km) outside of the source zone, and the Emb 6.1 earthquake is approximately 100 miles (160 km) outside of the source zone (Figure 2.5.2-6). The Emb 6.1 earthquake was well recorded and clearly lies outside the source zone (Reference 2.5.2-62). The Emb 5.5 earthquake was less well recorded (References 2.5.2-63 and 2.5.2-64), and attempts at relocating the event have resulted in significant (tens of kilometers) variation in the position of the earthquake epicenter (References 2.5.2-51, 2.5.2-63, and 2.5.2-65). Although the published location of the Emb 5.5 earthquake is outside the South Coastal Block source zone, the earthquake is conservatively considered to have occurred within the source zone given the uncertainty in the epicentral location of the earthquake. As such, the  $M_{\max}$  distribution for the source zone is updated to reflect this earthquake.

The updated  $M_{\max}$  values of 5.5 and 5.7, adopted here (Table 2.5.2-19) are derived using Law Engineering's methodology for developing  $M_{\max}$  distributions, as follows (Reference 2.5.2-16):

- The lower bound  $M_{\max}$  is the magnitude of the maximum observed earthquake in the zone.
- The upper bound  $M_{\max}$  magnitude defined by Law Engineering for regions with earthquakes occurring within 6.2 miles (10 km) of the surface is  $m_b$  5.7.

Weights for the original  $M_{\max}$  distribution (0.9 on the lower bound  $M_{\max}$  and 0.1 on the upper bound  $M_{\max}$ ) (Reference 2.5.2-18) are retained (Table 2.5.2-19).

#### 2.5.2.4.3.1.4 Rondout Associates Gulf Coast to Bahamas Fracture Zone (Zone 51)

Rondout Associates assigned  $M_{\max}$  values of 4.8, 5.5, and 5.8 to the Gulf Coast to Bahamas Fracture Zone source zone (zone 51) (Table 2.5.2-19). Because both the Emb 5.5 and Emb 6.1 earthquakes from the updated catalog occur well within this zone (Figure 2.5.2-7), and because these magnitudes are greater than the lowest  $M_{\max}$  values for the source zone, the  $M_{\max}$  distribution for this source zone has been updated.

The updated  $M_{\max}$  values of 6.1, 6.3, and 6.5 with weightings of 0.3, 0.55, and 0.15, respectively, used here (Table 2.5.2-19) follow from reclassifying the source zone as one capable of producing moderate earthquakes instead of the original classification of the source zone as one only capable of

producing smaller than moderate earthquakes ([Reference 2.5.2-16](#)). The original Rondout  $M_{\max}$  distribution for moderate earthquake source zones is 5.2, 6.3, and 6.5 with weightings of 0.3, 0.55, and 0.15, respectively. The updated  $M_{\max}$  distribution follows this distribution with the exception of an increase in the lower bound of the distribution to 6.1 to account for the observed Emb 6.1 earthquake within this zone.

#### 2.5.2.4.3.1.5 Weston Geophysical Corporation Gulf Coast Source Zone (Zone 107)

Weston Geophysical Corporation assigned  $M_{\max}$  values of 5.4 and 6.0 to the Gulf Coast source zone (zone 107) ([Table 2.5.2-19](#)). Both the Emb 5.5 and Emb 6.1 earthquakes from the updated catalog occur well within this zone ([Figure 2.5.2-8](#)). Because these magnitudes are greater than the original  $M_{\max}$  values for the source zone, the  $M_{\max}$  distribution for this source zone has been revised.

Weston Geophysical Corporation's ([Reference 2.5.2-16](#)) methodology for defining  $M_{\max}$  is based on developing discrete distributions for the probability of  $M_{\max}$  being a particular value. For the Gulf Coast source zone, these  $M_{\max}$  values and probabilities determined by the Weston Geophysical Corporation EST are: 3.6 (0.04628), 4.2 (0.11982), 4.8 (0.27542), 5.4 (0.34415), 6.0 (0.16169), 6.6 (0.04461), and 7.2 (0.00553) ([Reference 2.5.2-16](#)). Conservatively applying the Weston Geophysical Corporation's methodology, this discrete probability distribution is truncated at the magnitude that is closest to, yet greater than, the maximum observed earthquake within the source zone. For this study the distribution is truncated at 6.6 because the Emb 6.1 earthquake occurred within the source zone, and the next highest discrete magnitude in the distribution is 6.6. The truncated distribution is then renormalized so that the sum of all the probabilities is 1.0. The final  $M_{\max}$  values are the truncated distribution, and the weights are the renormalized probabilities.

#### 2.5.2.4.3.1.6 Woodward-Clyde Consultants Central U.S. Background Source Zone (Zone B43)

As described in [Subsection 2.5.2.2.1.6](#), Woodward-Clyde does not have any source zones within the site region, but a new source zone is constructed for the VCS site to represent the Central U.S. Background zone (see [Subsection 2.5.2.4.5.2](#)). The Emb 5.5 and Emb 6.1 earthquakes are well outside of this zone ([Figure 2.5.2-9](#)), so the  $M_{\max}$  distribution for this source zone is not revised.

#### 2.5.2.4.3.2 Law Engineering New Mexico-Texas Block

The Law Engineering New Mexico-Texas block (zone 124) is characterized by a  $M_{\max}$  distribution of  $m_b$  4.9 (0.3), 5.5 (0.5), and 5.8 (0.2) with weights shown in parentheses ([Table 2.5.2-9](#)). On January 2, 1992, an earthquake with an Emb magnitude of 5.0 occurred in the southeast corner of New Mexico. This event is located within the boundaries of the Law Engineering New Mexico-Texas block (zone 124) ([Figure 2.5.2-6](#)). Because the Emb magnitude of this event is greater than the lower-bound  $M_{\max}$  for this zone, the  $M_{\max}$  distribution is revised.

The Law Engineering methodology for developing the New Mexico-Texas block  $M_{\max}$  distribution is not explicitly stated within the EPRI-SOG study documentation ([Reference 2.5.2-16](#)). However, the EPRI-SOG for Law Engineering ([Reference 2.5.2-16](#)) does indicate that the 5.8 upper-bound  $M_{\max}$  is based on observations of seismicity within the zone, and that the lower-bound 4.9 is the maximum observed earthquake magnitude within the zone ([Reference 2.5.2-16](#)). Based on these statements, the  $M_{\max}$  distribution is updated by increasing the lower-bound  $M_{\max}$  value to 5.0 and maintaining the remaining  $M_{\max}$  values and original weights.

#### 2.5.2.4.4 New Seismic Source Characterizations

Geologic, geophysical, and seismological information developed since the EPRI-SOG study ([Reference 2.5.2-16](#)) was reviewed to identify seismic sources that were either not included in the original EPRI-SOG study or were included but require new characterizations based on more recent information or data. New seismic source characterizations are developed for three tectonic features with the potential to impact seismic hazard at the VCS site. These features are the NMSZ, the Meers fault, and the RGR ([Figure 2.5.2-10](#)). The development of these characterizations is described in [Subsections 2.5.2.4.4.1 through 2.5.2.4.4.3](#) and is based on post-EPRI-SOG information reviewed in [Subsection 2.5.1.1.4.3.5](#).

##### 2.5.2.4.4.1 New Madrid Seismic Zone

The NMSZ extends from southeastern Missouri to southwestern Tennessee and is located approximately 620 miles (1000 km) northeast of the VCS site ([Figure 2.5.2-10](#)). The NMSZ produced a series of large-magnitude earthquakes between December 1811 and February 1812 ([Reference 2.5.2-66](#)). [Subsection 2.5.1.1.4.3.5.6](#) presents a detailed description of the NMSZ. In brief, several post-EPRI-SOG studies demonstrate that the source parameters for geometry,  $M_{\max}$ , and recurrence of  $M_{\max}$  in the New Madrid region need to be updated to capture the current understanding of this seismic source ([References 2.5.2-33, 2.5.2-66, 2.5.2-67, 2.5.2-68, 2.5.2-69, and 2.5.2-97](#)).

The updated New Madrid seismic source model used for the VCS site is the same as that described in the Tennessee Valley Authority Bellefonte Nuclear Site COLA ([Reference 2.5.2-29](#)), itself a simplification of the NMSZ model developed for the Exelon Generation Company ESP site near Clinton, Illinois ([Reference 2.5.2-70](#)) ([Figure 2.5.2-15](#)). This source model accounts for new information on recurrence intervals for large earthquakes in the New Madrid area, for recent estimates of possible earthquake size on each of the active faults, and for the possibility of clustered

earthquake behavior. Within this model, three faults are identified in the NMSZ, each with two alternative geometries as follows (Figure 2.5.2-16):

Fault	Geometry
Blytheville	Blytheville arch/Bootheel lineament Blytheville arch/Blytheville fault zone
Northern	New Madrid north New Madrid north with extension
Reelfoot	Reelfoot central section Reelfoot full length

Also, earthquakes are treated as characteristic events in terms of magnitudes, with a weighted range of magnitudes for each fault (Figure 2.5.2-15). These magnitudes represent the centers of characteristic magnitude distributions that extend  $\pm 0.25$  moment magnitude units above and below the indicated magnitude.

Seismic hazard is calculated considering the possibility of clustered earthquake occurrences. The modeling of earthquake clusters in the NMSZ has undergone considerable study, and this model will continue to evolve as further field evidence of paleo-earthquakes is found and analyzed. In the Clinton cluster model for multiple earthquake occurrences, the possibility of three clustered earthquakes is taken into account, as is the possibility of clustered earthquakes on two of the faults (but not the third), or the possibility of two faults generating a characteristic earthquake magnitude and the third fault generating a smaller magnitude. The cluster model used for the Bellefonte COLA (Reference 2.5.2-29) is a conservative simplification of the Clinton model (Reference 2.5.2-70) in that hazard is computed assuming that all clustered events generate earthquakes on each of the three faults and that the magnitudes of those events correspond to the characteristic magnitude distribution.

Consistent with the Clinton model (Reference 2.5.2-70), the NMSZ faults used for the Bellefonte COLA are assumed to be vertical and extend from the surface to 12 miles (20 km) depth, and a finite rupture model is used to represent an extended rupture on all faults. An additional simplification was made in that only the preferred geometry of each fault is used. This is justified because of the large distance between the VCS site and the NMSZ (over 600 miles [965 km]) and the small differences between the preferred and alternative geometries. This simplification allows efficiency in calculations while providing an accurate estimate of seismic hazard.

#### 2.5.2.4.4.2 Meers Fault

The Meers fault is over 400 miles (640 km) from the VCS site. Two surface-rupturing earthquakes along the fault have occurred in the Holocene (Reference 2.5.2-71), making it one of the closest capable faults to the VCS site. The potential for Quaternary events on the Meers fault, and in

particular these two Holocene events, was identified in research (see summary in Subsection 2.5.1.1.4.3.5.4) ([References 2.5.2-31](#), [2.5.2-44](#), [2.5.2-72](#), and [2.5.2-73](#)) that post-dated the development of the EPRI-SOG source models ([Reference 2.5.2-16](#)); thus, this Holocene activity was not taken into account in the EPRI-SOG source models. A new source characterization of the Meers fault is developed for its use in determining whether the Meers fault contributes to hazard at the VCS site.

The seismic source characterization of the Meers fault is developed for the VCS site following the SSHAC guidelines for a Level 2 study ([Reference 2.5.2-27](#)) and based on a thorough review of existing literature and consultation with experts familiar with the Meers fault. As such, the new characterization attempts to represent the legitimate range of technically supportable interpretations of the seismic capability of the Meers fault among the informed technical community. A summary of the current state of knowledge regarding the tectonics and seismic capability of the Meers fault, as determined through the literature review and elicitation of expert opinion, is presented in Subsection 2.5.1.1.4.3.5.4, and the source model developed from this information is presented below.

As described in [Subsection 2.5.2.2.2.4](#), the USGS has developed a seismic source characterization of the Meers fault for use in the USGS National Seismic Hazard Maps. As stated in that subsection, the USGS does not use a formal expert elicitation process and does not explicitly attempt to represent the full uncertainty of source characterizations. However, the source models are developed from the range of published literature, and source characterizations are discussed in regional working groups so the USGS source model for the Meers fault is deemed a good base model on which to base the updated Meers fault characterization. These modifications result in a source model that better reflects uncertainty in the return periods and magnitude of characteristic earthquakes.

The USGS characterization of the Meers fault for the 2002 National Seismic Hazard Maps is summarized in the Frankel et al. 2002 study ([Reference 2.5.2-33](#)). The 2002 characterization of the Meers fault was used instead of the characterization from the 2008 hazard maps ([Reference 2.5.2-34](#)) because the documentation for the 2008 maps was not available when the model presented here was developed. There are no changes in the USGS Meers fault source model between 2002 and 2008 that impact the portion of that model adopted here. The USGS characterization of the Meers fault is a reasonable representation of the modern state of knowledge regarding the seismic capability of the fault. However, there is little epistemic uncertainty built into the USGS characterization, and where it is included there is no physical explanation provided by the USGS for the uncertainty values. The updated model developed here considers uncertainty in the characteristic magnitude, characteristic return period, and fault length that are not explicitly included in the USGS source model.

#### 2.5.2.4.4.2.1 Fault Location and Length

The surface trace of the Meers fault used in the updated source model is based on a simplified version of the USGS source model trace that is a discretized version of the fault trace from the USGS Quaternary Fault and Fold Database ([Reference 2.5.2-71](#)). The simplification used here ([Table 2.5.2-20](#)) uses the two endpoints of the 2002 USGS source model ([Reference 2.5.2-33](#)). The additional fault trace detail provided by the two additional points in the USGS model is insignificant to calculating seismic hazard at the VCS site given the distance between the site and fault.

The distance between the two endpoints of the fault trace is approximately 23 miles (37 km), representing the maximum expected length of the Meers fault Holocene rupture. The western 16 miles (26 km) of the fault is positively associated with the Holocene rupture given the mapping of the trace on aerial photographs, the continuous nature of the fault scarp over those 16 miles (26 km), and the trenching studies at different locations along the fault ([References 2.5.2-31](#), [2.5.2-44](#), [2.5.2-48](#), [2.5.2-49](#), and [2.5.2-71](#)). The easternmost portion of the fault scarp that extends the possible length of the Holocene scarp to 23 miles (37 km) was identified in low-sun-angle aerial photography and is more subtle and discontinuous ([References 2.5.2-48](#) and [2.5.2-49](#)). Field investigations of this easternmost extent of the scarp have not been conducted to determine if it is from the same Holocene events as is the western extent of the scarp because the area is within the U.S. Army's Fort Sill artillery range. To account for this uncertainty in the length of the Holocene surface ruptures, characteristic magnitudes for the fault are calculated using both 16 and 23 miles (26 and 37 km). However, to simplify the updated Meers fault source model, the location of the fault trace does not include this uncertainty.

It should be noted that one researcher ([Reference 2.5.2-74](#)) suggests that Quaternary activity on the Meers fault extends 19 miles (30 km) to the northwest of the westernmost extent of the fault traces used for the VCS site. Cetin ([Reference 2.5.2-74](#)) proposes this extension based on “displaced terrace deposits of Pleistocene age, displaced, buried and/or overthickened soil horizons, fault-related colluvium deposits (colluvial wedges) found near and only on the downthrown side of the fault, active seepage near the fault, deflection of stream alignments and the land use pattern along the fault.” However, as is summarized by Wheeler and Crone ([Reference 2.5.2-75](#)), the evidence presented by Cetin ([Reference 2.5.2-74](#)) for Quaternary faulting is inconclusive, has not been confirmed by other researchers who have attempted to visit the same field sites as Cetin ([Reference 2.5.2-74](#)), and has never been presented as peer-reviewed research. As such, this potential northwest extension of the capable Meers fault is not considered to be within the legitimate range of technically supportable interpretations.

#### 2.5.2.4.4.2.2 Characteristic Magnitude

Previous studies summarized in Subsections 2.5.1.1.4.3.5.4 and [Subsection 2.5.2.2.2](#) have characterized the Holocene events on the Meers fault with  $M_{\max}$  on the order of  $M_w$  7.0 ( $m_b$  6.9).

Characteristic magnitudes for the updated Meers fault source model are based on using the Holocene events identified on the Meers fault as proxies for the fault's characteristic magnitude. Magnitudes for the Holocene events are estimated using the empirical relationships of Wells and Coppersmith ([Reference 2.5.2-76](#)) between observed earthquake magnitude and characteristics of the earthquake rupture (e.g., surface rupture length, rupture area, and maximum surface displacement). For each of the empirical relationships described below, the “all faults” regression of Wells and Coppersmith ([Reference 2.5.2-76](#)) is used to estimate characteristic magnitudes.

### **Magnitude from Surface Rupture Length**

Mapping of the Meers fault scarp on aerial photographs by Ramelli et al. ([Reference 2.5.2-49](#)) and other researchers ([Reference 2.5.2-71](#)) indicates that the scarp associated with the Holocene events is between 16 and 23 miles (26 and 37 km) long. Because of this uncertainty in the length of the Holocene surface rupture, both 16 and 23 miles (26 and 37 km) are used with the regressions of Wells and Coppersmith (1994) ([Reference 2.5.2-76](#)) to estimate magnitude. Using the regression between rupture length and moment magnitude for all faults, estimated characteristic event magnitudes are:

- $M_w$  6.7 ( $m_b$  6.7) for a 16-mile (26-km) long rupture; and
- $M_w$  6.9 ( $m_b$  6.9) for a 23-mile (37-km) long rupture.

### **Magnitude from Rupture Area**

Rupture area for the Holocene ruptures of the Meers fault is estimated using the length of the scarp and the downdip width of the rupture, itself a function of the fault dip and depth of rupture bottom. The lengths of 16 and 23 miles (26 and 37 km) from above are used for rupture length. The dip of the Meers fault is taken from USGS source model, with an 89 degree dip to the southwest ([Reference 2.5.2-33](#)). The near-vertical orientation of the fault is supported by exposures of the fault in trenches, but the dip of the fault at depth is poorly constrained ([Reference 2.5.2-77](#)). The depth of the rupture bottom is taken as 9 to 12 miles (15 to 20 km) based on Luza and Lawson ([Reference 2.5.2-78](#)) that reports there is no indication of earthquakes occurring within Oklahoma at greater depths. Using the regressions of Wells and Coppersmith ([Reference 2.5.2-76](#)) between rupture area and moment magnitude for all faults results in the following values:

- $M_w$  6.6 ( $m_b$  6.7) for the minimum rupture area of 9 miles x 16 miles = 144 miles<sup>2</sup> (15 km x 26 km = 390 km<sup>2</sup>); and
- $M_w$  6.9 ( $m_b$  6.9) for the maximum rupture area of 12 miles x 23 miles = 276 miles<sup>2</sup> (20 km x 37 km = 740 km<sup>2</sup>).

## Magnitude from Maximum Surface Displacement

The best estimates of surface displacement per event on the Meers fault come from the 1993 study by Swan et al. ([Reference 2.5.2-31](#)) reviewed in Subsection 2.5.1.1.4.3.5.4, and these estimates are used with the regressions of Wells and Coppersmith ([Reference 2.5.2-76](#)) to estimate characteristic magnitudes. The regressions of Wells and Coppersmith ([Reference 2.5.2-76](#)) were determined using net surface displacements, and because the Meers fault exhibits oblique slip, there is only one combined observation of vertical and lateral displacement with which net displacement can be determined (7.5 feet or 2.29 meters per event). However, Swan et al. ([Reference 2.5.2-31](#)) report a best estimate of vertical displacement at a different location that is greater than this net displacement (8.5 feet or 2.6 meters per event). Both of these displacement values are used to estimate characteristic magnitudes for the Meers fault.

The regression on maximum surface displacement, and not the regression for the average surface displacement, of Wells and Coppersmith ([Reference 2.5.2-76](#)) is used to estimate magnitude because the average surface displacement regression is not appropriate for the displacement data available for the Meers fault. Wells and Coppersmith ([Reference 2.5.2-76](#)) explicitly state that the regression for maximum displacement was determined using the maximum reported displacement for an event, while the regressions for average displacement were done on faults where an average displacement was calculated from either an extensive study of the entire surface rupture or a minimum of 10 displacement measurements. The data available for the Meers fault is a maximum reported displacement and not an along-fault average.

Using the displacements described above, results in the following magnitude estimates:

- $M_w$  7.0 ( $m_b$  6.9) from a maximum vertical displacement of 8.5 feet (2.6 meters); and
- $M_w$  7.0 ( $m_b$  6.9) from a maximum net displacement of 7.5 feet (2.29 meters).

## Final Magnitude Distribution

The final characteristic magnitude distribution used for the Meers fault is:  $M_w$  6.7 ( $m_b$  6.7),  $M_w$  6.85 ( $m_b$  6.82), and  $M_w$  7.0 ( $m_b$  6.9) with weights 0.2, 0.6, and 0.2, respectively.  $M_w$  6.7 ( $m_b$  6.7) is chosen as the lower bound instead of  $M_w$  6.6 ( $m_b$  6.7) because it is not considered likely that only the 16 miles (26 km) of the Meers fault scarp is related to the Holocene ruptures.  $M_w$  7.0 ( $m_b$  6.9) is chosen as the maximum bound because it is the maximum estimated magnitude of any regression and it is roughly equivalent to other estimates of characteristic earthquake magnitude for the fault (e.g., [References 2.5.2-33](#) and [2.5.2-31](#)). The weighting of the distribution reflects the opinion that the best estimates of magnitude come from regressions on surface rupture length and rupture area.

#### 2.5.2.4.4.2.3 Characteristic Return Period

Epistemic uncertainty in return periods for characteristic earthquakes on the Meers fault is implemented through return period branches on a logic tree (Figure 2.5.2-17). The data presented by Swan et al. (Reference 2.5.2-31) on the timing of Meers earthquakes suggests that there have been two Holocene events preceded by a long period (greater than 200,000 years) of inactivity, indicating that the Meers fault exhibits clustered earthquake behavior. The initial branch of the logic tree represents uncertainty in whether the Meers fault is in an earthquake cluster.

Weightings of 0.9 and 0.1 are used for the logic tree branches describing the Meers fault as in an earthquake cluster or between earthquake clusters, respectively. High weighting on the “in earthquake cluster” conservatively reflects the observation that there is no information to suggest that the Meers fault is not in a cluster; insufficient time has elapsed since the most recent event to conclude that there is a moderate possibility that the period of increased Holocene activity has passed. Return periods for the inter-cluster branch are based on the work of Swan et al. (Reference 2.5.2-31) that estimates a minimum period of inactivity before the Holocene ruptures of 200,000 to 500,000 years. Based on this observation, return period branches of 500,000, 350,000, and 200,000 years with weights of 0.2, 0.6, and 0.2, respectively, are used for the inter-cluster branch.

Return periods for the intra-cluster branch are based on the elapsed time since the oldest Holocene event and the observation of two earthquakes during that time span. Assuming that the Meers fault is currently in an earthquake cluster, this method results in a reasonable estimate of the intra-cluster return period. Swan et al. (Reference 2.5.2-31) report two dates to constrain the maximum age of the oldest Holocene rupture: sample PITT-0477 with a calibrated age of 3397 years before present (B.P.; age before 1950, which is the conventional reference year for carbon dating) and sample PITT-0373 with a calibrated age of 2918 years B.P. The mean of these two ages is taken as the most-probable maximum age of the event, and half that age (1580 years) is taken as the most-probable maximum return period for intra-cluster events. Swan et al. (Reference 2.5.2-31) also report four ages that they believe best constrain the minimum age of the oldest Holocene event: PITT-0370 with a calibrated age of 1942 years B.P., PITT-0369 with a calibrated age of 1610 years B.P., PITT-0378 with a calibrated age of 1912 years B.P., and PITT-0478 with a calibrated age of 2093 years B.P. The mean of these four ages is taken as the most-probable minimum age of the event, and half the age (950 years) is taken as the most-probable minimum return period for intra-cluster events.

A direct inter-event return period for the two Holocene events can also be determined from ages reported by Swan et al. (Reference 2.5.2-31) that constrain the bounds of the oldest and youngest Holocene events. The return period determined using the time elapsed between the mean upper-bound age of the oldest Holocene event and the mean lower-bound age of the youngest Holocene event is 2000 years. The return period determined using the time elapsed between the mean lower-

bound age of the oldest Holocene event and the mean upper-bound age of the youngest Holocene event is 300 years. The large range in return period determined using this methodology is due to the compounded uncertainty from using the dates constraining both Holocene events as opposed to just the time elapsed since the oldest event. The 300-year lower-bound return period is unrealistic since it would imply significantly more events between the oldest Holocene event and the present time than the two observed. For this reason, and because the plausible range of return periods determined from the inter-event period is captured in the return periods previously described, the inter-event period is not used to estimate return periods.

The most probable minimum and maximum return periods are both given equal weight of 0.2 in the logic tree for the return period of intra-cluster events (Figure 2.5.2-17). The remaining 0.6 weight is given to the median of the most-probable minimum and maximum return periods (1265 years). This weighting reflects the belief that it is most likely for the intra-cluster return period to be somewhere between the minimum and maximum bounds.

#### 2.5.2.4.4.3 Rio Grande Rift

The RGR is a north-south-trending continental rift system recognized to extend from central Colorado through New Mexico, Texas, and into northern Mexico (References 2.5.2-57, 2.5.2-79, 2.5.2-80, and 2.5.2-81). The RGR is generally characterized by north- to north-northwest-trending grabens centered on a broad topographic high, a well-defined gravity low, elevated heat flow, and a tensile stress regime (e.g., References 2.5.2-53, 2.5.2-56, 2.5.2-57, and 2.5.2-58) (see description in Subsection 2.5.1.1.4.3.5.5). At the time of the EPRI-SOG study, relatively little was known about the seismogenic potential of faults within the RGR, and only the Weston EST explicitly included the RGR as a seismic source zone (Reference 2.5.2-16). Other ESTs either (1) did not extend their source model boundaries to include the RGR, or (2) included the RGR in large background source zones (Reference 2.5.2-16). Research post-dating the EPRI study has documented previously unrecognized late Quaternary fault activity within parts of the RGR (e.g., References 2.5.2-82, 2.5.2-83, 2.5.2-84, 2.5.2-85, 2.5.2-86, 2.5.2-87, and 2.5.2-88), as well as evidence that the RGR extends into western Texas and northern Mexico (References 2.5.2-89 and 2.5.2-56). These post-EPRI-SOG studies indicate that the RGR is a zone of distinct and elevated tectonic activity relative to other regions at a similar distance from the VCS site. Therefore, despite the greater than 400-mile (640-km) distance between the RGR and the VCS site (Figure 2.5.2-10), RGR sources are included in a screening study.

Two independent and complementary seismic characterizations of the RGR are developed. Because of the considerable distance between the RGR and the VCS site and the intent to use the sources for screening, the source characterizations are relatively simple. The first model of the RGR represents discrete faults within the RGR that have been characterized within the USGS National Seismic Hazard Map program (Reference 2.5.2-33). The second model of the RGR is a conservative

simplification of any RGR faults that may extend further south than those defined in the USGS hazard maps.

#### 2.5.2.4.4.3.1 RGR Fault Source Characterization

The fault source characterization of the RGR is based on a conservative simplification of the USGS representation of RGR faults in the 2002 version of the National Seismic Hazard Maps ([Reference 2.5.2-33](#)). The 2002 characterizations are used instead of the more recent 2008 characterizations ([Reference 2.5.2-34](#)) because the final 2008 characterizations were not available at the time of the screening study. Changes made to the RGR source characterizations for the 2008 maps were minor ([Reference 2.5.2-34](#)), relative to the distance between the VCS site and the RGR, and are not expected to affect the results of the screening study.

For the National Seismic Hazard Maps, the USGS characterizes the seismic behavior of 41 RGR faults ([Table 2.5.2-21](#) and [Figure 2.5.2-10](#)) based on the information within the USGS compilation of Quaternary folds and faults within the United States ([Reference 2.5.2-90](#)). As with all USGS source characterizations, a formal expert opinion elicitation process was not followed and the characterization is not designed to capture the full uncertainty of source characterizations. However, the source models are developed from published literature, and source characterizations are discussed in regional working groups. As such, the USGS source models are an adequate characterization of the RGR faults for the VCS screening study.

The USGS characterization includes alternative models of fault recurrence behavior including truncated Gutenberg-Richter and characteristic earthquake relationships. For the VCS site, the USGS characterization is simplified by assuming only a characteristic earthquake recurrence relationship parameterized by the characteristic recurrence rate and characteristic earthquake magnitude taken from the USGS parameterization of the faults ([Reference 2.5.2-33](#)). Uncertainty is added to the characteristic magnitudes using a magnitude distribution of  $\pm 0.2$  magnitude units about the USGS-reported magnitude with weightings of 0.2, 0.6, and 0.2 for the lowest to highest magnitudes. The surface trace of each fault is simplified from the USGS description by using only the endpoints of the fault trace. [Table 2.5.2-22](#) summarizes this model. These characterizations are implemented as vertical line sources extending to 9 miles (15 km) depth. Given the large distance between the RGR faults and the site, details of the geometry do not have a significant impact on ground motions.

#### 2.5.2.4.4.3.2 RGR Southern Extension Characterization

The fault source characterization of the RGR by the USGS represents the seismic hazard only from RGR faults as far south as western Texas ([Figure 2.5.2-10](#)). In addition to these faults the RGR is thought to extend into eastern Mexico, raising the potential for hazard at the site from the RGR within Mexico. However, there is very little information on the presence or activity of Quaternary faults in

eastern Mexico related to the RGR ([References 2.5.2-56, 2.5.2-57, 2.5.2-79, 2.5.2-80, 2.5.2-81, and 2.5.2-89](#)). Because of the uncertainty in the location and activity of capable RGR-related faults in Mexico, a simplified and conservative source model for the RGR is developed for use in the screening study. The simplified model of the RGR is based on defining the easternmost plausible extent of the RGR in Mexico and southernmost Texas and applying the bulk behavior of the RGR faults characterized in the United States to a set of hypothetical, or simplified, faults along this easternmost extent of the RGR. This model is conservative because: (1) there have been no RGR related faults identified as far east as the hypothetical faults used here, and (2) it is unlikely that potential RGR-related faults within Mexico have as high of recurrence rates or magnitudes as the those in the United States given the more pronounced topographic expression of active extension evident with the RGR-related faults in the United States.

The easternmost possible extent of the RGR in Texas and Mexico is based on an estimate of the easternmost position of the large-scale lithospheric expression (elevated topography, long-wavelength gravity anomaly, elevated heat flow, tensile stress regime, region of thinned crust, and elevated mantle) and topographic expression (range-front-bounded basins) of the RGR (e.g., [References 2.5.2-53, 2.5.2-54, 2.5.2-55, 2.5.2-56, 2.5.2-57, 2.5.2-58, 2.5.2-59, and 2.5.2-60](#)) ([Figure 2.5.2-10](#)). The exact position of the easternmost extent defined here is based on the location of thinned crust related to the RGR ([Reference 2.5.2-55](#)), the relationship between topography and gravitational potential energy thought to drive RGR-related deformation ([References 2.5.2-54, 2.5.2-91, 2.5.2-92, and 2.5.2-93](#)), the extent of the region of tensile stress related to the RGR ([References 2.5.2-54 and 2.5.2-60](#)), and the location of RGR-related earthquakes ([References 2.5.2-52, 2.5.2-61, and 2.5.2-94](#)). Essentially, the easternmost extent of each of these features roughly correlates with the elevated topography of the RGR that decays eastward to the coastal plains, so this topographic and physiographic transition to the coastal plains is used to delineate the easternmost extent of the RGR ([Figure 2.5.2-10](#)). The southernmost possible extent of the RGR is interpreted to terminate to the south at the Sierra Madre Oriental, a Laramide fold-and-thrust belt with no evidence of extensional faulting ([References 2.5.2-95 and 2.5.2-96](#)). The northern end of the easternmost extent is taken as the southernmost RGR fault characterized by the USGS ([Reference 2.5.2-33](#)).

The source characterizations of the hypothetical RGR faults in Mexico are each identical and based on the bulk characteristics of RGR-related faults within the USGS National Seismic Hazard Map database ([Reference 2.5.2-33](#)). The characteristic magnitude and return period distributions for this model are developed by assuming the 41 characteristic magnitudes and return periods defined by the USGS for RGR faults represent the distribution of characteristic earthquake magnitudes and return periods for the southern extent of the RGR in Mexico. As such, the observed distributions are used to derive simplified representative distributions for use in the updated characterization.

The characteristic magnitudes for RGR faults defined by the USGS ([Reference 2.5.2-33](#)) are shown in [Table 2.5.2-21](#) and vary between  $M_w$  6.1 ( $m_b$  6.3) and  $M_w$  7.5 ( $m_b$  7.2), with a mean magnitude of  $M_w$  6.9 ( $m_b$  6.9). Approximately 10 percent of observed magnitudes are between  $M_w$  6.1 and 6.5 ( $m_b$  6.3 and 6.6), 30 percent are between  $M_w$  6.5 and 6.8 ( $m_b$  6.6 and 6.8), 40 percent are between  $M_w$  6.8 and 7.1 ( $m_b$  6.8 and 7.0), and 20 percent are between  $M_w$  7.1 and 7.5 ( $m_b$  7.0 and 7.2). The model distribution of characteristic magnitude uses the midpoints of these magnitude ranges as the magnitude and the respective percentage as the weighting. This procedure results in a model magnitude distribution of  $M_w$  6.3 ( $m_b$  6.5), 6.65 ( $m_b$  6.7), 6.95 ( $m_b$  6.88), and 7.3 ( $m_b$  7.1) with weights of 0.1, 0.3, 0.4, and 0.2, respectively ([Table 2.5.2-23](#)).

The characteristic return periods for RGR faults defined by the USGS ([Reference 2.5.2-33](#)) are simply the reciprocal of the recurrence rates shown in [Table 2.5.2-21](#) and vary between 4000 years and 188,000 years, with a mean return period of 36,000 years. Approximately 40 percent of the observed return periods are between 4000 and 25,000 years, 40 percent are between 25,000 and 50,000 years, and 20 percent are between 50,000 and 188,000 years. The model return period distribution is based on using the midpoints of these return period ranges as the return period and the respective percentage as the weighting. This procedure results in model return period distributions of 14,500 years, 37,500 years, and 119,000 years with weights of 0.4, 0.4, and 0.2, respectively.

The model faults are aligned along the eastern extent of the RGR end-to-end with no overlap of the fault segments ([Figure 2.5.2-10](#)). The length of each hypothetical fault is 37 miles (60 km). This length is based on the subsurface rupture length of an earthquake with magnitude  $M_w$  7.3, the maximum magnitude of the fault model, as estimated by Wells and Coppersmith ([Reference 2.5.2-76](#)) for normal faults. This 37-mile (60-km) length is, therefore, the fault dimension required for the hypothetical faults to generate the maximum prescribed earthquake magnitude ( $M_w$  7.3). Given the large distance between the hypothetical faults and the site, other details of the fault geometry (i.e., dip direction) will not have a significant impact on ground motions at the site.

A summary of the seismic source characterization for the RGR source model in eastern Mexico is shown in [Table 2.5.2-23](#).

#### 2.5.2.4.5 Additional Revisions to the EPRI-SOG Source Model

##### 2.5.2.4.5.1 Revised Smoothing Parameters for Dames & Moore's South Coastal Margin Source Zone

In the EPRI-SOG model there are no seismicity parameters calculated and assigned to the degree cells adjacent to the VCS site for the Dames & Moore South Coastal Margin source zone (zone 20) ([Reference 2.5.2-1](#)). The lack of parameters in this region is due to the combination of Dames & Moore adopting zero smoothing for the source zone ([Reference 2.5.2-18](#)), and the absence of seismicity in the EPRI-SOG catalog within the degree cells that would be used to make estimates of

these parameters. Without parameters for these degree cells, the geographic regions adjacent to the VCS site do not contribute to the hazard at the site. The smoothing for Dames & Moore's South Coastal Margin source zone has been updated for the VCS hazard calculations to ensure that seismicity parameters are defined for degree cells adjacent to the site, and thus that these cells contribute to the calculated hazard at the site. The updated smoothing options and associated weights are (Table 2.5.2-19):

- Constant a, constant b, strong prior on b of 1.04 (weight 0.2)
- Medium smoothing on a, medium smoothing on b, strong prior on b of 1.04 (weight 0.4)
- High smoothing on a, high smoothing on b, strong prior on b of 1.04 (weight 0.4)

These smoothing options are based on those used by Dames & Moore for other source zones within the EPRI-SOG model (References 2.5.2-1, 2.5.2-3, 2.5.2-16, 2.5.2-18, 2.5.2-24, 2.5.2-25, and 2.5.2-26). This modification to the EPRI-SOG model was also made for the STPEGS Units 3 & 4 COLA (Reference 2.5.2-28).

#### 2.5.2.4.5.2 Woodward Clyde Central U.S. Background Source for the VCS Site

As described in Subsection 2.5.2.2.1.6, Woodward-Clyde consultants do not have a Central United States Background source zone defined for the VCS site because it is a greenfield site. Therefore, a Central U.S. Background source zone was constructed for the VCS site. The new source zone has the same dimensions, approximately 400 miles (640 km) square, as the Central U.S. Background source zone for the STPEGS Units 1 and 2 plant approximately 60 miles (100 km) east-northeast (Reference 2.5.2-1) and is centered on the VCS site. The vertices of the zone are (94.00° W, 31.60° N), (94.00° W, 25.60° N), (100.00° W, 25.60° N), and (100.00° W, 31.60° N). The  $M_{\max}$  values and smoothing options for the zone are those defined for the Central U.S. Background zone in the EPRI-SOG documentation (Reference 2.5.2-18) (Table 2.5.2-12).

#### 2.5.2.4.6 New Ground Motion Models

Since the 1989 EPRI (Reference 2.5.2-1) study, ground motion models for the CEUS have evolved. An EPRI project was conducted to summarize knowledge about CEUS ground motions, and results were published in 2004 by EPRI (Reference 2.5.2-98). These updated equations estimate median spectral acceleration and its uncertainty as a function of earthquake magnitude and distance. Epistemic uncertainty is modeled using multiple ground motion equations with weights, and multiple estimate of aleatory uncertainty, also with weights. Different sets of sources are recommended for seismic sources that represent rifted vs. non-rifted regions of the earth's crust. Equations are available for spectral frequencies at hard rock sites of 100 hertz (Hz) (which is equivalent to peak ground acceleration, PGA), 25 Hz, 10 Hz, 5 Hz, 2.5 Hz, 1 Hz, and 0.5 Hz.

The aleatory uncertainties published in the 2004 EPRI study ([Reference 2.5.2-98](#)) model were reexamined by Abrahamson and Bommer ([Reference 2.5.2-99](#)) because it was thought that the EPRI, 2004 aleatory uncertainties were probably too large, resulting in over-estimates of seismic hazard. The Abrahamson and Bommer ([Reference 2.5.2-99](#)) study recommends a revised set of aleatory uncertainties and weights that can be used to replace the original EPRI, 2004 aleatory uncertainties.

In summary, the ground motion model used in the seismic hazard calculations consisted of the median equations from EPRI 2004 combined with the updated aleatory uncertainties of the Abrahamson and Bommer ([Reference 2.5.2-99](#)) study.

#### 2.5.2.4.7 Updated Probabilistic Seismic Hazard Analysis and Deaggregation

The seismic hazard at the VCS site was investigated with the changes described in [Subsections 2.5.2.4.2](#) through [2.5.2.4.5](#) to seismic sources, seismicity parameters, maximum magnitudes, and ground motion equations. The initial investigation was made for hard rock conditions, with the incorporation of site-specific conditions at the VCS site to follow.

A PSHA consists of calculating annual frequencies of exceeding various ground motion amplitudes for all possible earthquakes that are hypothesized in a region. The seismic sources specify the rates of occurrence of earthquakes as a function of magnitude and location, and the ground motion model estimates the distribution of ground motions at the site for each event. Multiple weighted hypotheses on seismic sources, earthquake rates of occurrence, and ground motions (characterized by the median ground motion amplitude and its uncertainty) result in multiple weighted seismic hazard curves, and from these, the mean and fractile seismic hazard can be determined. The calculation is made separately for each of the six EPRI teams, and the seismic hazard distributions for the teams are combined, weighting each team equally. This combination gives the overall mean and distribution of rock seismic hazard at the site. The effects of local site conditions on seismic ground motions are taken into account below.

Seismic hazard was initially calculated using the EPRI team sources, the New Madrid faults, the Rio Grande Rift faults, and the Meers fault. These hazard calculations used the EPRI, 2004 ([Reference 2.5.2-98](#)) ground motion equations and the EPRI, 2004 ([Reference 2.5.2-98](#)) aleatory uncertainty model. As will be demonstrated below, the Rio Grande Rift faults and the Meers fault do not contribute significantly to the seismic hazard at the VCS site.

The base-case rock hazard was calculated with the 1989 EPRI ([Reference 2.5.2-1](#)) team sources, modified as described above for additional seismicity in the Gulf of Mexico, and adding the New Madrid fault model to each team's interpretations. The following EPRI team sources were included:

Bechtel: sources BZ1 and BZ2  
Dames & Moore: sources 20, 25, C08, and 67  
Law Engineering: sources 124 and 126  
Rondout: sources 51 and C02  
Woodward-Clyde: source BG  
Weston Geophysical: sources 107, 109, and C31

Figures 2.5.2-18 and 2.5.2-19 show mean rock hazard curves for 10 Hz and 1 Hz spectral accelerations, respectively. Separate mean hazard curves are shown for the EPRI teams' sources plus New Madrid faults, for the New Madrid faults alone, for the Rio Grande Rift faults alone, and for the Meers fault alone. These figures indicate that, at ground motions important for seismic design, the Rio Grande Rift faults and the Meers fault contribute less than 1 percent of the hazard calculated for the EPRI teams plus the New Madrid faults. For example, for 1 Hz spectral acceleration, at the amplitude for which the EPRI team sources plus the New Madrid faults equals  $10^{-4}$ , the hazard contribution from the Rio Grande Rift faults is about  $3 \times 10^{-7}$ , and the contribution from the Meers fault more than a factor of ten lower. The percent contribution for 10 Hz spectral acceleration is even less. On the basis of these comparisons, it is concluded that the Rio Grande Rift faults and Meers fault need not be included in the final hazard calculations.

Figures 2.5.2-20 through 2.5.2-23 show mean rock hazard curves by EPRI team for 10 Hz, 5 Hz, 2.5 Hz, and 1 Hz spectral accelerations, respectively. The mean hazard curves are similar, particularly for 2.5 Hz and 1 Hz, because the New Madrid seismic source is common to all teams and dominates the hazard at these low frequencies. This is further illustrated in Figures 2.5.2-24 through 2.5.2-27, where mean rock seismic hazard curves are plotted for individual sources and for the New Madrid faults for the same four spectral frequencies. In these figures, the probability of activity of each source is reflected in the hazard (the probability of exceedance of ground motion amplitudes). The New Madrid seismic source dominates the 2.5 Hz hazard for annual frequencies down to  $10^{-5}$ , and dominates the 1 Hz hazard for annual frequencies down to  $10^{-6}$ .

Figures 2.5.2-28 through 2.5.2-31 show median rock seismic hazard curves for individual sources and for the New Madrid faults for 10 Hz, 5 Hz, 2.5 Hz, and 1 Hz spectral accelerations, respectively.

Figures 2.5.2-32 through 2.5.2-38 show total rock hazard as the mean, 5th, 16th, 50th, 84th, and 95th fractile curves. One of the characteristics of the low spectral frequency hazard curves (1 Hz and 0.5 Hz in particular) is that the mean rock hazard curves exceed the 84th fractile at high ground motion amplitudes. This is the case when the New Madrid seismic source dominates the hazard, and is caused by a few EPRI (2004) (Reference 2.5.2-98) ground motion equations indicating relatively high hazards for the large distance between the New Madrid seismic source and the VCS site. This is shown in Figure 2.5.2-39, which plots the 1 Hz spectral acceleration hazard from the New Madrid seismic source only, for the 12 ground motion equations used for that source. The equation indicated

as “F9,” with a weight of 0.036, indicates the highest hazard, more than a factor of 10 above all other equations. This equation alone will cause the mean hazard to coincide with a very high fractile hazard curve for cases where the New Madrid seismic source dominates the hazard.

[Figures 2.5.2-40](#) and [2.5.2-41](#) show the mean and median  $10^{-4}$  and  $10^{-5}$  UHRS for hard rock conditions, based on the seven ground motion frequencies for which ground motion estimates are available. Numerical values for the mean UHRS are shown in [Table 2.5.2-24](#).

The seismic hazard was deaggregated following the guidelines of RG 1.165. Specifically, the mean contributions to seismic hazard for 1 Hz and 2.5 Hz were deaggregated by magnitude and distance for the mean  $10^{-4}$  ground motions at 1 Hz and 2.5 Hz, and these deaggregations were combined. [Figure 2.5.2-41](#) shows this combined deaggregation. Similar deaggregations of the mean hazard were performed for 5 and 10 Hz spectral accelerations ([Figure 2.5.2-44](#)). Deaggregations of the mean hazard for  $10^{-5}$  and  $10^{-6}$  ground motions are shown in [Figures 2.5.2-45](#) through [2.5.2-48](#). Deaggregation of the mean seismic hazard is recommended in RG 1.206. The contribution of the New Madrid source to seismic hazard is plotted in the deaggregation figures in the last distance interval, which represents 250+ miles (400+ km); the New Madrid source is actually about 560 miles (900 km) from the VCS site.

[Figures 2.5.2-42](#) through [2.5.2-47](#) include the contribution to hazard by  $\epsilon$ , which is the number of logarithmic standard deviations that the applicable ground motion ( $10^{-4}$ ,  $10^{-5}$ , or  $10^{-6}$ ) is above the logarithmic mean (log-mean). These figures indicate that the largest contribution to hazard for  $10^{-4}$  and  $10^{-5}$  ground motions comes from  $\epsilon$  values between 0 and 2 standard deviations above the mean, which is a common result.

The deaggregation plots in [Figures 2.5.2-42](#) through [2.5.2-45](#) for  $10^{-4}$  and  $10^{-5}$  ground motions indicate that the New Madrid seismic source has a major contribution to seismic hazard at the VCS site. For  $10^{-4}$  annual frequency of exceedance, this source is the largest contributor to seismic hazard for both 1 and 2.5 Hz ([Figure 2.5.2-42](#)) and 5 and 10 Hz ([Figure 2.5.2-43](#)). For an annual frequency of  $10^{-5}$ , the contribution is smaller, particularly for high frequencies (see [Figures 2.5.2-44](#) and [2.5.2-45](#)). For an annual frequency of  $10^{-6}$ , virtually all hazard at high frequencies comes from local sources ([Figure 2.5.2-47](#)), while low frequencies have about equal contributions from the New Madrid seismic source and from local sources ([Figure 2.5.2-46](#)). All of these observations are confirmed qualitatively in [Figures 2.5.2-24](#) through [2.5.2-27](#), which compare the mean hazard from the New Madrid source to the mean hazard from local sources for 10 Hz through 1 Hz.

[Table 2.5.2-25](#) summarizes the mean magnitude and distance resulting from these deaggregations, for all contributions to hazard and for contributions with distances exceeding 100 km. For the 1 and 2.5 Hz results, contributions from events with  $R > 100$  km exceed 5 percent of the total hazard. As a result, following the guidance of RG 1.165, the controlling earthquake for LF ground motions was

selected from the  $R > 100$  km calculation, and the controlling earthquake for HF ground motions was selected from the overall calculation. The values of  $M$  and  $R$  selected in this way are shown in shaded cells in [Table 2.5.2-25](#).

Smooth rock UHRS were developed from the UHRS amplitudes in [Table 2.5.2-24](#), using controlling earthquake  $M$  and  $R$  values shown in [Table 2.5.2-25](#) and using the hard rock spectral shapes for CEUS earthquake ground motions recommended in NUREG/CR-6728 ([Reference 2.5.2-2](#)). Separate spectral shapes were developed for high frequencies (HF) and low frequencies (LF).

In order to reflect accurately the UHRS values calculated by the PSHA as shown in [Table 2.5.2-24](#), the HF spectral shape was anchored to the UHRS values from [Table 2.5.2-24](#) at 100 Hz, 25 Hz, 10 Hz, and 5 Hz. In between these frequencies, the spectrum was calculated using shapes anchored to the next higher and lower frequency and weighting those shapes. The weighting was based on the inverse logarithmic difference between the intermediate frequency and the next higher or lower frequency. This technique provided a smooth, realistic spectral shape at these intermediate frequencies. Below 5 Hz, the HF shape was extrapolated from 5 Hz.

For the LF spectral shape a similar procedure was used except that the LF spectral shape was anchored to the UHRS values at all seven ground motion frequencies for which hazard calculations were made (100 Hz, 25 Hz, 10 Hz, 5 Hz, 2.5 Hz, 1 Hz, and 0.5 Hz). Anchoring the LF spectral shape to all frequencies was necessary because otherwise the LF spectral shape exceeded the HF spectral shape at high frequencies. This results from the contribution of extreme ground motions ( $\epsilon > 1$ , see [Figures 2.5.2-42](#), [2.5.2-44](#), and [2.5.2-46](#)) at low spectral frequencies and a resulting UHRS shape that differs from the median shape predicted in NUREG/CR-6728 ([Reference 2.5.2-2](#)).

[Figures 2.5.2-48](#) and [2.5.2-49](#) show the horizontal HF and LF spectra calculated in this way for  $10^{-4}$  and  $10^{-5}$  annual frequencies of exceedance, respectively. As mentioned previously, these spectra accurately reflect the UHRS amplitudes in [Table 2.5.2-24](#) that were calculated for the seven spectral frequencies at which PSHA calculations were done. Because the HF and LF spectra were scaled to the same high-frequency amplitudes, they are very similar at high frequencies. These spectra were used in site amplification calculations.

#### 2.5.2.4.8 Vertical Ground Motions

Vertical spectra were derived from horizontal spectra after accounting for site amplification. V:H ratios were used to estimate  $10^{-4}$  and  $10^{-5}$  vertical spectra from the consistent horizontal spectra. This process, and the resulting spectra, are described in [Subsection 2.5.2.6](#).

### 2.5.2.5 Seismic Wave Transmission Characteristics of the Site

The UHRS described in the previous section are defined on hard rock, characterized with shear wave velocity  $V_s = 9200$  feet per second (2.8 km per second), which is located at more than 20,000 feet (6096 meters) below the ground surface. This section describes the development of the site amplification factors that result from the transmission of the seismic waves through the thick soil column. The effect is modeled by a truncated soil column, extending from the finished ground surface (including fill) to a depth of about 8115 feet (2473 meters), and an adjustment to the soil damping within the truncated soil column to represent the anelastic attenuation of ground motion by the entire soil column (the  $\kappa$  ["kappa"] value).

To consider the seismic wave transmission characteristics for the site, subsurface conditions of the western and eastern portions of the power block area are considered (see Subsection 2.5.4.2). The western and eastern sites are referred to here as "Unit 1" and "Unit 2," respectively.

The development of the site amplification factors is performed in the following steps:

- (1) Develop a model of the base case soil column for each of the two units using site-specific geotechnical and geophysical data to a depth of about 615 feet (187 meters), augmented to a depth of about 8115 feet (2473 meters) with deep velocity profiles taken from industry or educational resources, as described in [Subsections 2.5.2.5.1](#) and 2.5.4. The model for the upper 615 feet (187 meters) is based on mean shear wave velocities measured at the sites of Units 1 and 2, except for the upper 15 feet (5 meters) of backfill, and shear modulus and damping strain dependencies taken from generic curves (see Subsection 2.5.4.7). The deeper soil layers are assumed to behave linearly. This model provides the base case representation of the dynamic properties of the VCS site subsurface for Units 1 and 2.
- (2) Confirm through sensitivity analyses that this model adequately captures the frequency-dependent response of the deep soil column over all frequencies of interest; i.e. greater than 0.1 Hz.
- (3) Calculate strain-independent (linear-elastic) material damping values for the deep soil strata (187 to 2473 meters), which experience small levels of strain during the earthquake to ensure that the truncated site model accurately accounts for the dissipation of energy in the deep soil site. This is done by constraining the damping within these deeper strata to replicate an estimate of the total  $\kappa$  for the site.
- (4) Generate a set of 60 artificial "randomized" soil profiles, for each of the two units, by using their respective base soil column and developing a probabilistic model that describes the uncertainties in the above soil properties, location of layer and hard rock

boundaries, correlation between the velocities in adjacent layers, and the overall dissipation of energy in the site. Use the  $10^{-4}$  and  $10^{-5}$  annual-frequency-of-exceedance smooth LF and HF hard rock spectra of [Subsection 2.5.2.4](#) for input into the base of the randomized soil columns, calculate dynamic response of the site for each of the 60 artificial profiles by using an equivalent-linear site-response formulation together with Random Vibration Theory (RVT), and calculate the mean of site response. Time histories for the site response analysis are not required for the frequency-domain RVT approach to site response analysis. This step is repeated for each of the four input motions ( $10^{-4}$  and  $10^{-5}$  annual frequencies, HF and LF smooth spectra).

These steps are described in the following subsections. The resulting site-specific amplification factors are used with the hard rock spectra of [Subsection 2.5.2.4](#) to develop GMRS in [Subsection 2.5.2.6](#).

#### 2.5.2.5.1 Base Case Soil Column and Uncertainties

Development of a base case soil column is described in detail in Subsection 2.5.4. Summaries of the low strain shear wave velocity, material damping, and strain-dependent properties of the base case soil strata are provided below in this section. These parameters, for the part of the soil column below the GMRS horizon at a depth of about 100 feet (30 meters) below finished ground surface (top of fill) serve as input for the GMRS site response analysis.

The VCS site is a deep soil site. The existing upper approximately 600 feet (183 meters) of the site soils were investigated using test borings, cone penetration testing (CPT), test pits, and geophysical methods. The soil layers encountered at the boring and CPT locations consist mainly of alternating layers of clays and sands and, therefore, are designated as CLAY 1, SAND 2, CLAY 3, SAND 4, etc. A total of 18 soil layers were identified within the maximum depth of 600 feet (183 meters) explored during the field investigation. In addition, a few sub-layers were identified.

The Primary-Secondary suspension measurements and CPT results provided shear and compression wave velocities of the soil at 1.6 feet (0.5 meters) intervals. This data was used to develop mean shear wave profiles for the upper 600 feet (183 meters) of insitu soil. Unit weights for these profiles are in the range of 120 pounds per cubic foot (pcf) to 130 pcf (1920 to 2080 kilograms per cubic meter).

As described in Subsection 2.5.4.7, the preliminary analysis for the development of site-specific amplification factors was conducted using measured wave velocity profiles combined with published shear modulus and damping degradation curves. The selected published curves were adopted to describe the strain dependencies of shear modulus and damping for the upper 600 feet (183 meters) of insitu soils and 15 feet (5 meters) of fill.

Information on subsurface conditions for depths 615 feet (187 meters) below top of fill was sought from available industry or academic resources. One resource identified was oil/gas sonic well log records for deep wells drilled in the vicinity of the VCS site. Shear wave velocity data at varying depths, ranging from 117 feet (36 meters) to 15,860 feet (4834 meters), were obtained from 6 sonic well logs located in proximity to the VCS site. The geology at the VCS site consists of layers of sand and clay. Below a depth of 1000 feet (305 meters) from ground surface, layers of sandstone, shale, and/or caliche of varying thickness are interbedded with the clay and sand layers. Average shear wave velocity values were derived at the well locations generally at 200-foot (61-meter) intervals of depth. Linear elastic properties are assigned to the soil at depths below 615 feet (187 meters) by assuming that the strains in these deep soil layers remain small during the earthquakes. Unit weight of the deep soils (below approximately 600 feet [183 meters]) range from 130 pcf to 140 pcf (2080 to 2240 kilograms per cubic meter). A value of 170 pcf (2720 kilograms per cubic meter) was assigned for the halfspace unit weight.

Damping values were developed for the linear deep soil layers to maintain the total  $\kappa$  for the site as described below.

A low-strain  $\kappa$  value, a near surface damping parameter for modeling site-dependent effects, is used as a measure of the total dissipation of energy of the site during small strain events. The site  $\kappa$  value is directly related to damping of the soil layers and scattering of the waves at layer interface boundaries. The  $\kappa$  associated for soil layer damping is additive for all layers. The following expression ([Reference 2.5.2-15](#)) shows the relationship between  $\kappa_i$  and the damping coefficient, ( $\zeta_i$ ) of the soil layer (i):

$$\kappa_i = \frac{2H_i \zeta_i}{V_{S_i}} \quad \text{Equation 2.5.2-6}$$

where  $H_i$  is the thickness and  $V_{S_i}$  the shear wave velocity of the soil layer (i). Total  $\kappa$  value of the site associated with material damping equals the sum of the  $\kappa_i$  values of all soil layers included in the model:

$$\kappa = \sum_i \kappa_i \quad (2.4.13-7)$$

The value of total  $\kappa$  is directly evaluated from recordings of earthquakes. One of the nearest and most applicable measures of total  $\kappa$  is a value of 0.058 sec based on inversions of regional earthquakes located and recorded within the deeper portions of the Mississippi Embayment in the area just south of Saint Louis, Missouri and Memphis, Tennessee ([Reference 2.5.2-102](#)). For various other study areas in the Mississippi Embayment also lacking in direct measurements of total ( $\kappa$ ), a more conservative value (i.e., corresponding to lower damping) of 0.046 sec has been used ([Reference 2.5.2-103](#)).

A  $\kappa$  value of 0.006 sec is assumed to apply to the CEUS crystalline basement and below (Reference 2.5.2-15), leaving a total soil  $\kappa$  value of 0.040 sec for the damping of the full depth of the Mississippi Embayment soils. EPRI (Reference 2.5.2-15) presents a standard deviation of 0.4 natural log units to be appropriate for sites in the eastern United States. This is consistent with (Reference 2.5.2-103) in considering  $\pm 50$  percent variation about the base case value of  $\kappa$  for Mississippi embayment sites. Therefore, a base case  $\kappa$  value of 0.040 sec is used for VCS site model with a standard deviation of 0.4 natural log units.

The following procedure is used to assign the damping to the models of the soil at depths below 600 feet (183 meters) in order to match the assigned  $\kappa$  value:

- (1) From Equations 2.5.2-6 and 2.5.2-7,  $\kappa$  associated with material damping is calculated for the top 600 feet (183 meters) of soil strata, i.e., excluding top fill, by using small strain damping for each soil layer.
- (2) The  $\kappa$  value of the top 600 feet (183 meters) of insitu soil is deducted from the total  $\kappa$  value, and a constant damping value is assigned to deep soil layers. In this calculation the  $\kappa$  associated with scattering of the waves in the randomized profiles is computed to ensure the  $\kappa$  associated with both soil layer damping and scattering of the waves in the layered profiles maintains the total  $\kappa$  adopted for the deep soil profile at the site.
- (3) The damping of each deep soil layer is randomized with consideration given to the mean and variation of the total  $\kappa$ .

The input motion for soil amplification analysis was specified at the bottom of the soil profile, below which the halfspace was modeled with shear wave velocity of 9200 feet per second (fps) (2.8 kilometers per second) and a damping ratio of 1 percent.

Multiple undisturbed samples, obtained at varying depths and representing the 18 soil layers in the 600 feet (183 meters) total depth of insitu soils explored, were assigned for resonant column torsional shear (RCTS) tests. The RCTS tests are completed, with results described in Subsection 2.5.4.7.3. Note that the RCTS test data is best fit to shear modulus and damping degradation curves from the literature. The preliminary analysis for the development of site-specific amplification factors was, therefore, conducted using measured shear wave velocity profiles combined with published shear modulus and damping degradation curves that are best fit to the RCTS test data. Results from 16 RCTS tests on insitu soils present at the power block (and two additional RCTS tests on re-compacted embankment fill soils at the cooling basin) have been obtained and are described in Subsection 2.5.4.7.3. Comparisons of these results with the selected literature curves for the corresponding soil strata in the base case soil column model, for each of the two units, demonstrate good agreement.

As described below in [Subsection 2.5.2.5.2](#), for each of the Unit 1 and 2 power blocks, the soil properties for each layer were randomized to account for the inherent natural variability of soil deposits, as well as the (epistemic) uncertainty associated with the choice of curves for variation of shear modulus and damping with strain level. Therefore, the actual site response analysis comprised a range of soil properties for each layer, and in particular, a range of initial small strain shear modulus and degradation curves. Because of different properties in each of the randomized profiles, the site response analysis generated a range of results, as reported in [Subsection 2.5.2.5.4](#).

#### 2.5.2.5.2 Site Properties Representing Uncertainties and Correlations

To account for variations in shear-wave velocity across the site, 60 artificial profiles were generated, for each of the two units (Units 1 and 2) separately, using the stochastic model described in ([Reference 2.5.2-104](#)), with some modifications to account for conditions at the VCS site. These randomized profiles represent the truncated soil column from the top of a halfspace with shear-wave velocity of 9200 fps (2.8 km per second) to the ground surface. This model uses as inputs the following quantities:

- A shear-wave velocity profile for each of the two units, which is equal to the base-case soil profile described above.
- The standard deviation of  $\ln(V_s)$  (the natural logarithm of the shear-wave velocity) as a function of depth, which was developed using available site and regional data (see [Subsection 2.5.4](#)).
- The correlation coefficient between  $\ln(V_s)$  in adjacent layers, which is taken from generic studies, using the inter-layer correlation model for category U.S. Geological Survey “C” soils ([Reference 2.5.2-104](#)), with modifications to some of the parameters to increase inter-layer correlation and reflect the smooth appearance of the input shear-wave velocity profiles for randomization.
- The probabilistic characterization of layer thickness consists of a function that describes the rate of layer boundaries as a function of depth. This study used a generic form of this function ([Reference 2.5.2-104](#)), and then modified it to allow for sharp changes and discontinuities in the adopted base-case velocity profile, especially near the surface.
- The profiles of the log-mean and plus/minus 1 standard deviation of the shear wave velocity profile are shown in [Figures 2.5.2-50](#) and [2.5.2-51](#) for Units 1 and 2, respectively. The variation was used in the randomization of the shear wave velocity profile.

- The depth to halfspace, 8115 feet (2473 meters) based on results of the study of soil column frequency to ensure frequencies lower than 0.1 Hz at the depth where the soil profiles are truncated.
- Log-mean values of shear stiffness (G/GMAX) and damping for each geologic unit are described in Subsection 2.5.4. Uncertainties in the strain-dependent properties for each soil unit are characterized using the values in [References 2.5.2-99](#) and [2.5.2-105](#). [Figures 2.5.2-52](#) and [2.5.2-53](#) illustrate the shear stiffness and damping curves generated for one of the geologic units, SAND 4, described in Subsection 2.5.4.

[Figures 2.5.2-54](#) and [2.5.2-55](#) illustrate the 60  $V_s$  profiles generated for Units 1 and 2, respectively, using the log-mean, logarithmic standard deviation, and correlation model described above. These same figures compare the log-mean of these 60  $V_s$  profiles to the log-mean  $V_s$  profile described in the previous section, indicating good agreement.

This set of 60 profiles, consisting of  $V_s$  versus depth, depth to half-space, stiffness, and damping, are used to calculate and quantify site response and its uncertainty, as described in the following sections.

#### 2.5.2.5.3 Correction of Damping for Scattering Effects to Maintain Total Site $\kappa$

The process of the randomization of soil velocity profiles introduces additional scattering of upward propagating shear waves (S-waves) in such a manner that the log-mean response of all randomized profiles is lower than the response obtained from the analyses of the log-mean profile. These scattering effects are accounted for by decreasing the damping value of the deep soil layers in the randomized profiles by 15 percent. Due to this modification, the log-mean damping value of deep soil layer changes from 0.62 to 0.53 percent for Unit 1, and from 0.65 to 0.55 percent for Unit 2. The log-mean values of total  $\kappa$  coefficient of the site is reduced by 0.005 sec. The modification has a very small effect on the variation of the randomized  $\kappa$  values as measured by the presented log-standard deviation.

#### 2.5.2.5.4 Site Response Analysis

The site response analysis performed for the VCS site is conducted using the program P-SHAKE (Appendix 2.5.2-A), which uses a procedure based on RVT ([References 2.5.2-106](#) and [2.5.2-107](#)) with the following assumptions:

- Vertically-propagating shear waves are the dominant contributor to site response.
- An equivalent-linear formulation of soil nonlinearity is appropriate for the characterization of site response.

These are the same assumptions that are implemented in the SHAKE program ([Reference 2.5.2-110](#)). With respect to RVT implementation, the major steps used in P-SHAKE are as follows:

- (1) The input motion is provided in terms of an accelerated response spectrum (ARS) and its associated spectral damping instead of spectrum-compatible acceleration time histories. The input ARS is converted to an acceleration power spectral density (PSD) using the RVT based procedure with the peak factor function.
- (2) From the frequency domain solution of the soil profile (following SHAKE approach), the transfer function for shear strain in each layer is obtained and convolved with the PSD of input motion to get the PSD and the maximum strain in each layer. The effective strain is obtained from the maximum strain and is used to obtain the new soil properties (soil shear modulus and damping) for the next iteration.
- (3) The iterations are repeated until convergence is reached in all layers to the convergence limit set by the user.
- (4) Once the final frequency domain solution is obtained, the acceleration response spectrum at each layer interface can be computed from the solution using an inverse process of obtaining PSD from the acceleration response spectrum.

The site-response analysis procedure, as described above, requires the following additional parameters:

- Strong-motion duration. The RVT methodology requires this parameter, but results are not very sensitive to it. These are calculated from the mean magnitudes from the deaggregation. Table 2.3-1 in [Reference 2.5.2-109](#) provides strong motion duration values as a function of magnitude. Accordingly, strong motion durations were assigned for each of the cases considered ( $10^{-4}$  and  $10^{-5}$  annual frequencies, HF and LF smooth spectra), presented in [Table 2.5.2-26](#).
- Effective strain ratio. A value of 0.65 is used. Effective strain ratio is defined as the ratio between the strain at the peak acceleration of earthquake time history and the strain at the equivalent harmonic wave going through the soil layers ([Reference 2.5.2-110](#)).

Note that the GMRS horizon is defined at the top of SAND 4 layer, which is at the 99 foot depth for Unit 1 and the 102 foot depth for Unit 2. To calculate the site response at the GMRS horizon, the top layers (above 99 feet [30 meters] and 102 feet [31 meters] for Units 1 and 2, respectively) are omitted when analyzing the soil columns. Envelope amplification factors for the two units are used to develop GMRS.

Figures 2.5.2-56 and 2.5.2-57 shows with thick red line the log-mean of site amplification factor at GMRS horizon (at 99-foot [30-meter] depth for Unit 1 and 102-foot [31-meter] depth for Unit 2) from analyses of the 60 modified random profiles with the  $10^{-4}$  LF input motion. As would be expected due to the large depth of sediments at the site, amplifications are largest at low frequencies (below 4.0 Hz) and smallest at high frequencies because of soil damping. Figure 2.5.2-58 shows the log-mean amplification factors of Units 1 and 2 at the GMRS horizon. As stated above, the envelope amplification factors are used to develop GMRS, refer to Subsection 2.5.2.6, for the VCS site. The maximum strains in the soil column are low for this motion, and this is shown in Figures 2.5.2-59 and 2.5.2-60, which plots the maximum strains versus depth that are calculated for the 60 profiles and their log-mean (in red thick line) for Units 1 and 2, respectively. The log-mean of maximum strains is less than 0.023 percent for Unit 1 and 0.028 percent for Unit 2. The maximum strain calculated from the analyses of all 120 profiles is 0.040 percent at depths above 615 feet (187 meters) of soil. The maximum strains in the deep soil layer at depths below 615 feet (187 meters) are very small and do not exceed 0.013 percent.

Figures 2.5.2-61 through 2.5.2-65 show similar plots of amplification factors and maximum strains obtained from the analyses with  $10^{-4}$  HF motion. The maximum strain results show that the soil column exhibits a lower level of strain as compared to the  $10^{-4}$  LF motion for this earthquake with maximum strains being less than 0.011 percent.

Figures 2.5.2-66 through 2.5.2-75 show comparable plots of amplification factors and maximum strains from the analyses performed with the  $10^{-5}$  input motion, both LF and HF. For this higher motion, larger maximum strains are observed, but the maximum log-mean does not exceed 0.1 percent for Units 1 and 2. From all of the 240 profiles (LF and HF, Units 1 and 2), a maximum strain of 0.15 percent is calculated at depths above 615 feet (187 meters) of soil. The maximum strain in the deep soil layers is very small, less than 0.05 percent.

Comparison of the profiles of log-mean maximum strain in Figures 2.5.2-76 and 2.5.2-77, for Units 1 and 2 respectively, clearly indicates that response of the site under the LF motions is stronger than under HF motions. Figures 2.5.2-78 and 2.5.2-79 show the log-mean profiles for the strain-compatible damping, for Units 1 and 2 respectively, that is a measure of energy dissipation in the soil profile during the shaking. Corresponding to the strains, a maximum damping value of 3.1 percent for Unit 1 and 2.8 percent for Unit 2 at depths above 615 feet (187 meters) of soil are calculated for the analyses with the  $10^{-5}$  LF motion. The strain compatible damping calculated for  $10^{-4}$  LF motion is small and does not exceed 2.0 percent. The small strain-compatible damping results in relatively small de-amplification of the site response at high frequencies.

A comparison of the envelope of the Unit 1 and Unit 2 log-mean soil amplification factors at the GMRS horizon for LF and HF,  $10^{-4}$  and  $10^{-5}$  input motions is shown in Figure 2.5.2-80. As shown in this figure, the amplifications at  $10^{-4}$  level of input motion between the LF and HF input motions are

larger for LF input motion and the difference increases for frequencies greater than about 5 Hz. De-amplification at higher frequencies is small particularly for the LF input motion, followed by amplification of the peak ground acceleration (about 1.5) at high frequencies (above 80 Hz). The amplification due to  $10^{-5}$  level of input motion follows the same trend compared to the amplification due to  $10^{-4}$  motion, indicating a limited extent of soil nonlinearity in the soil column.

The corresponding enveloping numerical values of the soil amplification factors are tabulated in [Table 2.5.2-27](#), refer to [Subsection 2.5.2.6](#).

#### 2.5.2.6 Ground Motion Response Spectra

The Safe Shutdown Earthquake (SSE) ground motion was developed starting from the  $10^{-4}$  and  $10^{-5}$ , HF and LF rock UHRS shown in [Figures 2.5.2-48](#) and [2.5.2-49](#). Site response was calculated for each of these rock input motions. [Figure 2.5.2-80](#) shows the resulting log-mean amplification factors for free surface conditions at the GMRS horizon for each of these input rock motions. The envelope amplification factors were used to multiply by the envelope of the HF and LF spectra shown in [Figures 2.5.2-48](#) and [2.5.2-49](#), to calculate  $10^{-4}$  and  $10^{-5}$  site spectra.

This procedure corresponds to Approach 2A in [References 2.5.2-2](#) and [2.5.2-111](#), wherein the rock UHRS (for example, at  $10^{-4}$ , column 2 in [Table 2.5.2-27](#)) is multiplied by a mean amplification factor at each frequency (column 3 in [Table 2.5.2-27](#)) to estimate the  $10^{-4}$  site UHRS (column 4 in [Table 2.5.2-27](#)).

Each of the  $10^{-4}$  and  $10^{-5}$  soil UHRS—originally processed at 305 frequency points between 0.1 and 100 Hz—were smoothed over  $\pm 5$  adjacent frequency spectral amplitudes. This smoothing removed minor variations in the response as appropriate for final seismic design response spectra. The resulting smoothed  $10^{-4}$  and  $10^{-5}$  soil UHRS are tabulated in columns 5 and 9 of [Table 2.5.2-27](#).

The low-frequency character of the spectra in [Figure 2.5.2-81](#) reflects the low-frequency amplification of the site. This is a deep soil site and there is a site resonance at about 0.6 Hz, with a dip in site response at about 1.5 Hz. This dip occurs for many of the 60 randomized soil profiles that were used to characterize the site profile and contributes to a dip in the site spectra for  $10^{-4}$  and  $10^{-5}$  at 1.2 Hz.

The horizontal GMRS was developed from the smoothed horizontal UHRS using the approach described in ASCE/SEI Standard 43-05 ([Reference 2.5.2-112](#)) and RG 1.208. The ASCE/SEI Standard 43-05 approach defines the GMRS using the site-specific UHRS, which is defined for Seismic Design Category SDC-5 at a mean  $10^{-4}$  annual frequency of exceedance. The procedure for computing the GMRS is as follows:

For each spectral frequency at which the UHRS is defined, a slope factor (AR) is determined from:

$$AR = SA(10^{-5}) / SA(10^{-4}) \qquad \text{Equation 2.5.2-8}$$

Where  $SA(10^{-4})$  is the spectral acceleration (SA) at a mean UHRS exceedance frequency of  $10^{-4}$  per year (and similarly for  $SA(10^{-5})$ ). A Design Factor (DF) is defined based on AR, which reflects the slope of the mean hazard curve between  $10^{-4}$  and  $10^{-5}$  mean annual frequencies of exceedance. The DF at each spectral frequency is given by:

$$DF = 0.6(AR)^{0.80} \quad \text{Equation 2.5.2-9}$$

and

$$GMRS = \max[SA(10^{-4}) \times \max(1, DF), 0.45 \times SA(10^{-5})] \quad \text{Equation 2.5.2-10}$$

The derivation of DF is described in detail in the Commentary to ASCE/SEI Standard 43-05 and in RG 1.208. [Table 2.5.2-27](#) shows the smoothed values of  $10^{-4}$  and  $10^{-5}$  UHRS calculated at each structural frequency and the resulting GMRS. The horizontal  $10^{-4}$  and  $10^{-5}$  UHRS and GMRS are plotted in [Figure 2.5.2-81](#).

A vertical SSE spectrum was calculated by deriving V:H ratios and applying them to the horizontal GMRS. The V:H ratios were obtained using the standard horizontal and vertical spectra recommended in RG 1.60, as described here.

For CEUS soil sites NUREG/CR-6728 ([Reference 2.5.2-2](#)) suggests a methodology for estimating V:H using available empirical Western United States (WUS) ground motion attenuation relations for both soil and rock, horizontal and vertical motions, and ground motion modeling to develop transfer functions to translate WUS V:H estimates to CEUS V:H estimates. This methodology results in several significant trends in the derived ratios that depend on the frequency of the ground motion, the magnitude and distance of an earthquake, and the subsurface material properties at a site. Among these trends are: the tendency for V:H to increase with frequency, and (for soil sites) to increase with higher magnitudes and smaller distances in the high-frequency range, but to decrease with higher magnitude and smaller distances in the low-frequency range.

Using the attenuation relations of ([Reference 2.5.2-113](#)) for WUS soil V:H values, and using the controlling earthquake magnitudes and distances for low- and broad-band frequency characterization of site-specific UHRS (for  $R > 100$  km and “overall” hazard, respectively, see [Table 2.5.2-25](#)), V:H ratios have been developed for the VCS site. [Figure 2.5.2-82](#) shows three V:H ratios as a function of magnitude and distance. Two of the V:H ratios consider the controlling high-frequency (5 to 10 Hz) events for  $10^{-4}$  and  $10^{-5}$  annual hazard levels. The third V:H ratio is for a single controlling low-frequency (1 to 2.5 Hz) event representative of both  $10^{-4}$  and  $10^{-5}$  annual hazard levels. The specification of the distance of 124 miles (200 km) for the low-frequency event is based on the far-distance limit of the dataset used by [Reference 2.5.2-113](#) in their ground motion attenuation relations. For distances greater than 124 miles (200 km) for the low-frequency event, WUS soil V:H values appear to decrease. Therefore, using a distance of 124 miles (200 km), conformal to the dataset used in [Reference 2.5.2-113](#), instead of the actual controlling distance of greater than 500 miles

(800 km), indicated in [Table 2.5.2-25](#), suggests appropriate, if not conservative guidance (i.e., higher value) on appropriate V:H for this event for the project site. To account for the WUS-to-CEUS high-frequency transformation, described in EPRI ([Reference 2.5.2-15](#)) and NUREG/CR-6728, these V:H ratios have been shifted toward higher frequencies. The value of this frequency shift (by a factor of 3.74) is derived by considering the V:H ratios presented in NUREG/CR-6728, and dividing the peak frequency for CEUS (~62.5Hz) by the peak frequency for WUS (~16.7Hz).

The V:H values from RG 1.60 are also shown in [Figure 2.5.2-82](#). They have been adopted for the VCS site because they are conservative, acceptable, and simple.

[Figure 2.5.2-83](#) shows the horizontal and vertical GMRS calculated in this way. The V:H ratios are documented in [Table 2.5.2-27](#). The recommended V:H ratio is nearly or exactly 1.0 for frequencies greater than 3.5 Hz, 0.668 for frequencies less than 0.25 Hz, and varies for intermediate frequencies. [Table 2.5.2-27](#) lists the vertical GMRS, which was calculated by applying the V:H ratios to the horizontal GMRS. This is mathematically equivalent to applying the V:H ratios to the  $10^{-4}$  and  $10^{-5}$  UHRS amplitudes, then calculating the vertical GMRS from the vertical  $10^{-4}$  and  $10^{-5}$  UHRS.

The GMRS and an updated assessment of the soil columns information will be used to develop the foundation input response spectra (FIRS) for the selected reactor technology at the COL application stage and to determine the adequacy of the CSDRS. The definitions of GMRS and FIRS will be taken from the NRC's "Interim Staff Guidance on Seismic Issues Associated with High Frequency Ground Motion in Design Certification and Combined License Applications" (ISG-17 [August 2009]). The definition of the CSDRS will be taken from the selected reactor technology DCD.

#### 2.5.2.7 References

- 2.5.2-1 Electric Power Research Institute (EPRI), *Probabilistic Seismic Hazard Evaluation at Nuclear Plant Sites in the Central and Eastern United States*, Resolution of the Charleston Earthquake Issue, Report 6395-D, 1989.
- 2.5.2-2 Risk Engineering, Inc., *Technical Basis for Revision of Regulatory Guidance on Design Ground Motions: Hazard- and Risk-Consistent Ground Motion Spectra Guidelines*, NUREG/CR-6728, U.S. Nuclear Regulatory Commission, Washington, D.C., 2001.
- 2.5.2-3 Electric Power Research Institute (EPRI), *Seismic Hazard Methodology for the Central and Eastern United States*, Vol. 1, part 2: Methodology (rev. 1), EPRI NP-4726-A, Rev. 1, 1988.
- 2.5.2-4 Frohlich, C. and Davis, S. D., *Texas Earthquakes*, pp. 40–255, 2002.

- 2.5.2-5 Engdahl, E. R., Hilst, R. V. D., and Buland, R., *Global Teleseismic Earthquake Relocation with Improved Travel Times and Procedures for Depth Procedures*, Bulletin of the Seismological Society of America, Vol. 88, no. 3, pp. 722–743, 1998.
- 2.5.2-6 Perez, O. J., *Revised World Seismicity Catalog (1950–1997) for Strong ( $M_S \geq 6$ ) Shallow ( $H \leq 70$  Km) Earthquakes*, Bulletin of the Seismological Society of America, Vol. 89, no. 2, pp. 335–341, 1999.
- 2.5.2-7 Advanced National Seismic System (ANSS), *ANSS/CNSS Worldwide Earthquake Catalog files*. Available at <http://www.ncedc.org/anss/catalog-search.html>, accessed September 19, 2007.
- 2.5.2-8 International Seismological Centre (ISC), *United Kingdom, On-line Bulletin*. Available at <http://www.isc.ac.uk>, accessed September 21, 2007.
- 2.5.2-9 National Earthquake Information Center (NEIC), Stover, C. W., and Coffman, J. L., *Seismicity of the United States, 1568–1989 (Revised)*, Professional Paper 1527, U.S. Geological Survey, 1993. Available at [http://neic.usgs.gov/neis/epic/code\\_catalog.html](http://neic.usgs.gov/neis/epic/code_catalog.html), accessed October 3, 2007.
- 2.5.2-10 Rinehart, W., Ganse, R., and Teik, P., National Geophysical Data Center (NGDC); Arnold, E., and Stover, C., U.S. Geological Survey (USGS), and Smith, R.H., (CIRES), National Earthquake Information Center (NEIC), *Seismicity of Middle America: National Geophysical Data Center and National Earthquake Information Service, U.S. Geological Survey, 1982*. Available at USGS website [http://neic.usgs.gov/neis/epic/code\\_catalog.html](http://neic.usgs.gov/neis/epic/code_catalog.html), accessed October 3, 2007.
- 2.5.2-11 National Earthquake Information Center (NEIC), Stover, C. W., Reagor, G., and Algermissen, S. T., *United States Earthquake Data File*, Open-File Report 84-225, 123 p., U.S. Geological Survey, 1984. Available at [http://neic.usgs.gov/neis/epic/code\\_catalog.html](http://neic.usgs.gov/neis/epic/code_catalog.html), accessed October 3, 2007.
- 2.5.2-12 National Earthquake Information Center (NEIC), *Preliminary Determination of Epicenter (PDE)*. Available at [http://neic.usgs.gov/neis/epic/code\\_catalog.html](http://neic.usgs.gov/neis/epic/code_catalog.html), accessed October 3, 2007.
- 2.5.2-13 Atkinson, G. M. and Boore, D. M., *Ground-Motion Relations for Eastern North America*, Bulletin of the Seismological Society of America, vol. 85, no. 1, pg. 17–30, 1995.
- 2.5.2-14 Frankel, A., Mueller, C., Barnhard, T., Perkins, D., Leyendecker, E.V., Dickman, N., Hanson, S., and Hopper, M., *National Seismic-Hazard Maps; Documentation*, Open-File Report 96-532, pp. 110, U.S. Geological Survey, 1996.

- 2.5.2-15 Electric Power Research Institute (EPRI), *Guidelines for Determining Design Basis Ground Motions*, Report TR-102293, Project 3302, Final Report, 1993.
- 2.5.2-16 Electric Power Research Institute (EPRI), *Seismic Hazard Methodology for the Central and Eastern United States*, Tectonic Interpretations, Vol. 5-10, EPRI Report NP-4726, Project P101-19, Final Report, 1986.
- 2.5.2-17 Frohlich, C., *Seismicity of the Central Gulf of Mexico*, Geology, pp. 103–106, 1982.
- 2.5.2-18 Electric Power Research Institute (EPRI), *EQHAZARD Primer*, prepared by Risk Engineering for Seismicity Owners Group and Electric Power Research Institute (EPRI), EPRI NP-6452-D, 1989.
- 2.5.2-19 National Earthquake Information Center (NEIC), *Information Regarding Technical and Scientific Information on the September 10, 2006 Earthquake in the Gulf of Mexico*, Available at <http://earthquake.usgs.gov/eqcenter/eqinthenews/2006/usslav/#scitech>, accessed September 13, 2006.
- 2.5.2-20 Engdahl, E. R. and Villaseñor, A., *Chapter 41: Global Seismicity: 1900–1999*, International Handbook of Earthquake & Engineering Seismology, pp. 665–690, 2002.
- 2.5.2-21 Johnston, A. C., Coppersmith, K. J., Kanter, L. R., and Cornell, C. A., *The Earthquakes of Stable Continental Regions*, Vol. 1: Assessment of Large Earthquake Potential, Final Report TR-102261-V1, Electric Power Research Institute (EPRI), 1994.
- 2.5.2-22 Deleted.
- 2.5.2-23 Bernreuter, D.L., Savy, J.B., Mensing, R.W., and Chen, J.C., *Seismic Characterization of 69 Nuclear Plant Sites East of the Rocky Mountains: Methodology*, Input Data and Comparisons to Previous Results for Ten Test Sites, NUREG/CR-5250, Vol. 1., p. 81 with 3 appendices, U.S. Nuclear Regulatory Commission, Washington, D.C., 1989.
- 2.5.2-24 Electric Power Research Institute (EPRI), *Seismic Hazard Methodology for the Central and Eastern United States*, Vol. 1, Part 1: Theory, EPRI NP-4726-A, 1988.
- 2.5.2-25 Electric Power Research Institute (EPRI), *Seismic Hazard Methodology for the Central and Eastern United States*, Vol. 2, Programmer's Manual, EPRI NP-4726-A, 1988.
- 2.5.2-26 Electric Power Research Institute (EPRI), *Seismic Hazard Methodology for the Central and Eastern United States*, Vol. 3, User's Manual, EPRI NP-4726-A, Rev. 1, 1989.

- 2.5.2-27 Budnitz, R.J., Apostolakis, G., Boore, D.M., Cluff, L.S., Coppersmith, K.J., Cornell, C.A., and Morris, P.A., *Recommendations for Probabilistic Seismic Hazard Analysis: Guidance on Uncertainty and Use of Experts*, NUREG/CR-6372, p. 278, U.S. NRC, Washington, D.C., 1997.
- 2.5.2-28 STPEGS, *South Texas Project COL Application for STP Site, Units 3 & 4*, rev. 0, NRC Docket Nos. 52-012 and 52-013, 2007.
- 2.5.2-29 TVA, *Tennessee Valley Authority (TVA) COL Application for Bellefonte Nuclear Site, Units 3 & 4*, Rev. 0, NRC Docket No. 52-014 and 52-015, (Proprietary), 2008.
- 2.5.2-30 Bernreuter, D.L., Savy, J.B., Mensing, R.W., and Chen, J.C., *Seismic Characterization of 69 Nuclear Plant Sites East of the Rocky Mountains: Results and Discussions for Batch 4 Sites*, NUREG/CR-5250, vol. 5., p. 247 with 2 appendices, U.S. Nuclear Regulatory Commission, Washington, D.C., 1989.
- 2.5.2-31 Swan, F.H., Wesling, J.R., Hanson, K.A., Kelson, K.I., and Perman, R.C., *Draft Report: Investigation of the Quaternary Structural and Tectonic Character of the Meers Fault (Southwestern Oklahoma)*, pp. 104 plus appendices, Geomatrix Consultants, Inc., San Francisco, CA, 1993.
- 2.5.2-32 Savy, J.B., Foxall, W., and Bernreuter, D.L., *Probabilistic Seismic Hazard Characterization and Design Parameters for the Pantex Plant*, UCRL-CR-132282, pp. 93, prepared for Mason and Hanger Corporation, Hazards Mitigation Center, Lawrence Livermore National Laboratory, 1998.
- 2.5.2-33 Frankel, A.D., Petersen, M.D., Muller, C.S., Haller, K.M., Wheeler, R.L., Leyendecker, E.V., Wesson, R.L., Harmsen, S.C., Cramer, C.H., Perkins, D.M., and Rukstales, K.S., *Documentation for the 2002 Update of the National Seismic Hazard Maps*, Open File Report 02-420, 33 p, U.S. Geological Survey, 2002.
- 2.5.2-34 Petersen, M.D., Frankel, A.D., Harmsen, S.C., Mueller, C.S., Haller, K.M., Wheeler, R.L., et al., *Documentation for the 2008 Update of the United States National Seismic Hazard Maps*, v.1.1, Open File Report 2008-1128, U.S. Geological Survey, 2008.
- 2.5.2-35 Sobel, P., *Revised Livermore Seismic Hazard Estimates for Sixty-Nine Nuclear Power Plant Sites East of the Rocky Mountains*, Washington, D.C., NUREG-1488, p. 95, U.S. NRC, 1994.
- 2.5.2-36 Crone, A.J., and Wheeler, R.L., *Data for Quaternary Faults, Liquefaction Features, and Possible Tectonic Features in the Central and Eastern United States, East of the Rocky Mountain Front*, Open-File Report 00-260, p. 342, U.S. Geological Survey, 2000.

- 2.5.2-37 Hanson, K.L., Swan, F.H., Wesling, J.R., and Kelson, K.I., *Quaternary Deformation along the Criner fault, Oklahoma: A Case Study for Evaluating Tectonic Versus Landslide Faulting*, 1997 Spring Meeting, American Geophysical Union, 1997.
- 2.5.2-38 Walker, W., Sralla, B., and Cronin, V.S., *A Reassessment of the Possible Activity of the Criner Hills Fault, South-Central Oklahoma*, 2005 Geological Society of America Annual Meeting, Vol. 37, p. 559, Geological Society of America, Salt Lake City, UT, 2005.
- 2.5.2-39 Wheeler, R.L., *Known or Suggested Quaternary Tectonic Faulting, Central and Eastern United States-New and Updated Assessments for 2005*, Open-File Report 2005-1336, U.S. Geological Survey, 2005.
- 2.5.2-40 Wheeler, R.L., *Quaternary Tectonic Faulting in the Eastern United States*, Engineering Geology, vol. 82, pp. 165–186, 2006.
- 2.5.2-41 Wheeler, R.L., *Earthquakes and the Cratonward Limit of Lapetan Faulting in Eastern North America*, Geology, Vol. 23, p. 105–108, 1995.
- 2.5.2-42 Wheeler, R.L., and Cramer, C.H., *Updated Seismic Hazard in the Southern Illinois Basin: Geological and Geophysical Foundations for Use in the 2002 USGS National Seismic-Hazard Maps*, Seismological Research Letters, Vol. 73, pp. 776–791, 2002.
- 2.5.2-43 Wheeler, R.L., and Frankel, A.D., *Geology in the 1996 USGS Seismic-Hazard Maps, Central and Eastern United States*, Research Letters, Vol. 71, pp. 273–282, 2000.
- 2.5.2-44 Crone, A.J., and Luza, K.V., *Style and Timing of Holocene Surface Faulting on the Meers Fault, Southwestern Oklahoma*, Geological Society of America Bulletin, Vol. 102, pp. 1–17, 1990.
- 2.5.2-45 Kelson, K.I., and Swan, F.H., *Paleoseismic History of the Meers Fault, Southwestern Oklahoma, and its Implications for Evaluations of Earthquake Hazards in the Central and Eastern United States*, Proceedings of the Seventeenth Water Reactor Safety Information Meeting, Weiss, A.J., ed., NUREG/CP-0105, pp. 341-365, U.S. NRC 1990.
- 2.5.2-46 Madole, R.F., *The Meers Fault: Quaternary Stratigraphy and Evidence for Late Holocene Movement, The Slick Hills of Southwestern Oklahoma — Fragments of an Aulacogen: Norman, OK*, Donovan, R.N., ed., Guidebook 24, pp. 55–67, Oklahoma Geological Society, 1986.

- 2.5.2-47 Madole, R.F., *Stratigraphic Evidence of Holocene Faulting in the Mid-Continent: The Meers Fault, Southwestern Oklahoma*, Geological Society of America Bulletin, Vol. 100, pp. 392–401, 1988.
- 2.5.2-48 Ramelli, A.R., and Slemmons, D.B., *Implications of the Meers Fault on Seismic Potential in the Central United States, Neotectonics in Earthquake Evaluation: Reviews in Engineering Geology*, Krinitzsky, E.L., and Slemmons, D.B., eds., Vol. 8, Geological Society of America, p. 59–75, 1990.
- 2.5.2-49 Ramelli, A.R., Slemmons, D.B., and Brocoum, S.J., *The Meers Fault: Tectonic Activity in Southwestern Oklahoma*, NUREG/CR-4852, p. 25, U.S. NRC, Washington, D.C., 1987.
- 2.5.2-50 Nettles, M., *Analysis of the 10 February 2006: Gulf of Mexico Earthquake from Global and Regional Seismic Data, 2007 Offshore Technology Conference: Houston, Texas*, p. OTC 19099, 2007.
- 2.5.2-51 Dellinger, J.A., Dewey, J.W., Blum, J., and Nettles, M., *Relocating and Characterizing the 10 Feb 2006 “Green Canyon” Gulf of Mexico Earthquake Using Oil-Industry Data*, EOS Transactions Vol. 88, no.52, Fall Meet. Suppl., Abstract S13F-01, American Geophysical Union, 2007.
- 2.5.2-52 Xie, J., *Spectral Inversion Of Lg From Earthquakes: A Modified Method With Applications To The 1995, Western Texas Earthquake Sequence*, Bulletin of the Seismological Society of America, vol. 88, pp. 1525–1537, 1998.
- 2.5.2-53 Aldrich, M.J., Chapin, C.E., and Laughlin, A.W., *Stress History and Tectonic Development of the Rio Grande Rift, New Mexico*, Journal of Geophysical Research, Vol. 91, pp. 6199–6211, 1986.
- 2.5.2-54 Humphreys, E.D., and Coblenz, D.D., *North American Dynamics and Western U.S. Tectonics*, Reviews of Geophysics, Vol. 45, p. RG3001, 2007.
- 2.5.2-55 Keller, G.R., *Geophysical Constraints on the Crustal Structure of New Mexico, The Geology of New Mexico: Special Publication*, Mack, G.H., and Giles, K.A., eds., p. 439–456, Socorro, NM, New Mexico Geologic Society, 2004.
- 2.5.2-56 Keller, G.R., Hinojosa, H., Dryer, R., Aiken, L.V., and Hoffer, J.M., *Preliminary Investigations of the Extent of the Rio Grande Rift in the Northern Portion of the State of Chihuahua*, Geofisica Internacional, Vol. 28, p. 1043–1049, 1989.
- 2.5.2-57 Keller, G.R., Morgan, P., and Seager, W.R., *Crustal Structure, Gravity Anomalies and Heat Flow in the Southern Rio Grande Rift and Their Relationship to Extensional Tectonics*, Tectonophysics, Vol. 174, pp. 21–37, 1990.
- 2.5.2-58 Olsen, K.H., Baldrige, W.S., and Callender, J.F., *Rio Grande Rift: An Overview*, Tectonophysics, Vol. 143, pp. 119–139, 1987.

- 2.5.2-59 Pazzaglia, F.J., and Hawley, J.W., *Neogene (Rift Flank) and Quaternary Geology and Geomorphology, The Geology of New Mexico: Special Publication*, Mack, G.H., and Giles, K.A., eds., pp. 407-437, Socorro, NM, New Mexico Geologic Society, 2004.
- 2.5.2-60 Heidelberg Academy of Sciences and Humanities, Reinecker, J., Heidbach, O., Tingay, M., Sperner, B., and Müller, B., 2005, *The Release 2005 of the World Stress Map*. Available at [www.world-stress-map.org](http://www.world-stress-map.org), accessed on March 13, 2007.
- 2.5.2-61 Doser, D.I., *Personal Communication on 14 April 1995, EQ in West Texas*, recorded by C. Fuller, September 26, 2007.
- 2.5.2-62 U.S. Geological Survey (USGS), *Preliminary Earthquake Report Magnitude 6.0 — Gulf of Mexico 2006 September 10 14:56:07 UTC*, USGS, 2006. Available at <http://earthquake.usgs.gov/eqcenter/eqinthenews/2006/usslav/index.php>, accessed May 4, 2007.
- 2.5.2-63 National Earthquake Information Center (NEIC), *NEIC Monthly Earthquake Data Report file for Event 200602104011, U.S. Geological Survey, 2007*. Available at <ftp://hazards.cr.usgs.gov/edr/mchedr/>, accessed November 11, 2007.
- 2.5.2-64 National Earthquake Information Center (NEIC), *NEIC PDE-W Earthquake Summary for 10 February 2006 041717 Event, United States Geological Survey, 2007*. Available at <http://neic.usgs.gov/cgi-bin/epic/epic.cgi?SEARCHMETHOD=2&CLAT=0.0&CLON=0.0&CRAD=0.0&FILEFORMAT=1&SEARCHRANGE=HH&SLAT2=28&SLAT1=27&SLON2=-90&SLON1=-91&SUBMIT=Submit+Search&SYEAR=&SMONTH=&SDAY=&EYEAR=&EMONTH=&EDAY=&LMAG=&UMAG=&NDEP1=&NDEP2=&IO1=&IO2=>, accessed August 23, 2007.
- 2.5.2-65 Dewey, J., *Draft Report on Green Canyon Event*, Denver, CO, 2007.
- 2.5.2-66 Hough, S.E., Armbruster, J.G., Seeber, L., and Hough, J.F., *On the Modified Mercalli Intensities and Magnitudes of the 1811-1812 New Madrid Earthquakes*, *Journal of Geophysical Research*, Vol. 105, pp. 23,839–23,864, 2000.
- 2.5.2-67 Bakun, W.H., and Hopper, M.G., *Magnitudes and Locations of the 1811–1812 New Madrid, Missouri and the 1886 Charleston, South Carolina, Earthquakes*, *Bulletin of the Seismological Society of America*, Vol. 94, pp. 64–75, 2004.
- 2.5.2-68 Cramer, C.H., *A Seismic Hazard Uncertainty Analysis for the New Madrid Seismic Zone*, *Engineering Geology*, Vol. 62, pp. 251–266, 2001.

- 2.5.2-69 Tuttle, M.P., Schweig, E.G., Sims, J.D., Lafferty, R.H., Wolf, L.W., and Haynes, M.L., *The Earthquake Potential of the New Madrid Seismic Zone*, *Bulletin of the Seismological Society of America*, Vol. 92, pp. 2080–2089, 2002.
- 2.5.2-70 Exelon Generation Company (EGC), *Exelon Generation Company (EGC) Early Site Permit (ESP) Application for the EGC ESP Site*, NRC Docket No. 52-007, rev. 4, April 4, 2006.
- 2.5.2-71 Crone, A. J., US Geological Survey (USGS), *Fault Number 1031b, Meers Fault, Quaternary Fault and Fold Database of the United States*, 1994. Available at <http://earthquakes.usgs.gov/regional/qfaults>, accessed December 7, 2007.
- 2.5.2-72 Gilbert, M.C., *The Meers Fault of Southwestern Oklahoma: Evidence for Possible Strong Quaternary Seismicity in the Midcontinent*, *EOS, Transactions of the American Geophysical Union*, Vol. 64, abstract T21B-13, pp. 313, 1983.
- 2.5.2-73 Gilbert, M.C., *The Meers Fault: Unusual Aspects and Possible Tectonic Consequences*, *Abstracts with Programs, Geological Society of America South Central Section Annual Meeting*, Vol. 15, abstract no. 17428, pp. 12,903, 1983.
- 2.5.2-74 Cetin, H., *Comment on 'Known and Suggested Quaternary Faulting in the Midcontinent United States' by Russell L. Wheeler and Anthony Crone*, *Engineering Geology*, Vol. 69, pp. 193–210, 2003.
- 2.5.2-75 Wheeler, R.L., and Crone, A.J., *Reply to Comment on Evaluation of Meers Fault, Oklahoma in 'Known and Suggested Quaternary Faulting in the Midcontinent United States' by Russell L. Wheeler and Anthony J. Crone*, *Engineering Geology*, Vol. 69, pp. 211–215, 2003.
- 2.5.2-76 Wells, D.L., and Coppersmith, K.J., *New Empirical Relationships Among Magnitude, Rupture Length, Rupture Width, Rupture Area, and Surface Displacement*, *Bulletin of the Seismological Society of America*, Vol. 84, pp. 974–1002, 1994.
- 2.5.2-77 McConnell, D.A., *Determination of Offset Across the Northern Margin of the Wichita Uplift, Southwest Oklahoma*, *Geological Society of America*, Vol. 101, pp. 1317–1332, 1989.
- 2.5.2-78 Luza, K.V., and Lawson, J.E., *Oklahoma Seismic Network*, NUREG/CR-6034, pp. 33, U.S. NRC, Washington, D.C., 1993.
- 2.5.2-79 Cook, F.A., McCullar, D.B., Decker, E.R., and Smithson, S.B., *Crustal Structure and Evolution of the Southern Rio Grande Rift, Rio Grande Rift in Southern New Mexico, West Texas, and Northern Chihuahua*, Riecker, R.E., ed., *American Geophysical Union*, Washington, D.C., 1979.

- 2.5.2-80 Seager, W.R., and Morgan, P., *Rio Grande Rift in Southern New Mexico, West Texas, and Northern Chihuahua, Rio Grande Rift: Tectonics and Magmatism*, Riecker, R.E., ed., p. 87–106, American Geophysical Union, Washington, D.C., 1979.
- 2.5.2-81 Tweto, O., *The Rio Grande Rift System in Colorado, Rio Grande Rift: Tectonics and Magmatism*, Riecker, R.E., ed., p. 33–56, American Geophysical Union, Washington, D.C., 1979.
- 2.5.2-82 Doser, D.I., *The 16 August 1931 Valentine, Texas, Earthquake: Evidence for Normal Faulting in West Texas, Bulletin of the Seismological Society of America*, Vol. 77, pp. 2005–2017, 1987.
- 2.5.2-83 Machette, M.N., *History of Quaternary Offset and Paleoseismicity Along the La Jencia Fault, Central Rio Grande Rift, New Mexico, Bulletin of the Seismological Society of America*, Vol. 76, p. 259–272, 1986.
- 2.5.2-84 McCalpin, J.P., *Frequency Distribution of Geologically Determined Slip Rates for Normal Faults in the Western United States, Bulletin of the Seismological Society of America*, Vol. 85, pp. 1867–1872, 1995.
- 2.5.2-85 McCalpin, J.P., *Late Quaternary Fault Activity of the Pajarito Fault, Rio Grande Rift of Northern New Mexico, USA, Tectonophysics*, Vol. 408, pp. 213–236, 2005.
- 2.5.2-86 Personius, S.F., and Mahan, S.A., *Paleoearthquake Recurrence on the East Paradise Fault Zone, Metropolitan Albuquerque, New Mexico, Bulletin of the Seismological Society of America*, Vol. 90, pp. 357–369, 2000.
- 2.5.2-87 Personius, S.F., and Mahan, S.A., *Paleoearthquakes and Eolian-Dominated Fault Sedimentation along the Hubbell Spring Fault Zone near Albuquerque, New Mexico, Bulletin of the Seismological Society of America*, Vol. 93, pp. 1355–1369, 2003.
- 2.5.2-88 Wong, I., Kelson, K.I., Olig, S., Kolbe, T., Hemphill-Haley, M., Bott, J., Green, R., Kanakari, H., et al., *Final Report: Seismic Hazards Evaluation of the Los Alamos National Laboratory*, Vol. 1, prepared for Los Alamos National Laboratory by Woodward-Clyde Federal Services, 1995.
- 2.5.2-89 Dickerson, P.W., and Muehlberger, W.R., *Basins of the Big Bend Segment of the Rio Grande Rift, Trans-Pecos Texas, Basins of the Rio Grande Rift: Structure, Stratigraphy, and Tectonic Setting*, Special Paper 291, Keller, G.R., and Cather, S.M., eds., Geologic Society of America, Boulder, CO, 1994.
- 2.5.2-90 U.S. Geological Survey (USGS), *Quaternary Fault and Fold Database for the United States, 2006*, Available at <http://earthquake.usgs.gov/regional/qfaults/>, accessed November 26, 2007.

- 2.5.2-91 Eaton, G., *The Basin and Range Province: Origin and Tectonic Significance*, *Annual Review of Earth and Planetary Sciences*, Vol. 10, pl. 409–440, 1982.
- 2.5.2-92 Eaton, G., *Topography and Origin of the Southern Rocky Mountains and Alvarado Ridge*, *Geological Society of London Special Publications*, Vol. 28, pp. 355–369, 1987.
- 2.5.2-93 Jones, C.H., Unruh, J.R., and Sonder, L.J., *The Role of Gravitational Potential Energy in Active Deformation in the Southwestern United States*, *Nature*, Vol. 381, pp. 37–41, 1996.
- 2.5.2-94 Doser, D.I., Baker, M.R., Luo, M., Marroquin, P., Ballesteros, L., Kingwell, J., Diaz, H.L., and Kaip, G., *The Not so Simple Relationship Between Seismicity and Oil Production in the Permian Basin, West Texas*, *Pure and Applied Geophysics*, Vol. 139, pp. 481–506, 1992.
- 2.5.2-95 Gray, G.G., Pottorf, R.J., Yurewic, D.A., Mahon, K.I., Pevear, D.R., and Chuchla, R.J., *Thermal and Chronological Record of Syn- to Post-Laramide Burial and Exhumation, Sierra Madre Oriental, Mexico, The Western Gulf of Mexico Basin: Tectonics, Sedimentary Basins, and Petroleum Systems*, Bartolini, C., Buffler, R.T., and Cantu-Chapa, A., eds., *Memoir 75*, pp. 159–181, American Association of Petroleum Geologists, 2001.
- 2.5.2-96 Murray, G.E., *Geology of the Atlantic and Gulf Coastal Province of North America*, pp. 692, New York, Harper and Brothers, 1961.
- 2.5.2-97 Johnston, A.C., *Seismic Moment Assessment of Earthquakes in Stable Continental Regions - III. New Madrid 1811–1812, Charleston 1886 and Lisbon 1755*, *Geophysical Journal International*, vol. 126, pp. 314–344, 1996.
- 2.5.2-98 Electric Power Research Institute (EPRI), *CEUS Ground Motion Project Final Report*, Technical Report 1009684, December 2004.
- 2.5.2-99 Abrahamson, N. A., and Bommer, J., *Program on Technology Innovation: Truncation of the Lognormal Distribution and Value of the Standard Deviation for Ground Motion Models in the Central and Eastern United States*, Technical Report 1014381, Electric Power Research Institute, August 2006.
- 2.5.2-100 Silva, W. J., Abrahamson, N. A., Toro, G. R., and Constantino, C. J., *Description and Validation of the Stochastic Ground Motion Model, Contract 770573*, Report to Brookhaven National Laboratory, Associated Universities, Inc., 1997.
- 2.5.2-101 Deleted.

- 2.5.2-102 Toro, G. and W. Silva, *Scenario Earthquakes For Saint Louis, MO, And Memphis, TN, and Seismic Hazard Maps for the Central United States Region Including the Effect of Site Conditions*, prepared under External Grant Number 1434-HQ-97-GR-02981 (Scenario Earthquakes and Seismic Hazard Mapping for the New Madrid Region), 2001.
- 2.5.2-103 Electric Power Research Institute (EPRI), *Program on Technology Innovation: Assessment of a Performance-Based Approach for Determining Seismic Ground Motions for New Plant Sites, Final Report*, Vol. 2, Seismic Hazard Results at 28 Sites, Report TR-1012045, August 2005.
- 2.5.2-104 Silva, W.J., *Probabilistic Models of Site Velocity Profiles for Generic and Site-Specific Ground Motion Amplification Studies, (Appendix), Description and Validation of the Stochastic Ground Motion Model*, Silva, W.J., N. Abrahamson, G. Toro and C. Costantino, report submitted to Brookhaven National Laboratory, contract No. 770573, Associated Universities, Inc. Upton New York 11973, 1996.
- 2.5.2-105 Constantino, C.J., *Recommendations for Uncertainty Estimates in Shear Modulus Reduction and Hysteretic Damping Relationships, (appendix), Description and Validation of the Stochastic Ground Motion Model*, Silva, W.J., N. Abrahamson, G. Toro and C. Costantino, report submitted to Brookhaven National Laboratory, contract No. 770573, Associated Universities, Inc. Upton New York 11973, 1996.
- 2.5.2-106 Der Kiureghian, A., *Structural Response to Stationary Excitation, Journal of the Engineering Mechanics Division*, Vol. 106, No. EM6, pp. 1195–1213, American Society of Civil Engineers, December, 1980.
- 2.5.2-107 Rathje, E. and Ozbey, C.M., *Site-Specific Validation of Random Vibration Theory-Based Seismic Site Response Analysis, Journal of Geotechnical and Geoenvironmental Engineering*, Vol. 132, no. 7, pp. 911–922, July 2006.
- 2.5.2-108 Idriss, I. M., and Sun, J. I., *SHAKE91: A Computer Program for Conducting Equivalent Linear Seismic Response Analyses of Horizontally Layered Soil Deposits*, Department of Civil and Environmental Engineering, Center for Geotechnical Modeling, University of California, 1992.
- 2.5.2-109 American Society of Civil Engineers (ASCE), *Seismic Analysis of Safety-Related Nuclear Structures and Commentary*, ASCE 4-98.
- 2.5.2-110 Schnabel, P. and Seed, H.B., *SHAKE- A Computer Program for Earthquake Response Analysis of Horizontally Layered Sites*, Report No. 72-12, Earthquake Engineering Research Center (EERC), December 1972.

- 2.5.2-111 Risk Engineering, Inc., *Technical Basis for Revision of Regulatory Guidance on Design Ground Motions: Development of Hazard- and Risk-Consistent Seismic Spectra for Two Sites*, Report No. NUREG/CR-6769, U.S. Nuclear Regulatory Commission, Washington, D.C., 2002.
- 2.5.2-112 American Society of Civil Engineers (ASCE), *Seismic Design Criteria for Structures, Systems, and Components in Nuclear Facilities*, Report No. ASCE/SEI 43-05, 2005.
- 2.5.2-113 Abrahamson, N.A, and Silva, W. J., *Empirical Response Spectral Attenuation Relations for Shallow Crustal Earthquakes*, *Seismological Research Letters*, Vol. 68, no. 1, pp. 94–127, 1997.

**Table 2.5.2-1**  
**Conversion Between Body-Wave ( $m_b$ ) and Moment ( $M_w$ ) Magnitudes<sup>(a)</sup>**

Convert	To	Convert	To
$m_b$	$M_w$	$M_w$	$m_b$
4.00	3.77	4.00	4.28
4.10	3.84	4.10	4.41
4.20	3.92	4.20	4.54
4.30	4.00	4.30	4.66
4.40	4.08	4.40	4.78
4.50	4.16	4.50	4.90
4.60	4.24	4.60	5.01
4.70	4.33	4.70	5.12
4.80	4.42	4.80	5.23
4.90	4.50	4.90	5.33
5.00	4.59	5.00	5.43
5.10	4.69	5.10	5.52
5.20	4.78	5.20	5.61
5.30	4.88	5.30	5.70
5.40	4.97	5.40	5.78
5.50	5.08	5.50	5.87
5.60	5.19	5.60	5.95
5.70	5.31	5.70	6.03
5.80	5.42	5.80	6.11
5.90	5.54	5.90	6.18
6.00	5.66	6.00	6.26
6.10	5.79	6.10	6.33
6.20	5.92	6.20	6.40
6.30	6.06	6.30	6.47
6.40	6.20	6.40	6.53
6.50	6.34	6.50	6.60
6.60	6.49	6.60	6.66
6.70	6.65	6.70	6.73
6.80	6.82	6.80	6.79
6.90	6.98	6.90	6.85
7.00	7.16	7.00	6.91
7.10	7.33	7.10	6.97
7.20	7.51	7.20	7.03
7.30	7.69	7.30	7.09
7.40	7.87	7.40	7.15
7.50	8.04	7.50	7.20
		7.60	7.26
		7.70	7.32
		7.80	7.37
		7.90	7.43
		8.00	7.49

(a) Average of relations given by [References 2.5.2-13, 2.5.2-15, and 2.5.2-14](#).

**Table 2.5.2-2**  
**Seismicity Catalog for Pre-1985 for the Gulf of Mexico Investigation Region [24°N to 32°N, 100°W to 83°W] for which the**  
**Events are Rmb Magnitude Greater than or Equal to 3.0 or Intensity Greater than or Equal to IV**

Catalog Reference	Year	Month	Day	Hour	Minute	Second	Lat (°N)	Lon (°W)	Depth (km)	Int (MMI)	Emb	Smb	Rmb
DPC	1847	2	14	2	0	0.00	29.600	98.000	0	V	3.60	0.56	3.96
DPC	1887	1	5	17	57	0.00	30.150	97.060	0	V	4.10	0.56	4.46
DPC	1887	1	31	22	14	0.00	30.530	96.300	0	IV	3.30	0.56	3.66
DPC	1902	10	9	19	0	0.00	30.100	97.600	0	IV	3.90	0.56	4.26
SRA	1981	2	13	2	15	0.00	30.000	91.800	0	IV	3.11	0.56	3.47
ANSS	1984	1	23	0	11	59.38	26.716	87.339	5	—	2.85	0.41	3.04

**Table 2.5.2-3 (Sheet 1 of 24)**  
**Seismicity Catalog from 1985 to Present for the Project Investigation Region [24°N to 40°N, 107°W to 83°W] for which the Events are Rmb Magnitude Greater than or Equal to 3.0 or Intensity Greater than or Equal to IV**

Catalog Reference	Year	Month	Day	Hour	Minute	Second	Lat (°N)	Lon (°W)	Depth (km)	Int (MMI)	Emb	Smb	Rmb
ANSS	1985	2	10	14	16	52.20	36.450	98.410	5		2.85	0.41	3.04
ANSS	1985	2	13	10	22	24.00	38.420	87.500	18		3.09	0.41	3.28
ANSS	1985	2	15	15	56	10.00	37.230	89.330	5		3.33	0.41	3.53
ANSS	1985	3	16	21	55	2.47	38.558	105.850	5		3.33	0.41	3.53
ANSS	1985	5	1	1	16	27.80	37.780	87.610	10		3.01	0.41	3.20
ANSS	1985	5	4	7	7	11.86	36.282	90.879	10		2.85	0.41	3.04
SRA	1985	5	6	2	11	16.20	34.969	97.482	5	V	2.30	0.10	2.31
ANSS	1985	6	5	10	36	0.60	32.562	106.916	6		3.01	0.41	3.20
SRA	1985	6	27	18	20	0.00	33.621	106.475	0		3.40	0.10	3.41
ANSS	1985	7	12	18	20	28.30	35.202	85.148	20		2.97	0.30	3.08
ANSS	1985	7	21	21	22	11.80	37.980	90.620	6		2.93	0.41	3.12
ANSS	1985	8	2	4	23	10.80	35.223	92.213	7		2.85	0.41	3.04
ANSS	1985	8	3	4	23	11.00	35.210	92.200	5		3.33	0.41	3.53
ANSS	1985	8	16	14	56	52.96	34.130	106.832	7		3.98	0.41	4.18
ANSS	1985	9	6	22	17	2.85	35.814	93.123	2		3.33	0.41	3.53
ANSS	1985	9	18	15	54	4.64	33.548	97.051	5		3.30	0.10	3.31
ANSS	1985	10	12	6	43	42.50	38.510	89.010	5		2.85	0.41	3.04
ANSS	1985	11	8	19	56	48.52	35.223	92.188	4		3.17	0.41	3.37
ANSS	1985	11	12	6	50	35.03	29.438	104.800	5		4.30	0.10	4.31
ANSS	1985	12	5	22	59	41.11	35.896	89.995	6		3.50	0.41	3.69
ANSS	1985	12	15	7	14	52.23	35.281	104.635	5		3.60	0.10	3.61
ANSS	1985	12	16	22	20	4.38	35.736	90.245	11		2.85	0.41	3.04
ANSS	1985	12	22	0	56	5.00	35.701	83.720	13		3.25	0.30	3.35
ANSS	1985	12	29	8	56	58.30	38.490	89.020	1		3.25	0.41	3.45
ANSS	1986	1	1	14	13	22.65	35.886	89.991	8		2.85	0.41	3.04
ANSS	1986	1	7	1	26	43.30	35.610	84.761	23		3.06	0.30	3.17
ANSS	1986	1	29	8	16	7.80	38.350	87.540	5		2.93	0.41	3.12

**Table 2.5.2-3 (Sheet 2 of 24)**  
**Seismicity Catalog from 1985 to Present for the Project Investigation Region [24°N to 40°N, 107°W to 83°W] for which the Events are Rmb Magnitude Greater than or Equal to 3.0 or Intensity Greater than or Equal to IV**

Catalog Reference	Year	Month	Day	Hour	Minute	Second	Lat (°N)	Lon (°W)	Depth (km)	Int (MMI)	Emb	Smb	Rmb
ANSS	1986	1	30	22	26	37.07	32.066	100.693	5		3.30	0.10	3.31
ANSS	1986	2	15	11	1	12.80	38.250	89.770	5		2.85	0.41	3.04
ANSS	1986	2	17	19	13	6.70	37.940	90.400	4		2.93	0.41	3.12
ANSS	1986	2	26	15	3	0.50	38.390	89.100	5		2.85	0.41	3.04
ANSS	1986	2	26	22	49	59.03	24.815	100.190	33		4.40	0.10	4.41
SRA	1986	2	28	4	12	57.90	33.296	83.245	1	IV	1.79	0.27	1.88
ANSS	1986	3	3	11	45	17.48	35.308	102.514	5		3.10	0.10	3.11
ANSS	1986	4	11	6	17	14.75	38.982	106.940	5		3.01	0.41	3.20
ANSS	1986	4	19	7	40	53.00	35.187	85.510	27		2.97	0.30	3.08
ANSS	1986	4	27	21	33	22.50	37.960	90.190	4		2.93	0.41	3.12
ANSS	1986	5	7	2	27	0.46	33.233	87.361	1		4.50	0.10	4.51
ANSS	1986	5	9	21	55	26.71	38.887	106.884	5		2.85	0.41	3.04
ISC	1986	5	12	4	18	2.70	27.714	88.726	10		3.50	0.10	3.51
ANSS	1986	5	12	4	18	48.30	30.900	89.150	10		2.93	0.41	3.12
ANSS	1986	5	24	8	16	1.50	35.118	92.217	4		3.17	0.41	3.37
ANSS	1986	5	24	12	48	14.43	36.484	89.917	13		3.17	0.41	3.37
ANSS	1986	6	2	4	4	5.20	39.344	99.781	5		3.00	0.10	3.01
ANSS	1986	6	4	4	38	10.68	25.211	100.717	33		3.50	0.10	3.51
ANSS	1986	6	8	8	52	55.36	24.497	100.015	10		3.70	0.10	3.71
ANSS	1986	7	11	14	26	14.80	34.937	84.987	13		3.74	0.41	3.93
ANSS	1986	8	26	16	41	24.80	38.320	89.790	5		3.58	0.41	3.77
ANSS	1986	8	27	18	6	56.38	35.160	105.094	5		3.25	0.41	3.45
ANSS	1986	10	20	4	32	49.00	37.918	101.372	5		3.00	0.10	3.01
ANSS	1986	10	29	5	3	41.30	38.440	89.040	5		3.09	0.41	3.28
ANSS	1986	11	6	19	21	47.20	38.110	90.420	9		2.85	0.41	3.04
ANSS	1986	12	12	23	51	48.26	36.903	89.128	12		2.85	0.41	3.04
ANSS	1986	12	30	7	15	19.09	36.418	89.629	13		3.25	0.41	3.45
ANSS	1987	1	16	3	25	35.96	35.902	90.012	8		2.93	0.41	3.12

**Table 2.5.2-3 (Sheet 3 of 24)**  
**Seismicity Catalog from 1985 to Present for the Project Investigation Region [24°N to 40°N, 107°W to 83°W] for which the Events are Rmb Magnitude Greater than or Equal to 3.0 or Intensity Greater than or Equal to IV**

Catalog Reference	Year	Month	Day	Hour	Minute	Second	Lat (°N)	Lon (°W)	Depth (km)	Int (MMI)	Emb	Smb	Rmb
ANSS	1987	1	24	16	8	17.00	35.828	98.097	5		3.10	0.10	3.11
ANSS	1987	3	13	18	37	7.00	39.090	89.410	1		3.25	0.41	3.45
ANSS	1987	3	14	11	51	1.29	36.117	89.770	10		2.85	0.41	3.04
ANSS	1987	3	27	7	29	30.50	35.565	84.230	19		4.07	0.41	4.26
ANSS	1987	4	16	10	55	9.49	38.358	105.651	5		2.85	0.41	3.04
ANSS	1987	4	26	0	56	21.50	38.540	89.410	5		3.17	0.41	3.37
ANSS	1987	5	2	19	51	28.81	36.290	89.553	10		3.01	0.41	3.20
PDE	1987	5	14	15	59	58.46	33.545	106.519	0		3.01	0.41	3.20
ANSS	1987	5	20	0	2	12.64	35.155	92.244	3		3.01	0.41	3.20
ANSS	1987	5	23	19	8	23.82	36.614	89.620	11		3.33	0.41	3.53
ANSS	1987	6	4	17	19	23.40	37.939	85.800	8		3.06	0.30	3.17
ANSS	1987	6	10	23	48	53.90	38.710	87.950	5		4.88	0.41	5.07
ANSS	1987	6	13	21	17	13.50	36.576	89.735	10		3.98	0.41	4.18
ANSS	1987	6	15	15	5	16.41	36.547	89.697	13		2.85	0.41	3.04
ANSS	1987	6	19	3	46	38.29	36.466	89.587	19		3.09	0.41	3.28
ANSS	1987	6	23	0	0	19.40	38.720	87.950	5		2.93	0.41	3.12
ANSS	1987	6	26	18	39	20.38	36.534	89.674	13		3.09	0.41	3.28
ANSS	1987	7	7	19	19	6.30	36.941	89.148	17		3.33	0.41	3.53
ANSS	1987	7	11	0	4	29.50	36.105	83.816	25		3.66	0.41	3.85
ANSS	1987	7	11	2	48	5.90	36.103	83.819	24		3.25	0.41	3.45
ANSS	1987	7	20	16	19	16.10	38.955	106.507	5		2.93	0.41	3.12
ANSS	1987	8	14	18	27	56.67	35.706	90.385	11		2.85	0.41	3.04
ANSS	1987	8	31	17	12	35.20	38.300	89.680	0		3.33	0.41	3.53
ANSS	1987	9	1	23	2	49.40	35.515	84.396	21		3.06	0.30	3.17
ANSS	1987	9	22	17	23	50.10	35.623	84.312	19		3.33	0.41	3.53
ANSS	1987	9	29	0	4	56.13	36.953	89.159	11		4.15	0.41	4.34
ANSS	1987	10	14	15	49	40.10	37.050	88.780	2		3.74	0.41	3.93
ANSS	1987	11	17	15	52	21.10	38.720	87.960	5		3.25	0.41	3.45

**Table 2.5.2-3 (Sheet 4 of 24)**  
**Seismicity Catalog from 1985 to Present for the Project Investigation Region [24°N to 40°N, 107°W to 83°W] for which the Events are Rmb Magnitude Greater than or Equal to 3.0 or Intensity Greater than or Equal to IV**

Catalog Reference	Year	Month	Day	Hour	Minute	Second	Lat (°N)	Lon (°W)	Depth (km)	Int (MMI)	Emb	Smb	Rmb
ANSS	1987	12	8	1	42	40.30	36.055	98.024	5		3.70	0.10	3.71
ANSS	1988	1	5	14	39	18.20	38.720	87.960	5		3.33	0.41	3.53
ANSS	1988	1	9	1	7	40.60	35.279	84.199	12		3.16	0.30	3.26
ANSS	1988	1	15	7	33	29.20	37.515	106.684	5		3.17	0.41	3.37
ANSS	1988	1	31	0	12	44.36	35.664	90.440	15		3.33	0.41	3.53
ANSS	1988	1	31	9	24	36.30	29.945	105.076	5		3.90	0.41	4.10
ANSS	1988	2	18	0	37	45.40	35.346	83.837	2		3.50	0.41	3.69
ANSS	1988	2	27	15	17	6.50	36.680	89.520	15		3.25	0.41	3.45
ANSS	1988	3	10	21	24	9.50	37.750	88.830	4		3.09	0.41	3.28
ANSS	1988	3	15	12	34	48.70	38.300	89.000	12		2.93	0.41	3.12
ANSS	1988	4	14	9	39	31.47	39.093	99.155	5		3.60	0.10	3.61
ANSS	1988	5	2	13	43	59.42	35.666	90.351	8		2.85	0.41	3.04
ANSS	1988	5	20	23	6	23.90	37.310	92.670	5		3.42	0.41	3.61
ANSS	1988	6	25	15	2	49.26	36.669	89.593	5		2.85	0.41	3.04
ANSS	1988	9	7	2	28	9.54	38.143	83.878	10		4.60	0.10	4.61
ANSS	1988	9	7	2	30	32.90	38.170	83.756	8		3.74	0.41	3.93
ANSS	1988	9	18	16	16	1.00	37.310	87.210	13		2.85	0.41	3.04
ANSS	1988	10	5	0	38	55.00	38.660	88.020	5		3.33	0.41	3.53
ANSS	1988	12	25	15	57	57.83	34.206	92.658	12		3.42	0.41	3.61
ANSS	1988	12	29	2	52	13.70	38.990	87.730	5		3.01	0.41	3.20
ANSS	1988	12	31	14	24	20.68	36.193	89.430	6		3.09	0.41	3.28
ANSS	1989	1	3	19	8	51.30	38.990	87.720	5		2.93	0.41	3.12
ANSS	1989	1	29	5	7	15.33	35.221	104.093	7		3.34	0.30	3.44
ANSS	1989	2	28	17	31	50.84	33.643	87.092	0		3.50	0.10	3.51
ANSS	1989	4	15	16	39	51.66	36.558	89.682	10		2.85	0.41	3.04
ANSS	1989	4	27	16	47	51.33	36.088	89.775	12		4.15	0.41	4.34
ANSS	1989	6	8	18	18	43.37	39.165	99.477	5		4.00	0.10	4.01
ANSS	1989	6	16	14	53	53.12	39.143	99.457	5		3.80	0.10	3.81

**Table 2.5.2-3 (Sheet 5 of 24)**  
**Seismicity Catalog from 1985 to Present for the Project Investigation Region [24°N to 40°N, 107°W to 83°W] for which the Events are Rmb Magnitude Greater than or Equal to 3.0 or Intensity Greater than or Equal to IV**

Catalog Reference	Year	Month	Day	Hour	Minute	Second	Lat (°N)	Lon (°W)	Depth (km)	Int (MMI)	Emb	Smb	Rmb
ANSS	1989	6	28	9	35	0.20	37.810	88.950	13		3.01	0.41	3.20
ANSS	1989	7	6	10	38	25.56	38.772	102.635	5		2.93	0.41	3.12
ANSS	1989	7	13	18	35	22.90	39.168	99.472	5		3.40	0.10	3.41
ANSS	1989	7	14	23	32	22.39	36.295	89.494	11		2.85	0.41	3.04
ANSS	1989	7	15	0	8	2.64	38.607	83.569	10		3.10	0.10	3.11
ANSS	1989	7	15	18	58	28.00	34.373	87.323	14		2.93	0.41	3.12
ANSS	1989	7	20	6	7	50.42	36.434	98.876	5		3.10	0.10	3.11
ANSS	1989	8	13	20	16	2.90	33.632	87.086	0		3.40	0.10	3.41
ANSS	1989	8	20	0	3	18.30	34.803	87.596	7		3.82	0.41	4.02
ANSS	1989	9	14	17	31	27.90	36.558	89.630	12		3.25	0.41	3.45
ANSS	1989	10	9	1	43	33.19	35.794	90.153	13		2.93	0.41	3.12
ANSS	1989	10	30	5	6	56.46	36.555	89.696	8		2.85	0.41	3.04
ANSS	1989	11	29	6	54	38.50	34.455	106.891	13		4.52	0.30	4.62
ANSS	1989	12	1	9	26	51.30	36.216	89.440	9		2.85	0.41	3.04
ANSS	1989	12	2	13	31	45.60	35.993	83.847	11		3.01	0.41	3.20
ANSS	1990	1	24	18	20	26.20	38.140	86.490	10		3.82	0.41	4.02
ANSS	1990	1	27	14	5	51.67	38.184	86.430	5		3.74	0.41	3.93
ANSS	1990	1	29	13	16	10.68	34.463	106.879	12		4.80	0.10	4.81
ANSS	1990	1	31	1	8	19.29	34.445	106.860	10		4.00	0.10	4.01
ANSS	1990	2	21	12	2	19.34	34.014	106.544	5		3.58	0.41	3.77
ANSS	1990	2	27	13	23	22.00	33.953	106.588	5		3.79	0.30	3.89
ANSS	1990	3	2	7	1	48.07	38.851	89.170	0		3.42	0.41	3.61
ANSS	1990	3	9	21	2	54.80	38.140	86.190	5		2.85	0.41	3.04
ANSS	1990	3	12	16	48	1.67	36.359	92.251	0		2.93	0.41	3.12
ANSS	1990	3	18	16	22	33.19	36.692	91.505	1		3.09	0.41	3.28
ANSS	1990	4	24	9	41	36.57	38.955	88.201	18		3.01	0.41	3.20
ANSS	1990	5	5	16	26	22.89	34.449	106.878	7		3.52	0.30	3.62
ANSS	1990	6	23	20	44	2.74	33.762	87.969	1		3.25	0.41	3.45

**Table 2.5.2-3 (Sheet 6 of 24)**  
**Seismicity Catalog from 1985 to Present for the Project Investigation Region [24°N to 40°N, 107°W to 83°W] for which the Events are Rmb Magnitude Greater than or Equal to 3.0 or Intensity Greater than or Equal to IV**

Catalog Reference	Year	Month	Day	Hour	Minute	Second	Lat (°N)	Lon (°W)	Depth (km)	Int (MMI)	Emb	Smb	Rmb
ANSS	1990	7	15	18	22	48.50	37.880	90.840	3		2.85	0.41	3.04
ANSS	1990	7	21	19	28	22.79	34.458	106.858	12		2.97	0.30	3.08
ANSS	1990	7	21	20	30	31.34	34.455	106.856	7		3.06	0.30	3.17
ANSS	1990	7	21	23	48	4.92	34.453	106.854	7		3.16	0.30	3.26
ANSS	1990	7	22	21	27	5.13	34.838	106.006	10		3.61	0.30	3.71
ANSS	1990	7	28	7	53	33.75	34.600	93.376	4		3.01	0.41	3.20
ANSS	1990	7	31	7	32	40.18	34.456	106.862	8		3.25	0.30	3.35
ANSS	1990	8	7	5	5	56.22	36.857	89.237	7		3.17	0.41	3.37
ANSS	1990	8	17	21	1	15.90	36.934	83.384	1		3.90	0.41	4.10
ANSS	1990	8	24	19	43	50.60	37.200	89.110	5		2.93	0.41	3.12
ANSS	1990	8	29	19	34	59.25	35.785	89.644	15		3.42	0.41	3.61
ANSS	1990	9	2	4	35	40.20	33.758	87.928	1		3.16	0.30	3.26
ANSS	1990	9	8	0	3	57.40	38.061	83.731	5		3.30	0.10	3.31
ANSS	1990	9	12	21	38	57.62	39.701	106.206	5		3.09	0.41	3.28
ANSS	1990	9	16	21	14	13.19	35.537	92.275	2		2.93	0.41	3.12
ANSS	1990	9	26	13	18	51.71	37.152	89.613	1		4.55	0.41	4.75
ANSS	1990	9	27	1	47	52.95	37.172	89.594	15		2.93	0.41	3.12
ANSS	1990	10	24	8	20	3.67	38.346	88.971	1		3.25	0.41	3.45
ANSS	1990	11	8	10	8	25.40	37.108	83.031	0		3.16	0.30	3.26
ANSS	1990	11	8	10	46	53.77	34.449	106.856	6		4.40	0.10	4.41
ANSS	1990	11	8	11	3	46.51	34.453	106.861	9		3.06	0.30	3.17
ANSS	1990	11	9	3	39	15.92	36.537	89.632	10		3.25	0.41	3.45
ANSS	1990	11	10	12	18	16.85	34.450	106.851	7		3.06	0.30	3.17
ANSS	1990	11	15	7	25	24.38	34.457	106.859	7		3.52	0.30	3.62
ANSS	1990	11	15	11	44	41.40	34.760	97.590	5		3.90	0.10	3.91
ANSS	1990	11	15	11	45	35.06	35.603	93.042	29		3.50	0.41	3.69
ANSS	1990	12	20	14	4	17.40	39.590	86.630	5		3.66	0.41	3.85
ANSS	1991	1	23	9	25	23.20	37.940	88.873	1		3.17	0.41	3.37

**Table 2.5.2-3 (Sheet 7 of 24)**  
**Seismicity Catalog from 1985 to Present for the Project Investigation Region [24°N to 40°N, 107°W to 83°W] for which the Events are Rmb Magnitude Greater than or Equal to 3.0 or Intensity Greater than or Equal to IV**

Catalog Reference	Year	Month	Day	Hour	Minute	Second	Lat (°N)	Lon (°W)	Depth (km)	Int (MMI)	Emb	Smb	Rmb
ANSS	1991	1	24	5	0	26.90	36.378	97.300	5		3.00	0.10	3.01
ANSS	1991	1	28	11	43	55.70	37.349	87.324	1		2.93	0.41	3.12
ANSS	1991	2	6	10	3	2.72	28.428	106.332	5		3.90	0.10	3.91
ANSS	1991	2	11	0	0	12.70	35.950	89.930	14		3.09	0.41	3.28
ANSS	1991	2	11	15	36	44.30	34.108	90.599	12		2.85	0.41	3.04
ANSS	1991	3	23	10	5	54.70	36.074	89.805	13		2.85	0.41	3.04
ANSS	1991	4	16	4	6	37.80	38.593	88.007	7		2.85	0.41	3.04
ANSS	1991	5	4	1	18	54.60	36.575	89.825	11		4.31	0.41	4.50
ANSS	1991	5	10	12	15	54.33	37.459	106.578	5		3.42	0.41	3.61
ANSS	1991	5	30	22	7	44.00	39.200	99.400	5		3.50	0.10	3.51
ANSS	1991	6	1	22	1	41.30	36.521	89.616	2		2.85	0.41	3.04
ANSS	1991	6	5	18	44	14.90	34.447	106.849	4		2.97	0.30	3.08
ISC	1991	6	20	16	5	0.00	33.619	106.475	0		3.50	0.41	3.69
ANSS	1991	7	7	21	24	3.60	36.685	91.567	8		3.82	0.41	4.02
ANSS	1991	7	22	3	31	0.30	36.468	89.546	9		2.85	0.41	3.04
ANSS	1991	9	24	7	21	7.00	35.701	84.117	13		3.09	0.41	3.28
ANSS	1991	10	3	11	46	4.90	36.856	89.449	2		2.85	0.41	3.04
ANSS	1991	10	30	14	54	12.60	34.904	84.713	8		3.06	0.30	3.17
ANSS	1991	11	11	9	20	44.00	38.905	87.710	0		3.74	0.41	3.93
ANSS	1991	11	13	9	43	15.70	35.728	90.292	13		2.85	0.41	3.04
ANSS	1991	11	16	3	39	2.01	25.895	100.581	5		3.60	0.10	3.61
ANSS	1991	12	9	12	47	16.50	34.850	106.553	14		3.10	0.10	3.11
ANSS	1991	12	13	11	41	46.50	35.856	90.085	14		3.01	0.41	3.20
ANSS	1992	1	2	11	45	35.61	32.336	103.101	5		5.00	0.10	5.01
ANSS	1992	1	21	11	36	21.00	38.000	92.670	5		3.06	0.30	3.17
ANSS	1992	2	23	16	17	52.51	30.646	105.507	5		3.40	0.10	3.41
ISC	1992	3	31	14	59	43.60	26.311	85.895	5		3.80	0.10	3.81
ANSS	1992	4	3	3	6	4.20	35.832	89.499	8		3.01	0.41	3.20

**Table 2.5.2-3 (Sheet 8 of 24)**  
**Seismicity Catalog from 1985 to Present for the Project Investigation Region [24°N to 40°N, 107°W to 83°W] for which the Events are Rmb Magnitude Greater than or Equal to 3.0 or Intensity Greater than or Equal to IV**

Catalog Reference	Year	Month	Day	Hour	Minute	Second	Lat (°N)	Lon (°W)	Depth (km)	Int (MMI)	Emb	Smb	Rmb
ANSS	1992	4	15	22	46	5.08	37.335	104.773	5		3.30	0.10	3.31
ANSS	1992	4	30	0	1	30.51	36.932	90.439	10		2.85	0.41	3.04
ANSS	1992	5	2	10	19	29.81	37.378	104.778	5		3.10	0.10	3.11
ANSS	1992	7	15	2	56	40.75	38.760	99.549	5		3.30	0.10	3.31
ANSS	1992	7	30	14	40	55.87	24.705	99.779	10		4.30	0.10	4.31
ANSS	1992	8	26	3	24	52.67	32.173	102.708	5		3.00	0.10	3.01
ANSS	1992	8	26	5	41	39.06	37.641	89.683	2		2.93	0.41	3.12
ANSS	1992	9	11	16	34	11.70	33.171	87.501	7		2.97	0.30	3.08
ISC	1992	9	27	17	2	34.40	28.192	88.431	10		3.58	0.41	3.77
ANSS	1992	10	1	1	31	48.97	27.832	102.374	5		3.80	0.10	3.81
ANSS	1992	11	10	17	16	46.80	35.644	84.132	10		2.97	0.30	3.08
ANSS	1992	12	17	7	18	4.27	34.744	97.581	5		3.60	0.10	3.61
ANSS	1992	12	27	10	12	58.76	37.501	89.616	10		3.25	0.41	3.45
ANSS	1993	1	3	21	14	54.14	35.194	90.244	17		2.85	0.41	3.04
ANSS	1993	1	8	13	1	18.70	35.929	90.036	22		3.50	0.41	3.69
ANSS	1993	1	14	17	6	10.45	36.595	98.275	5		3.10	0.10	3.11
ANSS	1993	1	15	2	2	50.90	35.039	85.025	8		3.17	0.41	3.37
ANSS	1993	1	21	19	46	20.07	36.229	89.597	6		3.09	0.41	3.28
ANSS	1993	1	29	13	56	24.17	39.033	89.030	5		3.25	0.41	3.45
ANSS	1993	2	6	2	9	45.63	36.664	89.733	8		3.33	0.41	3.53
ANSS	1993	2	24	12	41	21.80	36.167	89.473	13		2.93	0.41	3.12
ANSS	1993	2	28	21	48	1.33	26.063	101.930	5		3.80	0.10	3.81
ANSS	1993	3	2	0	29	11.86	36.673	89.494	9		3.09	0.41	3.28
ANSS	1993	3	16	7	38	10.27	35.605	90.478	12		3.09	0.41	3.28
ANSS	1993	3	24	2	32	3.50	35.391	104.195	5		3.00	0.10	3.01
ANSS	1993	3	29	15	37	21.13	36.555	89.586	10		2.85	0.41	3.04
ANSS	1993	3	31	20	23	21.30	36.799	89.423	4		3.17	0.41	3.37
ANSS	1993	4	28	22	40	1.96	36.196	89.442	7		3.42	0.41	3.61

**Table 2.5.2-3 (Sheet 9 of 24)**  
**Seismicity Catalog from 1985 to Present for the Project Investigation Region [24°N to 40°N, 107°W to 83°W] for which the**  
**Events are Rmb Magnitude Greater than or Equal to 3.0 or Intensity Greater than or Equal to IV**

Catalog Reference	Year	Month	Day	Hour	Minute	Second	Lat (°N)	Lon (°W)	Depth (km)	Int (MMI)	Emb	Smb	Rmb
ISC	1993	6	10	15	10	0.00	33.619	106.475	0		3.25	0.41	3.45
ANSS	1993	6	16	1	47	12.62	37.651	89.756	10		2.85	0.41	3.04
ANSS	1993	7	8	4	3	52.25	39.227	106.715	5		3.17	0.41	3.37
ANSS	1993	7	16	10	54	32.86	31.747	88.341	5		3.70	0.10	3.71
ANSS	1993	8	5	7	21	37.45	36.009	89.885	12		3.01	0.41	3.20
ANSS	1993	8	27	0	8	33.35	38.091	90.437	22		3.33	0.41	3.53
ANSS	1993	9	24	18	27	15.04	36.564	89.582	7		2.93	0.41	3.12
ANSS	1993	9	29	2	1	19.06	35.868	102.981	5		3.30	0.10	3.31
ANSS	1993	11	30	3	7	31.82	35.863	103.026	5		3.30	0.10	3.31
ANSS	1993	12	5	0	58	20.23	27.831	102.737	5		4.70	0.10	4.71
ANSS	1993	12	22	19	25	11.39	33.331	105.682	10		3.16	0.30	3.26
ANSS	1994	1	5	23	0	56.00	25.887	106.933	10		3.80	0.10	3.81
ANSS	1994	2	5	14	55	37.79	37.368	89.188	16		4.07	0.41	4.26
ANSS	1994	2	28	18	29	49.07	37.833	89.374	5		3.09	0.41	3.28
ANSS	1994	3	21	17	34	18.16	36.860	89.172	5		3.01	0.41	3.20
ANSS	1994	4	5	22	22	0.40	34.969	85.491	24		3.25	0.41	3.45
ANSS	1994	4	6	17	38	56.17	38.156	89.214	15		3.25	0.41	3.45
ISC	1994	4	16	7	20	20.00	34.660	97.710	5		3.17	0.23	3.23
ANSS	1994	4	23	19	46	47.90	35.965	90.050	5		3.25	0.41	3.45
ANSS	1994	4	29	3	28	58.68	36.250	98.090	5		3.00	0.10	3.01
ANSS	1994	5	4	9	12	3.40	34.222	87.195	19		3.09	0.41	3.28
ANSS	1994	6	10	23	34	2.92	33.013	92.671	5		3.20	0.10	3.21
ISC	1994	6	30	1	8	24.00	27.849	90.123	10		3.70	0.10	3.71
ANSS	1994	8	19	16	3	30.65	35.508	89.919	11		3.25	0.41	3.45
ANSS	1994	8	20	10	45	45.33	36.140	91.063	10		3.50	0.41	3.69
ANSS	1994	9	26	14	23	22.84	36.960	88.920	13		3.42	0.41	3.61
ANSS	1994	11	6	12	50	38.95	35.949	89.060	11		3.17	0.41	3.37
ANSS	1994	11	20	23	31	48.98	36.437	89.514	6		2.85	0.41	3.04

**Table 2.5.2-3 (Sheet 10 of 24)**  
**Seismicity Catalog from 1985 to Present for the Project Investigation Region [24°N to 40°N, 107°W to 83°W] for which the**  
**Events are Rmb Magnitude Greater than or Equal to 3.0 or Intensity Greater than or Equal to IV**

Catalog Reference	Year	Month	Day	Hour	Minute	Second	Lat (°N)	Lon (°W)	Depth (km)	Int (MMI)	Emb	Smb	Rmb
ANSS	1994	12	25	19	6	7.52	39.290	104.811	10		4.00	0.10	4.01
FDNC	1995	1	4	1	46	14.10	29.450	96.950	5	IV	2.70	0.10	2.71
ANSS	1995	1	18	15	51	39.42	34.774	97.596	5		4.20	0.10	4.21
ANSS	1995	1	31	11	33	52.17	27.739	105.114	10		3.50	0.10	3.51
ANSS	1995	2	19	12	57	6.00	39.120	83.470	10		3.52	0.30	3.62
ANSS	1995	3	11	8	15	52.32	36.959	83.133	1		3.80	0.10	3.81
ANSS	1995	3	11	9	50	4.44	36.990	83.180	1		3.30	0.10	3.31
ANSS	1995	3	18	22	6	20.80	35.422	84.941	26		3.25	0.30	3.35
ANSS	1995	3	19	18	36	43.97	35.000	104.212	5		3.30	0.10	3.31
ANSS	1995	4	5	5	31	16.23	35.200	99.028	5		3.00	0.10	3.01
ANSS	1995	4	14	0	32	56.17	30.285	103.347	18		5.60	0.10	5.61
ANSS	1995	4	14	2	19	38.50	30.300	103.350	10		3.30	0.10	3.31
ANSS	1995	4	15	14	33	29.51	30.271	103.324	10		4.00	0.10	4.01
ANSS	1995	4	27	0	42	35.00	36.690	89.480	5		2.93	0.41	3.12
ANSS	1995	5	27	19	51	8.00	36.180	89.390	10		3.09	0.41	3.28
ANSS	1995	5	28	15	28	36.95	33.191	87.827	1		3.40	0.10	3.41
ANSS	1995	5	31	19	57	36.23	24.948	103.869	10		3.80	0.10	3.81
ANSS	1995	6	1	1	6	15.70	30.300	103.350	10		3.50	0.10	3.51
ANSS	1995	6	1	4	49	29.32	34.287	96.732	5		3.00	0.10	3.01
ANSS	1995	6	6	21	27	8.00	36.180	89.370	8		3.17	0.41	3.37
ANSS	1995	6	29	9	27	19.00	36.630	89.780	12		3.09	0.41	3.28
ANSS	1995	6	29	20	7	48.00	36.580	89.770	10		2.93	0.41	3.12
ANSS	1995	7	4	3	59	4.53	36.246	104.814	5		3.74	0.41	3.93
ANSS	1995	7	5	14	16	44.70	35.334	84.163	10		3.66	0.41	3.85
ANSS	1995	7	9	12	42	56.00	35.880	91.400	5		2.93	0.41	3.12
ANSS	1995	7	15	1	3	28.35	33.478	87.665	1		3.30	0.10	3.31
ANSS	1995	7	20	2	10	34.00	36.540	89.620	9		2.85	0.41	3.04
ANSS	1995	7	31	0	47	48.00	37.690	90.810	5		2.93	0.41	3.12

**Table 2.5.2-3 (Sheet 11 of 24)**  
**Seismicity Catalog from 1985 to Present for the Project Investigation Region [24°N to 40°N, 107°W to 83°W] for which the Events are Rmb Magnitude Greater than or Equal to 3.0 or Intensity Greater than or Equal to IV**

Catalog Reference	Year	Month	Day	Hour	Minute	Second	Lat (°N)	Lon (°W)	Depth (km)	Int (MMI)	Emb	Smb	Rmb
ANSS	1995	8	17	23	18	52.00	36.110	89.370	18		3.09	0.41	3.28
ANSS	1995	8	28	15	13	39.05	34.205	106.942	4		2.93	0.41	3.12
ANSS	1995	9	5	23	1	21.00	38.360	89.040	4		3.01	0.41	3.20
ANSS	1995	9	15	0	31	33.26	36.870	98.690	5		3.98	0.41	4.18
ANSS	1995	10	2	18	0	54.00	35.340	90.120	9		2.85	0.41	3.04
ANSS	1995	10	26	0	37	28.96	37.053	83.121	1		3.90	0.41	4.10
ANSS	1995	11	12	17	45	59.40	30.300	103.350	10		3.58	0.41	3.77
ANSS	1995	11	24	1	52	35.00	36.600	89.820	18		2.93	0.41	3.12
ANSS	1995	12	1	14	37	40.44	35.061	99.337	5		3.01	0.41	3.20
ANSS	1995	12	15	10	16	39.90	36.193	83.694	10		2.93	0.41	3.12
ANSS	1995	12	23	6	51	48.88	38.732	104.917	5		3.58	0.41	3.77
ANSS	1995	12	31	0	37	38.19	38.716	104.910	5		2.93	0.41	3.12
ISC	1996	3	15	12	3	35.50	33.230	104.740	0		3.50	0.41	3.69
ANSS	1996	3	15	13	17	57.22	33.586	105.694	10		3.01	0.41	3.20
ANSS	1996	3	24	20	16	12.70	34.255	105.681	10		3.50	0.41	3.69
ANSS	1996	3	24	20	19	23.10	34.270	105.689	10		3.66	0.41	3.85
ANSS	1996	3	25	6	43	46.86	35.610	102.601	5		3.50	0.41	3.69
ANSS	1996	3	25	14	15	50.55	32.131	88.671	5		3.50	0.41	3.69
ISC	1996	3	31	18	39	42.60	37.077	83.899	0		3.50	0.10	3.51
ANSS	1996	4	4	23	55	5.00	35.520	90.540	9		2.85	0.41	3.04
ANSS	1996	4	11	21	54	56.00	34.900	91.310	6		2.93	0.41	3.12
ANSS	1996	4	19	8	50	14.01	36.981	83.018	0		3.90	0.10	3.91
ISC	1996	5	13	20	18	59.30	36.776	83.004	13		3.40	0.10	3.41
ANSS	1996	7	5	21	37	9.60	35.200	84.000	5		2.93	0.41	3.12
ANSS	1996	7	16	0	35	6.00	35.760	90.200	7		2.93	0.41	3.12
ANSS	1996	7	22	10	6	14.98	34.204	105.711	10		3.50	0.41	3.69
ANSS	1996	8	1	5	44	22.75	37.398	104.247	5		3.74	0.41	3.93
ANSS	1996	8	1	5	55	54.16	37.378	104.196	5		3.25	0.41	3.45

**Table 2.5.2-3 (Sheet 12 of 24)**  
**Seismicity Catalog from 1985 to Present for the Project Investigation Region [24°N to 40°N, 107°W to 83°W] for which the Events are Rmb Magnitude Greater than or Equal to 3.0 or Intensity Greater than or Equal to IV**

Catalog Reference	Year	Month	Day	Hour	Minute	Second	Lat (°N)	Lon (°W)	Depth (km)	Int (MMI)	Emb	Smb	Rmb
ANSS	1996	8	11	18	17	49.88	33.577	90.874	10		3.50	0.41	3.69
ANSS	1996	10	13	18	57	46.00	38.410	89.380	23		2.85	0.41	3.04
ANSS	1996	11	1	3	9	28.35	37.349	104.232	5		3.25	0.41	3.45
ANSS	1996	11	5	19	48	19.00	37.330	90.220	4		2.93	0.41	3.12
ANSS	1996	11	23	10	54	18.50	35.040	100.504	5		3.09	0.41	3.28
ANSS	1996	11	29	5	41	34.00	35.930	89.930	20		4.15	0.41	4.34
ANSS	1996	11	29	10	47	10.00	36.240	89.450	4		3.42	0.41	3.61
ANSS	1996	12	15	7	19	57.00	36.030	89.830	8		2.93	0.41	3.12
ANSS	1996	12	16	1	58	31.35	39.500	87.400	5		3.17	0.41	3.37
ANSS	1997	1	9	3	7	25.99	33.200	92.600	5		2.93	0.41	3.12
ANSS	1997	1	18	22	4	39.00	39.100	105.100	5		3.30	0.10	3.31
ANSS	1997	1	19	4	36	15.00	39.100	105.100	5		2.85	0.41	3.04
ANSS	1997	2	12	23	53	10.77	34.947	100.890	5		3.09	0.41	3.28
ANSS	1997	2	15	9	8	55.46	34.973	100.569	5		3.25	0.41	3.45
ANSS	1997	3	16	19	7	28.00	34.270	93.490	5		3.42	0.41	3.61
ISC	1997	4	18	14	57	46.30	26.922	87.284	33		3.80	0.10	3.81
ANSS	1997	5	4	3	39	12.99	31.000	87.400	5		3.17	0.41	3.37
ANSS	1997	5	19	19	45	35.80	34.622	85.353	3		3.01	0.41	3.20
ANSS	1997	5	20	9	41	5.82	34.188	105.742	10		3.25	0.41	3.45
ANSS	1997	5	31	3	26	41.34	33.182	95.966	5		3.42	0.41	3.61
ANSS	1997	7	19	17	6	34.40	34.953	84.811	3		3.50	0.41	3.69
ANSS	1997	7	30	12	29	25.30	36.512	83.547	23		3.74	0.41	3.93
ANSS	1997	9	6	23	38	0.91	34.660	96.435	5		4.31	0.41	4.50
ANSS	1997	9	13	19	50	32.00	38.290	89.710	16		2.93	0.41	3.12
ANSS	1997	9	17	18	16	32.00	35.670	90.490	7		3.74	0.41	3.93
ANSS	1997	9	24	4	20	26.00	36.580	89.890	12		2.93	0.41	3.12
ANSS	1997	9	27	12	14	10.00	36.200	89.420	9		3.01	0.41	3.20
ISC	1997	10	19	11	12	12.10	32.332	103.395	0		3.58	0.10	3.59

**Table 2.5.2-3 (Sheet 13 of 24)**  
**Seismicity Catalog from 1985 to Present for the Project Investigation Region [24°N to 40°N, 107°W to 83°W] for which the Events are Rmb Magnitude Greater than or Equal to 3.0 or Intensity Greater than or Equal to IV**

Catalog Reference	Year	Month	Day	Hour	Minute	Second	Lat (°N)	Lon (°W)	Depth (km)	Int (MMI)	Emb	Smb	Rmb
EHB98	1997	10	24	8	35	18.83	31.126	87.283	3	.	4.80	0.10	4.81
ISC	1997	12	6	11	11	23.60	34.895	95.968	5		3.01	0.10	3.02
ANSS	1997	12	11	11	34	57.00	37.101	98.480	5		2.85	0.41	3.04
ANSS	1997	12	12	8	42	20.25	33.466	87.306	1		3.90	0.41	4.10
ANSS	1997	12	31	13	28	30.05	34.533	106.154	5		3.50	0.41	3.69
ANSS	1997	12	31	13	32	6.60	34.550	106.150	5		3.50	0.41	3.69
ANSS	1997	12	31	13	33	58.90	34.550	106.150	5		3.42	0.41	3.61
ANSS	1998	1	2	15	47	16.43	37.828	103.408	5		3.42	0.41	3.61
ANSS	1998	1	4	8	5	31.87	34.553	106.191	5		3.90	0.41	4.10
ANSS	1998	1	28	22	5	12.00	36.100	89.770	8		2.85	0.41	3.04
ANSS	1998	2	12	9	37	49.00	36.140	89.710	9		3.09	0.41	3.28
ANSS	1998	2	19	14	5	27.00	36.530	89.580	8		2.85	0.41	3.04
ANSS	1998	4	8	18	16	49.00	36.940	89.010	8		3.25	0.41	3.45
ANSS	1998	4	9	5	13	41.00	36.400	89.500	7		2.85	0.41	3.04
ANSS	1998	4	15	10	33	42.42	30.188	103.303	10		3.58	0.41	3.77
ANSS	1998	4	18	22	45	43.10	39.100	105.100	5		2.85	0.41	3.04
ANSS	1998	4	27	15	22	46.25	35.453	102.383	5		3.25	0.41	3.45
ANSS	1998	4	28	14	13	1.68	34.782	98.416	5		4.07	0.41	4.26
ANSS	1998	5	7	12	24	41.40	32.370	88.110	10		2.85	0.41	3.04
ANSS	1998	6	17	8	0	23.90	35.944	84.392	11		3.58	0.41	3.77
ISC	1998	6	18	17	21	5.90	25.183	106.684	0		4.50	0.10	4.51
ANSS	1998	6	24	15	20	1.39	32.502	87.954	5		3.42	0.41	3.61
ISC	1998	7	6	6	54	4.10	25.035	93.626	10		3.40	0.10	3.41
ANSS	1998	7	7	18	44	44.46	34.719	97.589	5		3.25	0.41	3.45
ANSS	1998	7	14	5	38	48.75	35.344	103.473	5		3.01	0.41	3.20
ANSS	1998	7	15	4	24	51.00	36.690	89.520	14		3.17	0.41	3.37
ANSS	1998	7	22	22	11	57.00	37.670	90.020	5		2.85	0.41	3.04
ISC	1998	8	14	17	5	11.80	27.744	99.864	0		3.90	0.10	3.91

**Table 2.5.2-3 (Sheet 14 of 24)**  
**Seismicity Catalog from 1985 to Present for the Project Investigation Region [24°N to 40°N, 107°W to 83°W] for which the Events are Rmb Magnitude Greater than or Equal to 3.0 or Intensity Greater than or Equal to IV**

Catalog Reference	Year	Month	Day	Hour	Minute	Second	Lat (°N)	Lon (°W)	Depth (km)	Int (MMI)	Emb	Smb	Rmb
ANSS	1998	10	15	9	47	22.00	35.630	90.430	4		3.01	0.41	3.20
ANSS	1998	10	30	17	41	22.20	36.800	97.600	5		3.50	0.41	3.69
ANSS	1999	1	7	5	16	26.96	38.674	99.378	5		3.09	0.41	3.28
ANSS	1999	1	17	18	38	5.10	36.893	83.799	1		3.06	0.30	3.17
ANSS	1999	1	18	7	0	53.47	33.405	87.255	1		4.80	0.10	4.81
ANSS	1999	2	25	2	11	31.00	34.180	89.810	5		3.01	0.41	3.20
ANSS	1999	3	1	8	0	23.50	32.573	104.656	1		3.01	0.41	3.20
ANSS	1999	3	14	22	43	17.97	32.591	104.630	1		3.90	0.41	4.10
ANSS	1999	3	17	12	29	23.11	32.582	104.672	1		3.43	0.30	3.53
ANSS	1999	5	13	14	18	22.75	39.100	94.700	5		3.09	0.41	3.28
ANSS	1999	5	30	19	4	25.60	32.575	104.664	10		3.82	0.41	4.02
ANSS	1999	8	23	12	12	41.00	36.260	89.500	9		3.17	0.41	3.37
ANSS	1999	10	21	8	17	59.00	36.540	91.100	11		3.82	0.41	4.02
ANSS	1999	10	21	8	49	49.00	36.500	90.990	9		3.17	0.41	3.37
ANSS	1999	10	25	23	19	58.37	36.846	99.659	26		3.09	0.41	3.28
ANSS	1999	11	26	6	54	59.00	36.480	92.400	5		3.01	0.41	3.20
ANSS	1999	11	28	11	0	9.30	33.416	87.253	1		3.74	0.41	3.93
ISC	2000	1	14	10	39	34.90	34.674	95.095	18		3.09	0.23	3.15
ANSS	2000	1	18	22	19	32.20	32.920	83.465	19		3.50	0.41	3.69
ANSS	2000	2	2	7	14	20.26	32.582	104.629	5		2.85	0.41	3.04
ANSS	2000	2	4	1	36	26.88	39.092	99.417	5		2.93	0.41	3.12
ANSS	2000	2	26	3	1	0.83	30.243	103.612	5		2.93	0.41	3.12
ANSS	2000	3	6	15	2	28.00	38.100	87.570	5		2.85	0.41	3.04
ANSS	2000	4	14	3	54	20.00	39.760	86.750	5		3.58	0.41	3.77
ANSS	2000	4	28	23	36	26.00	37.690	88.460	5		3.01	0.41	3.20
ANSS	2000	5	28	11	32	7.02	33.809	87.820	5		3.09	0.41	3.28
ANSS	2000	6	15	23	17	14.63	25.450	100.999	33		4.60	0.10	4.61
ANSS	2000	6	27	1	28	45.00	35.800	92.750	0		3.82	0.41	4.02

**Table 2.5.2-3 (Sheet 15 of 24)**  
**Seismicity Catalog from 1985 to Present for the Project Investigation Region [24°N to 40°N, 107°W to 83°W] for which the Events are Rmb Magnitude Greater than or Equal to 3.0 or Intensity Greater than or Equal to IV**

Catalog Reference	Year	Month	Day	Hour	Minute	Second	Lat (°N)	Lon (°W)	Depth (km)	Int (MMI)	Emb	Smb	Rmb
ANSS	2000	6	27	6	2	57.00	37.130	88.870	4		3.01	0.41	3.20
ANSS	2000	8	2	12	21	30.06	35.200	101.900	5		2.85	0.41	3.04
ANSS	2000	8	7	17	19	8.00	35.392	101.812	5		3.33	0.41	3.53
ANSS	2000	8	7	18	34	9.00	35.392	101.812	5		3.09	0.41	3.28
ANSS	2000	8	7	21	36	21.00	35.392	101.812	5		3.09	0.41	3.28
ANSS	2000	8	10	13	39	50.00	35.392	101.812	5		3.09	0.41	3.28
ANSS	2000	8	17	1	8	5.45	35.390	101.814	5		3.82	0.41	4.02
ANSS	2000	8	22	20	12	15.00	36.490	91.110	11		3.82	0.41	4.02
ANSS	2000	9	20	6	24	59.00	24.622	99.933	33		4.20	0.10	4.21
ANSS	2000	12	7	14	8	50.00	38.010	87.680	5		3.82	0.41	4.02
ISC	2000	12	9	6	46	9.20	28.017	90.134	10		3.90	0.10	3.91
ANSS	2000	12	16	22	8	54.00	35.400	101.800	5		3.82	0.41	4.02
ANSS	2001	3	3	10	46	13.00	33.190	92.660	5		3.09	0.41	3.28
ANSS	2001	3	7	17	12	23.80	35.552	84.850	7		3.25	0.41	3.45
ISC	2001	3	16	4	39	9.30	28.545	88.946	10		3.70	0.10	3.71
ANSS	2001	3	21	23	35	34.90	34.847	85.438	0		3.16	0.30	3.26
ANSS	2001	3	30	17	13	55.60	37.933	93.327	5		3.17	0.41	3.37
ISC	2001	4	4	10	27	19.80	24.145	106.838	137		3.20	0.10	3.21
ANSS	2001	4	13	16	36	20.70	36.526	83.342	0		2.97	0.30	3.08
ANSS	2001	5	4	6	42	12.00	35.240	92.250	10		4.23	0.41	4.42
ANSS	2001	5	4	8	31	43.00	35.250	92.230	0		2.85	0.41	3.04
ANSS	2001	5	5	7	38	44.00	35.210	92.230	7		2.85	0.41	3.04
ANSS	2001	6	2	1	55	53.72	32.334	103.141	5		3.33	0.41	3.53
ANSS	2001	7	7	20	45	43.00	36.270	89.400	14		3.17	0.41	3.37
ANSS	2001	7	14	22	40	28.00	36.260	89.420	7		2.85	0.41	3.04
ANSS	2001	7	22	19	22	45.57	39.022	105.129	5		3.17	0.41	3.37
ANSS	2001	7	24	14	2	35.00	37.700	97.000	5		3.09	0.41	3.28
ANSS	2001	7	26	5	26	46.00	35.971	83.552	14		3.25	0.41	3.45

**Table 2.5.2-3 (Sheet 16 of 24)**  
**Seismicity Catalog from 1985 to Present for the Project Investigation Region [24°N to 40°N, 107°W to 83°W] for which the Events are Rmb Magnitude Greater than or Equal to 3.0 or Intensity Greater than or Equal to IV**

Catalog Reference	Year	Month	Day	Hour	Minute	Second	Lat (°N)	Lon (°W)	Depth (km)	Int (MMI)	Emb	Smb	Rmb
ANSS	2001	8	4	1	13	28.00	34.420	93.230	0		3.25	0.41	3.45
ANSS	2001	8	28	14	16	9.52	37.088	104.692	5		3.42	0.41	3.61
ANSS	2001	8	28	14	22	0.33	37.091	104.655	5		3.50	0.41	3.69
ANSS	2001	9	4	12	22	44.97	37.107	104.622	5		3.42	0.41	3.61
ANSS	2001	9	4	12	45	53.22	37.143	104.650	5		3.90	0.41	4.10
ANSS	2001	9	5	10	52	7.89	37.143	104.618	5		4.31	0.41	4.50
ANSS	2001	9	5	14	48	58.26	37.112	104.611	5		3.66	0.41	3.85
ANSS	2001	9	6	9	41	43.59	37.110	104.628	5		3.58	0.41	3.77
ANSS	2001	9	6	11	28	26.49	37.140	104.585	5		3.50	0.41	3.69
ANSS	2001	9	10	18	56	0.37	37.108	104.602	5		3.42	0.41	3.61
ANSS	2001	9	13	11	22	16.48	37.108	104.703	5		2.93	0.41	3.12
ANSS	2001	9	13	16	39	5.44	37.091	104.593	5		3.09	0.41	3.28
ANSS	2001	9	21	19	10	59.67	37.121	104.706	5		3.42	0.41	3.61
ANSS	2001	11	13	1	56	13.13	39.996	100.208	5		3.33	0.41	3.53
ANSS	2001	11	22	0	7	8.02	31.786	102.631	5		3.17	0.41	3.37
ANSS	2001	12	8	1	8	22.40	34.710	86.231	0		3.82	0.41	4.02
ANSS	2001	12	15	7	58	31.36	36.859	104.797	5		3.33	0.41	3.53
ANSS	2001	12	17	1	54	44.76	33.200	92.700	10		2.93	0.41	3.12
ANSS	2002	1	26	1	6	3.86	36.860	104.784	5		3.42	0.41	3.61
ANSS	2002	2	7	5	19	55.41	36.857	104.744	5		2.93	0.41	3.12
ANSS	2002	2	8	16	7	13.60	34.727	98.361	5		3.74	0.41	3.93
ANSS	2002	2	17	23	1	41.00	36.540	89.640	8		3.01	0.41	3.20
ANSS	2002	3	12	8	30	47.00	37.250	89.960	10		3.17	0.41	3.37
ANSS	2002	3	31	2	54	8.13	35.359	101.824	5		2.93	0.41	3.12
ANSS	2002	4	14	3	35	2.13	39.939	100.320	5		2.93	0.41	3.12
ANSS	2002	4	20	20	0	0.00	36.130	89.390	7		2.93	0.41	3.12
ANSS	2002	4	27	2	33	43.00	35.960	89.960	5		2.85	0.41	3.04
ANSS	2002	5	21	20	35	34.43	32.797	88.102	5		3.17	0.41	3.37

**Table 2.5.2-3 (Sheet 17 of 24)**  
**Seismicity Catalog from 1985 to Present for the Project Investigation Region [24°N to 40°N, 107°W to 83°W] for which the Events are Rmb Magnitude Greater than or Equal to 3.0 or Intensity Greater than or Equal to IV**

Catalog Reference	Year	Month	Day	Hour	Minute	Second	Lat (°N)	Lon (°W)	Depth (km)	Int (MMI)	Emb	Smb	Rmb
ISC	2002	5	27	0	28	22.00	27.664	94.530	10		3.90	0.10	3.91
ANSS	2002	5	31	9	57	10.02	34.025	97.619	5		3.33	0.41	3.53
ANSS	2002	6	18	9	12	36.66	36.881	104.779	5		3.50	0.41	3.69
ANSS	2002	6	18	17	37	15.17	37.987	87.780	5		5.01	0.10	5.02
ANSS	2002	6	19	12	14	20.30	36.568	103.028	5		3.66	0.41	3.85
ANSS	2002	7	29	11	28	7.00	35.920	90.030	8		2.93	0.41	3.12
ANSS	2002	8	11	23	19	47.00	34.340	90.180	5		2.93	0.41	3.12
ANSS	2002	9	8	9	3	24.00	35.670	89.640	6		2.85	0.41	3.04
ANSS	2002	9	17	15	45	14.47	32.581	104.630	10		3.50	0.41	3.69
ANSS	2002	9	17	23	34	19.35	32.576	104.631	10		3.33	0.41	3.53
ISC	2002	9	19	14	44	36.20	27.820	89.131	10		3.80	0.10	3.81
ANSS	2002	10	13	22	18	54.59	39.203	106.654	5		2.93	0.41	3.12
ANSS	2002	10	20	2	18	13.00	34.274	96.079	5		3.42	0.41	3.61
ANSS	2002	10	26	14	8	39.00	36.470	89.550	8		3.01	0.41	3.20
ANSS	2002	10	26	20	5	55.00	33.950	90.720	5		3.17	0.41	3.37
ANSS	2002	11	1	11	8	56.28	39.119	99.089	5		3.09	0.41	3.28
ANSS	2002	11	1	14	19	56.16	39.077	99.101	5		2.93	0.41	3.12
ANSS	2002	11	14	4	56	52.26	36.917	104.768	5		3.25	0.41	3.45
ANSS	2002	12	11	14	25	23.54	39.360	99.403	5		2.93	0.41	3.12
ISC	2002	12	31	19	2	29.10	37.034	104.620	0		4.66	0.10	4.67
ANSS	2003	1	1	7	43	37.91	39.155	106.759	5		3.01	0.41	3.20
ANSS	2003	1	3	16	17	7.00	37.830	88.090	5		3.01	0.41	3.20
ISC	2003	1	4	23	25	5.90	24.344	100.159	10		3.30	0.10	3.31
ANSS	2003	1	10	10	29	22.46	38.256	102.622	5		3.01	0.41	3.20
ANSS	2003	4	1	13	9	49.61	39.244	99.487	5		2.93	0.41	3.12
ANSS	2003	4	7	10	2	12.51	33.892	97.695	5		3.01	0.41	3.20
ISC	2003	4	13	4	52	53.90	26.096	86.080	10		3.50	0.10	3.51
ANSS	2003	4	17	17	31	59.07	39.255	99.482	5		3.09	0.41	3.28

**Table 2.5.2-3 (Sheet 18 of 24)**  
**Seismicity Catalog from 1985 to Present for the Project Investigation Region [24°N to 40°N, 107°W to 83°W] for which the  
 Events are Rmb Magnitude Greater than or Equal to 3.0 or Intensity Greater than or Equal to IV**

Catalog Reference	Year	Month	Day	Hour	Minute	Second	Lat (°N)	Lon (°W)	Depth (km)	Int (MMI)	Emb	Smb	Rmb
ANSS	2003	4	28	7	32	26.04	36.844	104.923	5		3.58	0.41	3.77
ANSS	2003	4	29	8	59	38.10	34.445	85.620	9		4.39	0.41	4.58
ANSS	2003	4	29	9	45	45.00	34.440	85.640	3		3.01	0.41	3.20
ANSS	2003	4	30	4	56	22.00	35.920	89.920	24		3.90	0.41	4.10
ANSS	2003	5	2	3	25	3.00	36.730	89.680	2		2.85	0.41	3.04
ANSS	2003	5	2	8	10	13.00	37.960	88.650	1		3.25	0.41	3.45
ANSS	2003	5	2	10	48	44.00	34.490	85.610	15		3.17	0.41	3.37
ANSS	2003	5	30	2	18	24.00	36.130	89.390	6		2.93	0.41	3.12
ANSS	2003	6	3	18	9	27.84	36.994	104.768	5		3.33	0.41	3.53
ANSS	2003	6	6	12	29	34.00	36.870	88.980	3		3.90	0.41	4.10
ANSS	2003	6	10	7	46	31.00	36.020	91.390	5		2.85	0.41	3.04
ANSS	2003	6	15	0	22	17.97	36.910	104.763	5		3.58	0.41	3.77
ANSS	2003	6	21	2	3	9.56	32.665	104.505	5		3.58	0.41	3.77
ANSS	2003	7	8	5	55	5.00	38.150	91.500	3		3.17	0.41	3.37
ANSS	2003	7	29	21	52	46.86	24.595	105.120	10		4.33	0.30	4.44
ANSS	2003	7	30	2	50	19.00	36.520	89.530	4		2.93	0.41	3.12
ANSS	2003	8	14	0	11	8.96	36.945	104.870	5		3.33	0.41	3.53
ANSS	2003	8	26	2	26	58.00	37.100	88.680	2		3.17	0.41	3.37
ANSS	2003	9	8	11	2	49.31	37.369	104.685	5		3.09	0.41	3.28
ANSS	2003	9	13	15	22	40.99	36.831	104.907	5		3.74	0.41	3.93
ANSS	2003	9	16	2	22	45.00	36.100	89.760	7		2.85	0.41	3.04
ISC	2003	9	19	18	14	25.40	36.982	104.751	0		4.50	0.10	4.51
ANSS	2003	9	24	15	2	9.09	35.277	101.742	5		3.33	0.41	3.53
ANSS	2003	9	30	2	28	3.38	31.115	87.520	5		3.33	0.41	3.53
ANSS	2003	10	25	12	55	55.58	37.031	104.836	5		3.01	0.41	3.20
ANSS	2003	11	24	7	5	57.72	36.958	104.828	5		3.17	0.41	3.37
ANSS	2003	12	14	10	16	41.00	35.200	92.250	5		2.93	0.41	3.12
ANSS	2003	12	15	5	57	18.00	35.200	92.240	5		2.85	0.41	3.04

**Table 2.5.2-3 (Sheet 19 of 24)**  
**Seismicity Catalog from 1985 to Present for the Project Investigation Region [24°N to 40°N, 107°W to 83°W] for which the Events are Rmb Magnitude Greater than or Equal to 3.0 or Intensity Greater than or Equal to IV**

Catalog Reference	Year	Month	Day	Hour	Minute	Second	Lat (°N)	Lon (°W)	Depth (km)	Int (MMI)	Emb	Smb	Rmb
ANSS	2003	12	21	5	20	6.00	36.290	89.500	9		2.85	0.41	3.04
ANSS	2003	12	28	2	55	2.32	37.596	105.280	5		3.50	0.41	3.69
ANSS	2003	12	28	3	57	3.21	37.584	105.298	5		3.17	0.41	3.37
ANSS	2003	12	29	9	2	8.00	38.130	90.170	5		3.09	0.41	3.28
ANSS	2003	12	31	15	8	5.68	33.668	91.695	5		2.93	0.41	3.12
ANSS	2004	1	14	1	14	15.47	37.018	104.842	5		3.01	0.41	3.20
ANSS	2004	2	3	14	34	22.57	36.932	104.861	5		3.42	0.41	3.61
ANSS	2004	2	8	5	56	45.00	39.490	91.880	5		3.01	0.41	3.20
ANSS	2004	2	9	18	21	49.00	36.350	90.750	13		3.01	0.41	3.20
ANSS	2004	3	20	10	40	35.47	33.232	87.008	5		2.93	0.41	3.12
ANSS	2004	3	22	12	9	56.46	36.855	104.851	5		4.40	0.10	4.41
ANSS	2004	3	30	1	2	55.40	36.892	104.876	5		3.09	0.41	3.28
ANSS	2004	3	30	2	23	37.86	36.876	104.831	5		3.17	0.41	3.37
ANSS	2004	3	30	2	41	4.15	37.036	104.931	5		3.50	0.41	3.69
ANSS	2004	4	6	19	1	2.70	25.172	99.532	38		4.33	0.30	4.44
ANSS	2004	4	22	16	13	2.25	34.804	97.677	5		3.01	0.41	3.20
ANSS	2004	5	3	19	25	48.00	36.280	89.450	3		2.85	0.41	3.04
ANSS	2004	5	9	8	56	10.43	33.231	86.960	5		3.33	0.41	3.53
ANSS	2004	5	23	9	22	5.28	32.525	104.566	5		4.00	0.10	4.01
ANSS	2004	5	24	21	36	28.56	34.465	106.899	5		3.50	0.41	3.69
ANSS	2004	5	31	3	27	43.77	36.935	104.835	5		3.33	0.41	3.53
ANSS	2004	6	8	0	15	9.99	34.233	97.254	5		3.50	0.41	3.69
ANSS	2004	6	10	12	30	9.86	34.236	97.267	5		3.01	0.41	3.20
ANSS	2004	6	15	8	34	21.00	36.730	89.680	5		3.42	0.41	3.61
ANSS	2004	6	16	4	7	21.00	36.730	89.690	4		2.93	0.41	3.12
ISC	2004	6	18	19	20	56.40	27.027	86.997	10		3.50	0.10	3.51
ANSS	2004	6	22	8	55	28.23	32.528	104.584	5		3.66	0.41	3.85
ANSS	2004	7	16	3	25	17.00	36.860	89.180	4		3.58	0.41	3.77

**Table 2.5.2-3 (Sheet 20 of 24)**  
**Seismicity Catalog from 1985 to Present for the Project Investigation Region [24°N to 40°N, 107°W to 83°W] for which the Events are Rmb Magnitude Greater than or Equal to 3.0 or Intensity Greater than or Equal to IV**

Catalog Reference	Year	Month	Day	Hour	Minute	Second	Lat (°N)	Lon (°W)	Depth (km)	Int (MMI)	Emb	Smb	Rmb
ANSS	2004	8	1	6	50	47.63	36.874	105.104	5		4.66	0.10	4.67
ANSS	2004	8	19	23	51	49.42	33.203	86.968	5		3.70	0.10	3.71
ANSS	2004	8	26	18	45	18.62	32.582	104.505	5		3.42	0.41	3.61
ANSS	2004	8	28	5	6	43.67	33.221	86.924	5		2.93	0.41	3.12
ANSS	2004	9	10	6	39	21.00	35.369	98.048	5		2.93	0.41	3.12
ANSS	2004	9	12	13	5	19.00	39.590	85.790	5		3.58	0.41	3.77
ANSS	2004	9	12	23	31	23.00	36.420	89.920	5		2.85	0.41	3.04
ANSS	2004	9	17	15	21	43.60	36.933	84.004	1		3.66	0.41	3.85
ANSS	2004	10	28	2	59	4.82	32.604	104.499	5		3.09	0.41	3.28
ANSS	2004	11	7	11	20	21.43	32.649	87.933	5		4.66	0.10	4.67
ANSS	2004	11	14	21	27	49.90	33.253	106.201	5		3.50	0.41	3.69
ANSS	2004	11	22	23	42	13.45	34.864	97.672	5		3.09	0.41	3.28
ANSS	2004	11	30	23	59	34.00	36.940	93.890	9		3.01	0.41	3.20
ANSS	2004	11	30	23	59	34.20	36.936	83.893	10		2.97	0.30	3.08
ANSS	2004	12	23	6	54	20.70	35.429	84.204	8		2.97	0.30	3.08
ANSS	2005	1	5	3	37	56.76	27.750	104.987	5		3.25	0.41	3.45
ANSS	2005	1	10	10	14	59.15	37.007	104.675	5		3.42	0.41	3.61
ANSS	2005	1	27	17	52	55.00	35.200	92.220	4		2.85	0.41	3.04
ANSS	2005	2	10	14	4	54.00	35.760	90.250	16		3.98	0.41	4.18
ANSS	2005	3	18	1	2	16.00	35.720	84.160	9		2.85	0.41	3.04
ANSS	2005	3	22	8	11	50.51	31.836	88.060	5		3.33	0.41	3.53
ANSS	2005	4	3	14	39	16.97	28.393	100.305	5		3.50	0.41	3.69
ANSS	2005	4	5	20	37	43.00	36.150	83.690	10		3.01	0.41	3.20
ANSS	2005	4	6	8	45	24.57	36.881	104.794	5		3.01	0.41	3.20
ANSS	2005	4	14	15	38	16.00	35.470	84.090	15		2.93	0.41	3.12
ANSS	2005	4	22	5	17	4.09	34.179	95.192	5		3.09	0.41	3.28
ANSS	2005	4	24	11	2	35.90	36.920	105.070	5		3.42	0.41	3.61
ANSS	2005	5	1	12	37	32.00	35.830	90.150	10		3.98	0.41	4.18

**Table 2.5.2-3 (Sheet 21 of 24)**  
**Seismicity Catalog from 1985 to Present for the Project Investigation Region [24°N to 40°N, 107°W to 83°W] for which the Events are Rmb Magnitude Greater than or Equal to 3.0 or Intensity Greater than or Equal to IV**

Catalog Reference	Year	Month	Day	Hour	Minute	Second	Lat (°N)	Lon (°W)	Depth (km)	Int (MMI)	Emb	Smb	Rmb
ANSS	2005	5	16	22	29	46.84	35.250	97.608	5		2.93	0.41	3.12
ANSS	2005	5	18	19	59	42.90	38.460	93.967	5		3.33	0.41	3.53
ANSS	2005	6	2	11	35	11.00	36.150	89.470	15		3.82	0.41	4.02
ANSS	2005	6	7	16	33	36.71	33.531	87.304	5		2.93	0.41	3.12
ANSS	2005	6	20	2	0	32.00	36.930	88.990	10		2.85	0.41	3.04
ANSS	2005	6	20	12	21	42.00	36.920	89.000	19		3.58	0.41	3.77
ANSS	2005	6	27	15	46	52.00	37.630	89.420	10		3.09	0.41	3.28
ANSS	2005	7	4	10	45	24.50	36.860	105.097	5		3.09	0.41	3.28
ANSS	2005	7	8	6	24	1.12	36.938	104.886	5		3.09	0.41	3.28
ANSS	2005	7	13	12	8	13.00	35.810	90.160	11		2.93	0.41	3.12
ANSS	2005	7	31	7	7	7.97	38.718	92.725	5		3.33	0.41	3.53
ANSS	2005	8	10	22	8	16.96	36.952	104.822	5		4.10	0.10	4.11
ANSS	2005	8	10	22	24	33.94	36.982	104.959	5		3.09	0.41	3.28
ANSS	2005	8	15	0	12	57.00	35.870	90.010	6		3.01	0.41	3.20
ANSS	2005	10	12	6	27	30.00	35.510	84.540	8		3.58	0.41	3.77
ANSS	2005	10	20	8	15	36.58	36.970	104.849	5		3.09	0.41	3.28
ANSS	2005	11	16	3	11	32.64	37.099	104.897	5		3.01	0.41	3.20
ANSS	2005	12	6	16	24	14.00	38.420	89.200	4		2.85	0.41	3.04
ANSS	2005	12	19	20	27	40.37	32.528	104.549	5		4.41	0.10	4.42
ANSS	2005	12	20	0	52	20.51	30.258	90.708	5		3.09	0.41	3.28
ISC	2005	12	22	14	30	12.40	32.599	104.390	0		3.25	0.10	3.26
ANSS	2005	12	25	14	33	45.00	36.530	89.660	12		2.93	0.41	3.12
ANSS	2006	1	2	21	48	57.00	37.840	88.420	11		3.58	0.41	3.77
ANSS	2006	1	27	16	7	45.84	32.551	104.577	5		3.17	0.41	3.37
ANSS	2006	1	27	18	48	49.23	37.030	104.968	5		3.33	0.41	3.53
ANSS	2006	2	4	19	55	10.68	32.575	104.617	5		2.85	0.41	3.04
ANSS	2006	2	10	4	14	17.80	27.597	90.163	5		5.52	0.41	5.71
ANSS	2006	2	11	13	3	50.48	37.076	105.444	5		3.01	0.41	3.20

**Table 2.5.2-3 (Sheet 22 of 24)**  
**Seismicity Catalog from 1985 to Present for the Project Investigation Region [24°N to 40°N, 107°W to 83°W] for which the Events are Rmb Magnitude Greater than or Equal to 3.0 or Intensity Greater than or Equal to IV**

Catalog Reference	Year	Month	Day	Hour	Minute	Second	Lat (°N)	Lon (°W)	Depth (km)	Int (MMI)	Emb	Smb	Rmb
ANSS	2006	2	18	5	49	41.45	35.672	101.794	5		3.50	0.41	3.69
ANSS	2006	3	1	17	42	42.00	37.500	88.980	6		3.09	0.41	3.28
ANSS	2006	3	4	17	14	58.25	30.289	103.674	5		2.85	0.41	3.04
ANSS	2006	3	11	2	37	20.00	35.200	88.010	2		2.85	0.41	3.04
ANSS	2006	3	15	8	30	25.86	35.091	96.300	5		2.97	0.30	3.08
ANSS	2006	3	20	17	55	29.12	32.600	104.563	5		3.09	0.41	3.28
ANSS	2006	3	28	23	55	11.49	35.363	101.871	5		3.09	0.41	3.28
ANSS	2006	4	5	18	46	23.14	34.069	97.314	5		3.09	0.41	3.28
ANSS	2006	4	8	15	59	43.25	28.010	105.123	10		3.58	0.41	3.77
ANSS	2006	4	8	18	8	35.23	31.954	101.419	5		3.01	0.41	3.20
ANSS	2006	4	9	14	41	29.00	35.240	92.240	8		2.93	0.41	3.12
ANSS	2006	4	11	3	29	21.00	35.360	84.480	20		3.33	0.41	3.53
ANSS	2006	4	17	16	25	12.29	24.432	100.091	17		4.10	0.10	4.11
ANSS	2006	5	6	17	7	1.34	37.014	104.768	5		3.17	0.41	3.37
ANSS	2006	5	10	12	17	29.00	35.530	84.400	25		3.25	0.41	3.45
ISC	2006	5	14	3	4	0.50	26.058	106.944	33		4.10	0.10	4.11
ANSS	2006	5	18	13	1	15.00	38.050	90.530	6		3.01	0.41	3.20
ANSS	2006	5	26	6	14	25.12	36.795	104.832	5		3.17	0.41	3.37
ANSS	2006	6	16	0	57	27.00	35.510	83.200	1		3.42	0.41	3.61
ANSS	2006	7	11	11	53	37.78	36.964	104.929	5		3.25	0.41	3.45
ANSS	2006	8	7	8	44	28.00	34.940	85.460	14		3.01	0.41	3.20
ANSS	2006	8	12	10	49	9.67	32.895	100.894	5		2.93	0.41	3.12
ANSS	2006	8	24	14	4	25.88	37.014	105.013	5		3.17	0.41	3.37
ANSS	2006	9	7	13	51	13.00	36.270	89.500	8		3.33	0.41	3.53
ANSS	2006	9	9	9	54	6.65	37.296	104.770	5		3.25	0.41	3.45
ANSS	2006	9	9	12	53	14.21	37.368	104.865	5		3.09	0.41	3.28
ANSS	2006	9	9	18	5	41.79	37.374	104.736	5		3.01	0.41	3.20
ANSS	2006	9	9	23	14	35.54	37.298	104.794	5		3.58	0.41	3.77

**Table 2.5.2-3 (Sheet 23 of 24)**  
**Seismicity Catalog from 1985 to Present for the Project Investigation Region [24°N to 40°N, 107°W to 83°W] for which the Events are Rmb Magnitude Greater than or Equal to 3.0 or Intensity Greater than or Equal to IV**

Catalog Reference	Year	Month	Day	Hour	Minute	Second	Lat (°N)	Lon (°W)	Depth (km)	Int (MMI)	Emb	Smb	Rmb
ANSS	2006	9	10	14	56	8.16	26.319	86.606	14		6.11	0.10	6.12
ANSS	2006	9	14	13	3	24.26	37.010	104.867	5		3.09	0.41	3.28
ANSS	2006	9	30	12	40	0.12	37.061	104.971	5		2.93	0.41	3.12
ANSS	2006	10	6	22	13	16.78	34.122	97.625	5		3.50	0.41	3.69
ANSS	2006	10	17	5	18	4.00	35.230	92.290	4		2.93	0.41	3.12
ANSS	2006	10	18	20	59	21.00	36.540	89.640	8		3.42	0.41	3.61
ANSS	2006	10	30	2	35	13.47	36.811	104.963	5		3.50	0.41	3.69
ANSS	2006	11	24	23	22	24.10	37.040	104.996	5		3.17	0.41	3.37
ANSS	2006	12	18	8	34	26.60	35.356	84.347	15		3.33	0.41	3.53
ANSS	2006	12	24	11	50	21.47	36.935	104.750	5		3.58	0.41	3.77
ANSS	2007	1	3	14	34	38.54	37.067	104.895	5		4.78	0.10	4.79
ANSS	2007	1	3	23	5	45.00	35.920	83.950	15		2.85	0.41	3.04
ANSS	2007	1	14	5	17	36.69	36.878	104.930	5		3.25	0.41	3.45
ANSS	2007	1	31	23	47	43.00	36.910	89.010	16		3.01	0.41	3.20
ANSS	2007	2	12	18	32	33.66	35.441	97.459	5		2.93	0.41	3.12
ANSS	2007	2	13	0	15	48.89	35.459	97.482	5		2.93	0.41	3.12
ANSS	2007	2	25	11	24	19.15	37.099	104.773	5		3.17	0.41	3.37
ANSS	2007	3	12	6	32	14.59	37.061	104.937	5		3.42	0.41	3.61
ANSS	2007	3	23	8	15	49.84	39.464	95.341	5		3.17	0.41	3.37
ANSS	2007	4	6	1	34	37.00	36.090	89.410	11		2.85	0.41	3.04
ANSS	2007	5	4	16	16	28.18	33.797	87.299	5		3.09	0.41	3.28
ANSS	2007	5	14	6	39	32.00	36.780	91.310	8		2.85	0.41	3.04
ANSS	2007	5	16	13	22	21.42	33.300	92.587	5		3.09	0.41	3.28
ANSS	2007	5	23	5	16	55.15	34.067	106.940	5		3.42	0.41	3.61
ISC	2007	5	23	19	10	5.00	29.470	93.579	33		3.60	0.10	3.61
ANSS	2007	5	27	21	3	22.11	35.149	95.976	5		3.16	0.30	3.26
ISC	2007	6	5	16	19	42.80	32.616	98.608	10		6.10	0.10	6.11
ANSS	2007	6	9	10	45	44.71	36.929	104.793	1		3.33	0.41	3.53

**Table 2.5.2-3 (Sheet 24 of 24)**  
**Seismicity Catalog from 1985 to Present for the Project Investigation Region [24°N to 40°N, 107°W to 83°W] for which the Events are Rmb Magnitude Greater than or Equal to 3.0 or Intensity Greater than or Equal to IV**

Catalog Reference	Year	Month	Day	Hour	Minute	Second	Lat (°N)	Lon (°W)	Depth (km)	Int (MMI)	Emb	Smb	Rmb
ANSS	2007	6	15	1	8	38.09	35.527	101.000	5		3.01	0.41	3.20
ANSS	2007	6	19	18	16	27.00	35.790	85.360	4		3.50	0.41	3.69
ISC	2007	7	3	15	44	52.80	31.900	105.302	10		6.20	0.10	6.21
PDE-W	2007	9	7	10	40	47.00	36.210	93.100	0	III	3.06	0.27	3.15
ANSS	2007	9	15	23	16	42.73	30.740	96.745	5		2.85	0.41	3.04
PDE-Q	2007	9	27	15	21	2.06	35.471	100.108	5		3.00	0.10	3.01
PDE-Q	2007	10	7	13	54	21.55	34.510	100.146	5		3.10	0.10	3.11

**Table 2.5.2-4  
Seismicity Events Recommended for Recurrence Analysis within the Gulf of Mexico**

Catalog	Year	Month	Day	Hour	Minute	Second	Lat (°N)	Lon (°W)	Depth (km)	Int (MMI)	Emb	Smb	Rmb
EPRI	1927	12	15	4	30	0.00	28.900	89.400	0	IV	3.80	0.30	3.90
EPRI	1929	7	28	17	0	0.00	28.900	89.400	0	IV	3.80	0.30	3.90
EPRI	1958	11	6	23	8	0.00	29.900	90.100	0	IV	3.11	0.56	3.47
EPRI	1963	11	5	22	45	3.40	27.490	92.580	15		4.71	0.20	4.76
EPRI	1978	7	24	8	6	16.90	26.380	88.720	15		4.88	0.10	4.89
EPRI	1980	1	10	19	16	23.50	24.130	85.710	15		3.88	0.10	3.89
SRA	1981	2	13	2	15	0.00	30.000	91.800	0	IV	3.11	0.56	3.47
ANSS	1984	1	23	0	11	59.38	26.716	87.339	5		2.85	0.41	3.04
ISC	1986	5	12	4	18	2.70	27.714	88.726	10		3.50	0.10	3.51
ISC	1992	3	31	14	59	43.60	26.311	85.895	5		3.80	0.10	3.81
ISC	1992	9	27	17	2	34.40	28.192	88.431	10		3.58	0.41	3.77
ISC	1994	6	30	1	8	24.00	27.849	90.123	10		3.70	0.10	3.71
ISC	1997	4	18	14	57	46.30	26.922	87.284	33		3.80	0.10	3.81
ISC	1998	7	6	6	54	4.10	25.035	93.626	10		3.40	0.10	3.41
ISC	2000	12	9	6	46	9.20	28.017	90.134	10		3.90	0.10	3.91
ISC	2001	3	16	4	39	9.30	28.545	88.946	10		3.70	0.10	3.71
ISC	2002	5	27	0	28	22.00	27.664	94.530	10		3.90	0.10	3.91
ISC	2002	9	19	14	44	36.20	27.820	89.131	10		3.80	0.10	3.81
ISC	2003	4	13	4	52	53.90	26.096	86.080	10		3.50	0.10	3.51
ISC	2004	6	18	19	20	56.40	27.027	86.997	10		3.50	0.10	3.51
ANSS	2006	2	10	4	14	17.80	27.597	90.163	5		5.52	0.41	5.71
ANSS	2006	9	10	14	56	8.16	26.319	86.606	14		6.11	0.10	6.12

**Table 2.5.2-5**  
**Region 2 Matrix of Detection Probabilities; Modified to Extend the Matrix to Year 2007**

Matrix of Detection Probabilities: EPRI (Reference 2.5.2-18) Incompleteness Region 2 [Modified]							
	Year Intervals						
	1625–1779	1780–1859	1860–1909	1910–1949	1950–1974	1975–1983	1984–2007
<b>Magnitude Intervals</b>	155 years	80 years	50 years	40 years	25 years	9 years	24 years
<b>3.3-3.89</b>	0.00	0.00	0.10	0.51	0.63	1.00	1.00
<b>3.9-4.49</b>	0.00	0.00	0.15	0.90	1.00	1.00	1.00
<b>4.5-5.09</b>	0.00	0.00	0.24	0.98	1.00	1.00	1.00
<b>5.1-5.69</b>	0.00	0.00	0.24	0.98	1.00	1.00	1.00
<b>5.7-6.29</b>	0.00	0.00	0.70	1.00	1.00	1.00	1.00
<b>6.3-7.5</b>	0.00	0.01	1.00	1.00	1.00	1.00	1.00

**Table 2.5.2-6**  
**Matrix of Detection Probabilities for the Gulf of Mexico**

Matrix of Detection Probabilities: Gulf of Mexico											
	Year Intervals										
	1625–1779	1780–1859	1860–1899	1900–1924	192–1949	1950–1959	1960–1964	1965–1969	1970–974	1975–1979	1980–2007
<b>Magnitude Intervals</b>	155 years	80 years	40 years	25 years	25 years	10 years	5 years	5 years	5 years	5 years	28 years
<b>3.3-3.89</b>	0.00	0.00	0.00	0.00	0.00	0.00	0.00	0.00	0.00	0.00	0.30
<b>3.9-4.49</b>	0.00	0.00	0.00	0.00	0.00	0.00	0.00	0.00	0.00	0.50	0.60
<b>4.5-5.09</b>	0.00	0.00	0.00	0.00	0.00	0.00	0.00	0.50	0.70	0.70	0.90
<b>5.1-5.69</b>	0.00	0.00	0.00	0.00	0.00	0.00	0.70	0.90	1.00	1.00	1.00
<b>5.7-6.29</b>	0.00	0.00	0.00	0.00	0.70	0.90	1.00	1.00	1.00	1.00	1.00
<b>6.3-7.5</b>	0.00	0.00	0.00	0.30	0.90	1.00	1.00	1.00	1.00	1.00	1.00

**Table 2.5.2-7  
Summary of Bechtel Group Seismic Source Zones**

Source	Description	Distance <sup>(a)</sup>		Pa <sup>(b)</sup>	M <sub>max</sub> (m <sub>b</sub> ) and Wts. <sup>(c)</sup>	Smoothing Options and Wts. <sup>(d)</sup>	New Information to Suggest Change in Source		
		(km)	(mi)				Geometry <sup>(e)</sup>	M <sub>max</sub> <sup>(f)</sup>	RI <sup>(g)</sup>
BZ1	Gulf Coast	0	0	1.0	5.4 [0.1] 5.7 [0.4] 6.0 [0.4] 6.6 [0.1]	1 [0.33] 2 [0.34] 3 [0.33]	No	Yes	No
BZ2	Texas Platform	15	9.3	0.1	5.4 [0.1] 5.7 [0.4] 6.0 [0.4] 6.6 [0.1]	1 [0.33] 2 [0.34] 4 [0.33]	No	No	No

- (a) Shortest distance between VCS site and source zone.
- (b) Probability of activity ([Reference 2.5.2-18](#)).
- (c) Maximum earthquake magnitude (M<sub>max</sub>) in body-wave magnitude (m<sub>b</sub>) and weighting (Wts.) ([Reference 2.5.2-18](#)).
- (d) Smoothing options ([Reference 2.5.2-18](#)):  
 1 = constant a, constant b, no b prior  
 2 = low smoothing on a, high smoothing on b, no b prior  
 3 = low smoothing on a, low smoothing on b, no b prior  
 4 = low smoothing on a, low smoothing on b, weak b prior of 1.05  
 Weights on magnitude intervals are [1.0, 1.0, 1.0, 1.0, 1.0, 1.0, 1.0]
- (e) No, unless updated geometry supported by post-EPRI-SOG data.
- (f) No, unless greater M<sub>max</sub> supported by post-EPRI-SOG data.
- (g) RI = recurrence interval. Assumed no change unless supported by post-EPRI-SOG data. Rate evaluations based on observed seismicity are not considered here and are described in [Subsection 2.5.2.4.2](#).

**Table 2.5.2-8  
Summary of Dames & Moore Seismic Source Zones**

Source	Description	Distance <sup>(a)</sup>		Pa <sup>(b)</sup>	M <sub>max</sub> (m <sub>b</sub> ) and Wts. <sup>(c)</sup>	Smoothing Options and Wts. <sup>(d)</sup>	New Information to Suggest Change in Source		
		(km)	(mi)				Geometry <sup>(e)</sup>	M <sub>max</sub> <sup>(f)</sup>	RI <sup>(g)</sup>
20	South Coastal Margin	0	0	1.0	5.3 [0.8] 7.2 [0.2]	1 [0.75] 2 [0.25]	No	Yes	No
25	Ouachitas Fold Belt	110	68	0.35	5.5 [0.8] 7.2 [0.2]	1 [0.75] 2 [0.25]	No	No	No
C08	Combination zone: 25 (Ouachitas Fold Belt) excluding 25A (Kink in Fold Belt)	110	68	NA	5.5 [0.8] 7.2 [0.2]	1 [0.75] 2 [0.25]	No	No	No
67	New Mexico	230	140	1.0	5.0 [0.8] 7.2 [0.2]	1 [0.75] 2 [0.25]	No	No	No

- (a) Shortest distance between VCS site and source zone.  
(b) Probability of activity ([Reference 2.5.2-18](#)).  
(c) Maximum earthquake magnitude (M<sub>max</sub>) in body-wave magnitude (m<sub>b</sub>) and weighting (Wts.) ([Reference 2.5.2-18](#)).  
(d) Smoothing options ([Reference 2.5.2-18](#)):  
1 = no smoothing on a, no smoothing on b, strong b prior of 1.04  
2 = no smoothing on a, no smoothing on b, weak b prior of 1.04  
Weights on magnitude intervals are [0.1, 0.2, 0.4, 1.0, 1.0, 1.0, 1.0]  
(e) No, unless updated geometry supported by post-EPRI-SOG data.  
(f) No, unless greater M<sub>max</sub> supported by post-EPRI-SOG data.  
(g) RI = recurrence interval. Assumed no change unless supported by post-EPRI-SOG data. Rate evaluations based on observed seismicity are not considered here and are described in [Subsection 2.5.2.4.2](#).

**Table 2.5.2-9  
Summary of Law Engineering Seismic Source Zones**

Source	Description	Distance <sup>(a)</sup>		Pa <sup>(b)</sup>	M <sub>max</sub> (m <sub>b</sub> ) and Wts. <sup>(c)</sup>	Smoothing Options and Wts. <sup>(d)</sup>	New Information to Suggest Change in Source		
		(km)	(mi)				Geometry <sup>(e)</sup>	M <sub>max</sub> <sup>(f)</sup>	RI <sup>(g)</sup>
124	New Mexico — Texas Block	69	43	1.0	4.9 [0.3] 5.5 [0.5] 5.8 [0.2]	1a [1.0]	No	Yes	No
126	South Coastal Block	0	0	1.0	4.6 [0.9] 4.9 [0.1]	1a [1.0]	No	Yes	No

- (a) Shortest distance between VCS site and source zone.
- (b) Probability of activity ([Reference 2.5.2-18](#)).
- (c) Maximum earthquake magnitude (M<sub>max</sub>) in body-wave magnitude (m<sub>b</sub>) and weighting (Wts.).
- (d) Smoothing options:  
1a = high smoothing on a, constant b, strong b prior of 1.05  
Weights on magnitude intervals are all 1.0.
- (e) No, unless updated geometry supported by post-EPRI-SOG data.
- (f) No, unless greater M<sub>max</sub> supported by post-EPRI-SOG data.
- (g) RI = recurrence interval. Assumed no change unless supported by post-EPRI-SOG data. Rate evaluations based on observed seismicity are not considered here and are described in [Subsection 2.5.2.4.2](#).

**Table 2.5.2-10  
Summary of Rondout Associates Seismic Source Zones**

Source	Description	Distance <sup>(a)</sup>		Pa <sup>(b)</sup>	M <sub>max</sub> (m <sub>b</sub> ) and Wts. <sup>(c)</sup>	Smoothing Options and Wts. <sup>(d)</sup>	New Information to Suggest Change in Source		
		(km)	(mi)				Geometry <sup>(e)</sup>	M <sub>max</sub> <sup>(f)</sup>	RI <sup>(g)</sup>
51	Gulf Coast to Bahamas Fracture Zone	0	0	1.0	4.8 [0.2] 5.5 [0.6] 5.8 [0.2]	3 [1.0]	No	Yes	No
C02	Background 50	150	93	NA	4.8 [0.2] 5.5 [0.6] 5.8 [0.2]	3 [1.0]	No	No	No

- (a) Shortest distance between VCS and source zone.
- (b) Probability of activity ([Reference 2.5.2-18](#)).
- (c) Maximum earthquake magnitude (M<sub>max</sub>) in body-wave magnitude (m<sub>b</sub>) and weighting (Wts.) ([Reference 2.5.2-18](#)).
- (d) Smoothing options ([Reference 2.5.2-18](#)):  
3 = low smoothing on a, constant b, strong b prior of 1.0
- (e) No, unless updated geometry supported by post-EPRI-SOG data.
- (f) No, unless greater M<sub>max</sub> supported by post-EPRI-SOG data.
- (g) RI = recurrence interval. Assumed no change unless supported by post-EPRI-SOG data. Rate evaluations based on observed seismicity are not considered here and are described in [Subsection 2.5.2.4.2](#).

**Table 2.5.2-11  
Summary of Weston Geophysical Corporation Seismic Source Zones**

Source	Description	Distance <sup>(a)</sup>		p <sup>(b)</sup>	M <sub>max</sub> (m <sub>b</sub> ) and Wts. <sup>(c)</sup>	Smoothing Options and Wts. <sup>(d)</sup>	New Information to Suggest Change in Source		
		(km)	(mi)				Geometry <sup>(e)</sup>	M <sub>max</sub> <sup>(f)</sup>	RI <sup>(g)</sup>
107	Gulf Coast	0	0	1.0	5.4 [0.71] 6.0 [0.29]	1a [0.2] 2a [0.8]	No	Yes	No
109	Southwest	154	97	1.0	5.4 [0.33] 6.0 [0.49] 6.6 [0.18]	1a [0.2] 2a [0.8]	No	No	No
C31	Combination zone: 109 (Southwest) excluding 37 (Delaware Basin)	154	97	NA	5.4 [0.33] 6.0 [0.49] 6.6 [0.18]	1a [0.7] 2a [0.3]	No	No	No

- (a) Shortest distance between VCS site and source zone.
- (b) Probability of activity for earthquakes with magnitudes greater than the minimum magnitude of m<sub>b</sub> 5.0 ([Reference 2.5.2-18](#)).
- (c) Maximum earthquake magnitude (M<sub>max</sub>) in body-wave magnitude (m<sub>b</sub>) and weighting (Wts.) ([Reference 2.5.2-18](#)).
- (d) Smoothing options ([Reference 2.5.2-18](#)):  
1b = constant a, constant b, medium b prior of 0.9  
2a = medium smoothing on a, medium smoothing on b, medium b prior of 1.0
- (e) No, unless updated geometry supported by post-EPRI-SOG data.
- (f) No, unless greater M<sub>max</sub> supported by post-EPRI-SOG data.
- (g) RI = recurrence interval. Assumed no change unless supported by post-EPRI-SOG data. Rate evaluations based on observed seismicity are not considered here and are described in [Subsection 2.5.2.4.2](#).

**Table 2.5.2-12  
 Summary of Woodward-Clyde Consultants Seismic Source Zones**

Source	Description	Distance <sup>(a)</sup>		p <sup>(b)</sup>	M <sub>max</sub> (m <sub>b</sub> ) and Wts. <sup>(c)</sup>	Smoothing Options and Wts. <sup>(d)</sup>	New Information to Suggest Change in Source		
		(km)	(mi)				Geometry <sup>(e)</sup>	M <sub>max</sub> <sup>(f)</sup>	RI <sup>(g)</sup>
BG	Central U.S. Background	0	0	NA	4.9 [0.17] 5.4 [0.28] 5.8 [0.27] 6.5 [0.28]	1 [0.25] 6 [0.25] 7 [0.25] 8 [0.25]	Yes <sup>(h)</sup>	No	No

- (a) Shortest distance between VCS site and source zone.
- (b) Probability of activity for earthquakes with magnitudes greater than the minimum magnitude of m<sub>b</sub> 5.0 ([Reference 2.5.2-18](#)).
- (c) Maximum earthquake magnitude (M<sub>max</sub>) in body-wave magnitude (m<sub>b</sub>) and weighting (Wts.) ([Reference 2.5.2-18](#)).
- (d) Smoothing options ([Reference 2.5.2-18](#)):
  - 1 = low smoothing on a, high smoothing on b, no b prior
  - 6 = low smoothing on a, high smoothing on b, moderate b prior of 1.0
  - 7 = low smoothing on a, high smoothing on b, moderate b prior of 0.9
  - 8 = low smoothing on a, high smoothing on b, moderate b prior of 0.8
 Weights on magnitude intervals are all 1.0.
- (e) No, unless updated geometry supported by post-EPRI-SOG data.
- (f) No, unless greater M<sub>max</sub> supported by post-EPRI-SOG data.
- (g) RI = recurrence interval. Assumed no change unless supported by post-EPRI-SOG data. Rate evaluations based on observed seismicity are not considered here and are described in [Subsection 2.5.2.4.2](#).
- (h) Revised geometry reflects new source centered on VCS site (see [Subsection 2.5.2.4.5.2](#)).

**Table 2.5.2-13**  
**Comparison of 1989 EPRI (Reference 2.5.2-1) Hazard Results for STPEGS Site and Current**  
**Hazard Results for VCS Site for Bechtel Team Using**  
**1989 EPRI (Reference 2.5.2-1) Assumptions**

PGA amp, cm/sec <sup>2</sup>	Hazard	EPRI-SOG for STPEGS	Current results for VCS	% diff
100	mean	1.19E-05	1.06E-05	-11%
	15%	4.22E-06	3.72E-06	-12%
	50%	9.09E-06	8.22E-06	-10%
	85%	1.82E-05	1.70E-05	-7%
250	mean	1.35E-06	1.28E-06	-6%
	15%	4.62E-07	4.37E-07	-6%
	50%	9.58E-07	1.00E-06	4%
	85%	2.28E-06	2.29E-06	0%
500	mean	1.30E-07	1.29E-07	-1%
	15%	3.08E-08	3.16E-08	3%
	50%	8.87E-08	8.91E-08	0%
	85%	2.23E-07	2.34E-07	5%

**Table 2.5.2-14**  
**Comparison of 1989 EPRI (Reference 2.5.2-1) Hazard Results for STPEGS Site and Current**  
**Hazard Results for VCS Site for Dames & Moore Team Using**  
**1989 EPRI (Reference 2.5.2-1) Assumptions**

PGA amp, cm/sec <sup>2</sup>	Hazard	EPRI-SOG for STPEGS	Current results for VCS	% diff
100	mean	9.52E-06	3.71E-07	-96%
	15%	2.13E-06	8.91E-14	-100%
	50%	5.03E-06	4.12E-09	-100%
	85%	1.02E-05	3.31E-07	-97%
250	mean	1.21E-06	1.76E-08	-99%
	15%	1.66E-07	1.02E-28	-100%
	50%	4.50E-07	1.08E-11	-100%
	85%	1.70E-06	4.90E-09	-100%
500	mean	1.70E-07	7.59E-10	-100%
	15%	6.64E-09	1.02E-28	-100%
	50%	2.42E-08	5.62E-15	-100%
	85%	2.92E-07	4.79E-11	-100%

**Table 2.5.2-15**  
**Comparison of 1989 EPRI (Reference 2.5.2-1) Hazard Results for STPEGS Site and Current**  
**Hazard Results for VCS Site For Law Engineering Inc. Team Using**  
**1989 EPRI (Reference 2.5.2-1) Assumptions**

PGA amp, cm/sec <sup>2</sup>	Hazard	EPRI-SOG for STPEGS	Current results for VCS	% diff
100	mean	1.13E-07	8.90E-08	-21%
	15%	1.19E-10	1.45E-28	-100%
	50%	1.20E-07	1.20E-08	-90%
	85%	2.09E-07	3.09E-07	48%
250	mean	7.38E-09	3.34E-10	-95%
	15%	1.19E-10	1.45E-28	-100%
	50%	8.80E-09	6.92E-12	-100%
	85%	1.22E-08	7.08E-10	-94%
500	mean	2.69E-10	1.04E-12	-100%
	15%	1.19E-10	1.45E-28	-100%
	50%	4.18E-10	2.46E-15	-100%
	85%	5.20E-10	1.23E-12	-100%

**Table 2.5.2-16**  
**Comparison of 1989 EPRI (Reference 2.5.2-1) Hazard Results for STPEGS Site and Current**  
**Hazard Results for VCS Site for Rondout Using**  
**1989 EPRI (Reference 2.5.2-1) Assumptions**

PGA amp, cm/sec <sup>2</sup>	Hazard	EPRI-SOG for STPEGS	Current results for VCS	% diff
100	mean	1.25E-05	1.08E-05	-13%
	15%	4.44E-07	6.76E-29	-100%
	50%	1.26E-05	1.12E-05	-11%
	85%	2.43E-05	2.09E-05	-14%
250	mean	1.22E-06	1.11E-06	-9%
	15%	2.67E-08	6.76E-29	-100%
	50%	1.25E-06	1.15E-06	-8%
	85%	2.18E-06	1.93E-06	-12%
500	mean	8.77E-08	8.40E-08	-4%
	15%	9.87E-10	6.76E-29	-100%
	50%	8.18E-08	8.32E-08	2%
	85%	1.89E-07	1.50E-07	-21%

**Table 2.5.2-17**  
**Comparison of 1989 EPRI (Reference 2.5.2-1) Hazard Results for STPEGS Site and Current**  
**Hazard Results for VCS Site for Weston Geophysical Team Using**  
**1989 EPRI (Reference 2.5.2-1) Assumptions**

<b>PGA amp, cm/sec<sup>2</sup></b>	<b>Hazard</b>	<b>EPRI-SOG for STPEGS</b>	<b>Current results for VCS</b>	<b>% diff</b>
100	mean	1.95E-05	1.77E-05	-9%
	15%	6.86E-06	6.92E-06	1%
	50%	1.23E-05	1.12E-05	-9%
	85%	2.74E-05	2.40E-05	-12%
250	mean	2.02E-06	1.90E-06	-6%
	15%	5.89E-07	5.75E-07	-2%
	50%	1.44E-06	1.32E-06	-8%
	85%	3.43E-06	3.24E-06	-6%
500	mean	1.68E-07	1.63E-07	-3%
	15%	2.64E-08	2.75E-08	4%
	50%	9.35E-08	9.55E-08	2%
	85%	3.50E-07	3.55E-07	1%

**Table 2.5.2-18**  
**Comparison of 1989 EPRI (Reference 2.5.2-1) Hazard Results for STPEGS Site and Current**  
**Hazard Results for VCS Site for Woodward-Clyde Team Using**  
**1989 EPRI (Reference 2.5.2-1) Assumptions**

PGA amp, cm/sec <sup>2</sup>	Hazard	EPRI-SOG for STPEGS	Current results for VCS	% diff
100	mean	2.24E-05	1.87E-05	-17%
	15%	3.49E-07	2.40E-29	-100%
	50%	1.35E-05	1.12E-05	-17%
	85%	4.63E-05	3.89E-05	-16%
250	mean	2.80E-06	2.43E-06	-13%
	15%	2.92E-08	2.40E-29	-100%
	50%	1.32E-06	1.23E-06	-7%
	85%	5.80E-06	4.90E-06	-16%
500	mean	3.39E-07	3.05E-07	-10%
	15%	1.29E-09	2.40E-29	-100%
	50%	7.81E-08	7.76E-08	-1%
	85%	6.69E-07	5.75E-07	-14%

**Table 2.5.2-19**  
**Comparison of Original EPRI-SOG Gulf Coastal Source Zones Characterizations and**  
**Modifications Made for the VCS Site**

EPRI Team	Source	Description	EPRI-SOG Model	Updated Model for VCS Site	
			$M_{max}$ ( $m_b$ ) and Wts. <sup>(a)</sup>	$M_{max}$ ( $m_b$ ) and Wts.	Smoothing Options and Wts.
Bechtel Group	BZ1	Gulf Coast	5.4 [0.1] 5.7 [0.4] 6.0 [0.4] 6.6 [0.1]	6.1 [0.10] 6.4 [0.40] 6.6 [0.50]	No Update
Dames & Moore	20	South Coastal Margin	5.3 [0.8] 7.2 [0.2]	5.5 [0.80] 7.2 [0.20]	I (0.2) II (0.4) III (0.4)
Law Engineering	126	South Coastal Block	4.6 [0.9] 4.9 [0.1]	5.5 [0.90] 5.7 [0.10]	No Update
Rondout Associates	51	Gulf Coast to Bahamas Fracture Zone	4.8 [0.2] 5.5 [0.6] 5.8 [0.2]	6.1 [0.30] 6.3 [0.55] 6.5 [0.15]	No Update
Weston Geophysical Corporation	107	Gulf Coast	5.4 [0.71] 6.0 [0.29]	6.6 [0.89] 7.2 [0.11]	No Update
Woodward-Clyde Consultants	B43	Central U.S. Background	4.9 [0.17] 5.4 [0.28] 5.8 [0.27] 6.5 [0.28]	No Update	No Update

(a)  $M_{max}$  distribution and weights from EPRI-SOG model ([Reference 2.5.2-18](#)).

**Table 2.5.2-20**  
**Seismic Source Characterization of the Meers Fault**

<b>Probability of Activity</b>	1
<b>Recurrence Model</b>	Characteristic
<b>Characteristic Magnitude</b>	6.7 (0.2), 6.85 (0.6), 7.0 (0.2)
<b>Characteristic Return Period</b>	See logic tree in <a href="#">Figure 2.5.2-17</a> .
<b>Dip</b>	89°
<b>Dip Direction</b>	SW
<b>Rupture Top</b>	0 km
<b>Rupture Bottom</b>	15 to 20 km
<b>Width</b>	15 to 20 km
<b>Length</b>	26 to 37 km
<b>Fault Trace Coordinates (Lat., Lon.)</b>	(34.85°, -98.64°) (34.71°, -98.29°)

**Table 2.5.2-21  
 Rio Grande Rift Faults Modeled as Discrete Fault Sources**

<b>Fault Name</b>	<b>Recurrence Rate (EQs/yr)</b>	<b>Magnitude (M<sub>w</sub>)</b>
Puye fault	4.0140E-05	6.6
Sawyer Canyon fault	5.4280E-05	6.2
La Canada del Amagre fault zone	9.5530E-05	6.5
Embudo fault	3.7700E-05	7.2
Lobato Mesa fault zone	6.3390E-05	6.6
Canones fault	2.0724E-05	6.8
Black Mesa fault zone	3.4270E-05	6.5
Gallina fault	1.8790E-05	6.9
Southern Sangre de Cristo fault	5.7220E-05	7.4
Northern Sangre de Cristo fault	1.0040E-04	7.5
Southern Sawatch fault	4.6820E-05	7.0
West Lobo Valley fault zone	1.7700E-05	7.2
West Indio Mountains fault	4.8600E-05	6.7
Caballo fault	7.8790E-05	7.0
West Eagle Mountains-Red Hills fault	1.5140E-05	6.7
Amargosa fault	6.5170E-05	7.2
East Baylor Mountain - Carizzo Mountain fault	5.3200E-06	7.0
Arroyo Diablo fault	2.4520E-05	6.4
East Sierra Diablo fault	1.6510E-05	6.9
Campo Grande fault	3.6540E-05	7.0
Acala fault	2.4770E-04	6.1
West Delaware Mountains fault zone	2.8590E-05	6.7
East Franklin Mountains fault	8.1530E-05	7.0
Organ Mountains fault	1.4976E-04	6.8
San Andres Mountains fault	3.9120E-05	7.5
Alamogordo fault	3.9970E-05	7.5
Caballo fault	3.7440E-05	6.6
La Jencia fault	2.3120E-05	6.8
Hubbell Springs fault	5.3650E-05	7.0
Tijeras-Canoncito fault	3.2820E-05	7.3
County Dump fault	3.3260E-05	6.9
Zia fault	4.2010E-05	6.8
San Francisco fault	6.6380E-05	6.8
San Felipe fault zone	3.1180E-05	7.0
La Bajada fault	4.9530E-05	7.0
Jemez-San Ysidro fault	1.2850E-05	7.1
Picuris-Pecos fault	2.1030E-05	7.4
Nacimiento fault	9.9400E-06	7.3
Nambe fault	1.6790E-05	7.0
Pajarito fault	5.7380E-05	7.0
Pojoaque fault	1.6260E-05	7.0

**Table 2.5.2-22**  
**Summary of Rio Grande Rift Fault Source Characterization**

<b>Dip, Dip Direction</b>	90°, NA
<b>Recurrence Model</b>	Characteristic Earthquake
<b>Recurrence Rate (EQs/yr)</b>	<a href="#">Table 2.5.2-21</a>
<b>Magnitude (<math>M_w</math>) and weights</b>	Take magnitude from <a href="#">Table 2.5.2-21</a> and use $M_w -0.2$ [0.2], $M_w$ [0.6], $M_w +0.2$ [0.2] with weights in parentheses
<b>Probability of Activity</b>	1.0

**Table 2.5.2-23**  
**Rio Grande Rift Southern Extension Characterization**

<b>Individual Fault Trace Coordinates (Lon., Lat.)</b>	Fault 1: (103.19°W, 30.52°N) (102.86°W, 30.06°N) Fault 2: (102.86°W, 30.06°N) (102.54°W, 29.60°N) Fault 3: (102.54°W, 29.60°N) (102.25°W, 29.12°N) Fault 4: (102.25°W, 29.12°N) (101.95°W, 28.64°N) Fault 5: (101.95°W, 28.64°N) (101.67°W, 28.17°N) Fault 6: (101.67°W, 28.17°N) (101.38°W, 27.69°N) Fault 7: (101.38°W, 27.69°N) (101.10°W, 27.21°N) Fault 8: (101.10°W, 27.21°N) (100.82°W, 26.73°N) Fault 9: (100.82°W, 26.73°N) (100.55°W, 26.25°N) Fault 10: (100.55°W, 26.25°N) (100.28°W, 25.77°N)
<b>Recurrence Model</b>	Characteristic Earthquake
<b>Return Period (yrs) and weights</b>	14,500 [0.4], 37,500 [0.4], 119,000 [0.2]
<b>Magnitude (<math>M_w</math>) and weights</b>	6.3 [0.1], 6.65 [0.3], 6.95 [0.4], 7.3 [0.2]
<b>Probability of Activity</b>	1.0

**Table 2.5.2-24  
 Mean and Median Rock UHS Accelerations (g)**

UHS amps, base rock						
Freq.	1E-4		1E-5		1E-6	
	Mean	Median	Mean	Median	Mean	Median
PGA	3.10E-02	1.76E-02	1.32E-01	1.01E-01	5.57E-01	4.08E-01
25	7.43E-02	3.94E-02	3.56E-01	2.64E-01	1.52E+00	1.06E+00
10	6.44E-02	3.84E-02	2.60E-01	2.02E-01	9.58E-01	7.54E-01
5	5.77E-02	3.23E-02	1.99E-01	1.35E-01	6.15E-01	4.82E-01
2.5	5.08E-02	2.62E-02	1.48E-01	7.70E-02	3.57E-01	2.38E-01
1	3.75E-02	1.60E-02	1.07E-01	3.87E-02	2.26E-01	8.96E-02
0.5	3.05E-02	1.01E-02	1.06E-01	2.11E-02	2.31E-01	4.03E-02

**Table 2.5.2-25  
 Controlling Magnitudes and Distances From Deaggregation**

Structural Frequency	Annual Frequency Exceedance	Overall Hazard		Hazard from R >100 km	
		M	R, km	M	R, km
1 & 2.5 Hz	1E-04	7.4	550	7.6	880
5 & 10 Hz	1E-04	6.6	190	7.5	780
1 & 2.5 Hz	1E-05	7.2	330	7.7	890
5 & 10 Hz	1E-05	5.9	36	7.7	850
1 & 2.5 Hz	1E-06	6.8	102	7.8	890
5 & 10 Hz	1E-06	5.6	12	7.8	840

Note: shaded cells indicate values used to construct UHS; see [Subsection 2.5.2.4.7](#).

**Table 2.5.2-26**  
**Assigned Strong Motion Durations in P-SHAKE**

Set of Runs	Description	Recurrence	Input Rock Spectra	
			Magnitude	Duration [sec]
LF4	Low Frequency	$10^{-4}$	7.6	13
HF4	High Frequency	$10^{-4}$	6.6	10
LF5	Low Frequency	$10^{-5}$	7.7	13
HF5	High Frequency	$10^{-5}$	5.9	6
LF6	Low Frequency	$10^{-6}$	7.8	13
HF6	High Frequency	$10^{-6}$	5.6	6

**Table 2.5.2-27 (Sheet 1 of 2)**  
**Horizontal  $10^{-4}$  and  $10^{-5}$  UHRS and GMRS, and Vertical GMRS**

Frequency	1E-4				1E-5				Horizontal GMRS	V/H	Vertical GMRS
	1E-4 Rock UHRS	AF	Soil UHRS	Smooth UHRS	1E-5 Rock UHRS	AF	Soil UHRS	Smooth UHRS			
100	3.10E-02	1.522	4.72E-02	4.72E-02	1.32E-01	1.246	1.64E-01	1.64E-01	7.69E-02	1.000	7.69E-02
90	3.39E-02	1.489	5.04E-02	5.06E-02	1.46E-01	1.207	1.76E-01	1.76E-01	8.25E-02	1.000	8.25E-02
80	3.87E-02	1.418	5.49E-02	5.46E-02	1.69E-01	1.123	1.90E-01	1.88E-01	8.83E-02	1.000	8.83E-02
70	4.62E-02	1.254	5.79E-02	5.76E-02	2.04E-01	0.963	1.97E-01	1.96E-01	9.19E-02	1.000	9.19E-02
60	5.57E-02	1.053	5.86E-02	5.88E-02	2.50E-01	0.796	1.99E-01	2.00E-01	9.37E-02	1.000	9.37E-02
50	6.48E-02	0.914	5.92E-02	5.94E-02	2.96E-01	0.682	2.02E-01	2.03E-01	9.51E-02	1.000	9.51E-02
45	6.85E-02	0.873	5.97E-02	5.98E-02	3.16E-01	0.648	2.05E-01	2.05E-01	9.61E-02	1.000	9.61E-02
40	7.12E-02	0.849	6.05E-02	6.05E-02	3.32E-01	0.627	2.08E-01	2.08E-01	9.76E-02	1.000	9.76E-02
35	7.32E-02	0.839	6.14E-02	6.14E-02	3.44E-01	0.618	2.13E-01	2.13E-01	9.97E-02	1.000	9.97E-02
30	7.42E-02	0.844	6.26E-02	6.27E-02	3.53E-01	0.622	2.19E-01	2.20E-01	1.03E-01	1.000	1.03E-01
25	7.43E-02	0.869	6.46E-02	6.49E-02	3.56E-01	0.648	2.31E-01	2.32E-01	1.08E-01	1.000	1.08E-01
20	7.38E-02	0.936	6.91E-02	6.92E-02	3.43E-01	0.737	2.53E-01	2.54E-01	1.17E-01	1.000	1.17E-01
15	7.12E-02	1.073	7.64E-02	7.62E-02	3.15E-01	0.909	2.86E-01	2.85E-01	1.32E-01	1.000	1.32E-01
12.5	6.85E-02	1.153	7.90E-02	7.91E-02	2.92E-01	1.010	2.95E-01	2.95E-01	1.36E-01	1.000	1.36E-01
10	6.44E-02	1.311	8.45E-02	8.39E-02	2.60E-01	1.199	3.12E-01	3.09E-01	1.43E-01	1.000	1.43E-01
9	6.40E-02	1.339	8.57E-02	8.67E-02	2.52E-01	1.236	3.12E-01	3.16E-01	1.46E-01	1.000	1.46E-01
8	6.33E-02	1.439	9.10E-02	9.09E-02	2.43E-01	1.354	3.29E-01	3.28E-01	1.52E-01	1.000	1.52E-01
7	6.21E-02	1.528	9.48E-02	9.51E-02	2.31E-01	1.461	3.37E-01	3.38E-01	1.57E-01	1.000	1.57E-01
6	6.03E-02	1.647	9.93E-02	9.91E-02	2.16E-01	1.597	3.46E-01	3.45E-01	1.61E-01	0.999	1.61E-01
5	5.77E-02	1.807	1.04E-01	1.05E-01	1.99E-01	1.776	3.53E-01	3.56E-01	1.68E-01	0.999	1.68E-01
4	5.51E-02	2.153	1.19E-01	1.18E-01	1.80E-01	2.137	3.84E-01	3.81E-01	1.81E-01	0.999	1.81E-01
3	5.28E-02	2.277	1.20E-01	1.21E-01	1.60E-01	2.273	3.63E-01	3.67E-01	1.76E-01	0.857	1.51E-01
2.5	5.08E-02	2.455	1.25E-01	1.24E-01	1.48E-01	2.460	3.64E-01	3.64E-01	1.76E-01	0.715	1.26E-01
2	4.87E-02	2.340	1.14E-01	1.14E-01	1.41E-01	2.352	3.31E-01	3.31E-01	1.61E-01	0.710	1.14E-01

**Table 2.5.2-27 (Sheet 2 of 2)**  
**Horizontal 10<sup>-4</sup> and 10<sup>-5</sup> UHRS and GMRS, and Vertical GMRS**

Frequency	1E-4				1E-5				Horizontal GMRS	V/H	Vertical GMRS
	1E-4 Rock UHRS	AF	Soil UHRS	Smooth UHRS	1E-5 Rock UHRS	AF	Soil UHRS	Smooth UHRS			
1.5	4.40E-02	2.206	9.71E-02	9.74E-02	1.27E-01	2.189	2.77E-01	2.79E-01	1.35E-01	0.704	9.53E-02
1.25	4.07E-02	2.329	9.49E-02	9.58E-02	1.17E-01	2.329	2.72E-01	2.75E-01	1.33E-01	0.701	9.35E-02
1	3.75E-02	2.685	1.01E-01	1.02E-01	1.07E-01	2.715	2.91E-01	2.96E-01	1.42E-01	0.696	9.91E-02
0.9	3.62E-02	2.896	1.05E-01	1.04E-01	1.08E-01	2.876	3.12E-01	3.11E-01	1.49E-01	0.694	1.03E-01
0.8	3.53E-02	2.917	1.03E-01	1.05E-01	1.11E-01	2.912	3.22E-01	3.26E-01	1.57E-01	0.691	1.09E-01
0.7	3.48E-02	3.195	1.11E-01	1.09E-01	1.13E-01	3.155	3.58E-01	3.52E-01	1.66E-01	0.689	1.15E-01
0.6	3.39E-02	3.135	1.06E-01	1.08E-01	1.14E-01	3.167	3.62E-01	3.65E-01	1.72E-01	0.686	1.18E-01
0.5	3.05E-02	3.279	1.00E-01	9.46E-02	1.06E-01	3.333	3.53E-01	3.32E-01	1.56E-01	0.682	1.06E-01
0.4	2.21E-02	2.534	5.60E-02	5.92E-02	7.71E-02	2.600	2.01E-01	2.10E-01	9.85E-02	0.678	6.68E-02
0.3	1.40E-02	3.395	4.76E-02	4.59E-02	4.91E-02	3.433	1.69E-01	1.62E-01	7.58E-02	0.672	5.09E-02
0.2	6.75E-03	1.897	1.28E-02	1.39E-02	2.38E-02	1.903	4.52E-02	4.95E-02	2.55E-02	0.668	1.71E-02
0.15	3.50E-03	2.794	9.77E-03	9.74E-03	1.23E-02	2.817	3.47E-02	3.46E-02	1.61E-02	0.668	1.08E-02
0.125	2.22E-03	3.064	6.80E-03	6.81E-03	7.81E-03	3.083	2.41E-02	2.41E-02	1.12E-02	0.668	7.52E-03
0.1	1.19E-03	2.811	3.35E-03	3.35E-03	4.18E-03	2.816	1.18E-02	1.18E-02	5.50E-03	0.668	3.67E-03

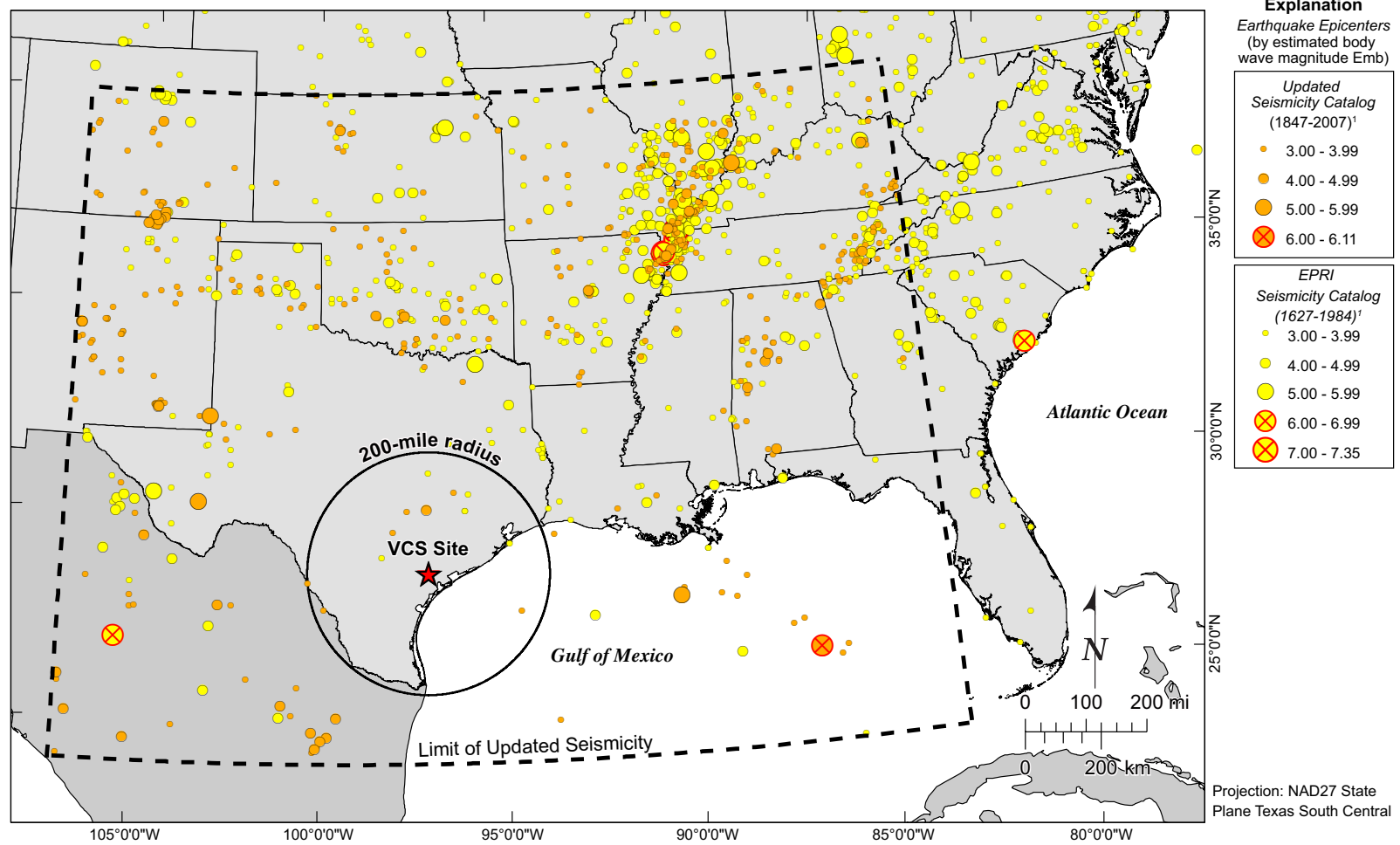


**Figure 2.5.2-1 The VCS Site, Large Project Seismicity Investigation Window (24° to 40° N, 107° to 83° W), the 200 Mile Radius Site Region, and both EPRI Catalog and Supplemental Earthquakes**

Note: See [Subsection 2.5.2.1](#)

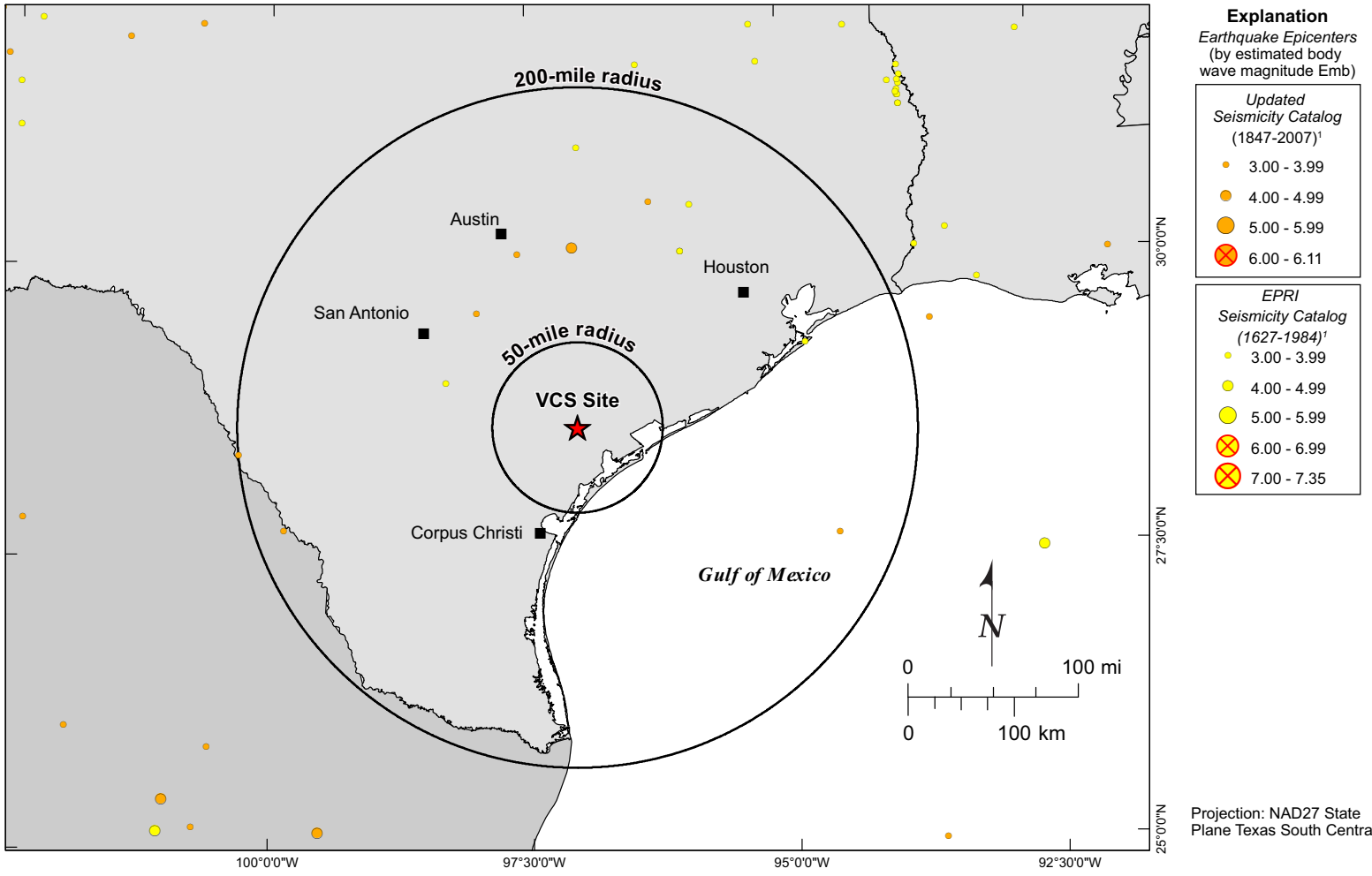
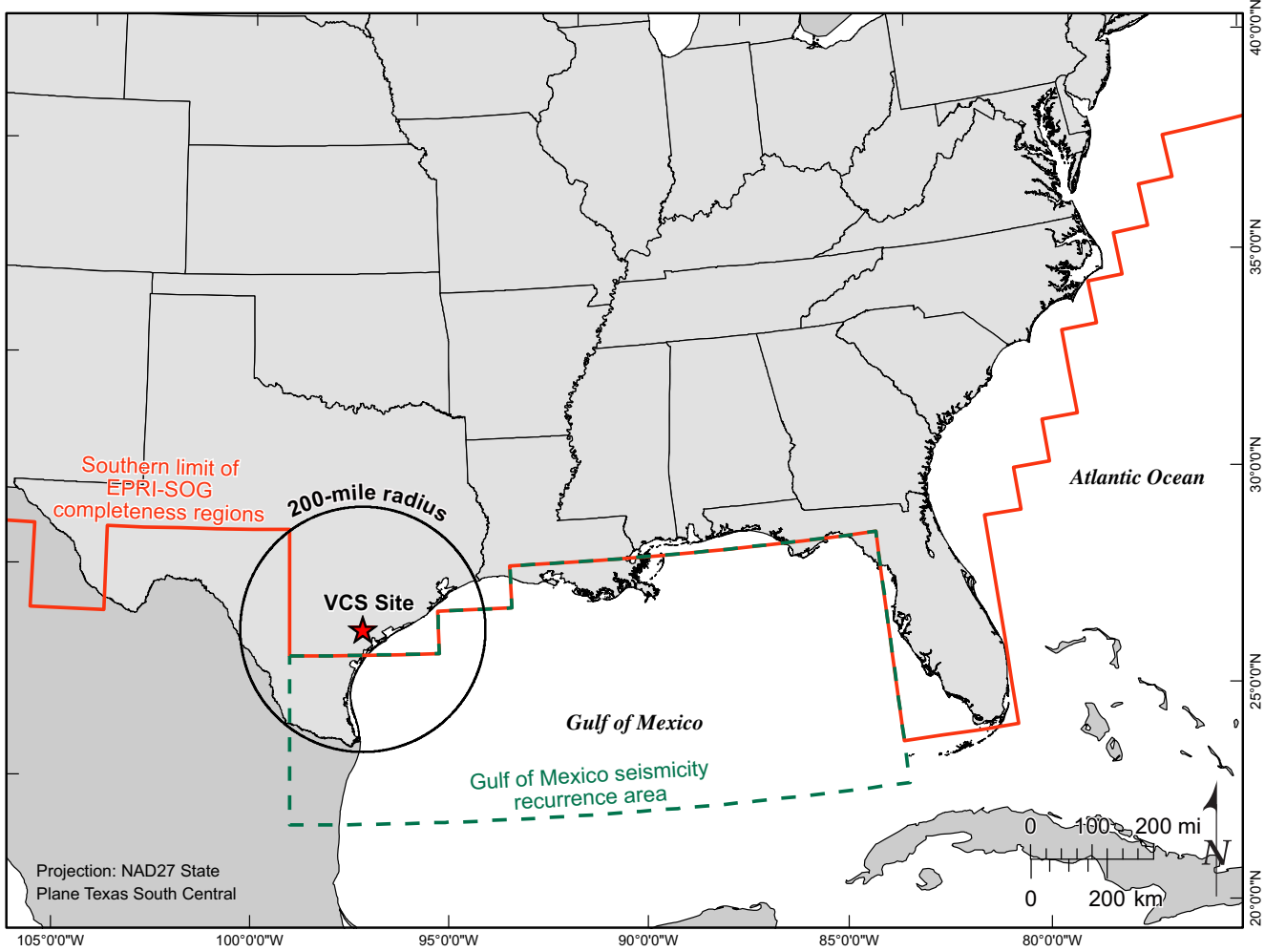


Figure 2.5.2-2 VCS Site Region Seismicity

Note: See [Subsection 2.5.2.1](#)



**Figure 2.5.2-3 Gulf of Mexico Seismicity Recurrence Area**

Note: Probability of earthquake detection parameters were developed within this area to supplement EPRI-SOG information

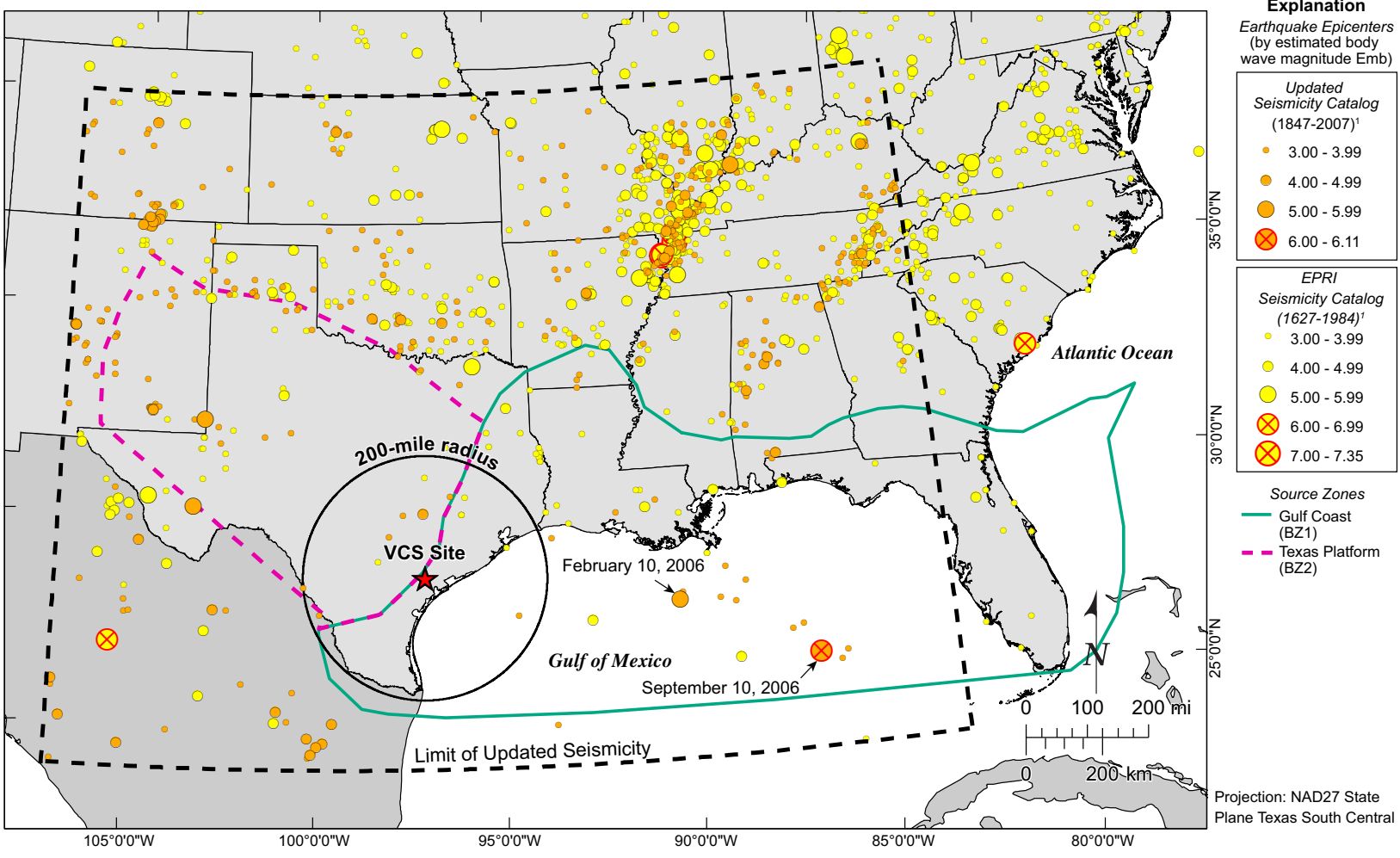


**Figure 2.5.2-4 Bechtel Group Source Zones Contributing Most Significantly to Seismic Hazard at the VCS Site**

Note: See [Subsection 2.5.2.1](#)

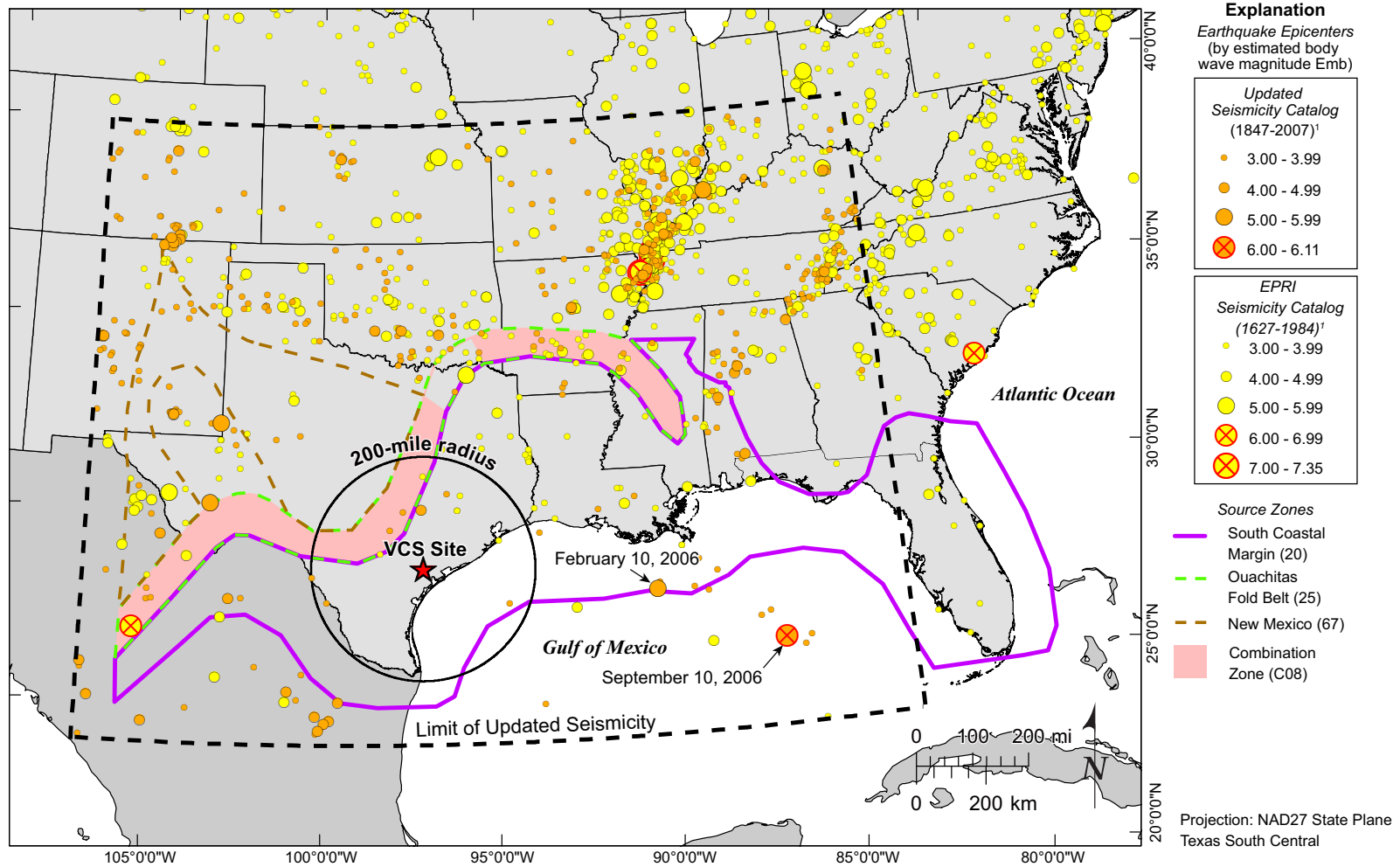


**Figure 2.5.2-5 Dames and Moore Source Zones Contributing Most Significantly to Seismic Hazard at the VCS Site**

Note: See [Subsection 2.5.2.1](#)

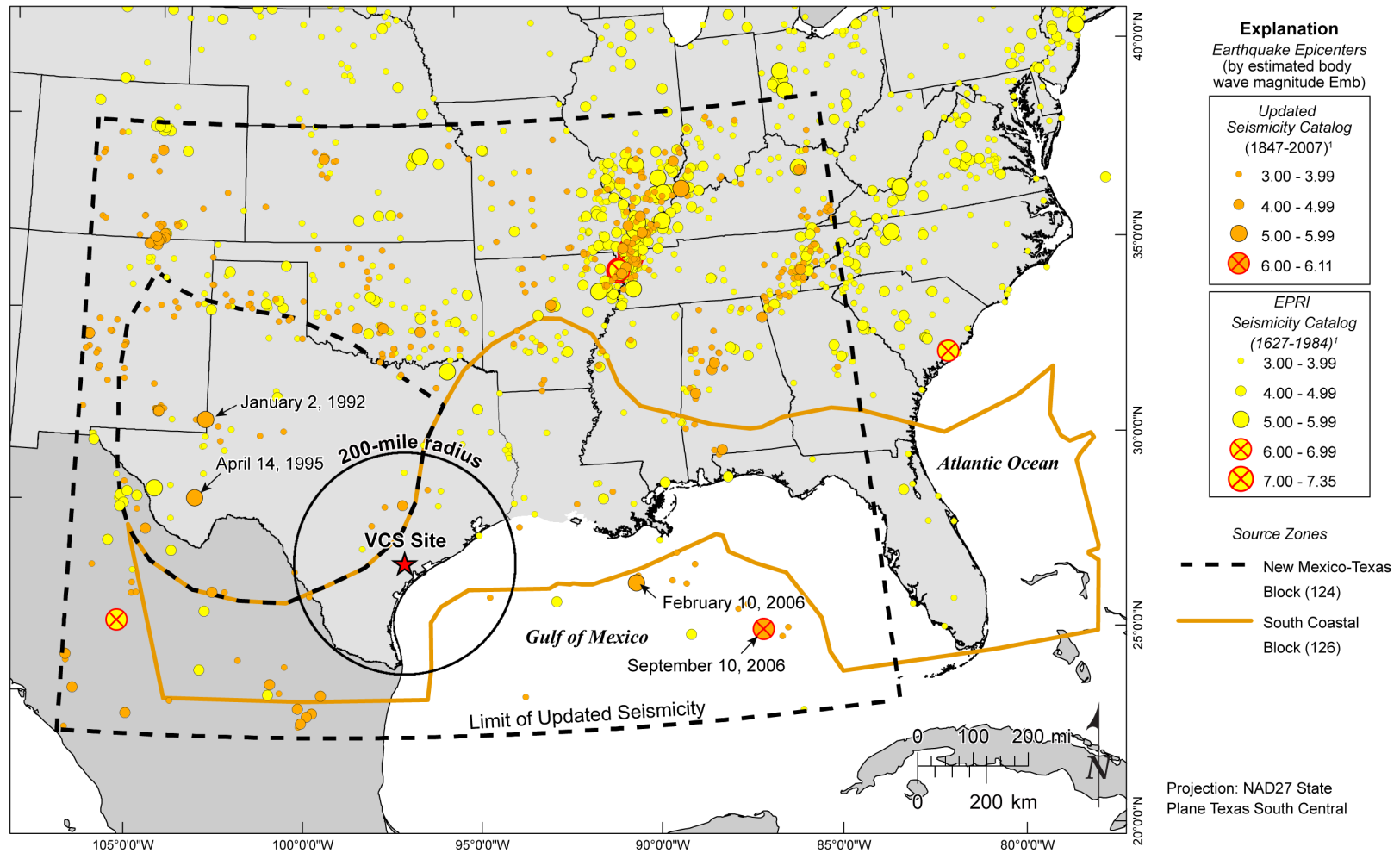
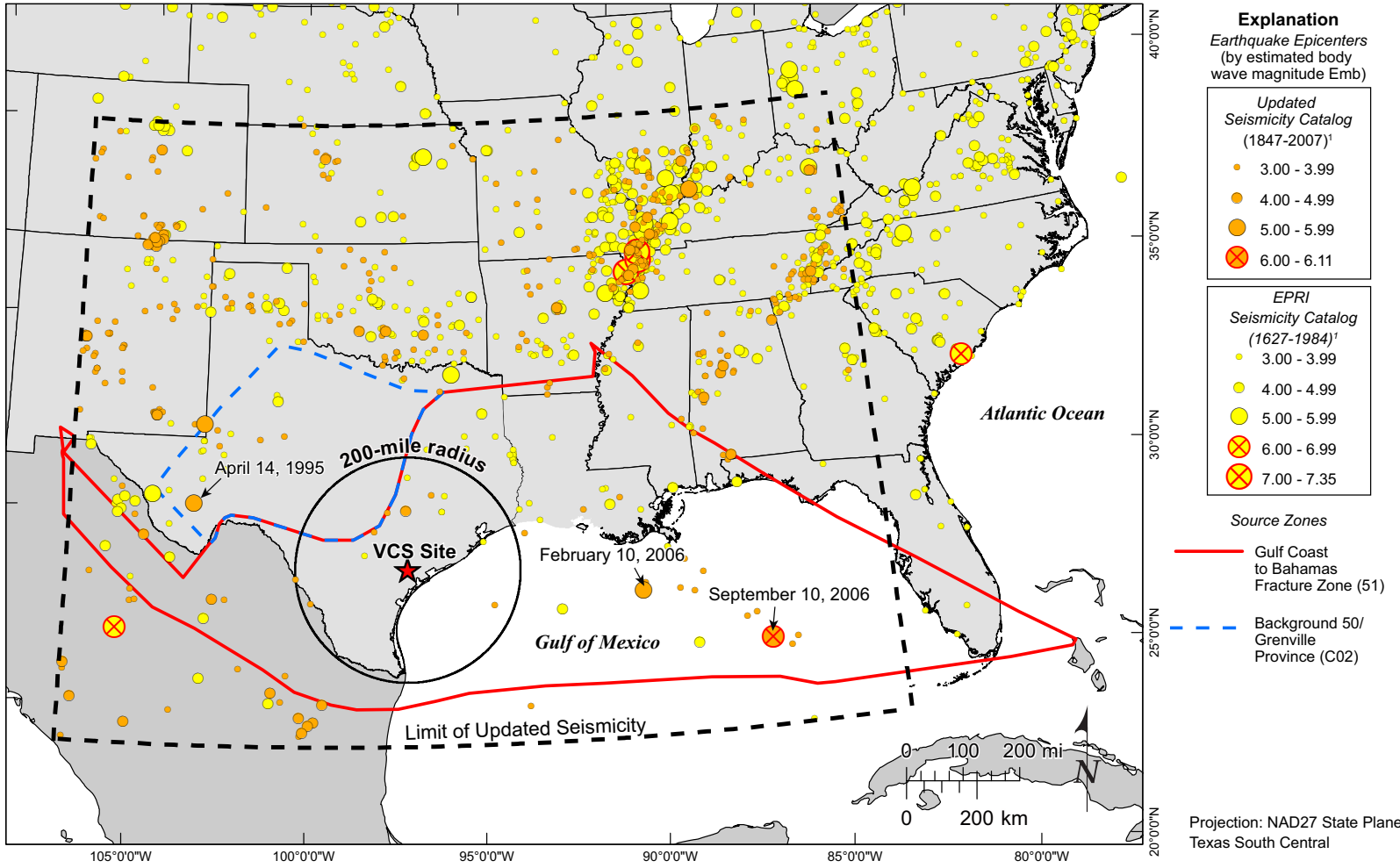


Figure 2.5.2-6 Law Engineering Source Zones Contributing Most Significantly to Seismic Hazard at the VCS Site

Note: See [Subsection 2.5.2.1](#)



**Figure 2.5.2-7 Rondout Source Zones Contributing Most Significantly to Seismic Hazard at the VCS Site**

Note: See [Subsection 2.5.2.1](#)

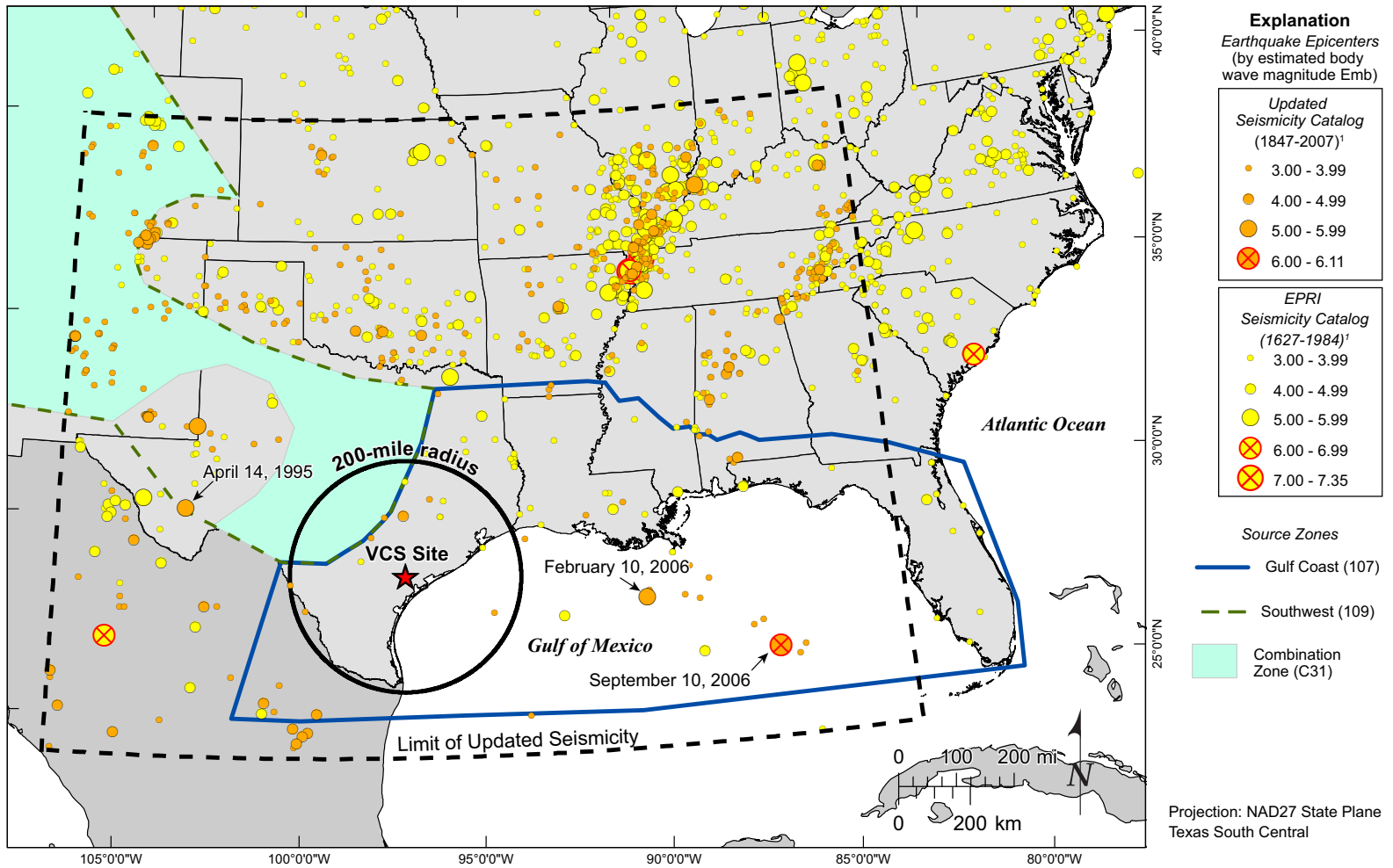


**Figure 2.5.2-8 Weston Geophysical Source Zones Contributing Most Significantly to Seismic Hazard at the VCS Site**

Note: See [Subsection 2.5.2.1](#)

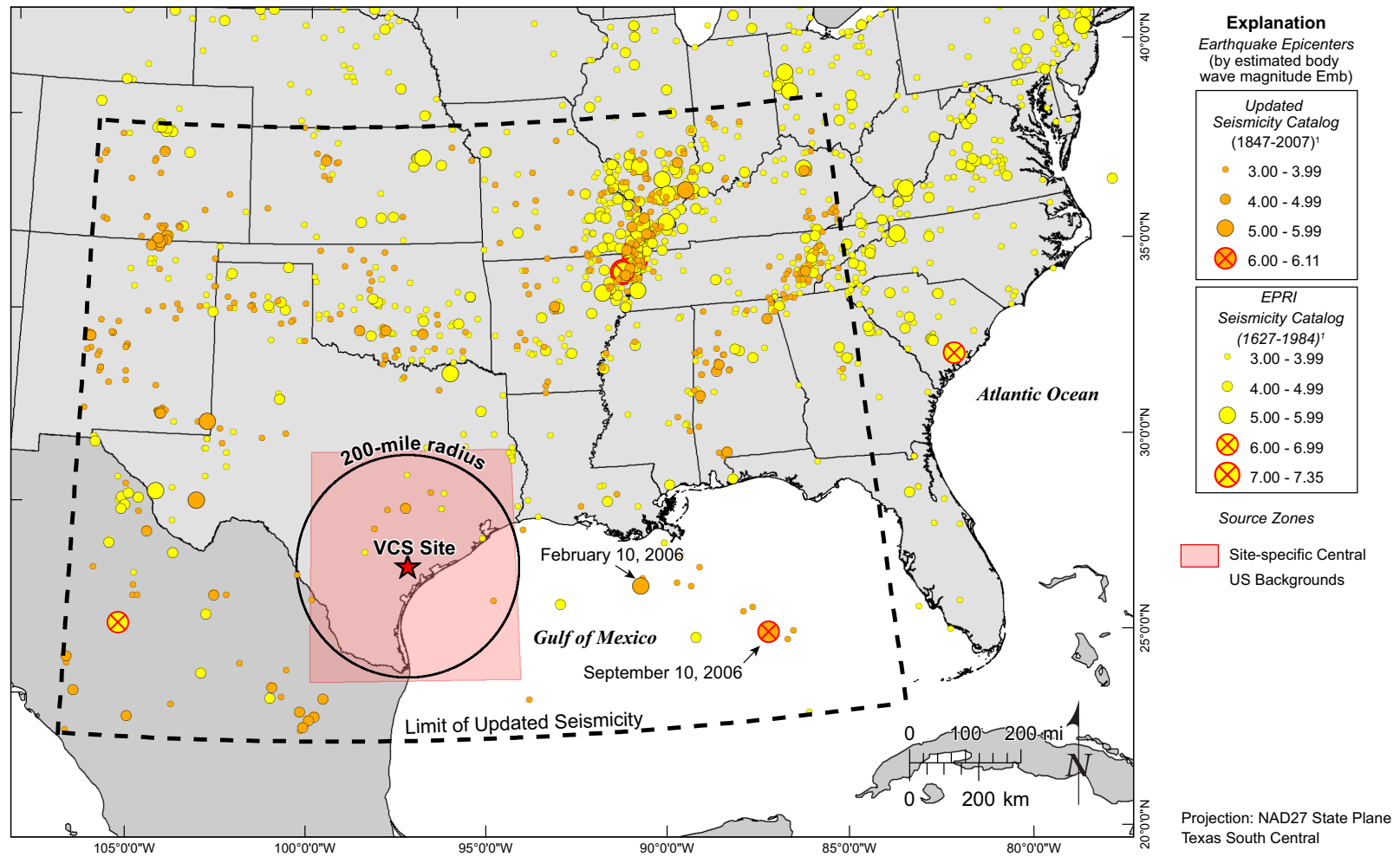
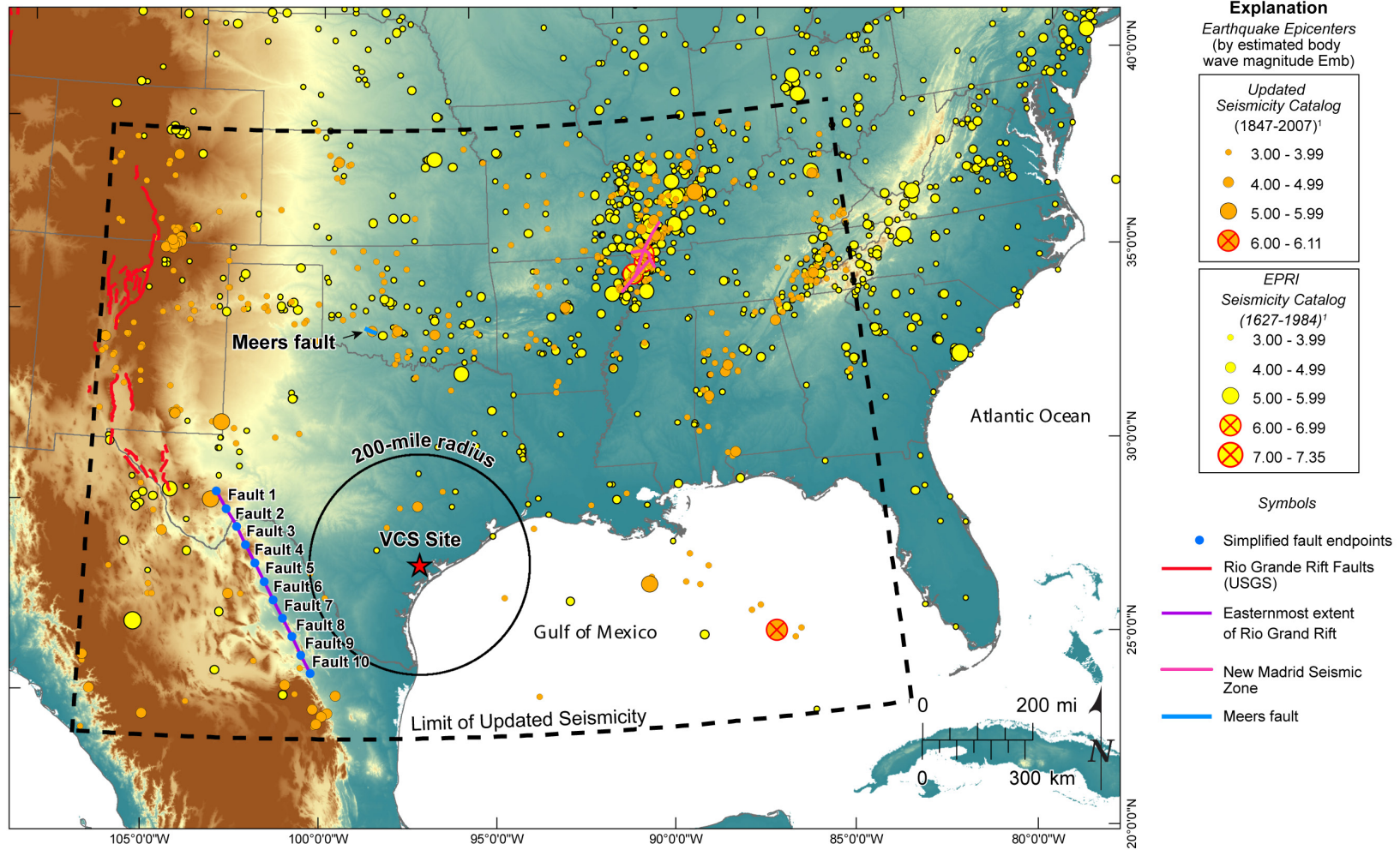


Figure 2.5.2-9 Woodward-Clyde Source Zones Contributing Most Significantly to Seismic Hazard at the VCS Site

Note: See [Subsection 2.5.2.1](#)



**Figure 2.5.2-10 Location of the Meers Fault, Simplified Fault Segments to Model the Rio Grande Rift (RGR) Faults, and Fault of the New Madrid Seismic Zone (NMSZ)**

Note: See [Subsection 2.5.2.1](#)

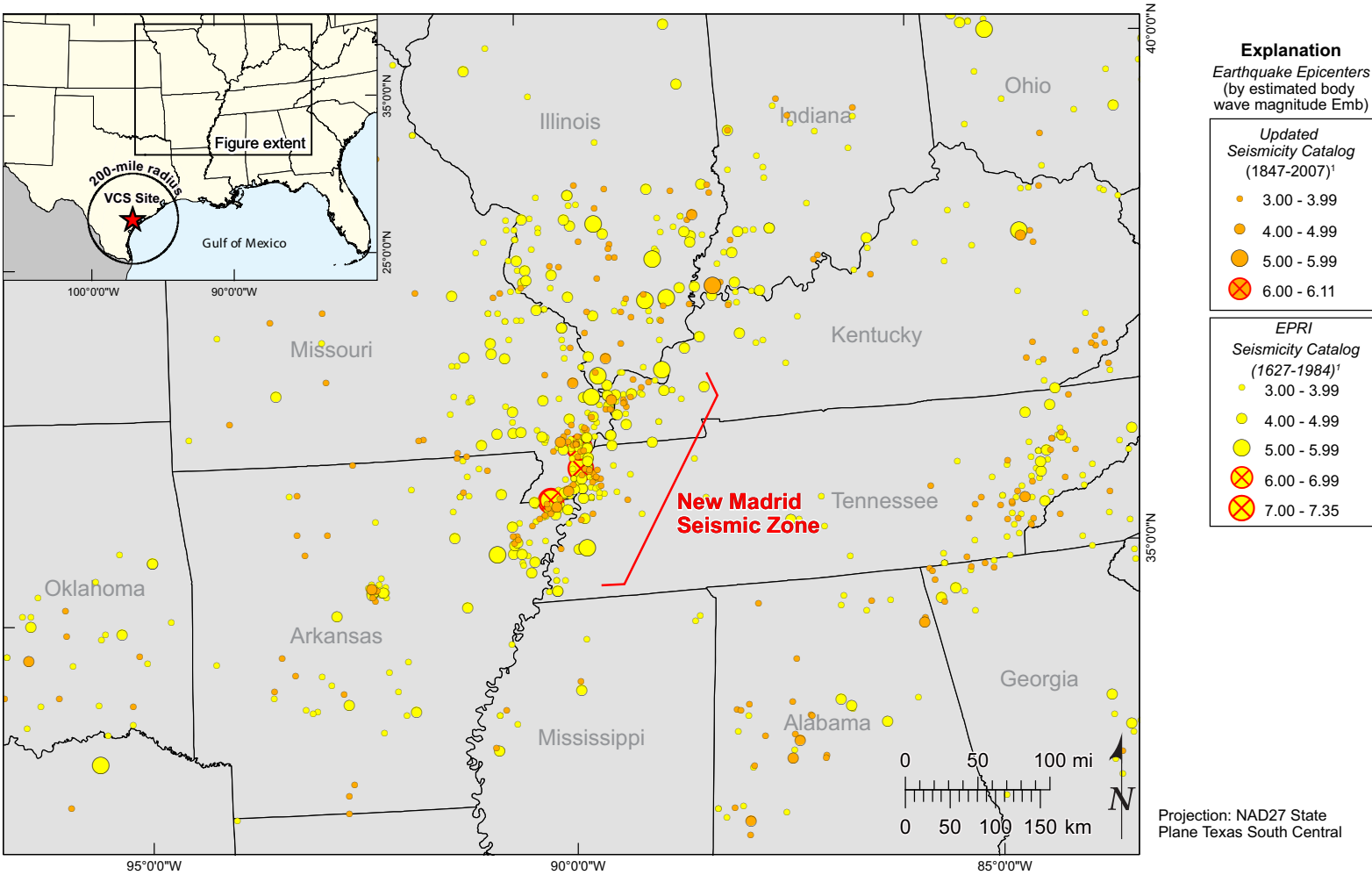


**Figure 2.5.2-11 Pattern of Concentrate Seismicity in the New Madrid Seismic Zone (NMSZ)**

Note: See [Subsection 2.5.2.1](#)

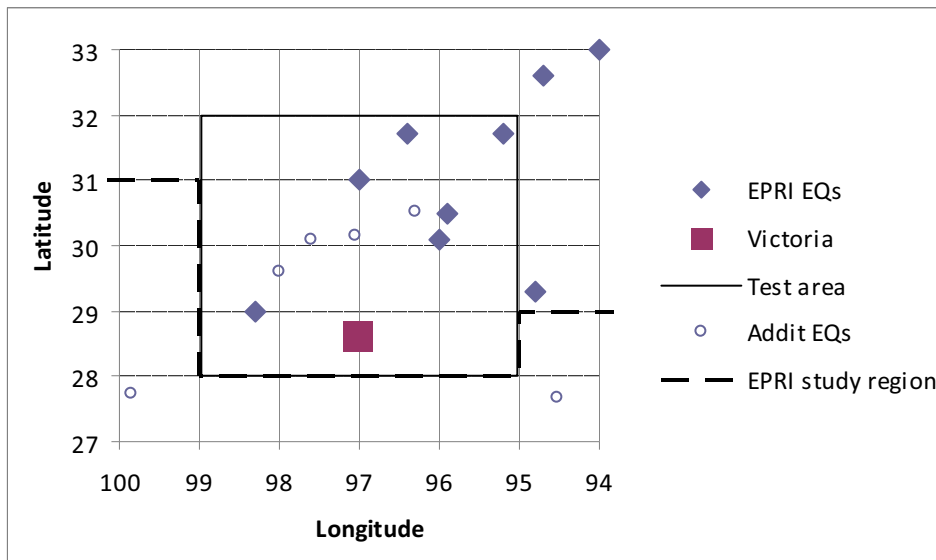


**Figure 2.5.2-12 Historical Seismicity in the Vicinity of the VCS Site and Test Area Used to Test the Effects of Additional Seismicity**

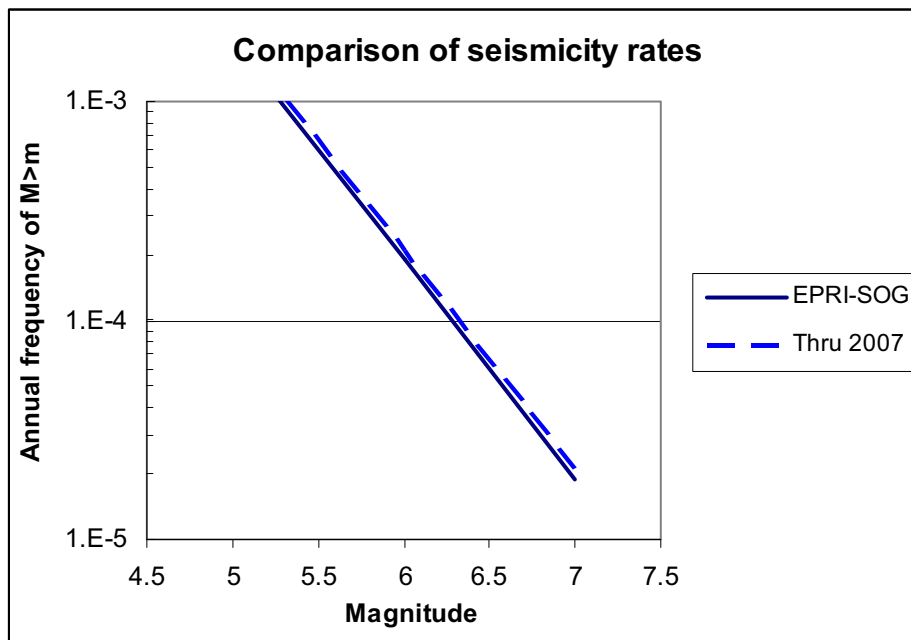


**Figure 2.5.2-13 Earthquake Occurrence Rates for EPRI (1989) Catalog and for Catalog Extended Through 2007 for Test Area**

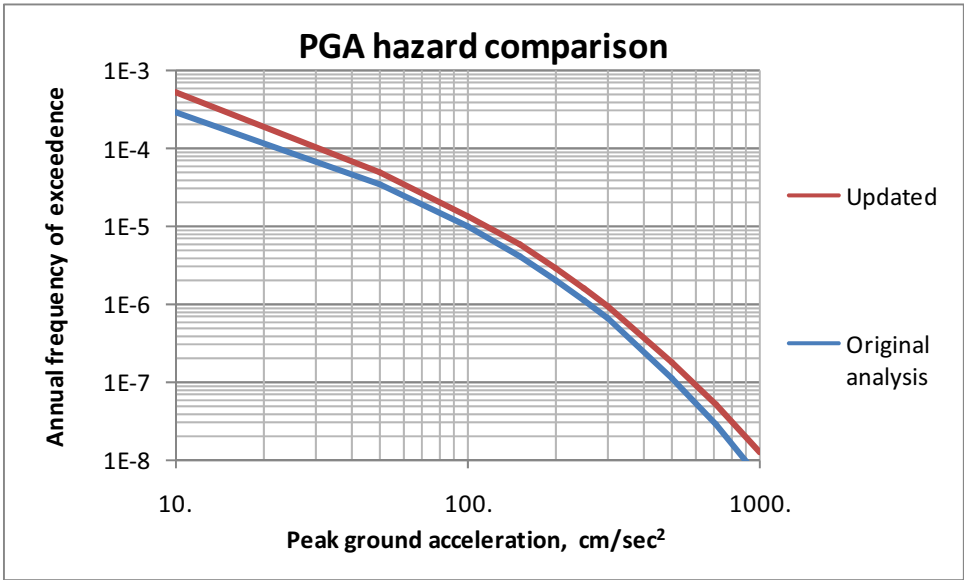


**Figure 2.5.2-14 Mean Peak Ground Acceleration (PGA) Rock Hazard from Original EPRI Analysis Compared to Mean PGA Hazard Using the Updated Catalog and Extended Seismic Sources**

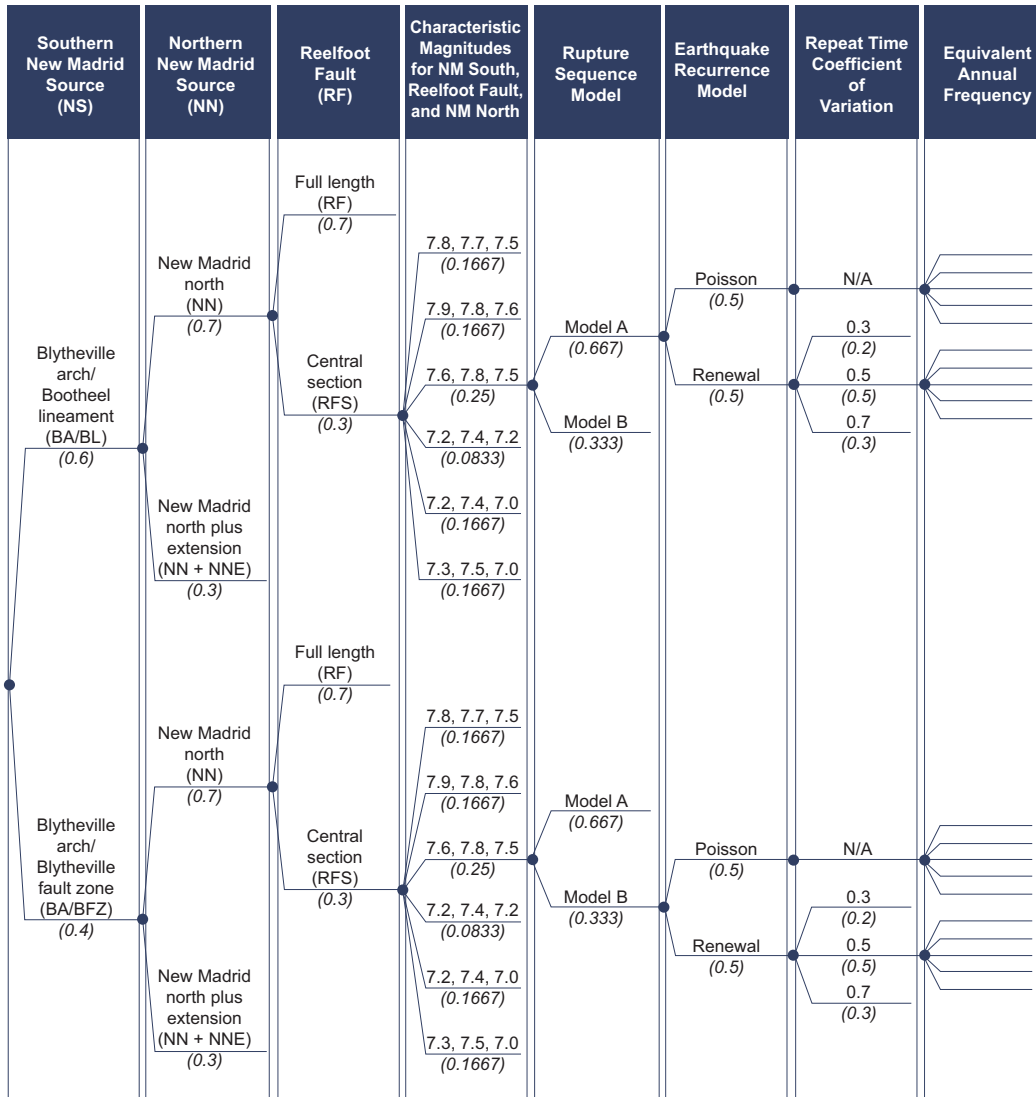
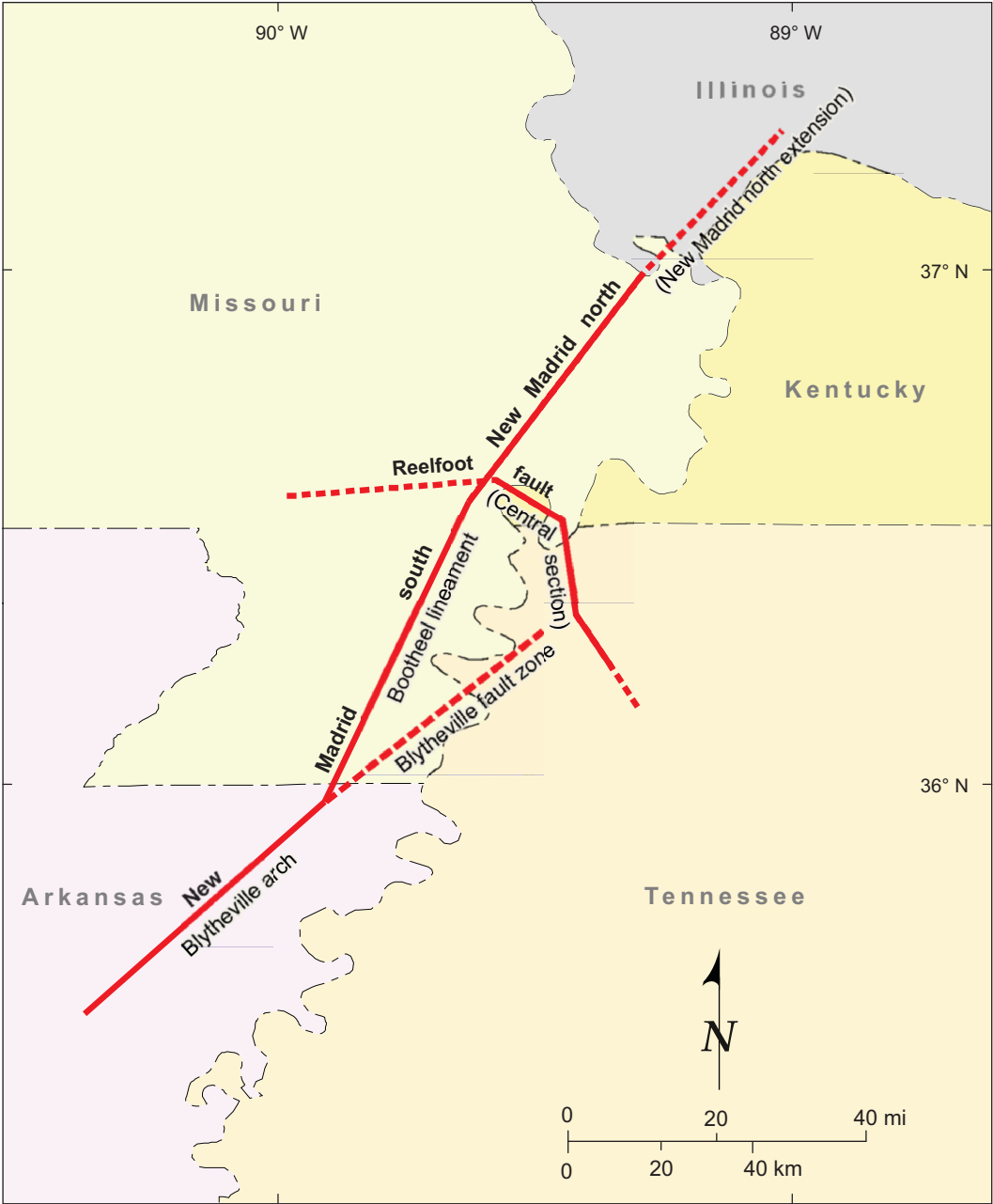
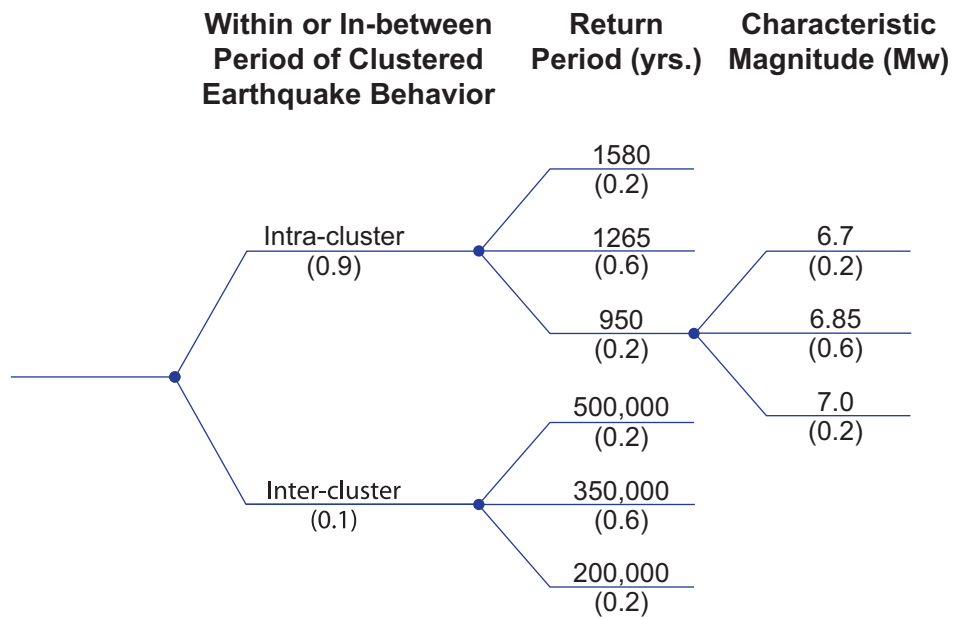


Figure 2.5.2-15 Clinton Source Characterization Logic Tree for the NMSZ  
 (Reference 2.5.2-70)



**Figure 2.5.2-16 NMSZ Source Model**  
(source geometry from [Reference 2.5.2-29](#))



**Figure 2.5.2-17 Logic Tree of Return Period and Characteristic Magnitude for the Meers Fault**

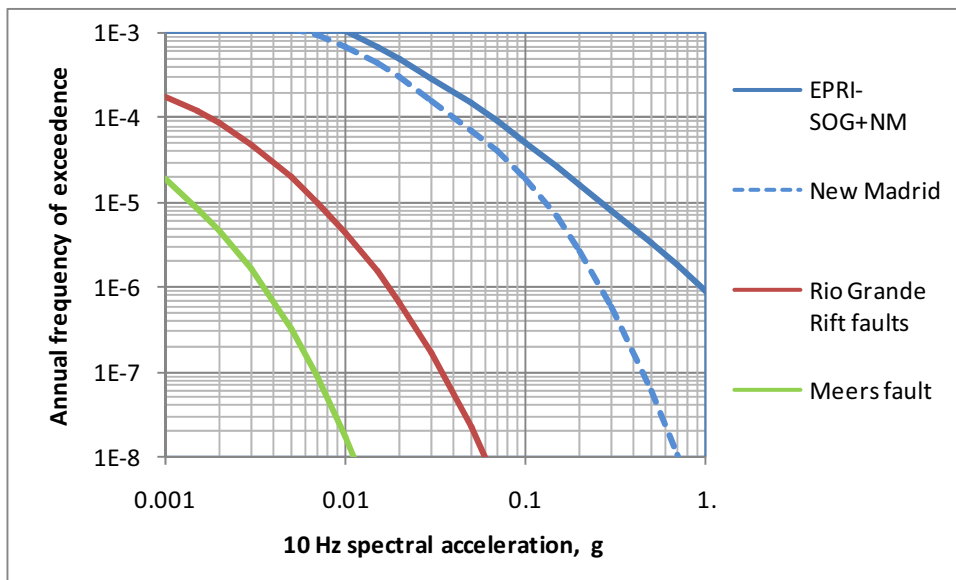


**Figure 2.5.2-18 10 Hz Mean Rock Seismic Hazard Curves for EPRI-SOG Teams Plus New Madrid, for New Madrid Alone, for Rio Grande Rift Faults Alone, and for Meers Fault Alone**

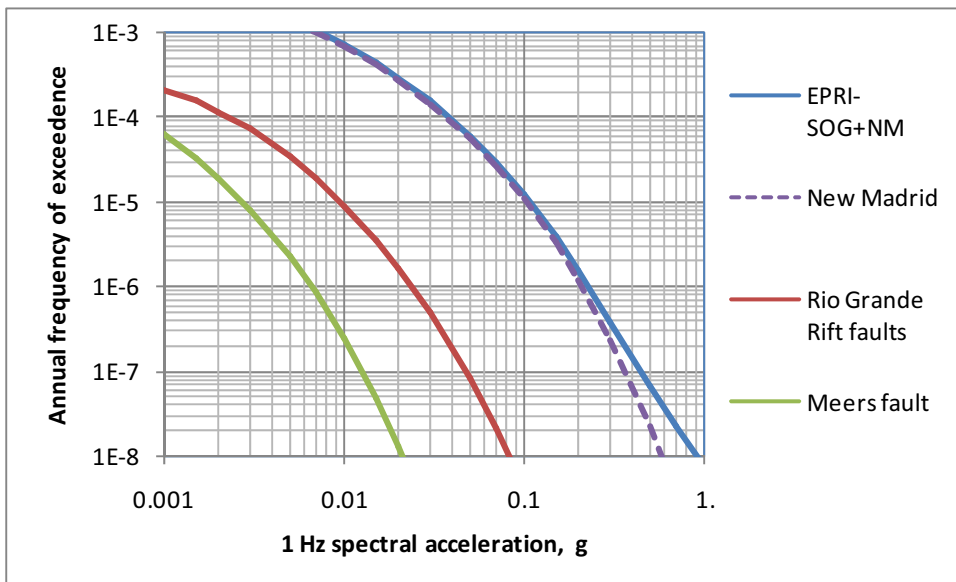


**Figure 2.5.2-19 1 Hz Mean Rock Seismic Hazard Curves For EPRI-SOG Teams Plus New Madrid, for New Madrid Alone, for Rio Grande Rift Faults Alone, and for Meers Fault Alone**

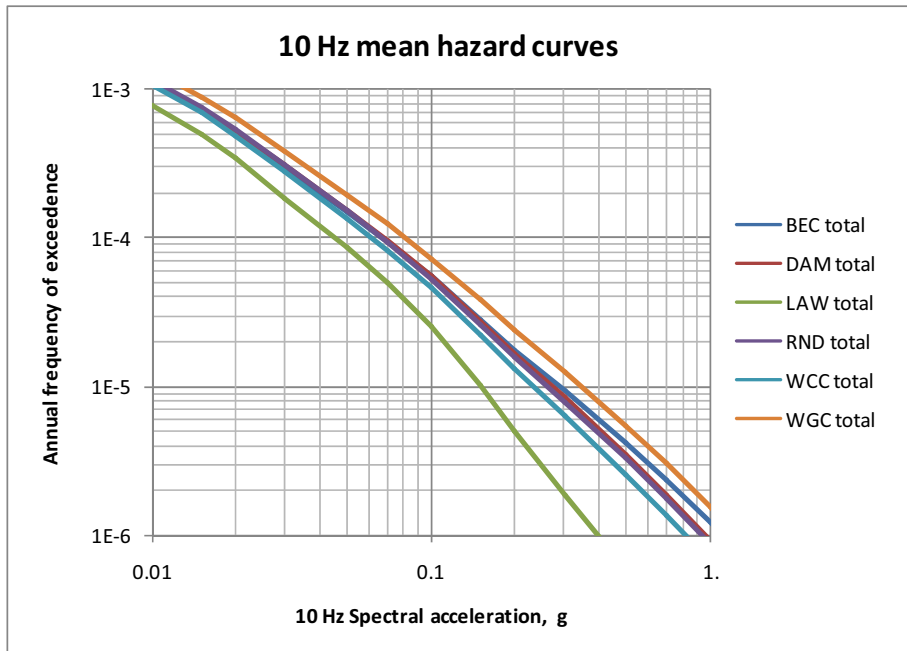


Figure 2.5.2-20 10 Hz Mean Rock Seismic Hazard Curves for EPRI Teams (Each Team Curve Includes the New Madrid Source)

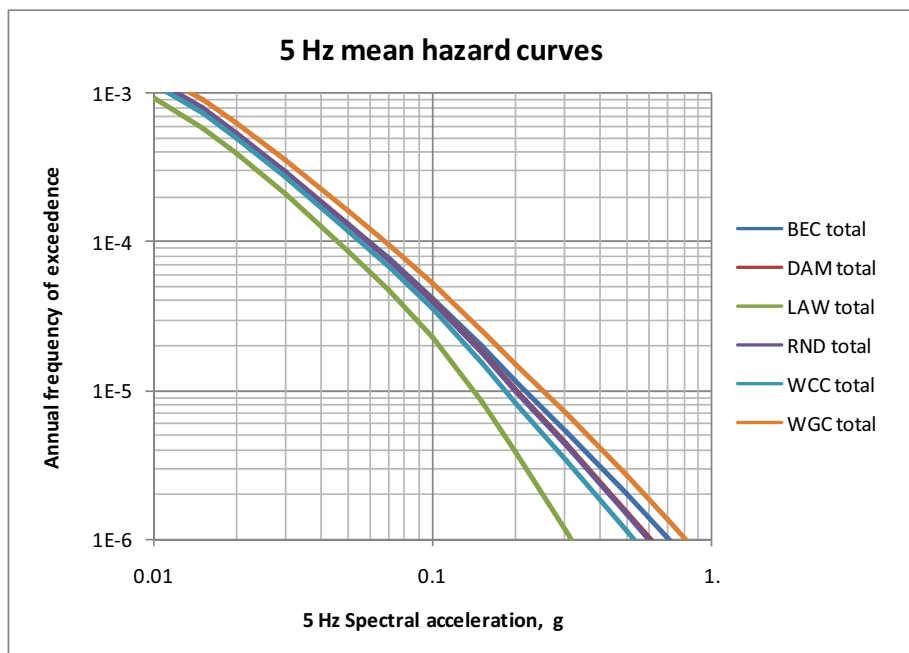


Figure 2.5.2-21 5 Hz Mean Rock Seismic Hazard Curves for EPRI Teams (Each Team Curve Includes the New Madrid Source)

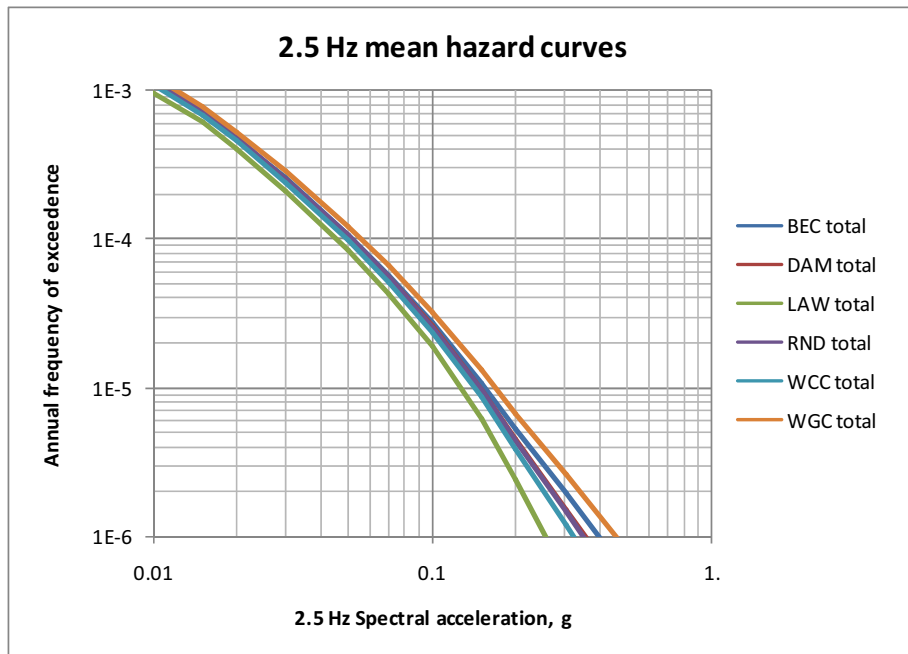


Figure 2.5.2-22 2.5 Hz Mean Rock Seismic Hazard Curves for EPRI Teams (Each Team Curve Includes the New Madrid Source)

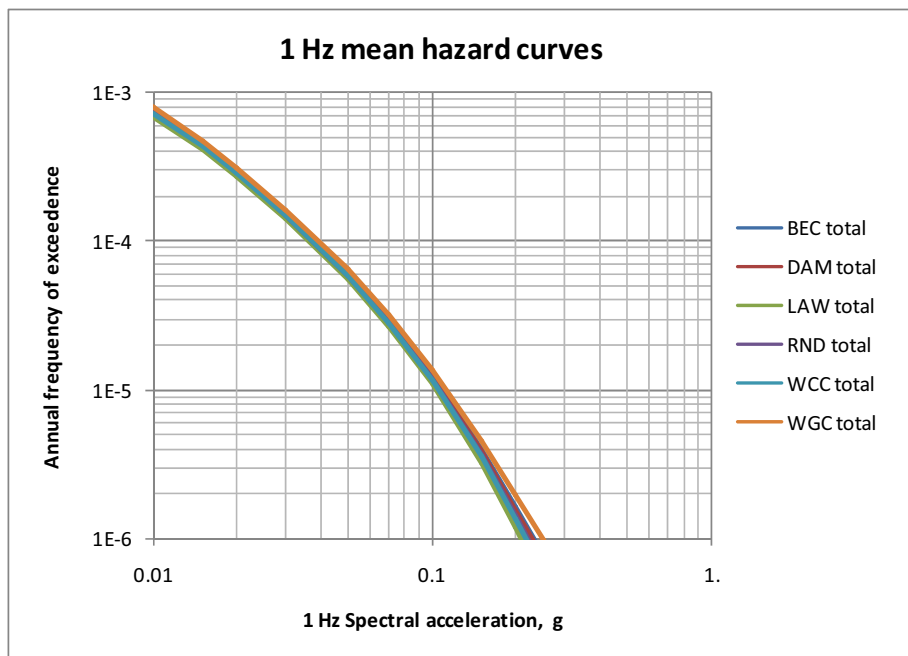
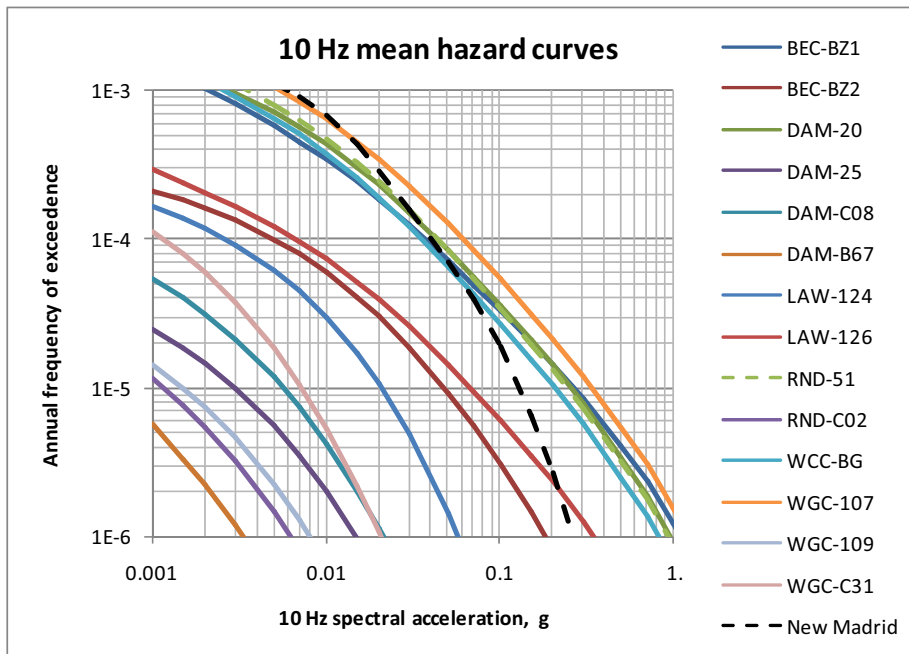
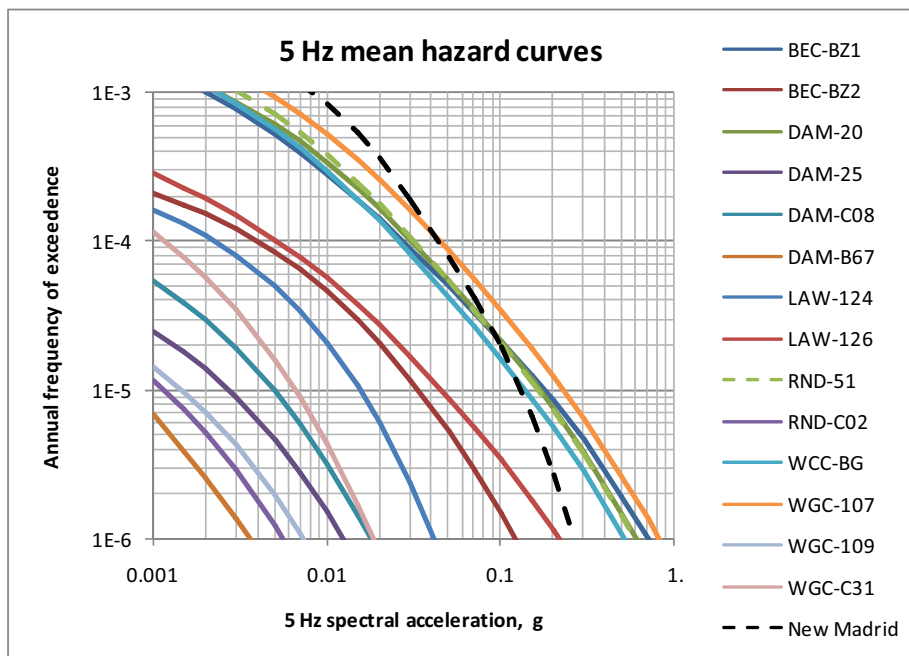


Figure 2.5.2-23 1 Hz Mean Rock Seismic Hazard Curves for EPRI Teams (Each Team Curve Includes the New Madrid Source)



**Figure 2.5.2-24 10 Hz Mean Rock Seismic Hazard Curves by Source for Each EPRI Team and for The New Madrid Source**



**Figure 2.5.2-25 5 Hz Mean Rock Seismic Hazard Curves by Source for Each EPRI Team and for The New Madrid Source**

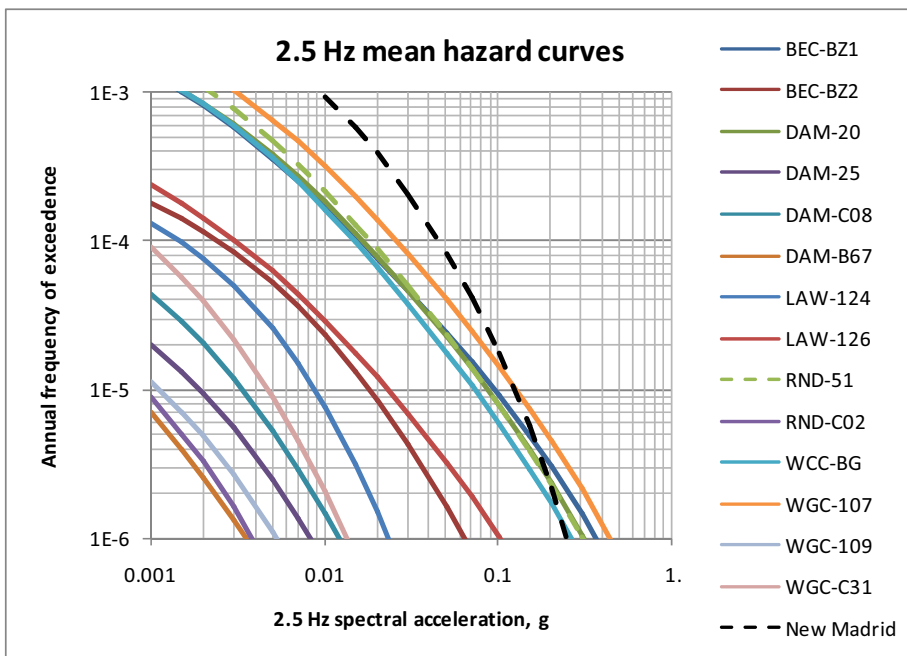


**Figure 2.5.2-26 2.5 Hz Mean Rock Seismic Hazard Curves by Source for Each EPRI Team and for the New Madrid Source**

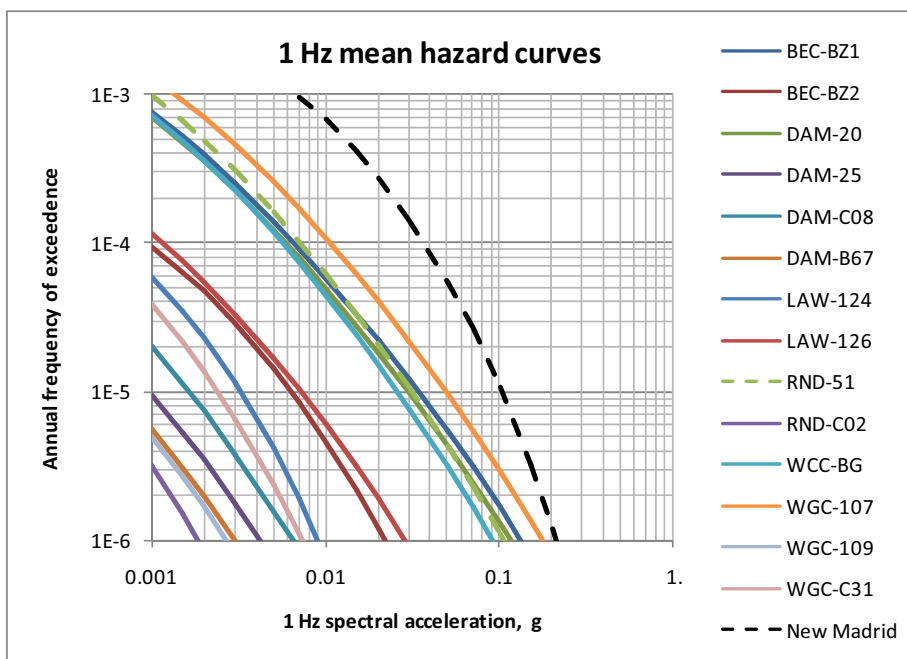


**Figure 2.5.2-27 1 Hz Mean Rock Seismic Hazard Curves by Source for Each EPRI Team and for the New Madrid Source**

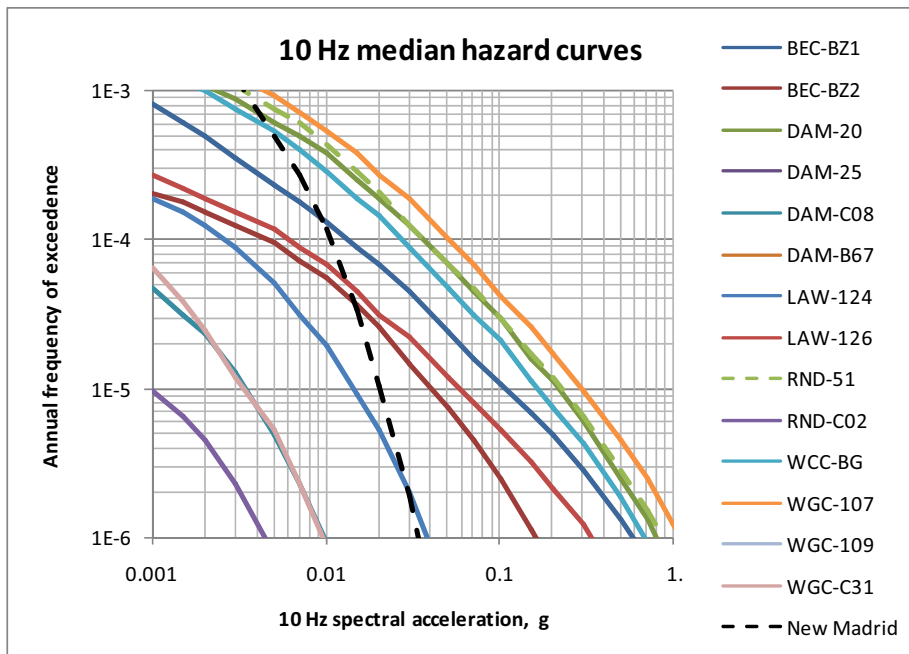


**Figure 2.5.2-28 10 Hz Median Rock Seismic Hazard Curves by Source for each EPRI Team and for the New Madrid Source**

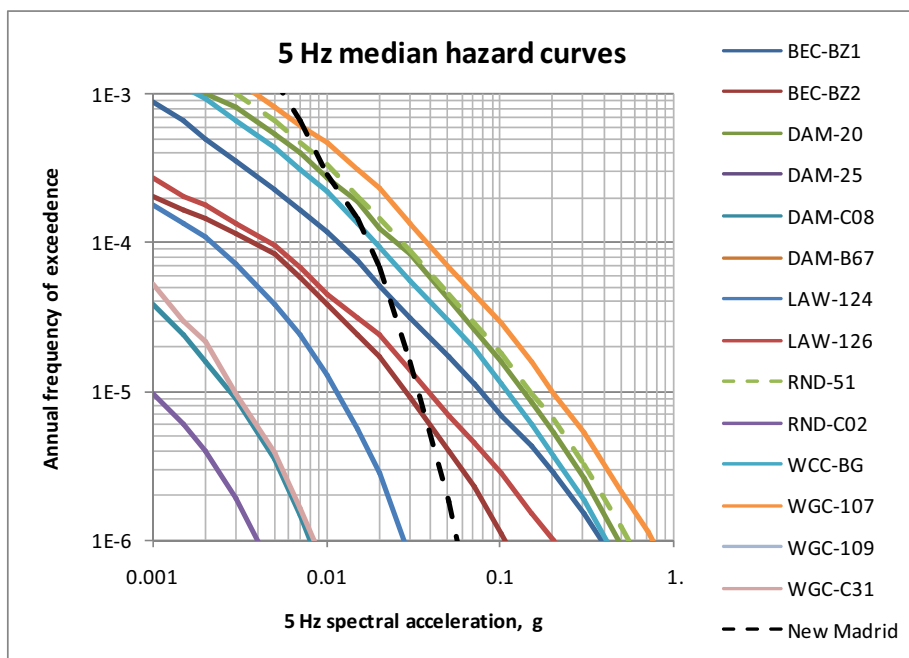


**Figure 2.5.2-29 5 Hz Median Rock Seismic Hazard Curves by Source for each EPRI Team and for the New Madrid Source**

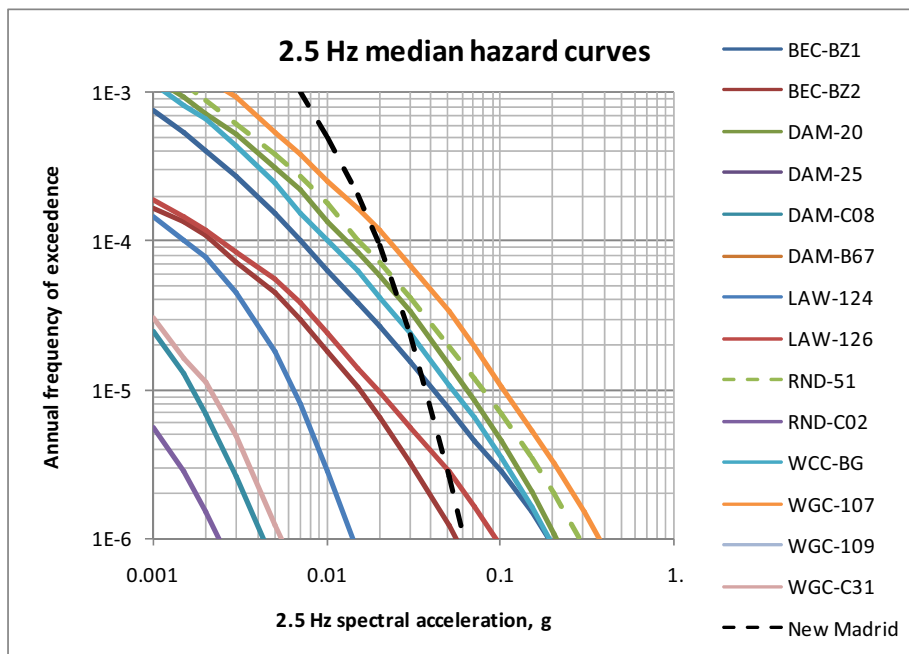


Figure 2.5.2-30 2.5 Hz Median Rock Seismic Hazard Curves by Source for each EPRI Team and for the New Madrid Source

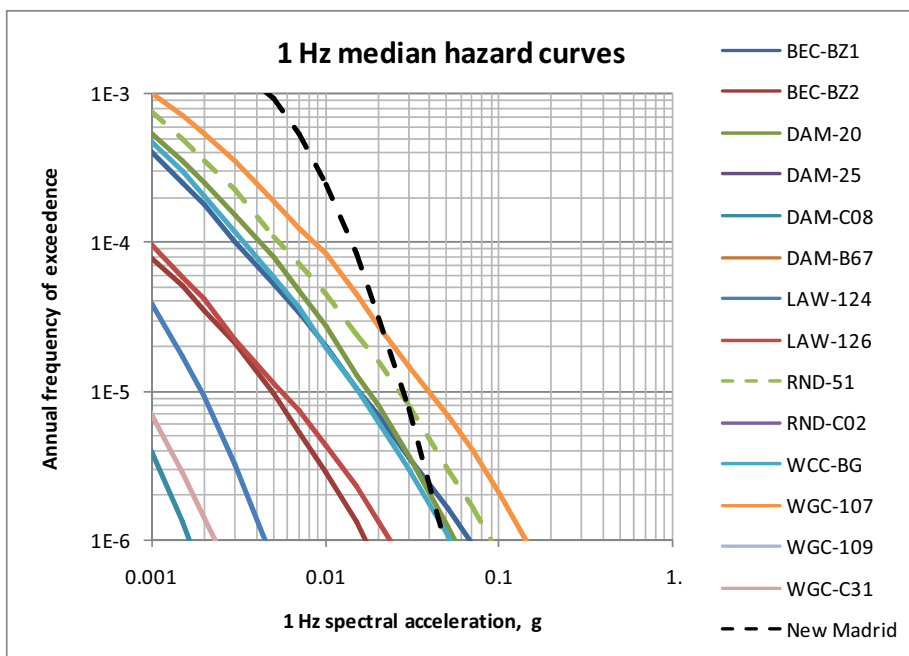


Figure 2.5.2-31 1 Hz Median Rock Seismic Hazard Curves by Source for each EPRI Team and for the New Madrid Source

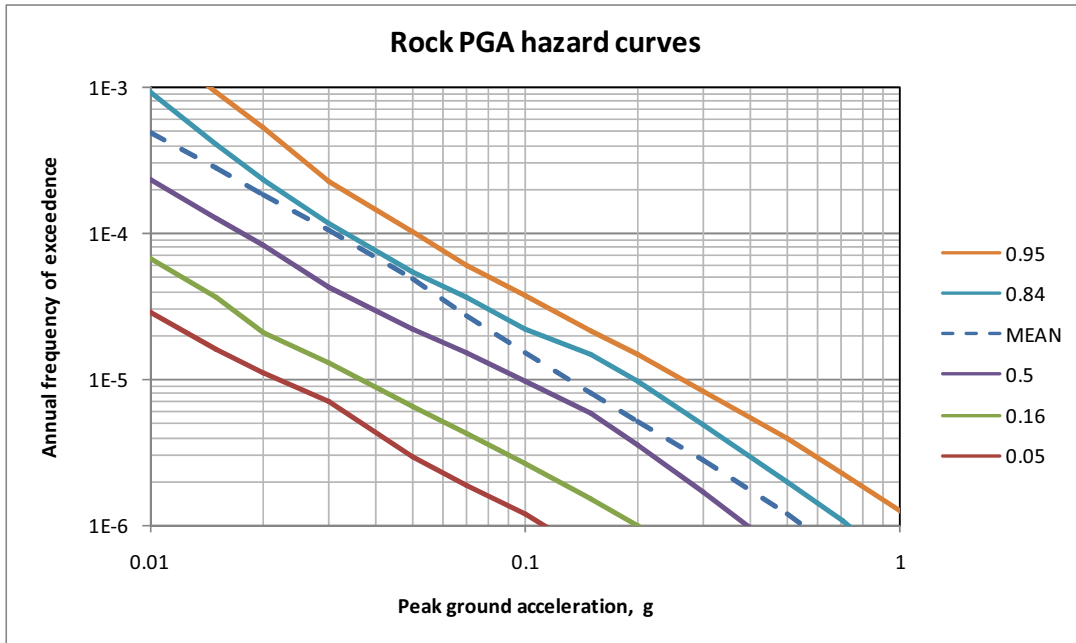


Figure 2.5.2-32 Mean and Fractile PGA Rock Hazard Curves

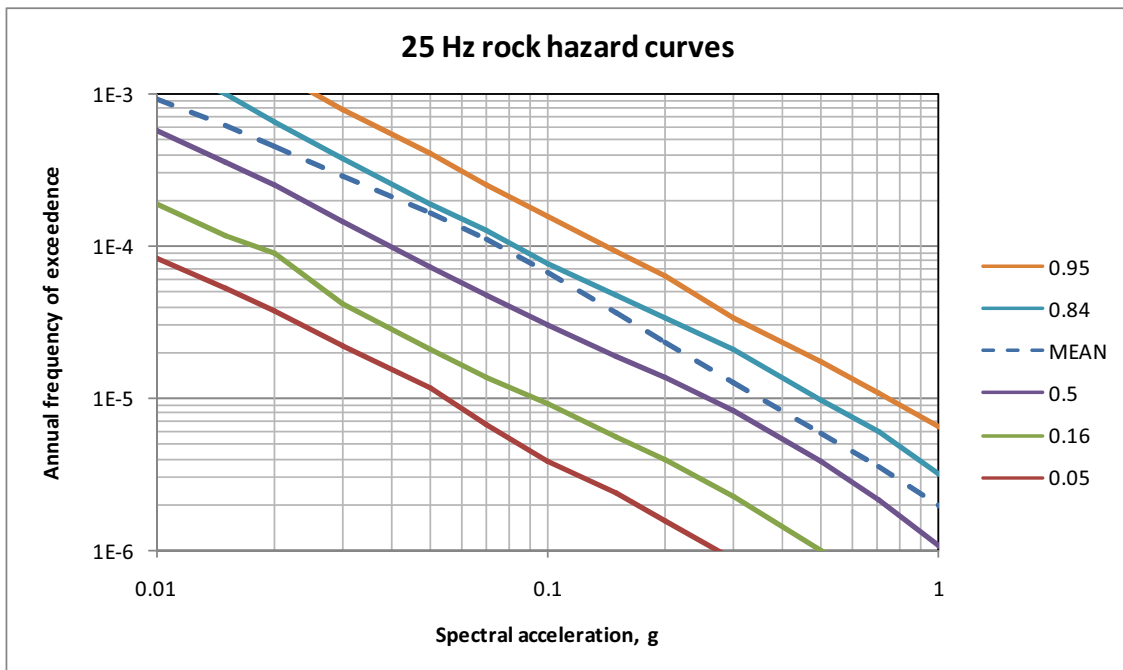


Figure 2.5.2-33 Mean and Fractile 25 Hz Rock Hazard Curves

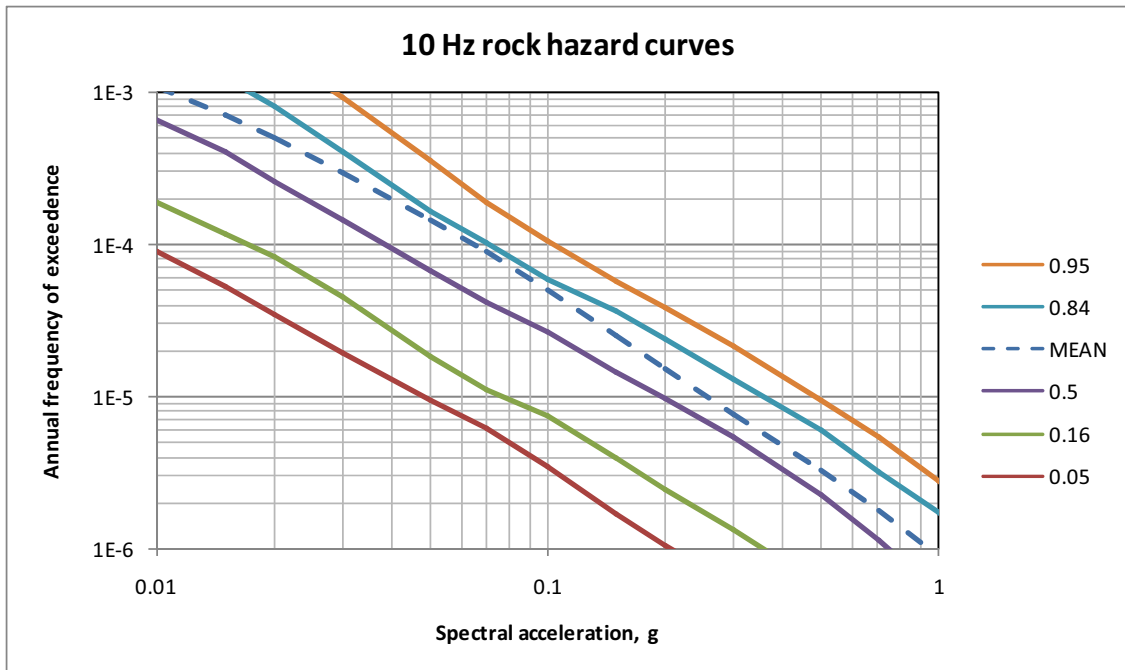


Figure 2.5.2-34 Mean and Fractile 10 Hz Rock Hazard Curves

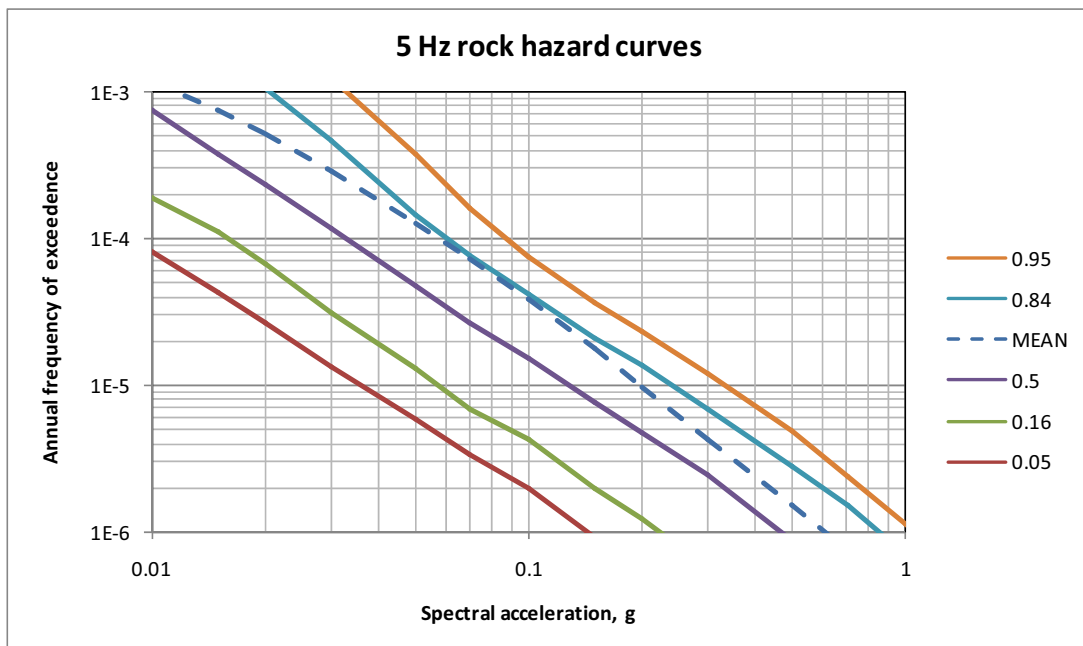


Figure 2.5.2-35 Mean and Fractile 5 Hz Rock Hazard Curves

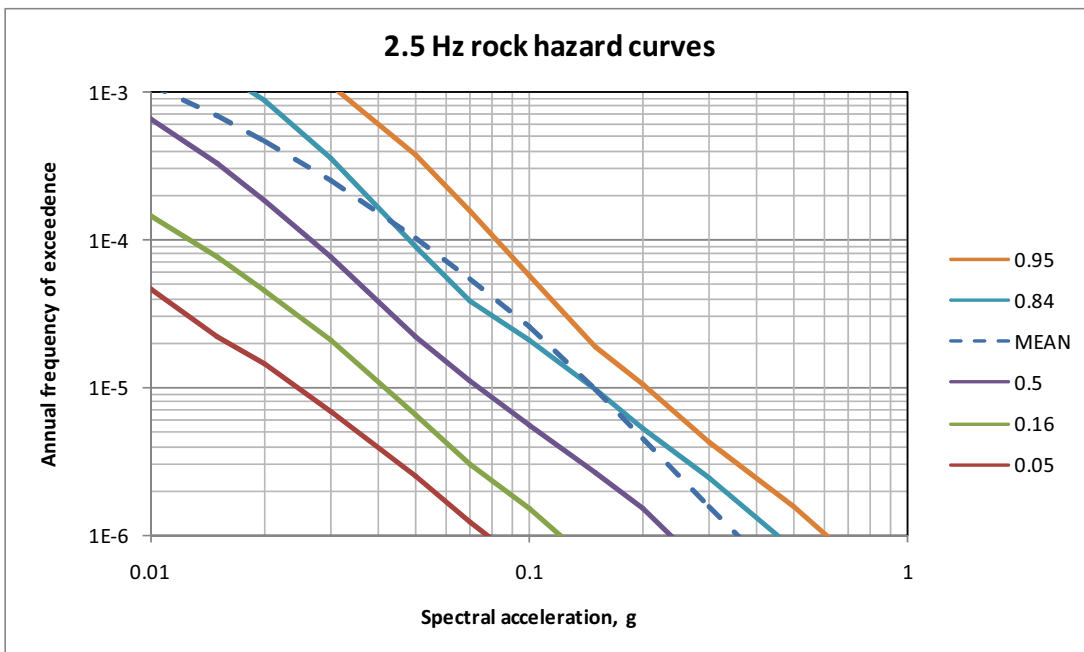


Figure 2.5.2-36 Mean and Fractile 2.5 Hz Rock Hazard Curves

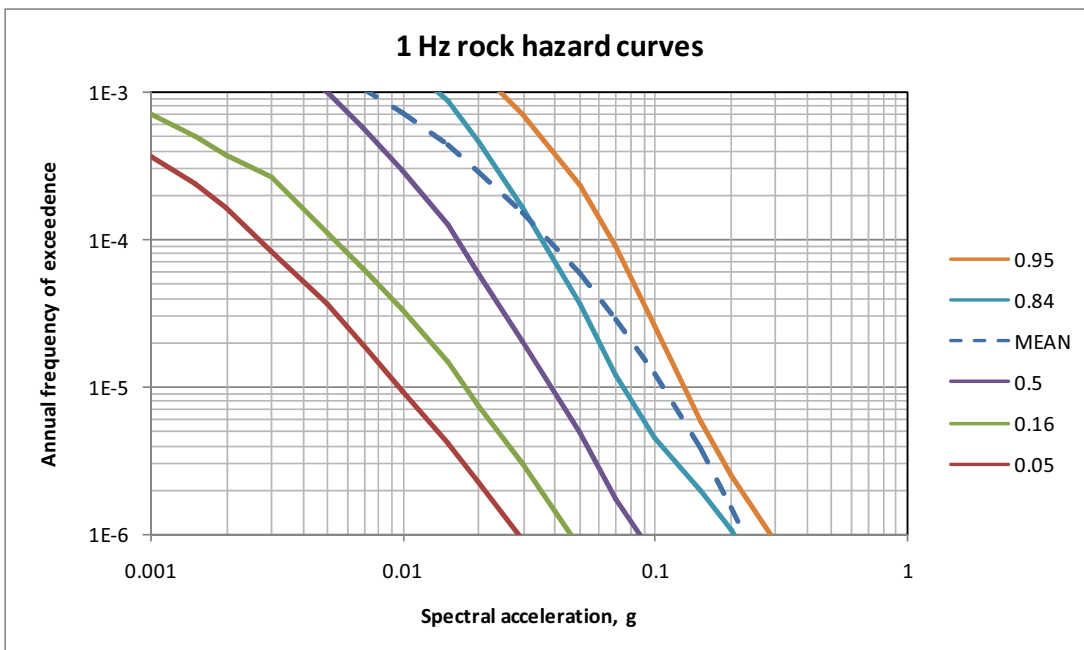


Figure 2.5.2-37 Mean and Fractile 1 Hz Rock Hazard Curves

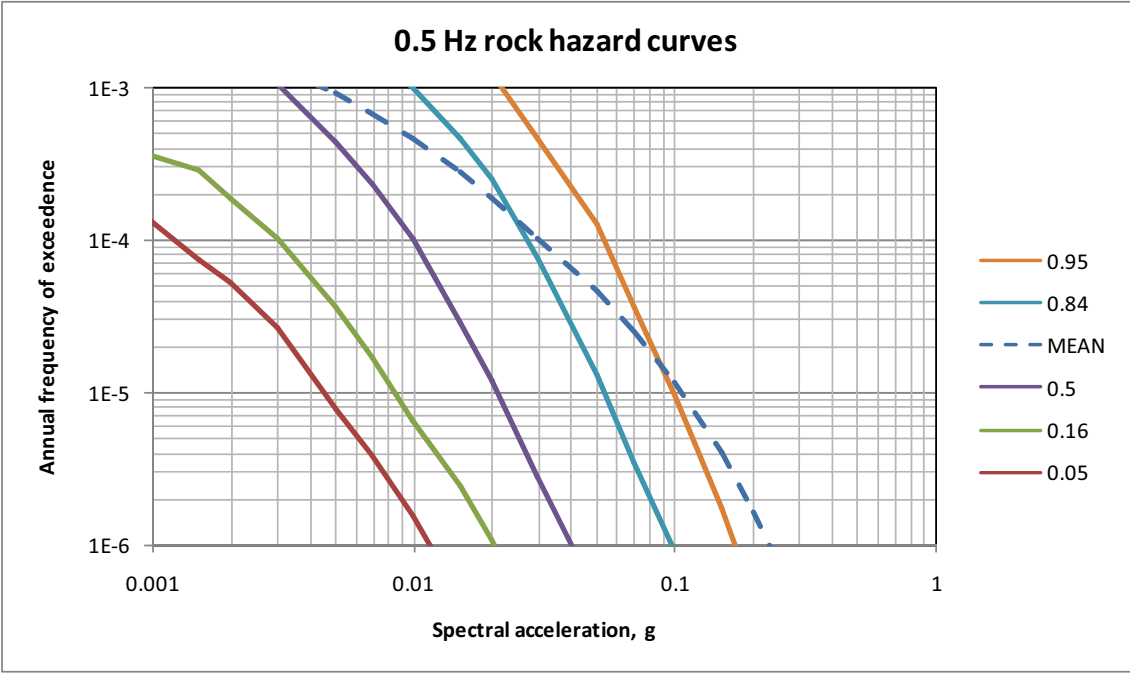
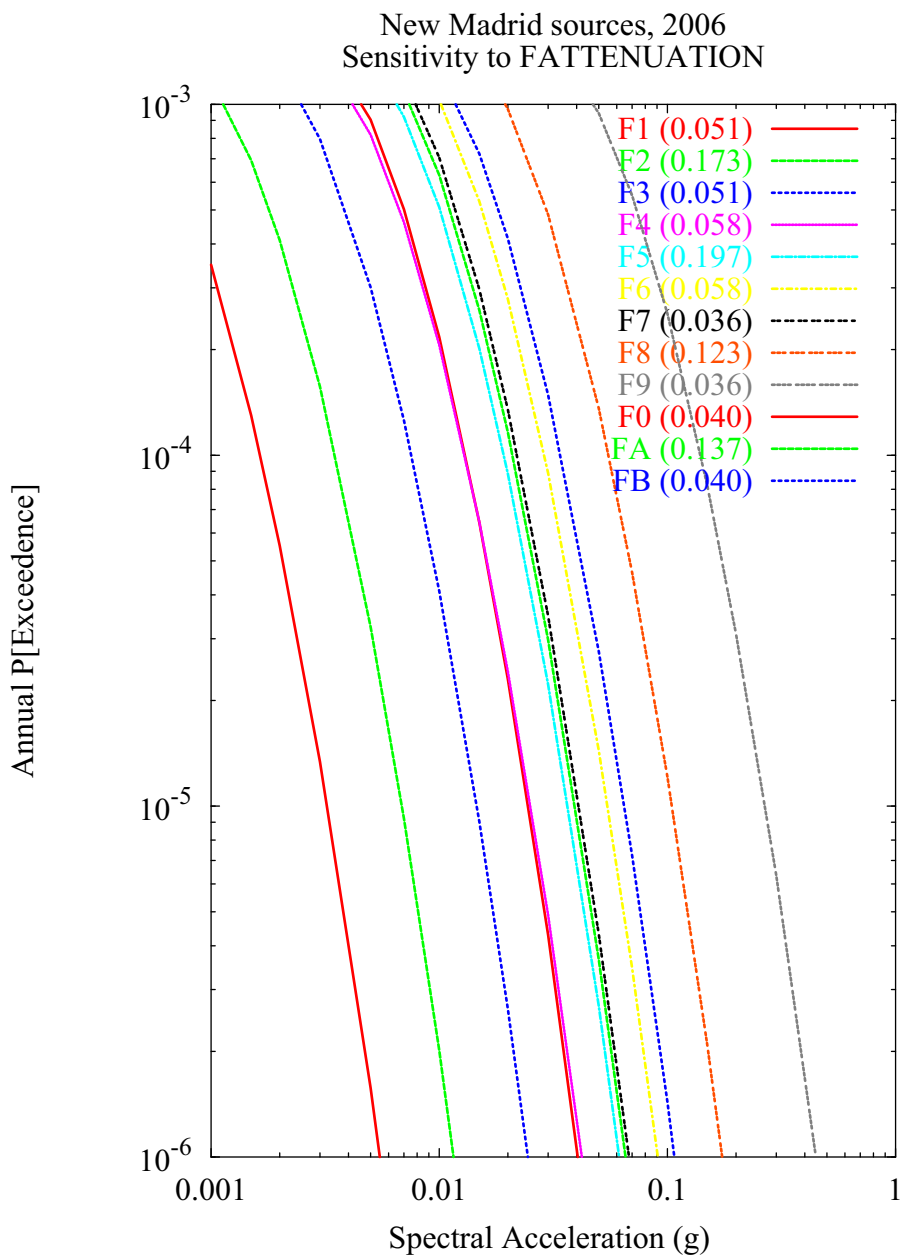


Figure 2.5.2-38 Mean and Fractile 0.5 Hz Rock Hazard Curves



**Figure 2.5.2-39 Sensitivity of 1 Hz Mean Hazard to Ground Motion Equation for the New Madrid Source**

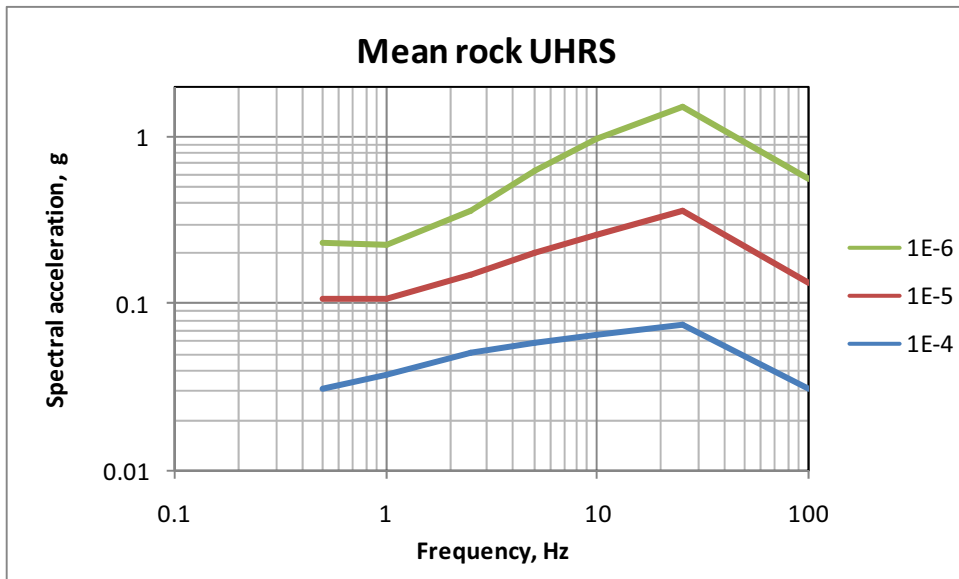


Figure 2.5.2-40 Mean Rock UHRS for  $10^{-4}$ ,  $10^{-5}$ , and  $10^{-6}$

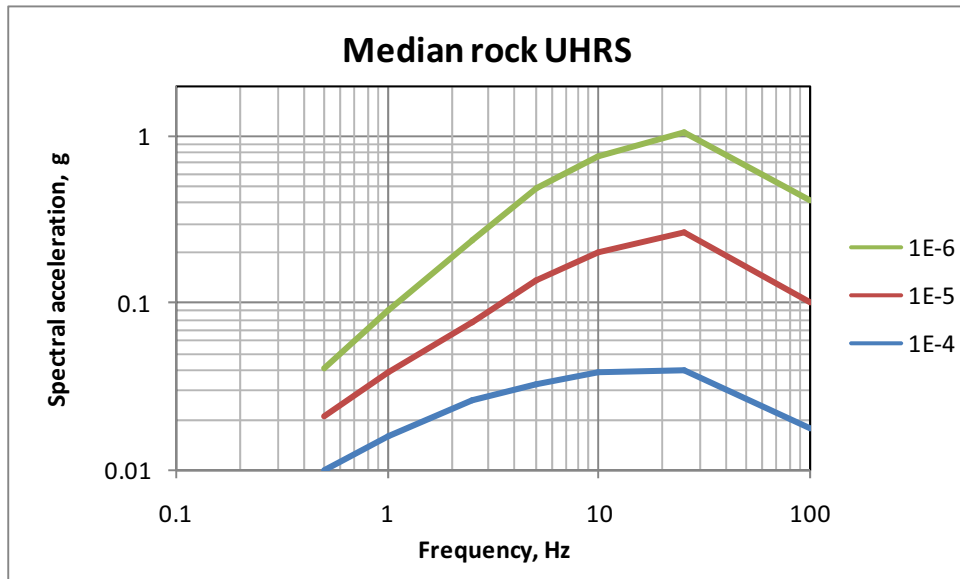


Figure 2.5.2-41 Median Rock UHRS for  $10^{-4}$ ,  $10^{-5}$ , and  $10^{-6}$

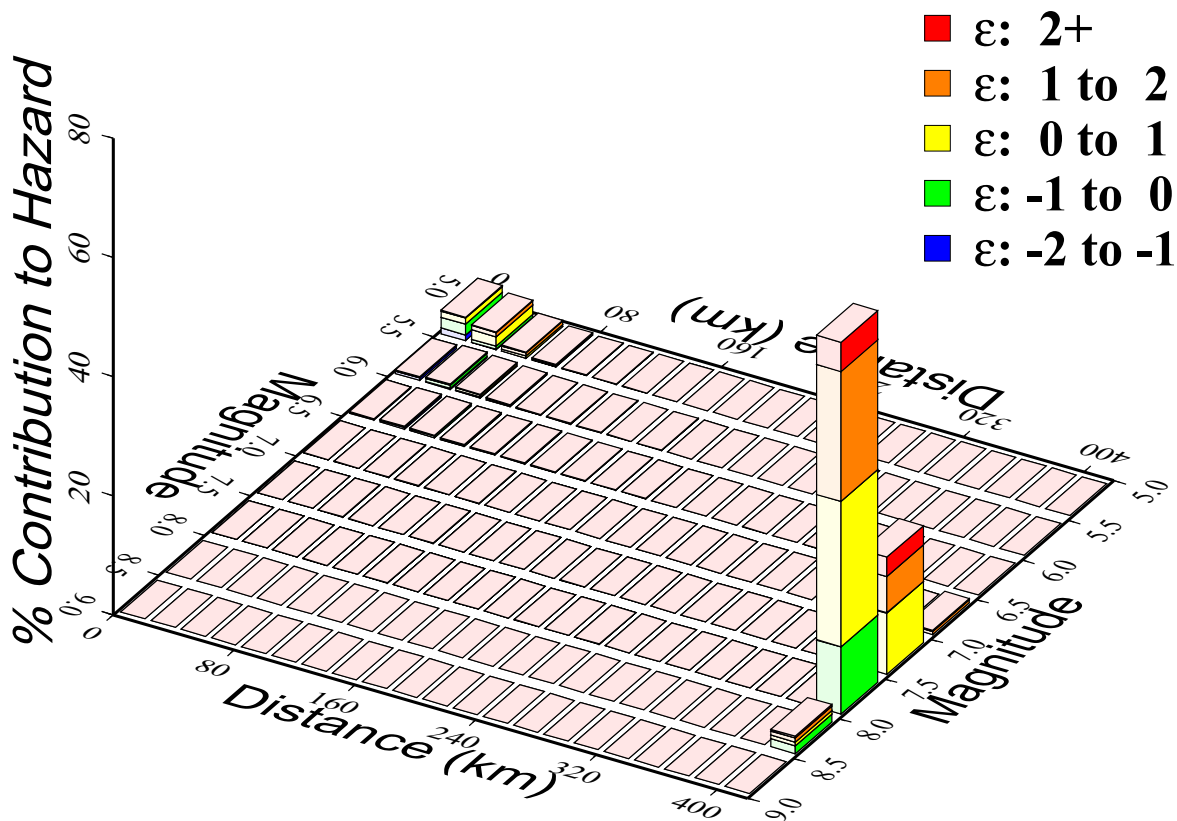


Figure 2.5.2-42 1 and 2.5 Hz Deaggregation of Mean Hazard for  $10^{-4}$

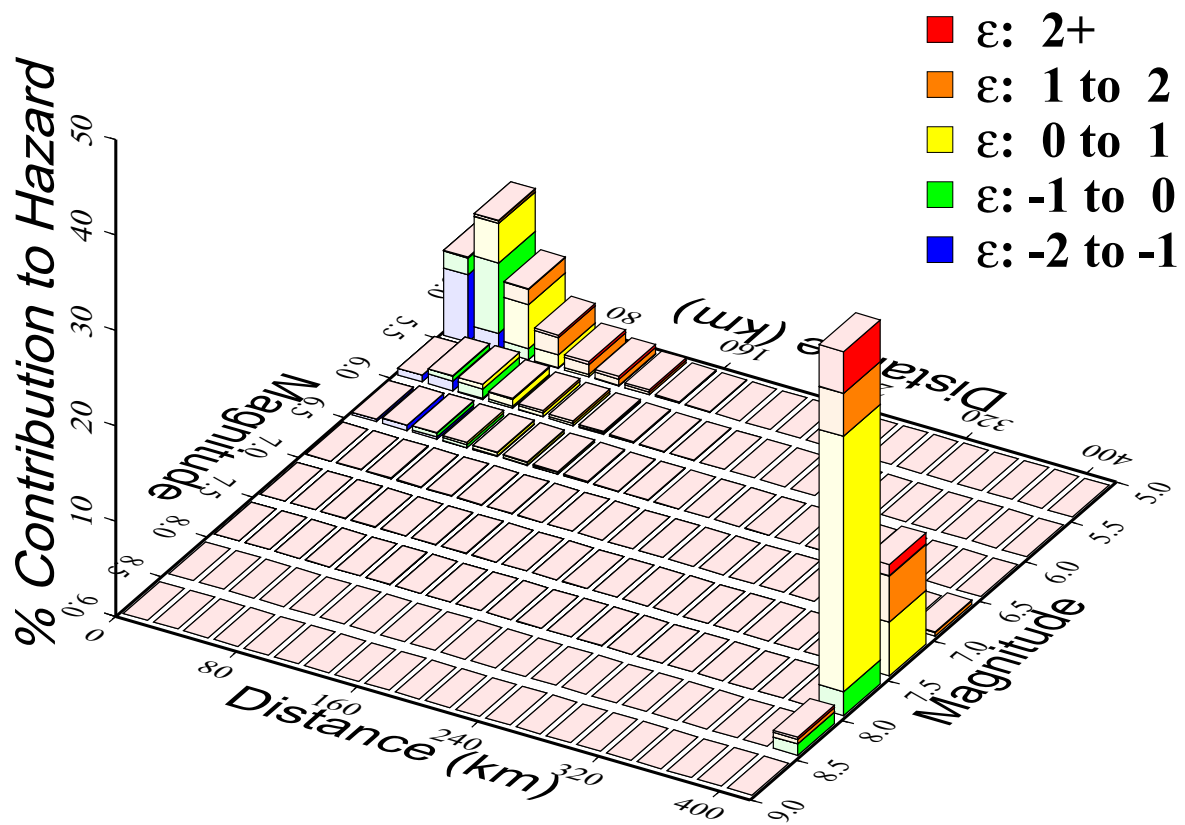


Figure 2.5.2-43 5 and 10 Hz Deaggregation of Mean Hazard for  $10^{-4}$

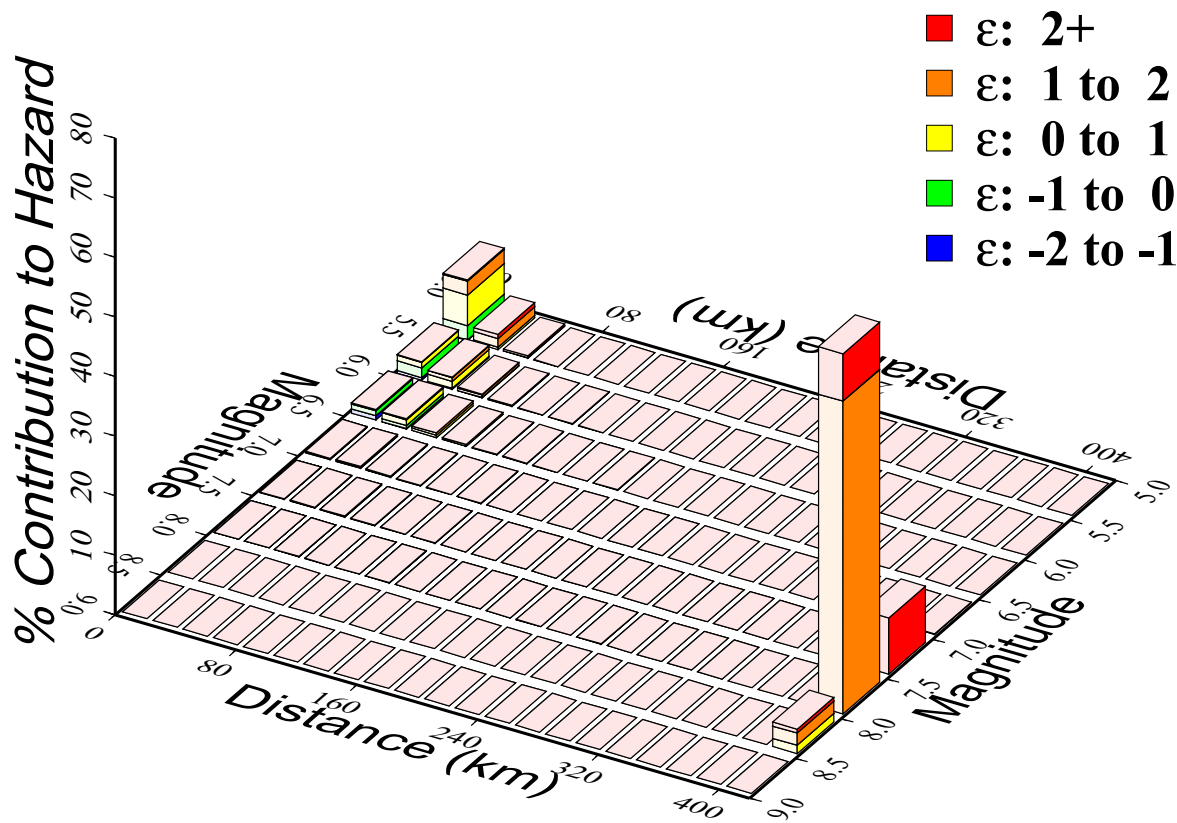


Figure 2.5.2-44 1 and 2.5 Hz Deaggregation of Mean Hazard for  $10^{-5}$

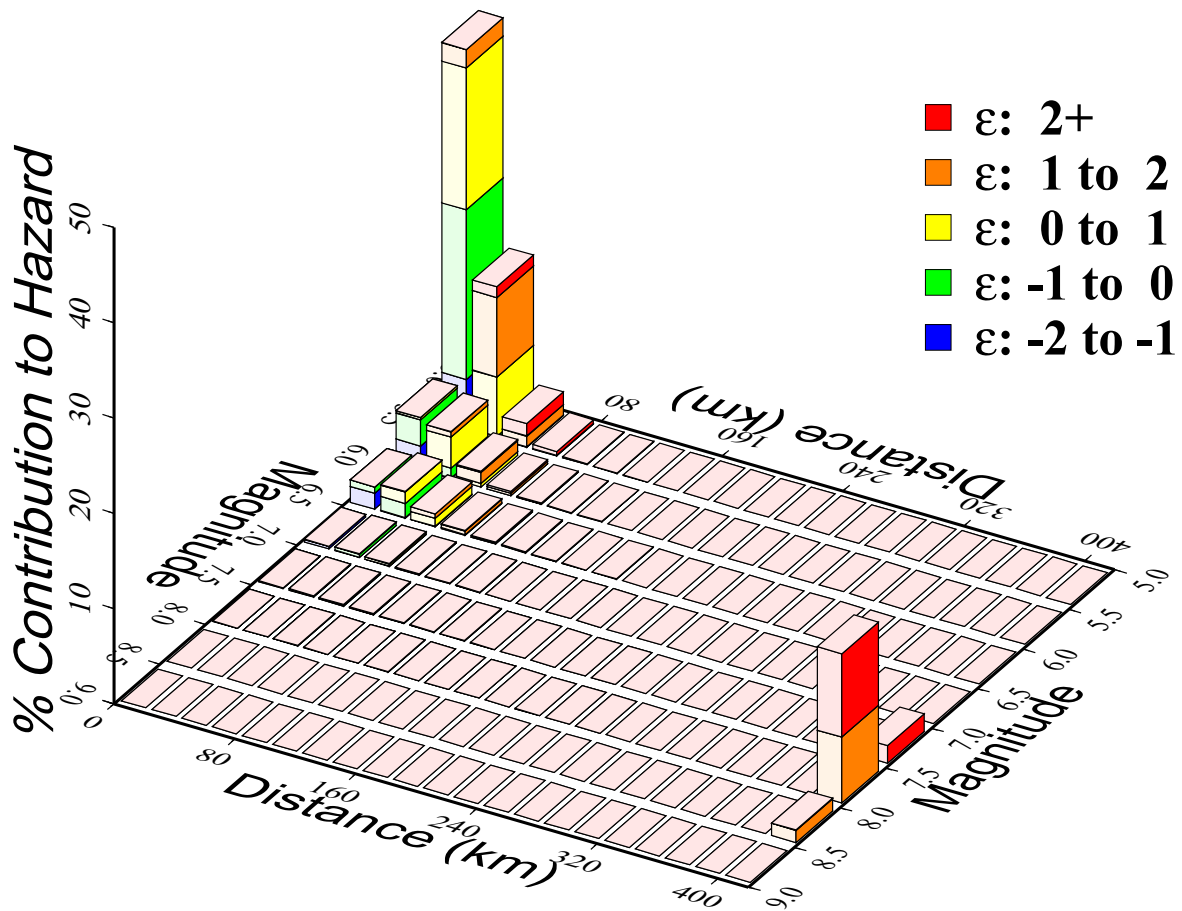


Figure 2.5.2-45 5 and 10 Hz Deaggregation of Mean Hazard for  $10^{-5}$

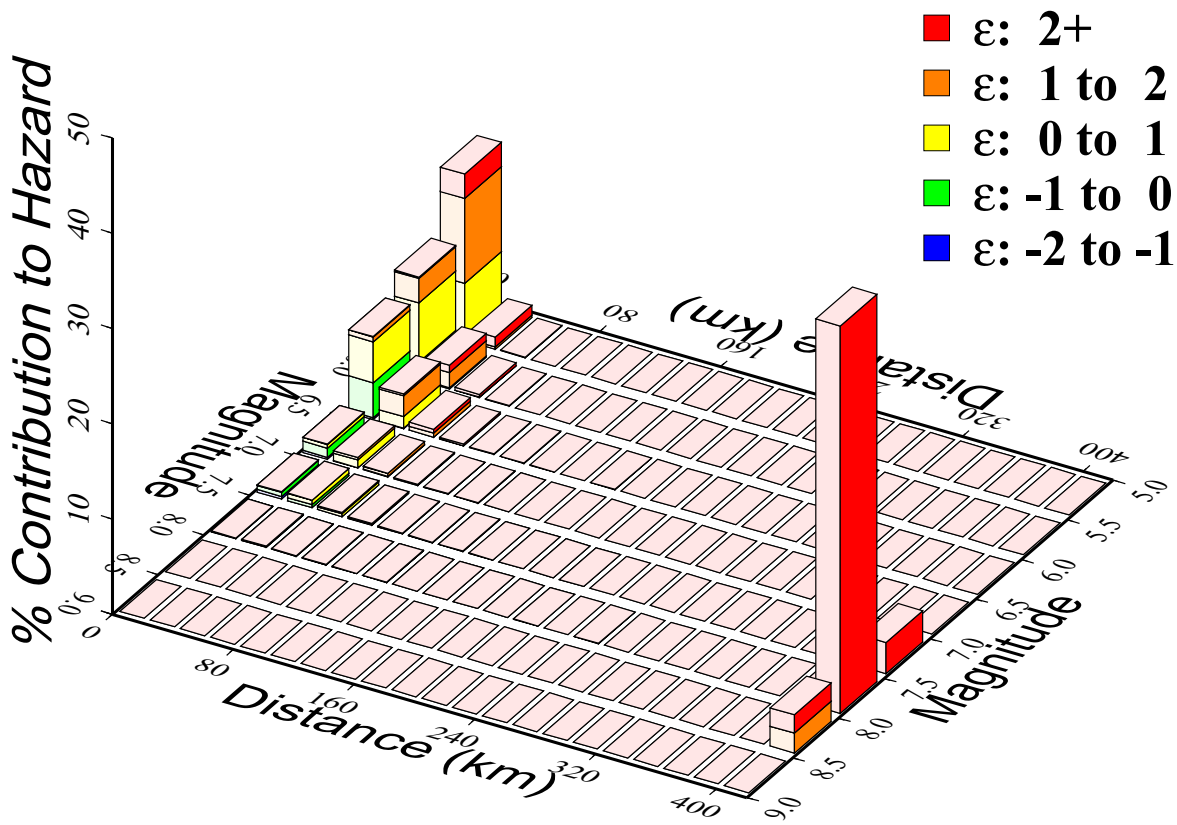


Figure 2.5.2-46 1 and 2.5 Hz Deaggregation of Mean Hazard for 10<sup>-6</sup>

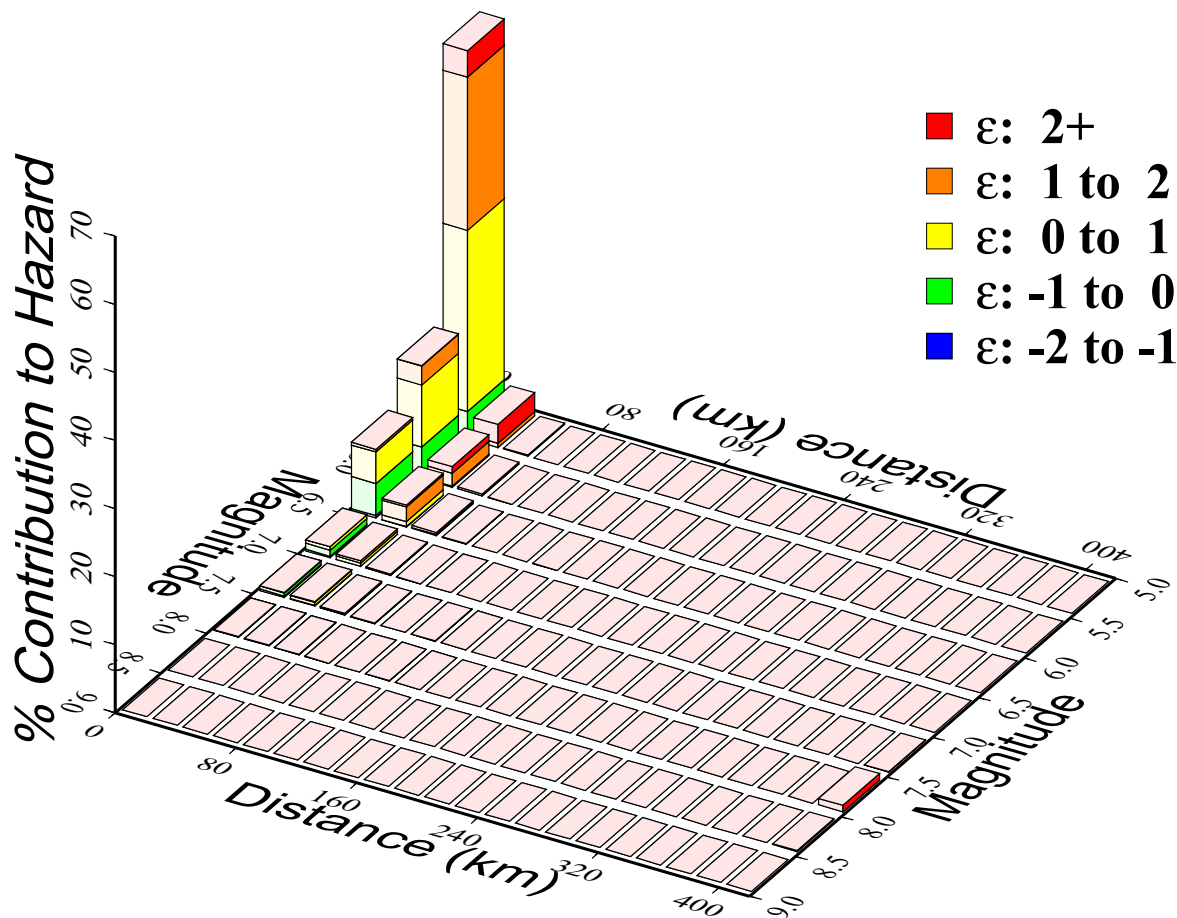


Figure 2.5.2-47 5 and 10 Hz Deaggregation of Mean Hazard for 10<sup>-6</sup>

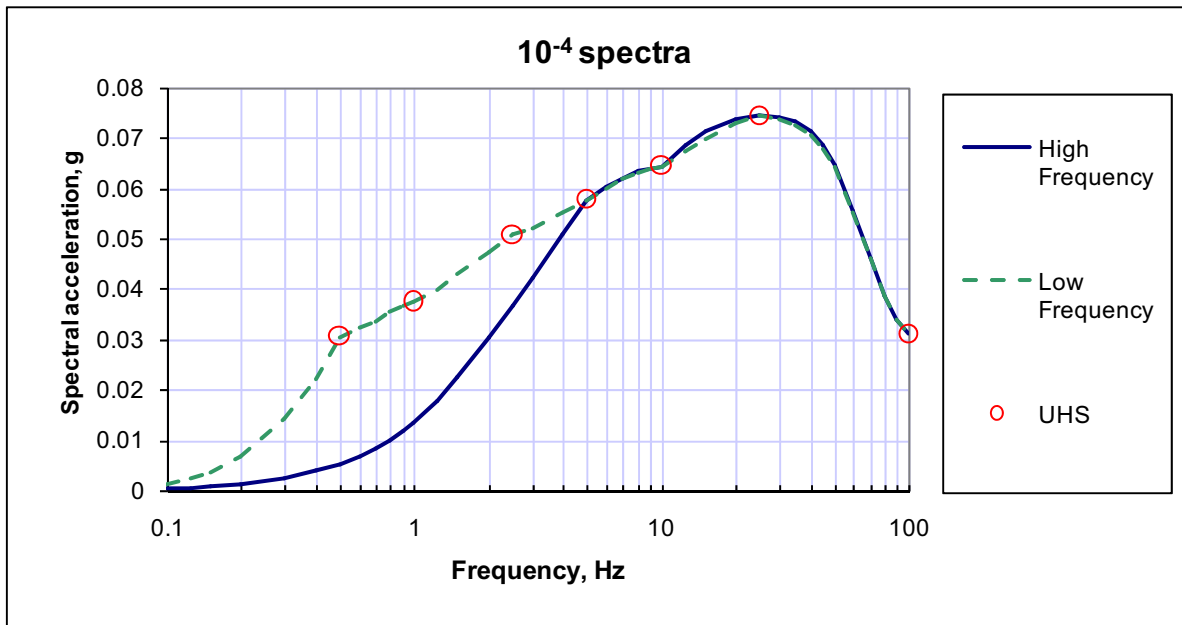


Figure 2.5.2-48 Mean HF and LF Rock Spectra for 10<sup>-4</sup>

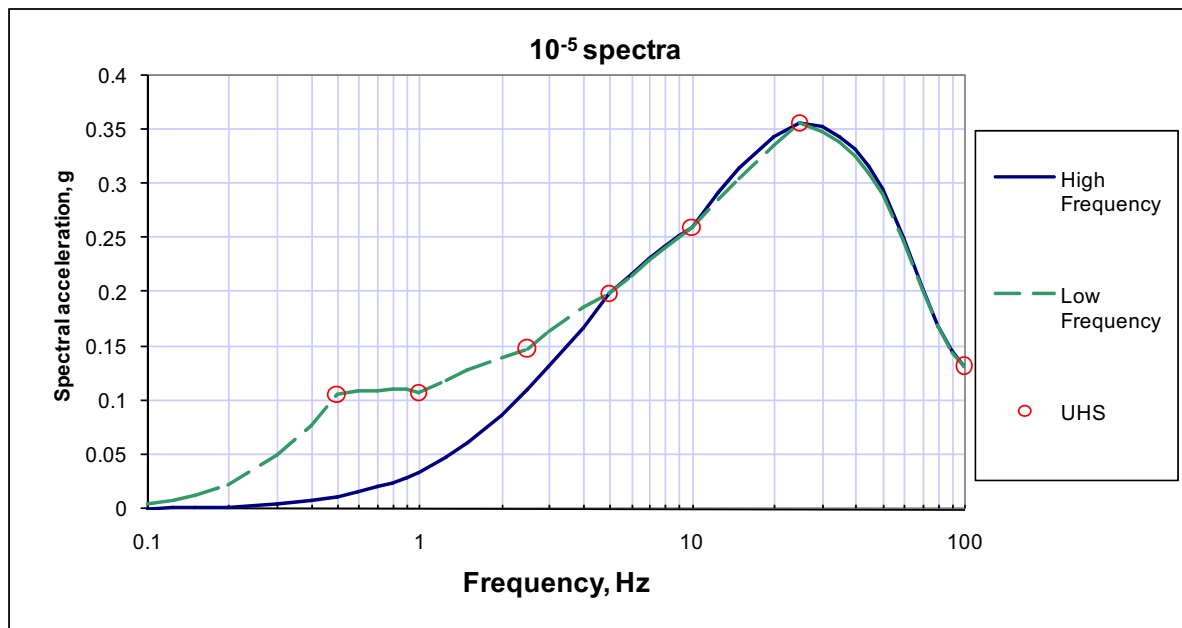
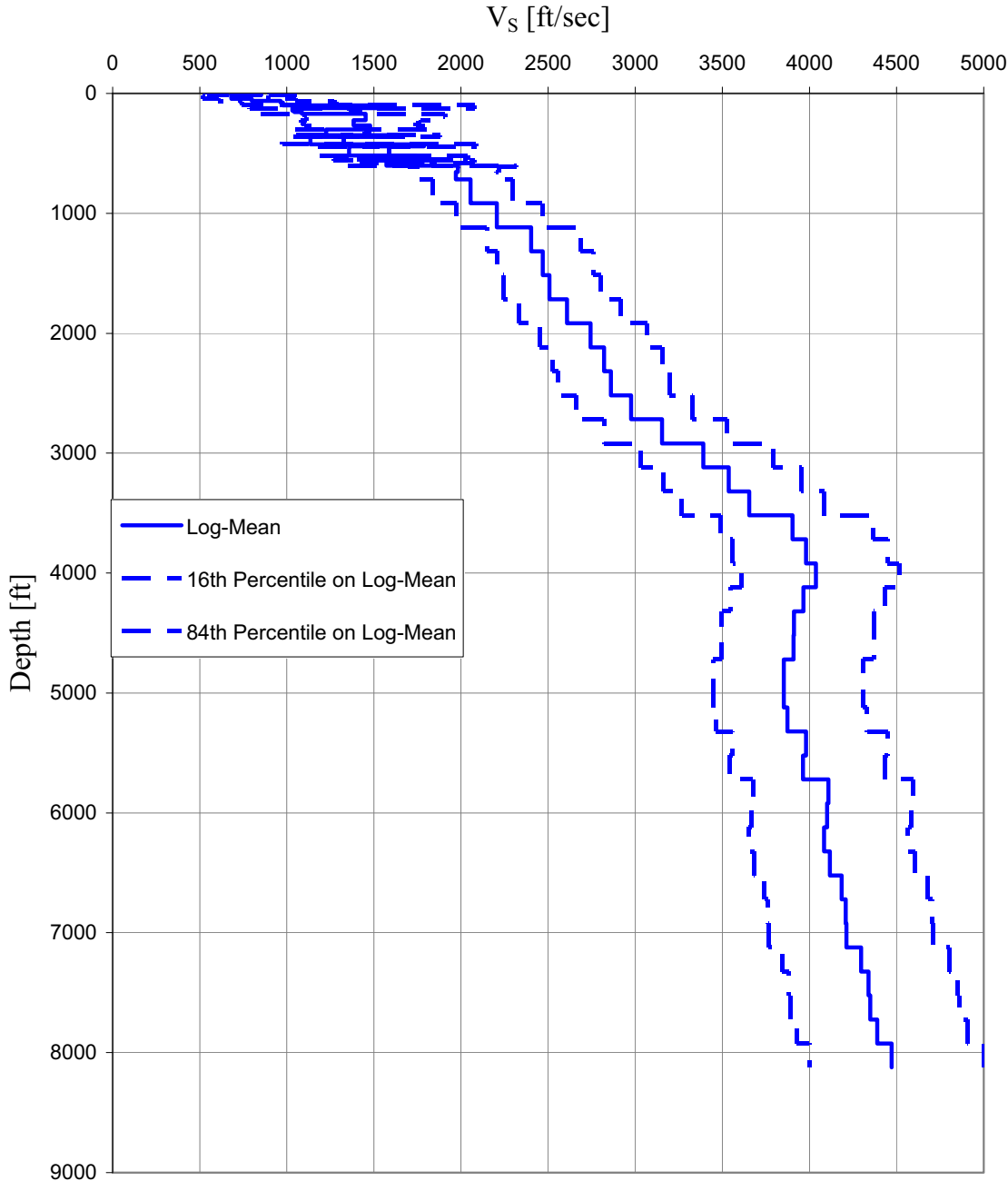
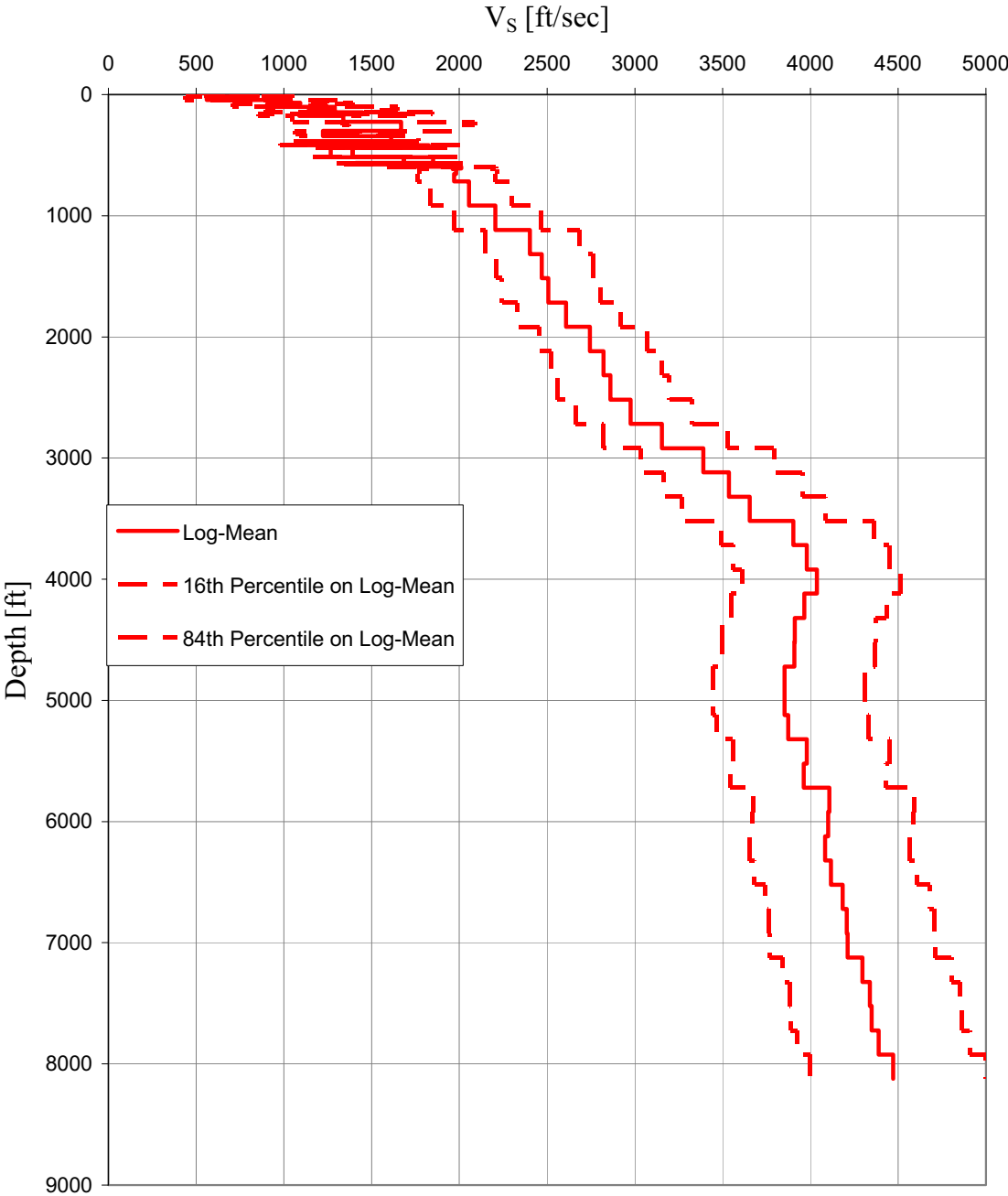


Figure 2.5.2-49 Mean HF and LF Rock Spectra for 10<sup>-5</sup>



**Figure 2.5.2-50 Input Log-Mean Shear Wave Velocity Profile (Plus/Minus One Standard Deviation) for Randomization Process — Unit 1**



**Figure 2.5.2-51 Input Log-Mean Shear Wave Velocity Profile (Plus/Minus One Standard Deviation) for Randomization Process — Unit 2**

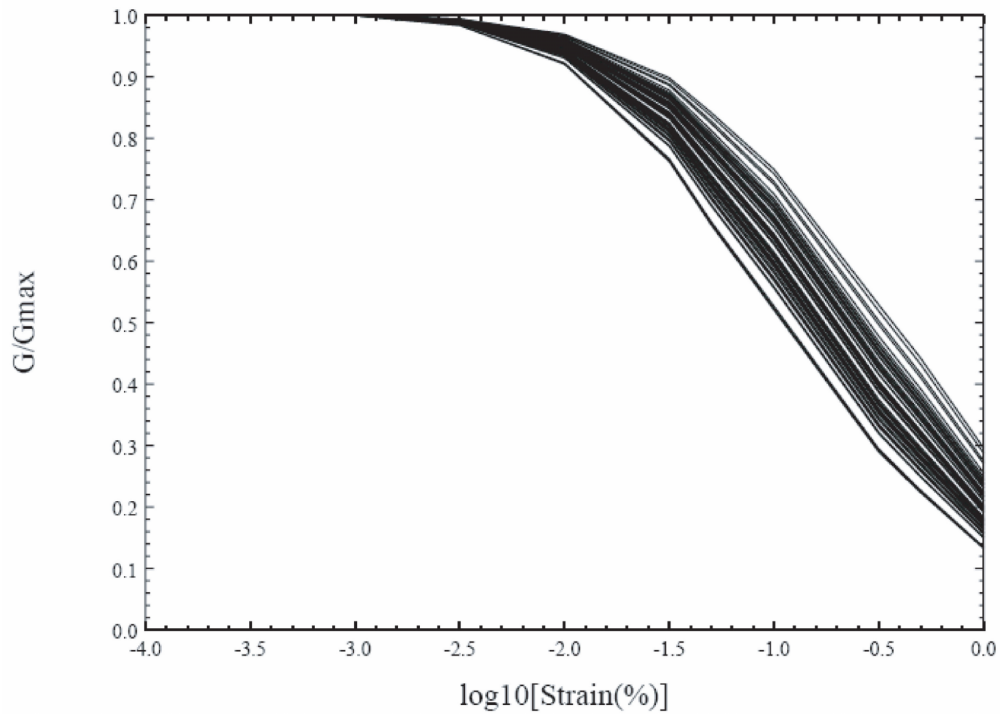


**Figure 2.5.2-52 Strain Dependent Degradation Curves for Sand 4**

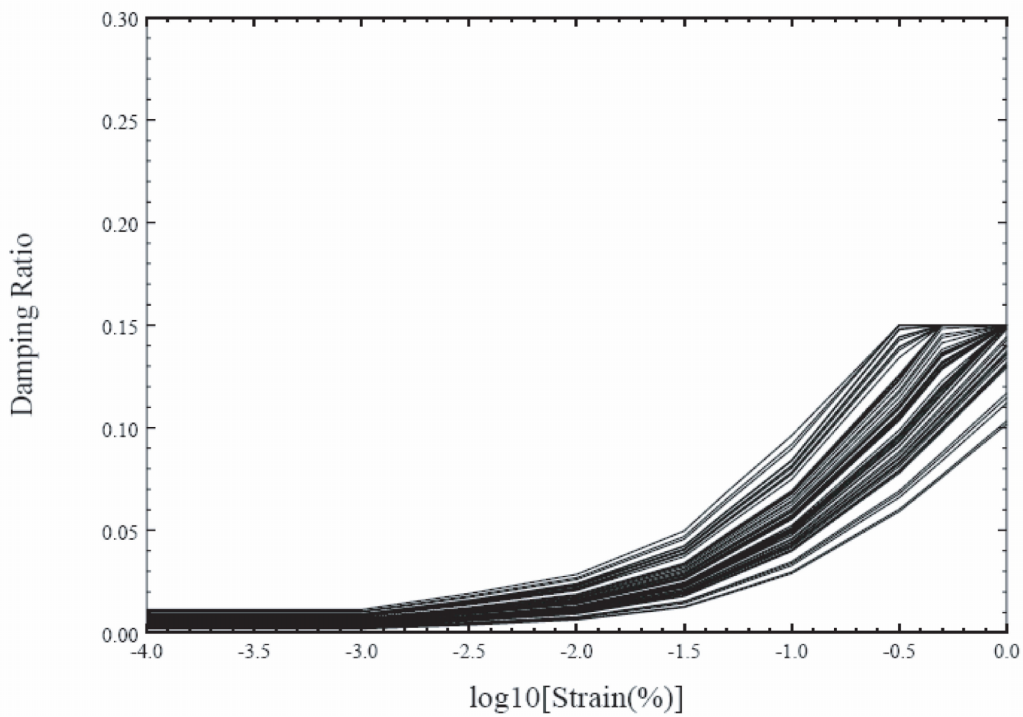


**Figure 2.5.2-53 Strain Dependent Damping Ratio Properties for Sand 4**

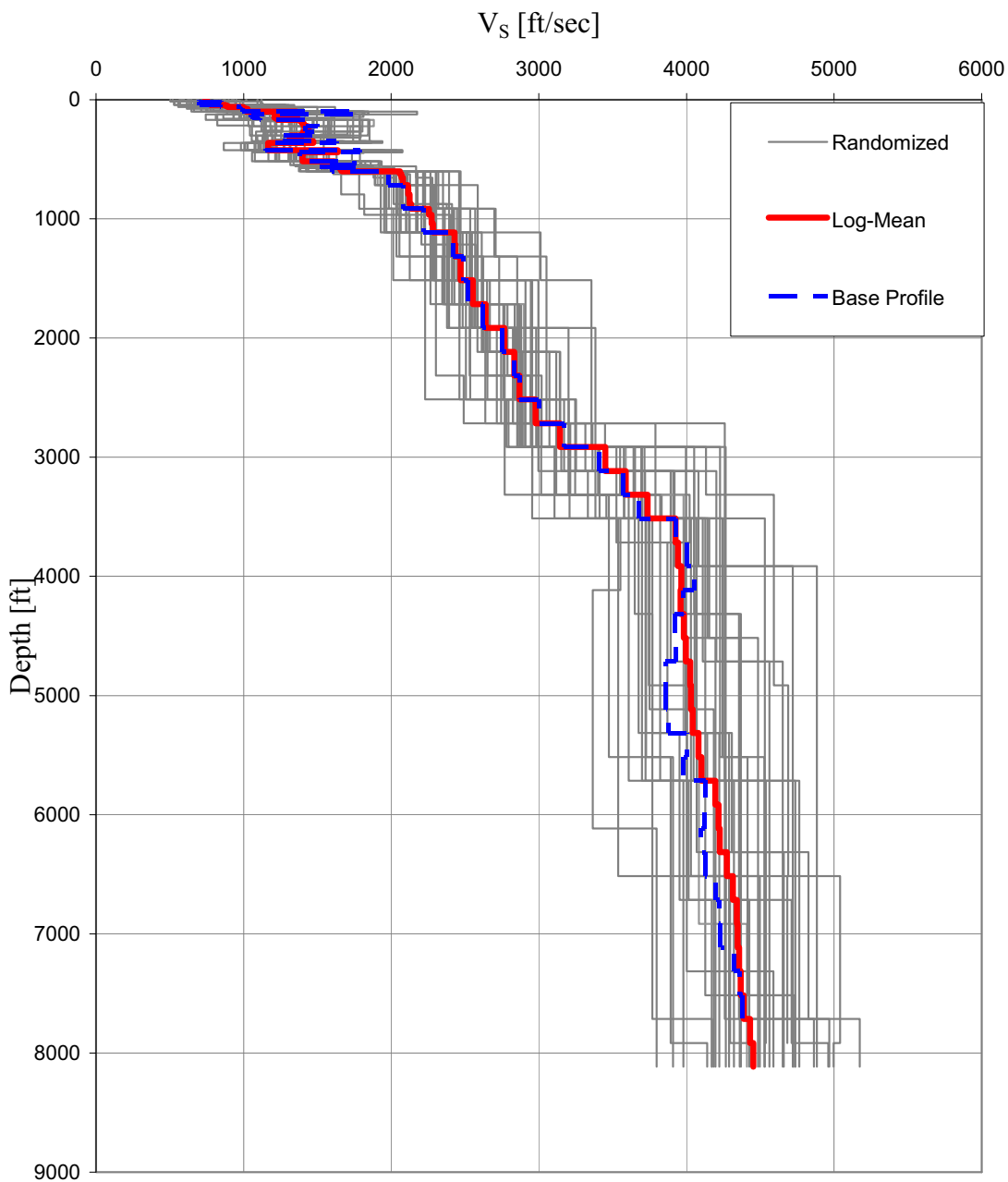


**Figure 2.5.2-54 Randomized Shear Wave Velocity Profiles, Log-Mean Shear Wave Velocity Profile and the Base Profile Used for Randomization — Unit 1**

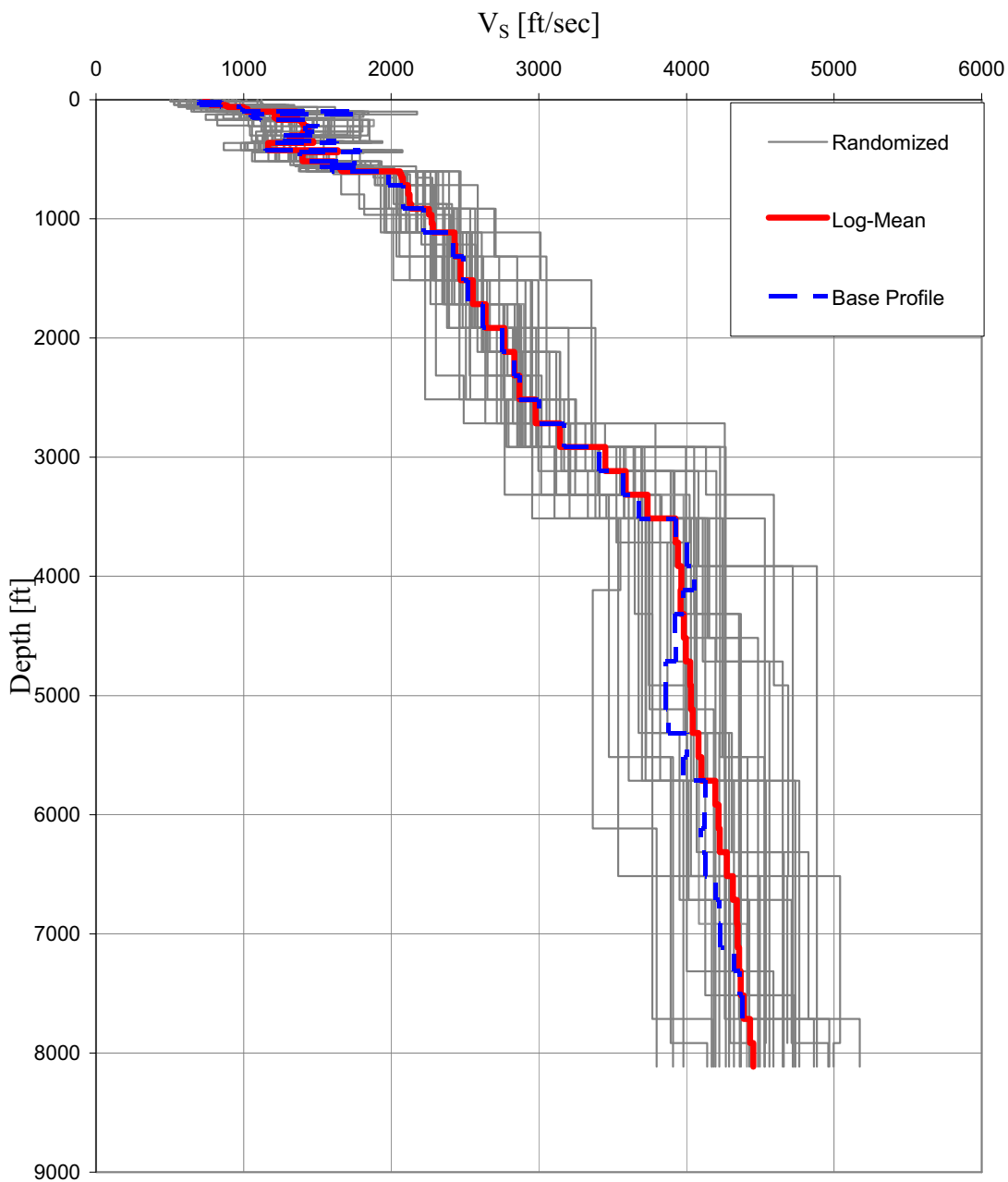


**Figure 2.5.2-55 Randomized Shear Wave Velocity Profiles, Log-Mean Shear Wave Velocity Profile and the Base Profile Used for Randomization — Unit 2**

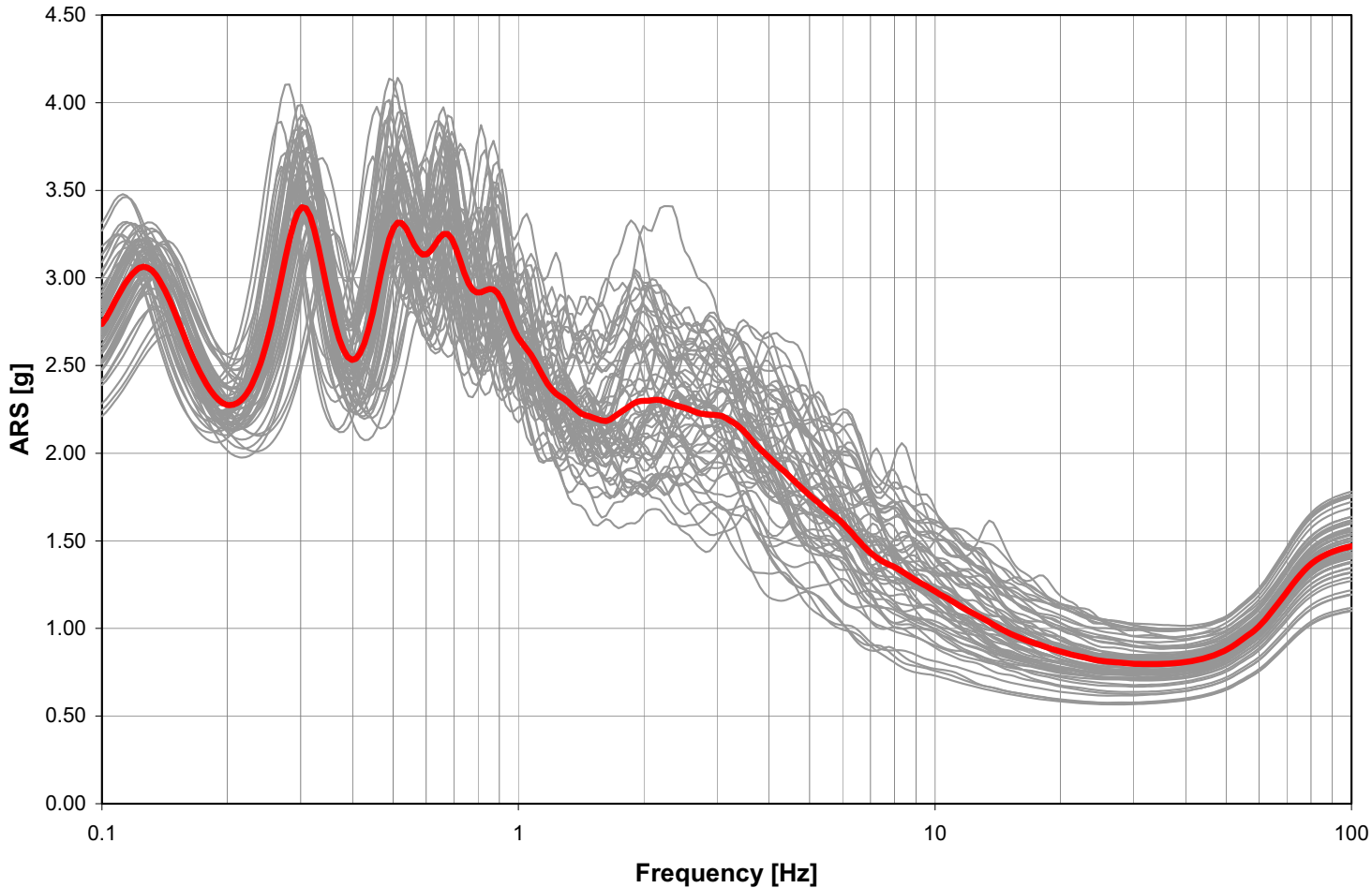


**Figure 2.5.2-56 Log-Mean of Site Amplification Factor at the GMRS Horizon (99 ft Depth) from Analysis of the 60 Modified Random Profiles with the  $10^{-4}$  LF Input Motion — Unit 1**

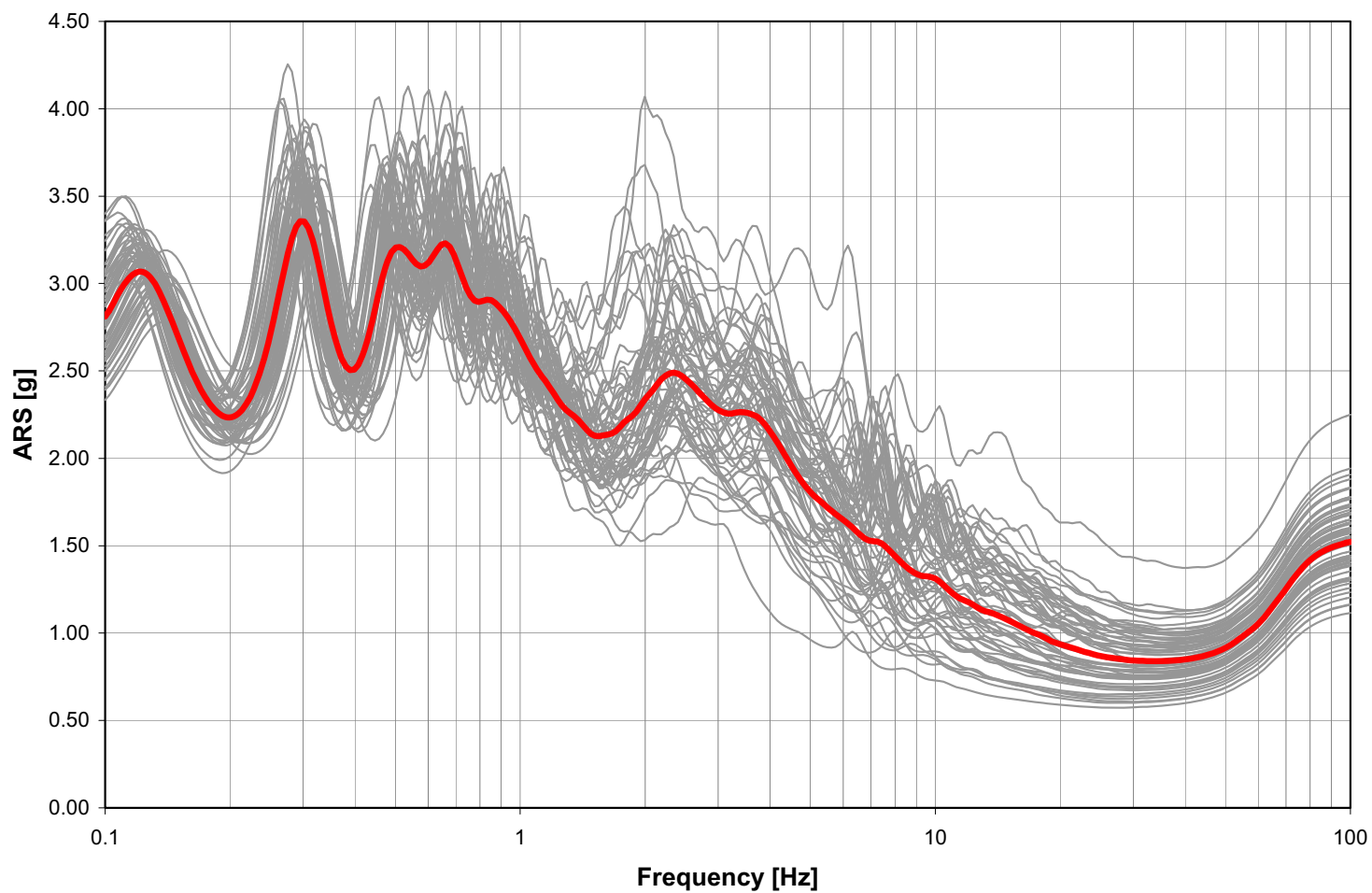


**Figure 2.5.2-57 Log-Mean of Site Amplification Factor at the GMRS Horizon (102 ft Depth) from Analysis of the 60 Modified Random Profiles with the  $10^{-4}$  LF Input Motion — Unit 2**

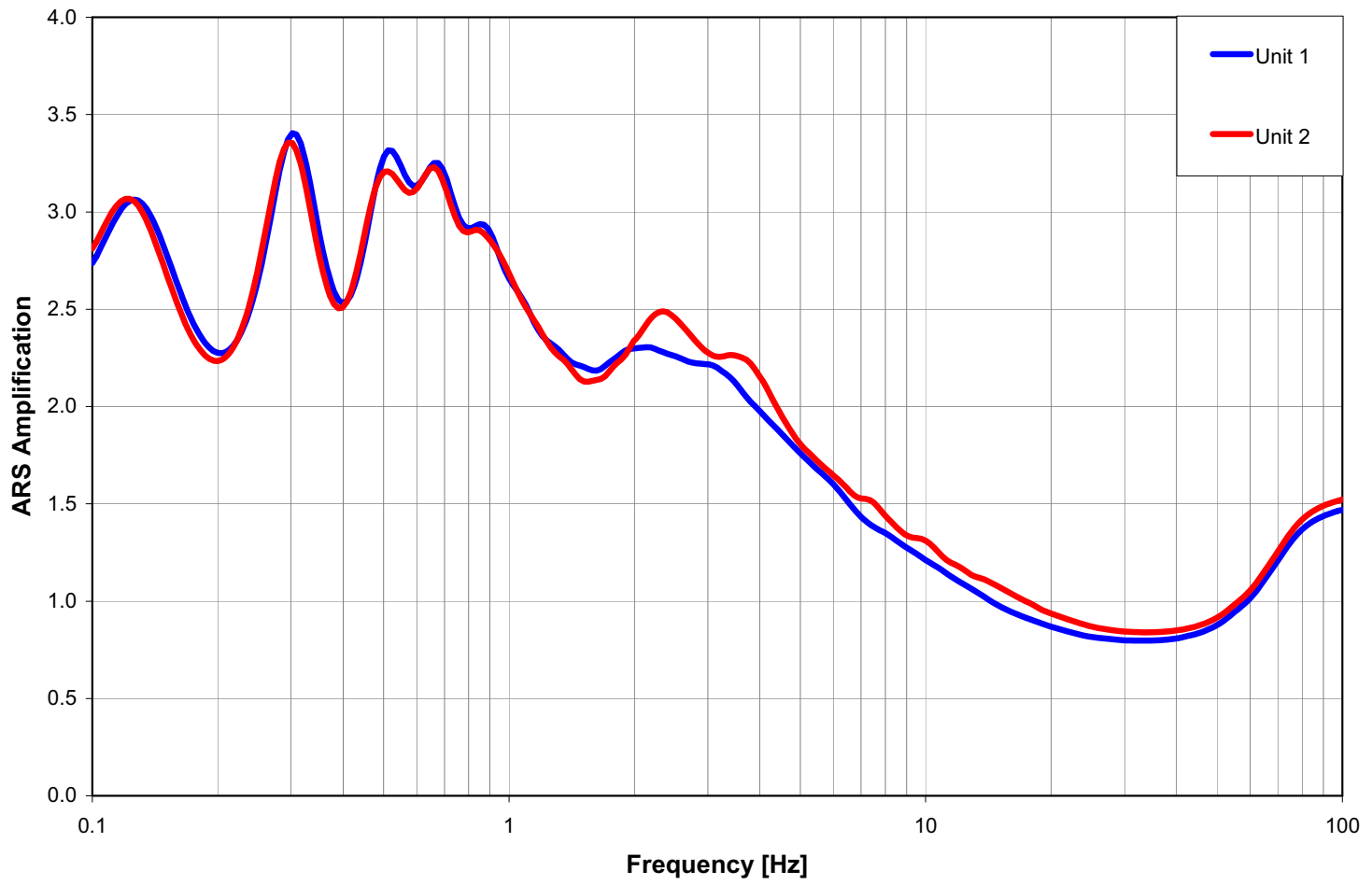


**Figure 2.5.2-58 Log-Mean of Site Amplification Factor at the GMRS Horizons (Unit 1 at 99 ft Depth and Unit 2 at 102 ft Depth) with the  $10^{-4}$  LF Input Motion**

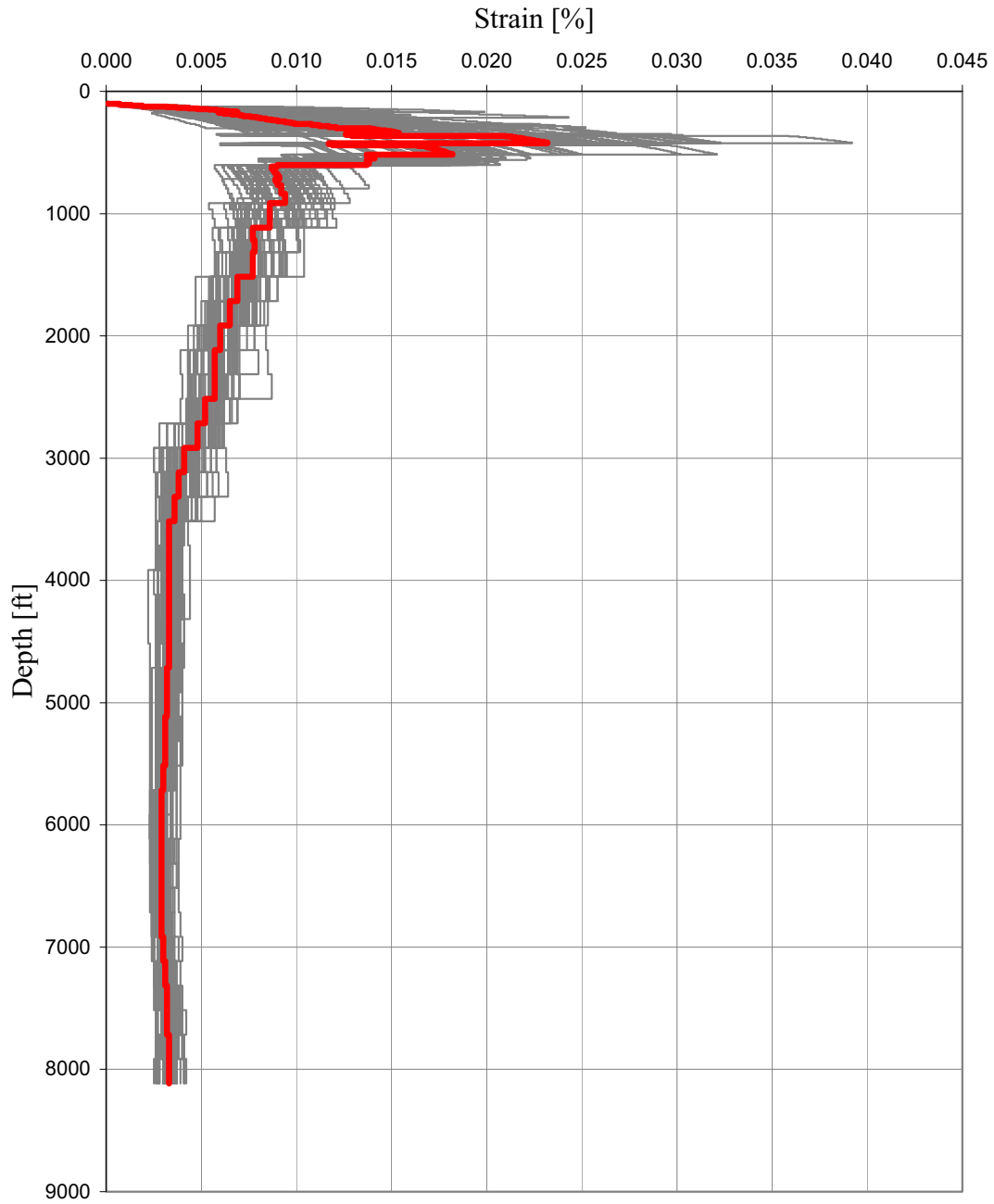


**Figure 2.5.2-59 Maximum Strain Versus Depth Calculated for the 60 Profiles and their Log-Mean (Thick Red Line) with the  $10^{-4}$  LF Input Motion — Unit 1**

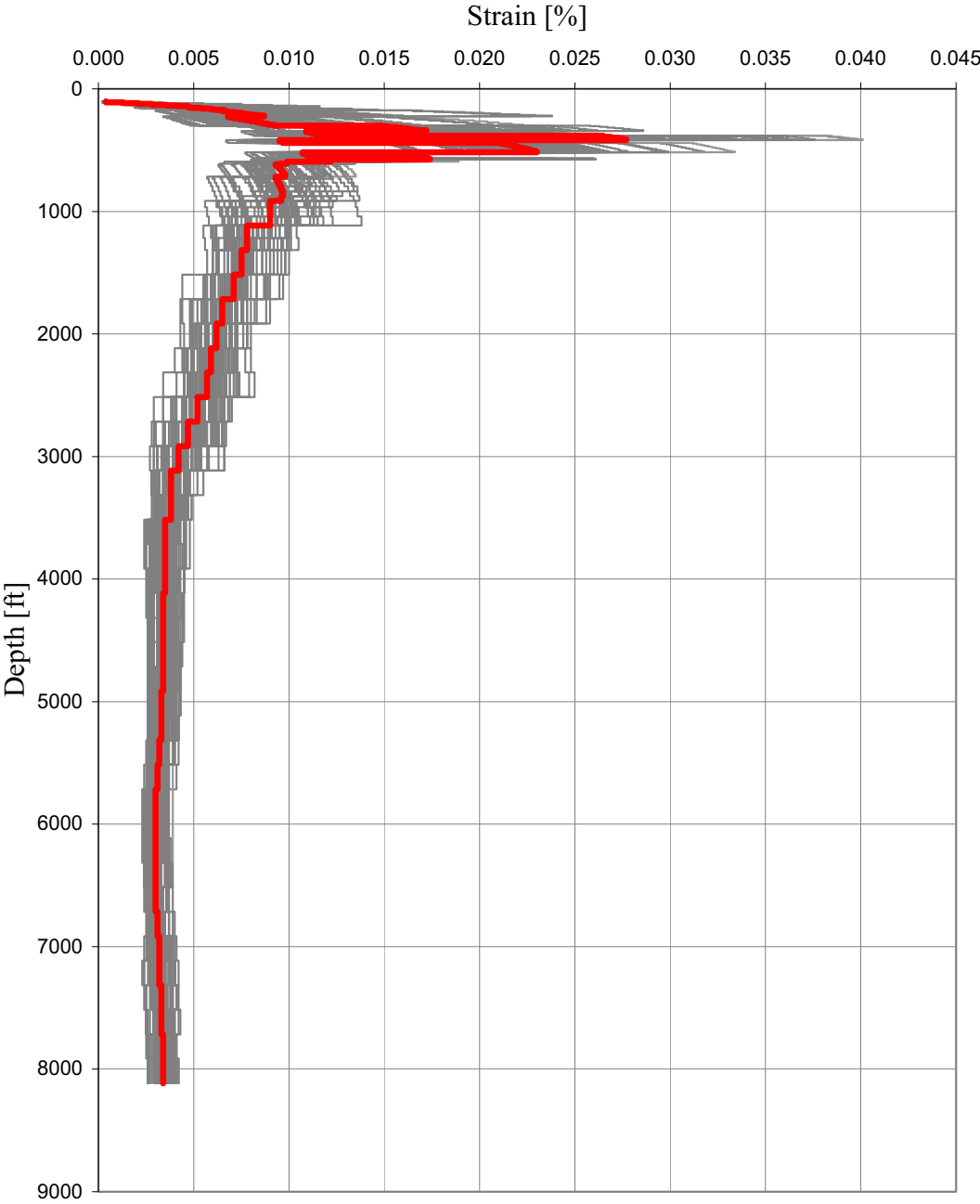


**Figure 2.5.2-60 Maximum Strain Versus Depth Calculated for the 60 Profiles and their Log-Mean (Thick Red Line) with the  $10^{-4}$  LF Input Motion — Unit 2**

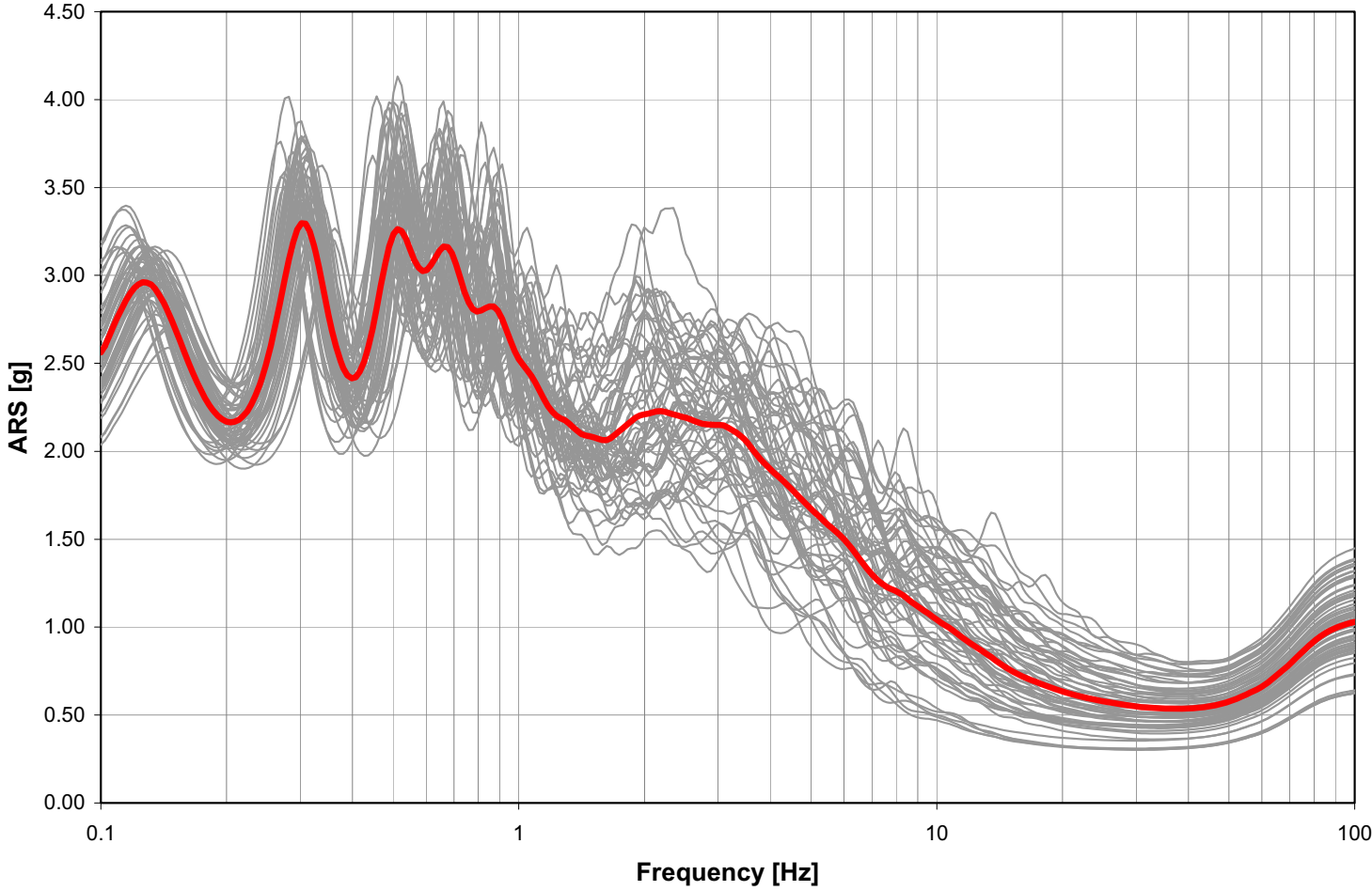


**Figure 2.5.2-61 Log-Mean of Site Amplification Factor at the GMRS Horizon (99 ft Depth) from Analyses of the 60 Modified Random Profiles with the  $10^{-4}$  HF Input Motion — Unit 1**

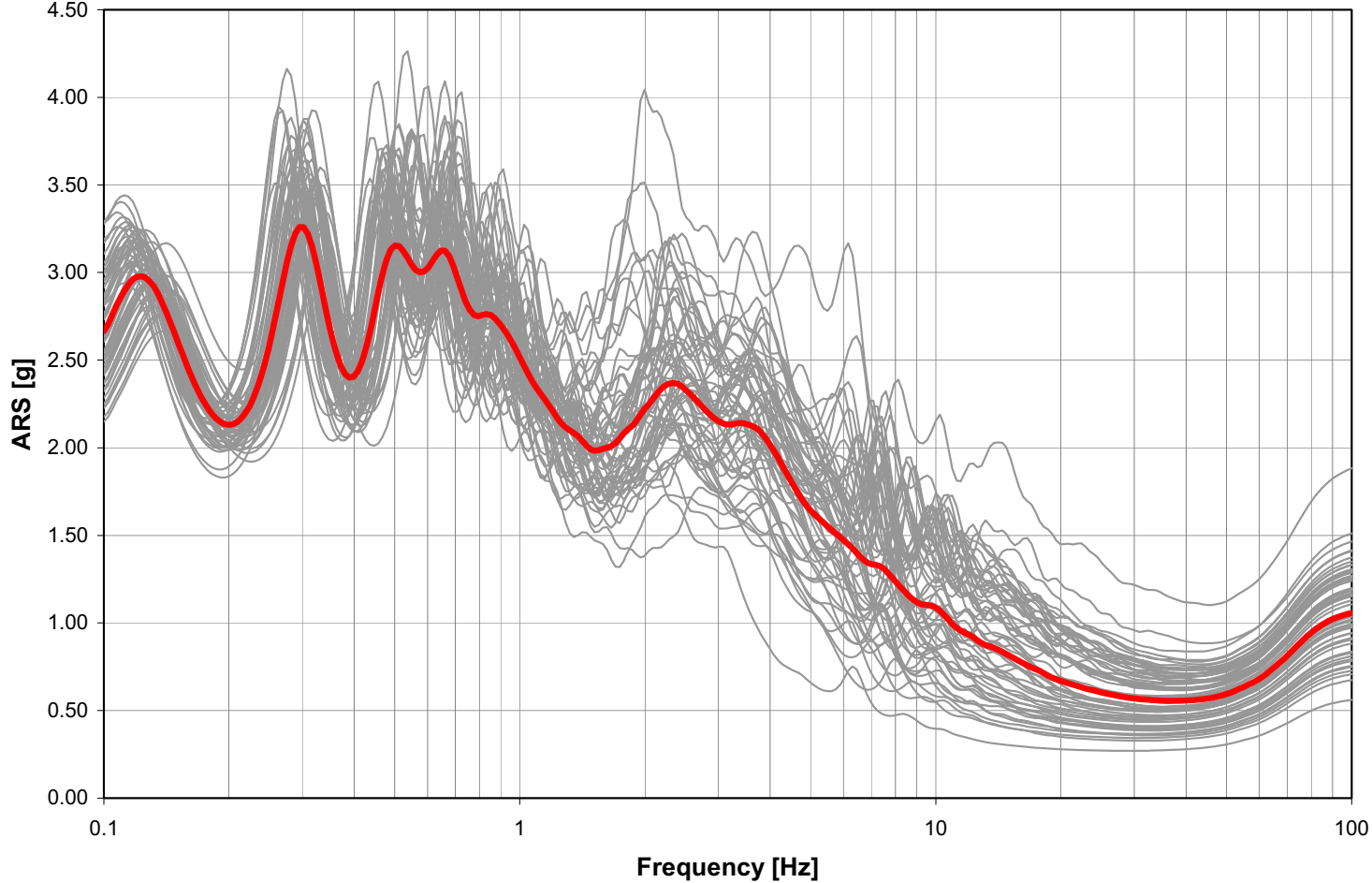


**Figure 2.5.2-62 Log-Mean of Site Amplification Factor at the GMRS Horizon (102 ft Depth) from Analysis of the 60 Modified Random Profiles with the  $10^{-4}$  HF Input Motion — Unit 2**

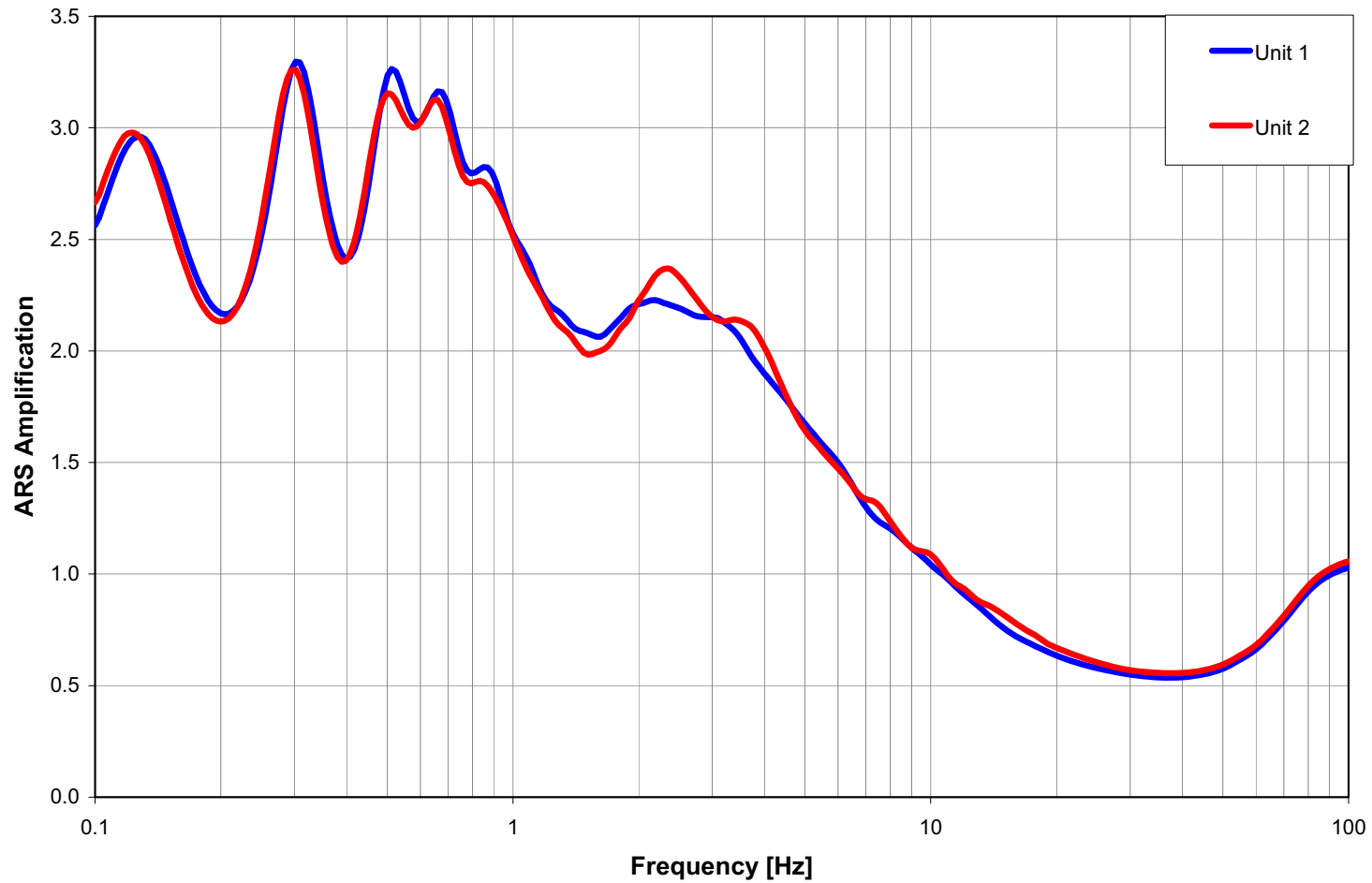


**Figure 2.5.2-63 Log-Mean of Site Amplification Factor at the GMRS Horizons  
(Unit 1 at 99 ft Depth and Unit 2 at 102 ft Depth) with the  $10^{-4}$  HF Input Motion**

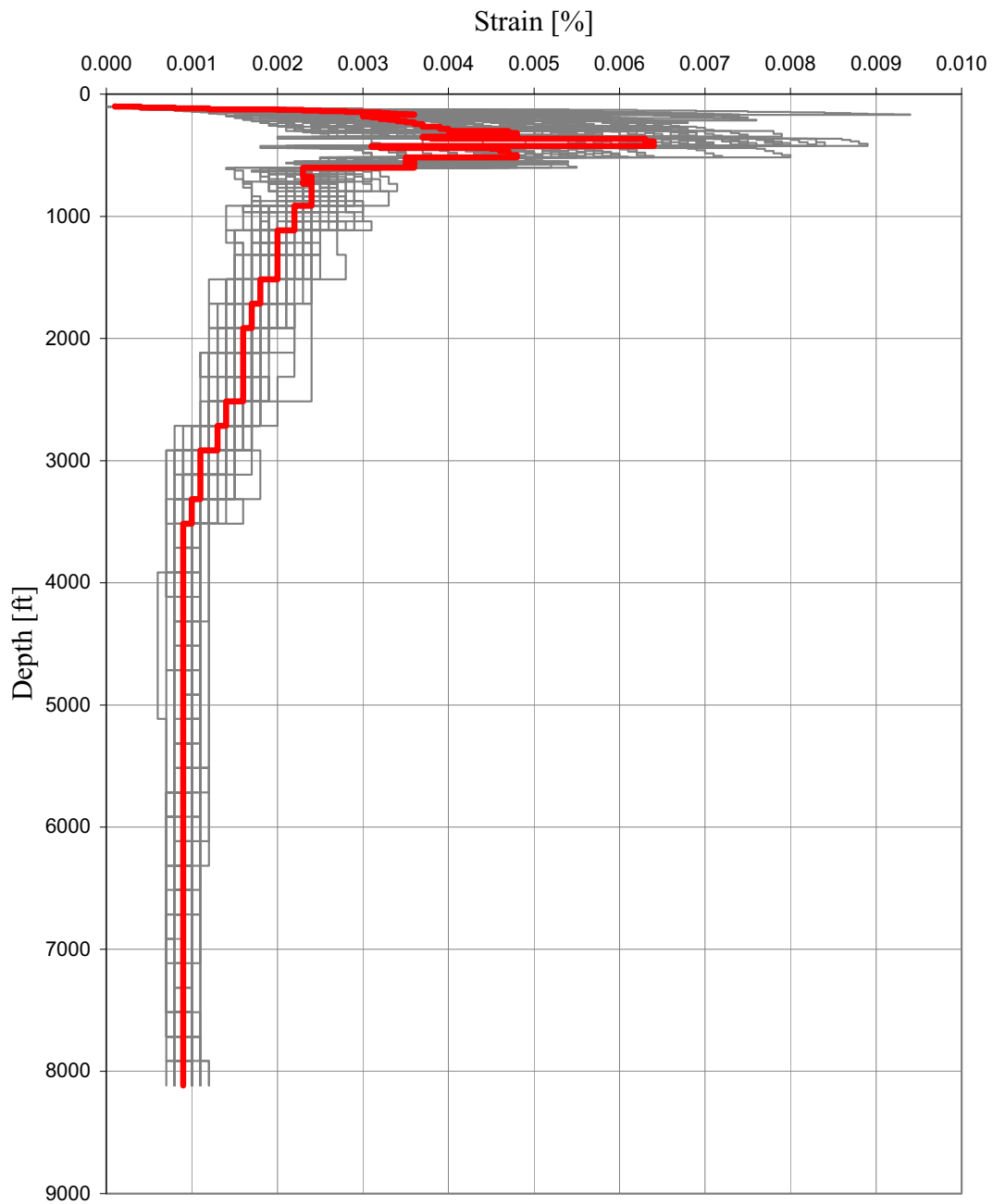


**Figure 2.5.2-64 Maximum Strain Versus Depth Calculated for the 60 Profiles and their Log-Mean (Thick Red Line) with the  $10^{-4}$  HF Input Motion — Unit 1**

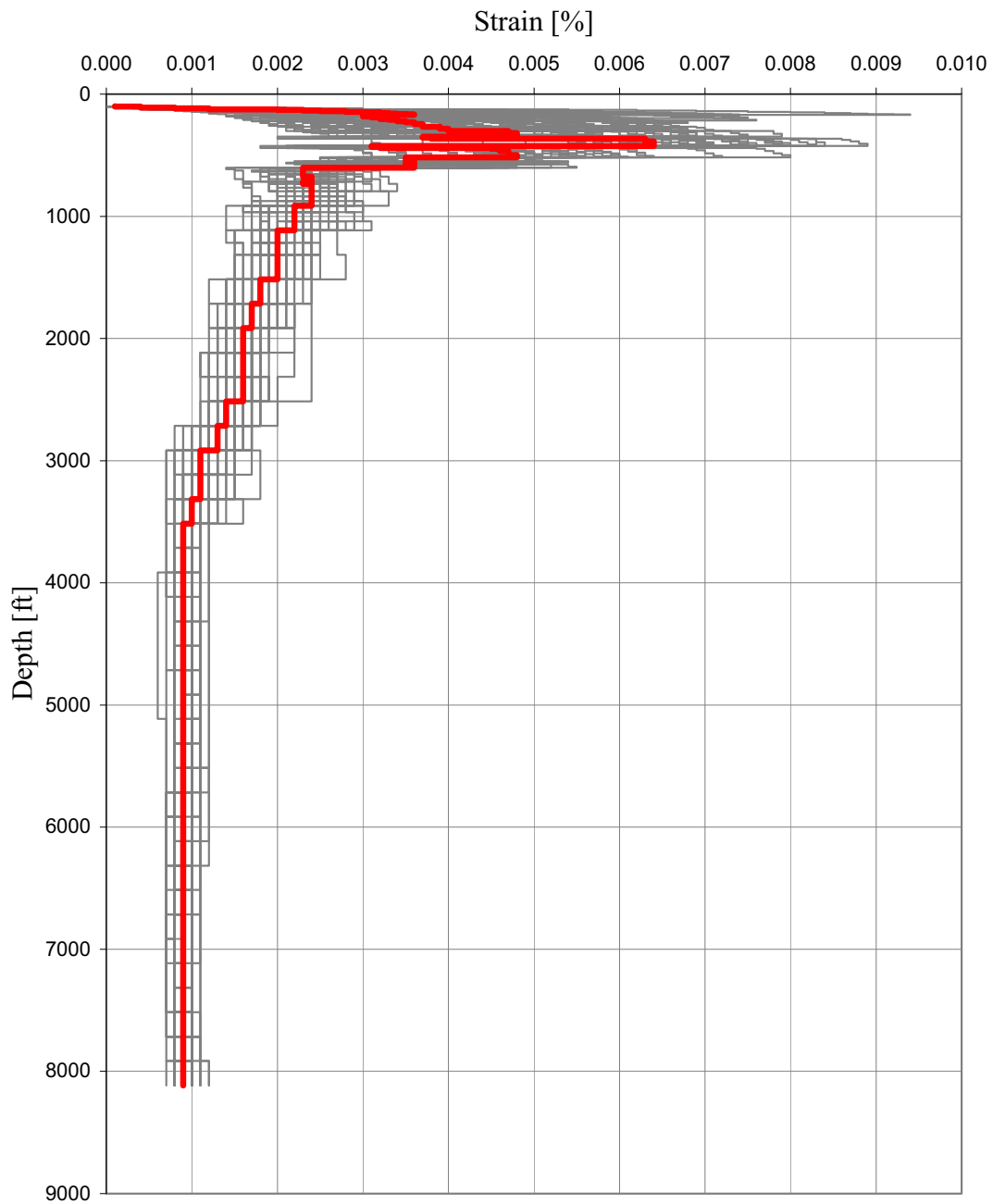


**Figure 2.5.2-65 Maximum Strain Versus Depth Calculated for the 60 Profiles and their Log-Mean (Thick Red Line) with the  $10^{-4}$  HF Input Motion — Unit 2**

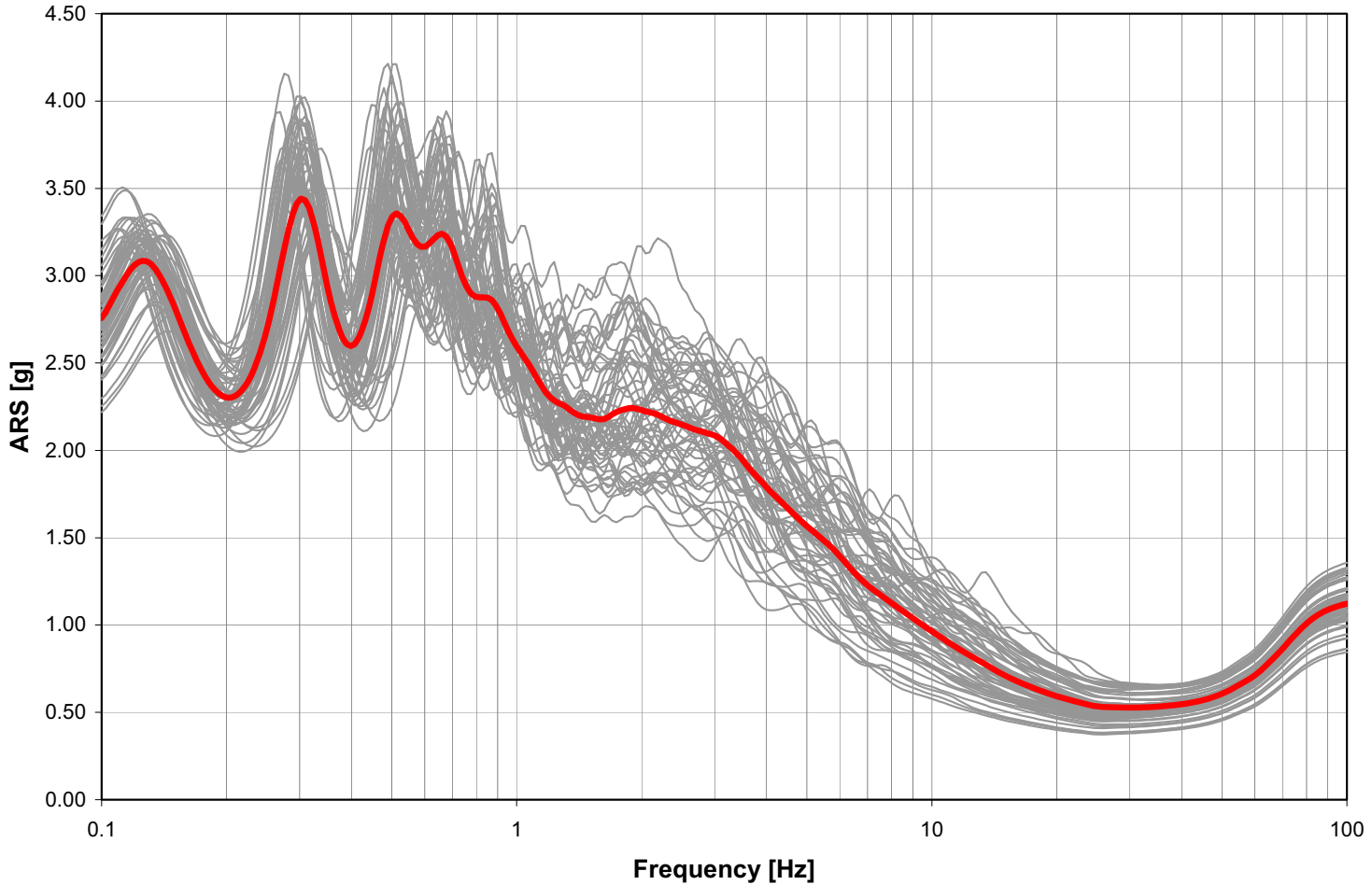


**Figure 2.5.2-66 Log-Mean of Site Amplification Factor at the GMRS Horizon (99 ft Depth) from Analysis of the 60 Modified Random Profiles with the  $10^{-5}$  LF Input Motion — Unit 1**

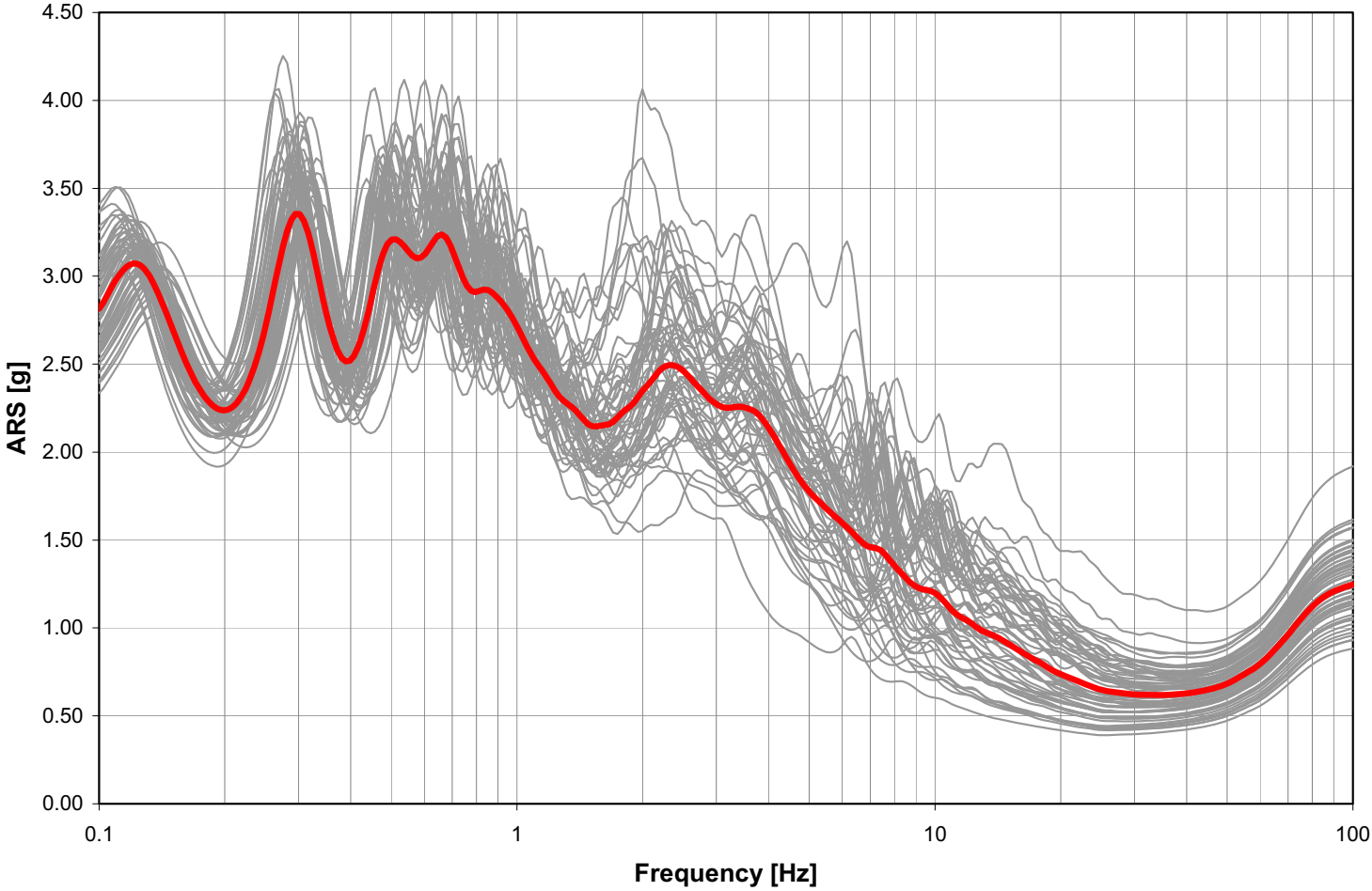


**Figure 2.5.2-67 Log-Mean of Site Amplification Factor at the GMRS Horizon (102 ft Depth) from Analysis of the 60 Modified Random Profiles with the  $10^{-5}$  LF Input Motion — Unit 2**

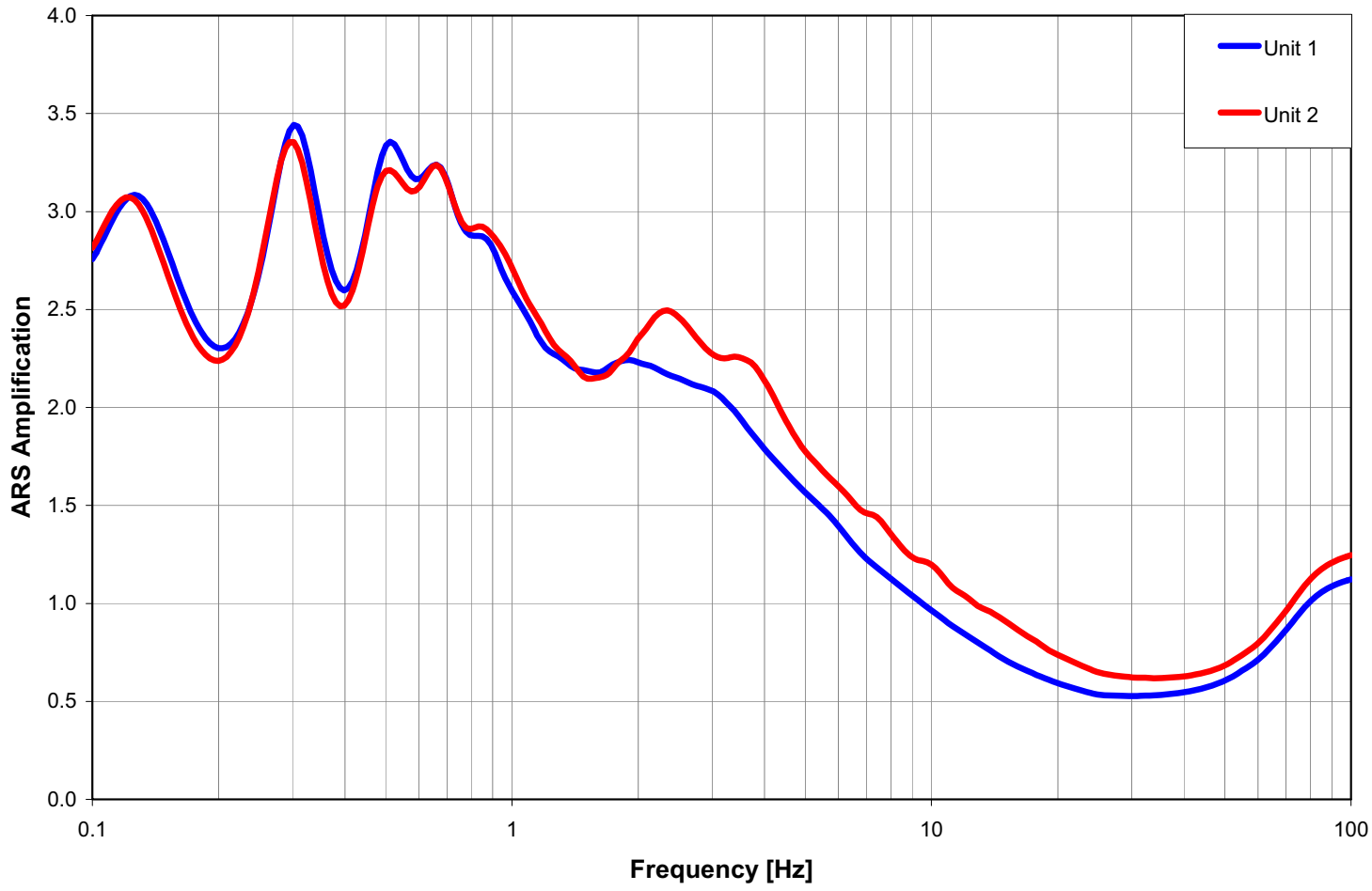


**Figure 2.5.2-68 Log-Mean of Site Amplification Factor at the GMRS Horizons  
(Unit 1 at 99 ft Depth and Unit 2 at 102 ft Depth) with the  $10^{-5}$  LF Input Motion**

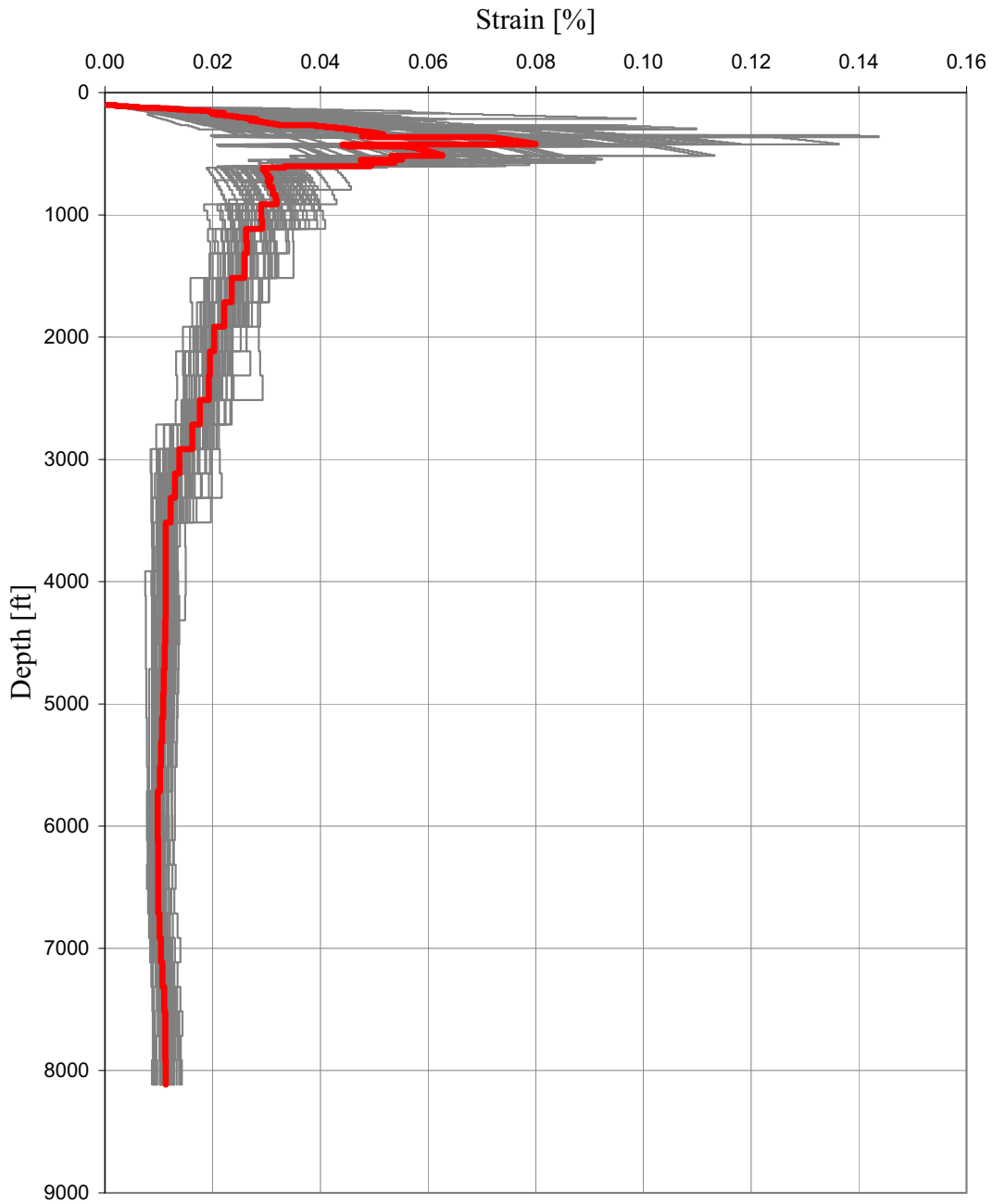


**Figure 2.5.2-69 Maximum Strain Versus Depth Calculated for the 60 Profiles and their Log-Mean (Thick Red Line) with the  $10^{-5}$  LF Input Motion — Unit 1**

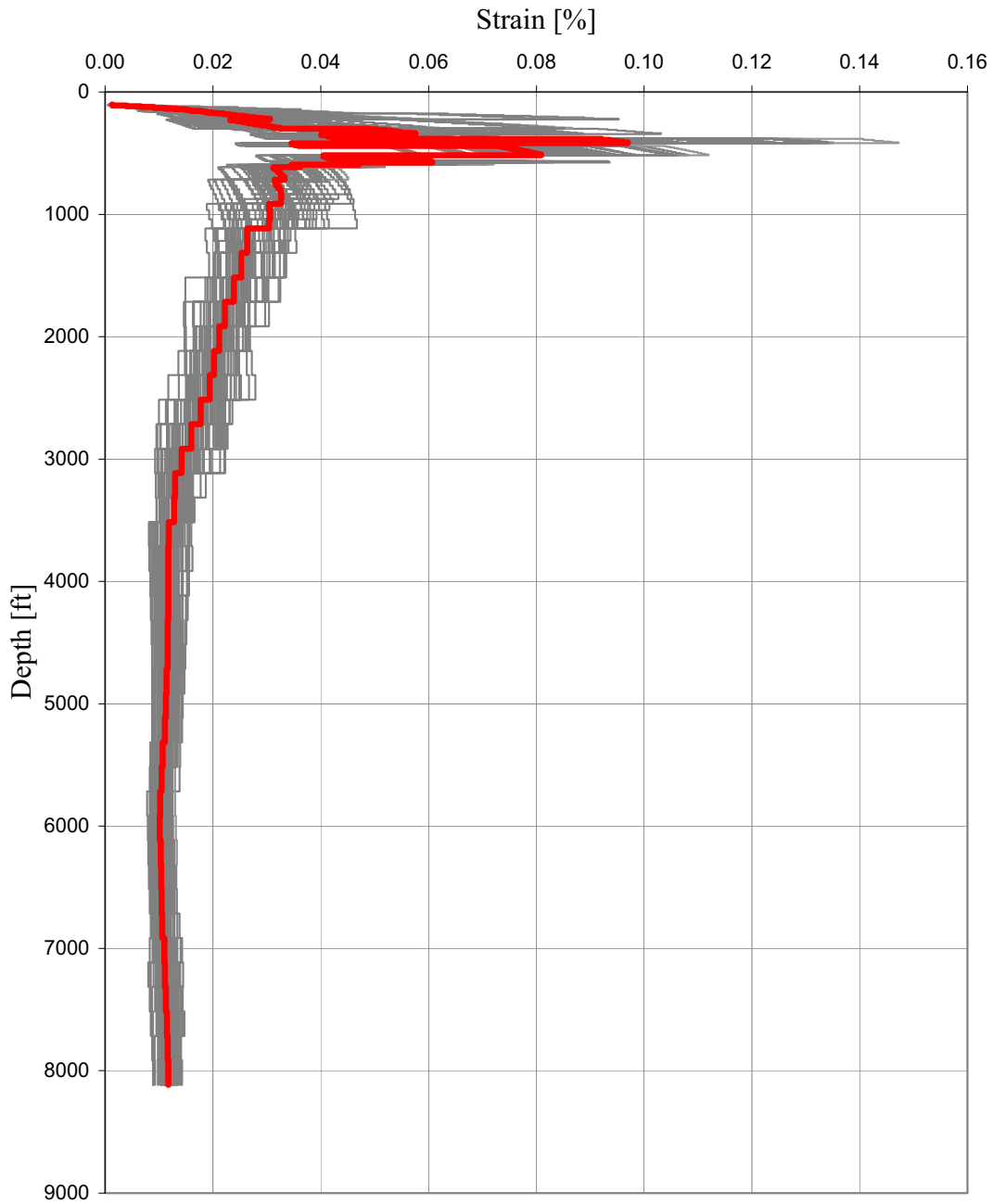


**Figure 2.5.2-70 Maximum Strain Versus Depth Calculated for the 60 Profiles and their Log-Mean (Thick Red Line) with the  $10^{-5}$  LF Input Motion — Unit 2**

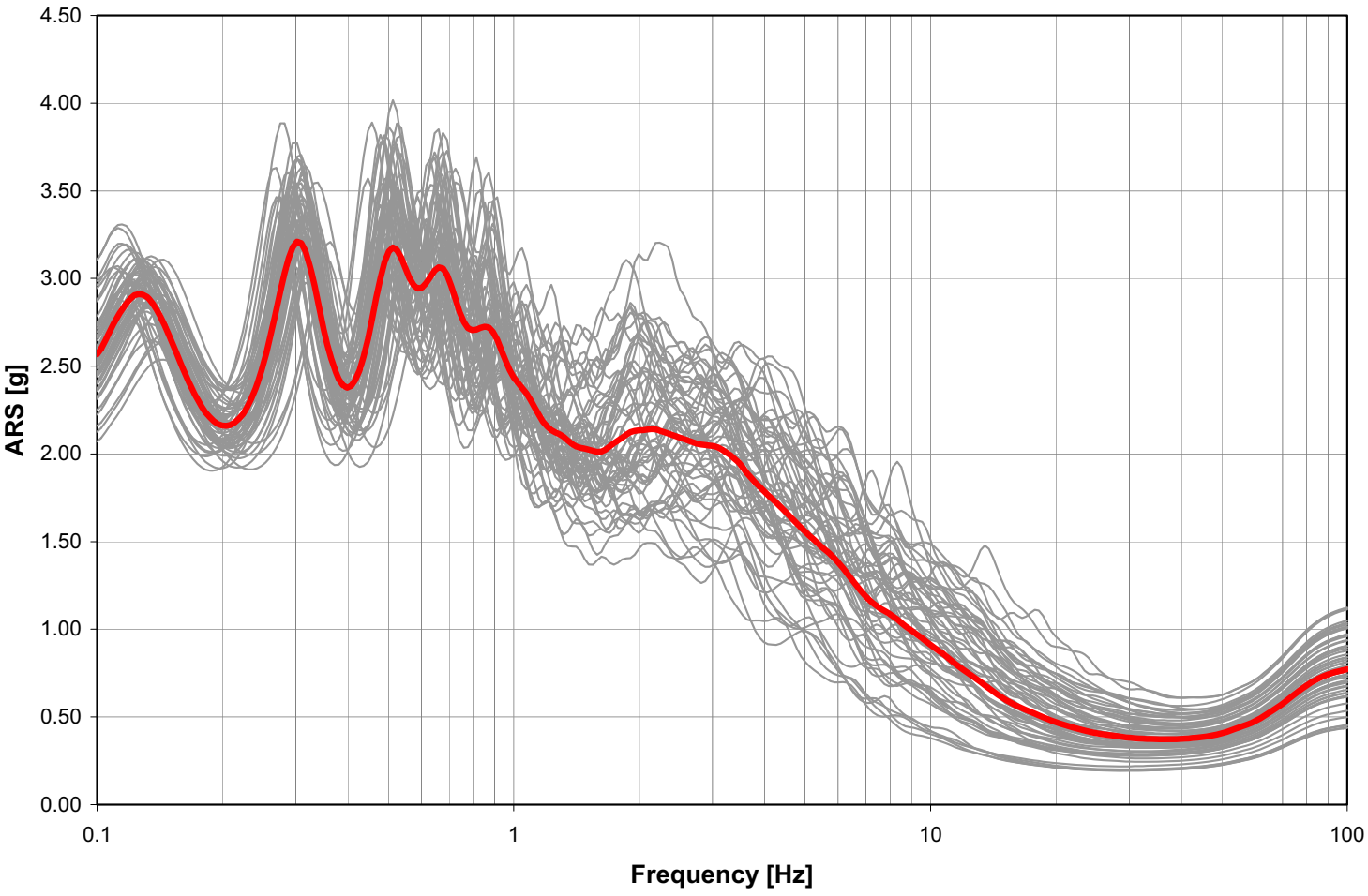


**Figure 2.5.2-71 Log-Mean of Site Amplification Factor at the GMRS Horizon (99 ft Depth) from Analysis of the 60 Modified Random Profiles with the  $10^{-5}$  HF Input Motion — Unit 1**

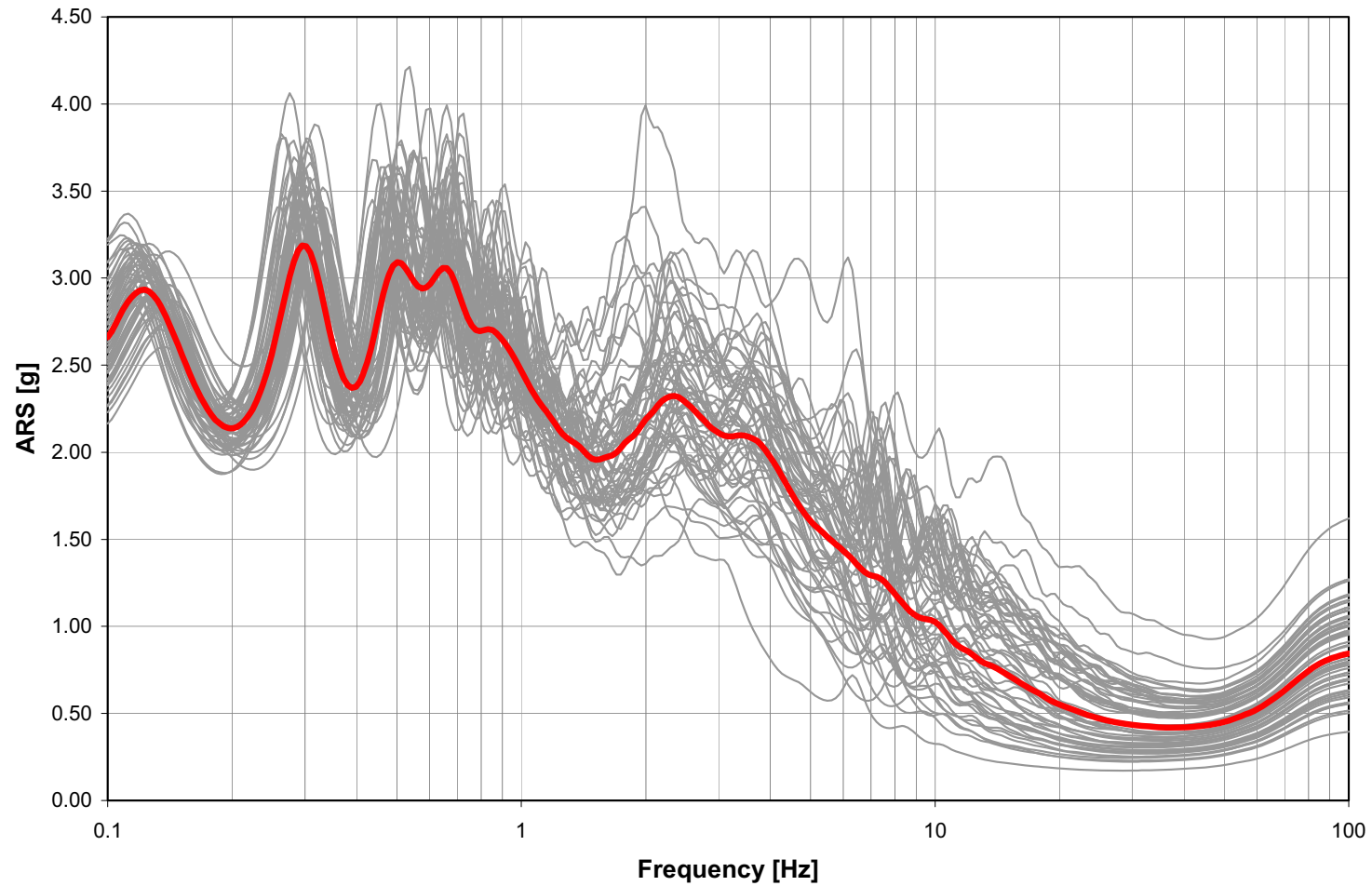


**Figure 2.5.2-72 Log-Mean of Site Amplification Factor at the GMRS Horizon (102 ft Depth) from Analysis of the 60 Modified Random Profiles with the  $10^{-5}$  HF Input Motion — Unit 2**

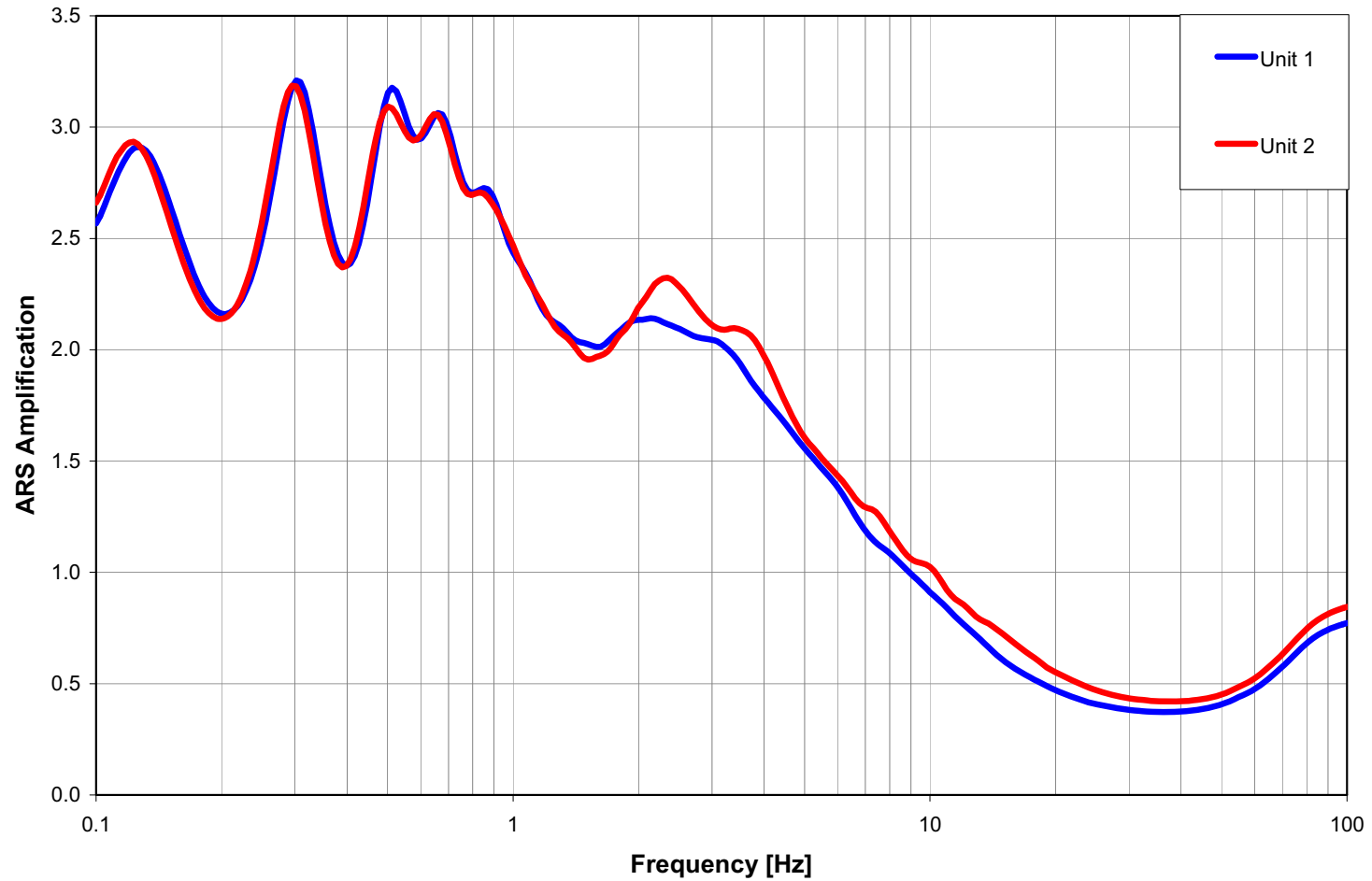


**Figure 2.5.2-73 Log-Mean of Site Amplification Factor at the GMRS Horizons (Unit 1 at 99 ft Depth and Unit 2 at 102 ft Depth) with the  $10^{-5}$  HF Input Motion**

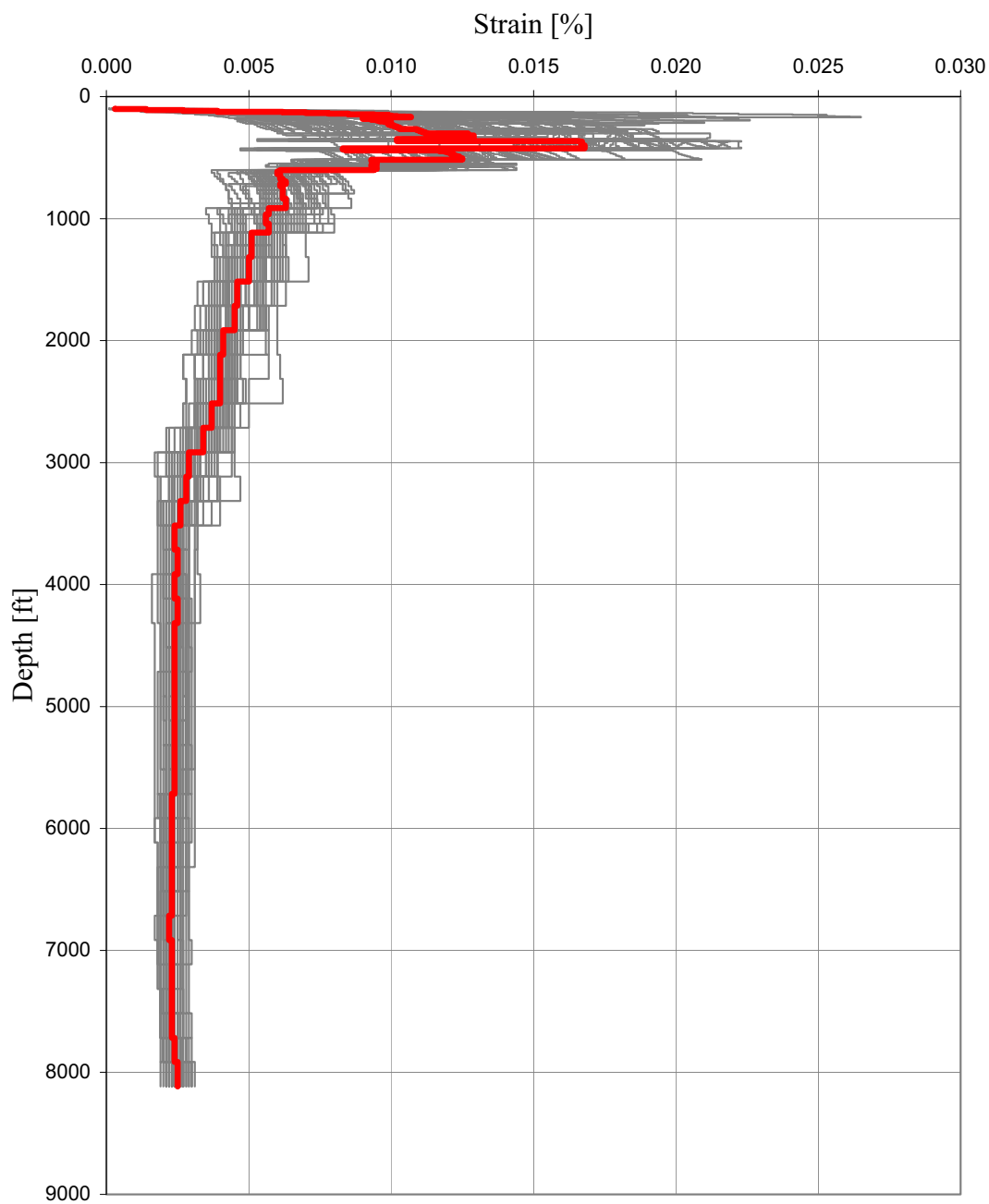


**Figure 2.5.2-74 Maximum Strain Versus Depth Calculated for the 60 Profiles and their Log-Mean (Thick Red Line) with the  $10^{-5}$  HF Input Motion — Unit 1**

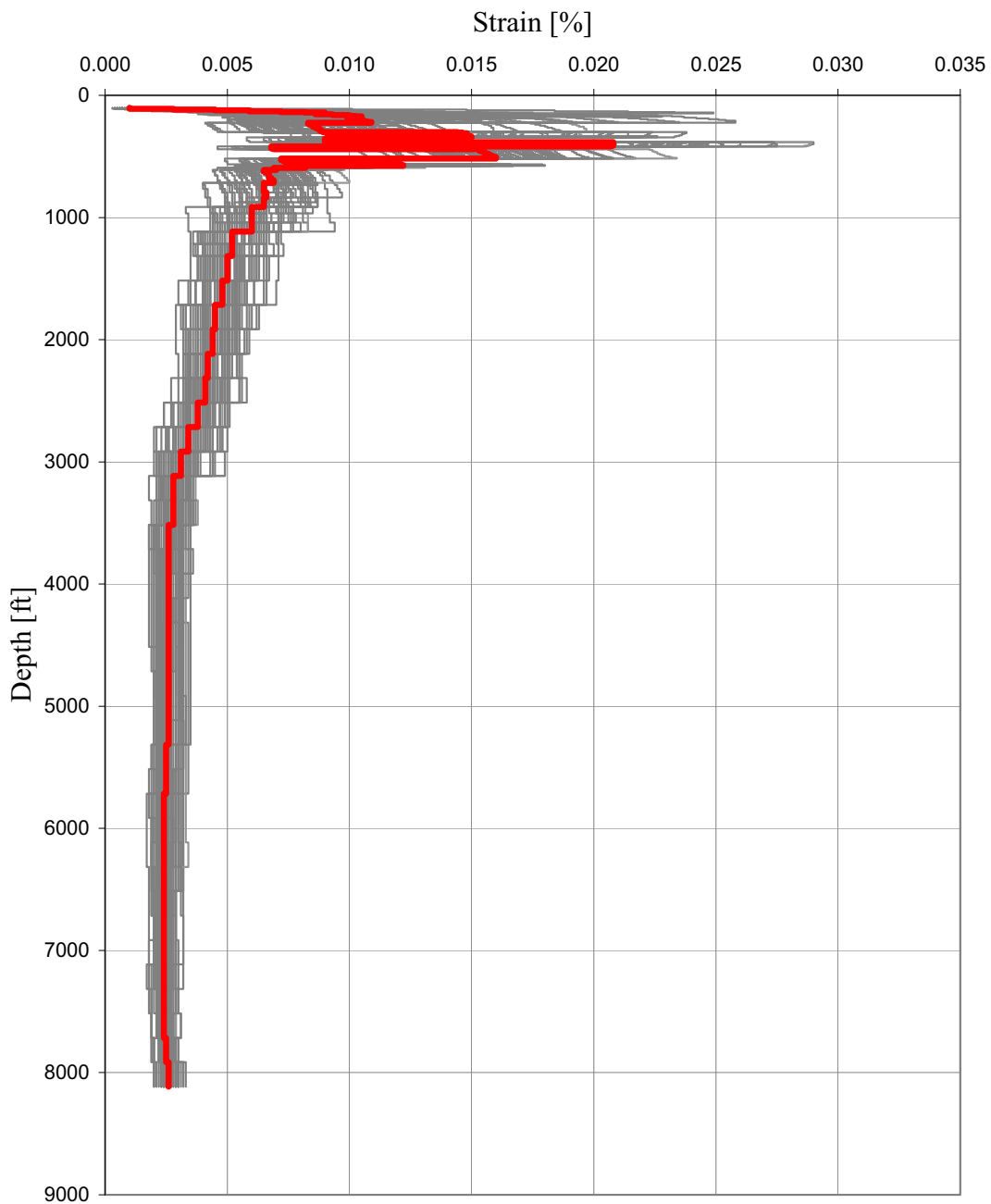


**Figure 2.5.2-75 Maximum Strain Versus Depth Calculated for the 60 Profiles and their Log-Mean (Thick Red Line) with the  $10^{-5}$  HF Input Motion — Unit 2**

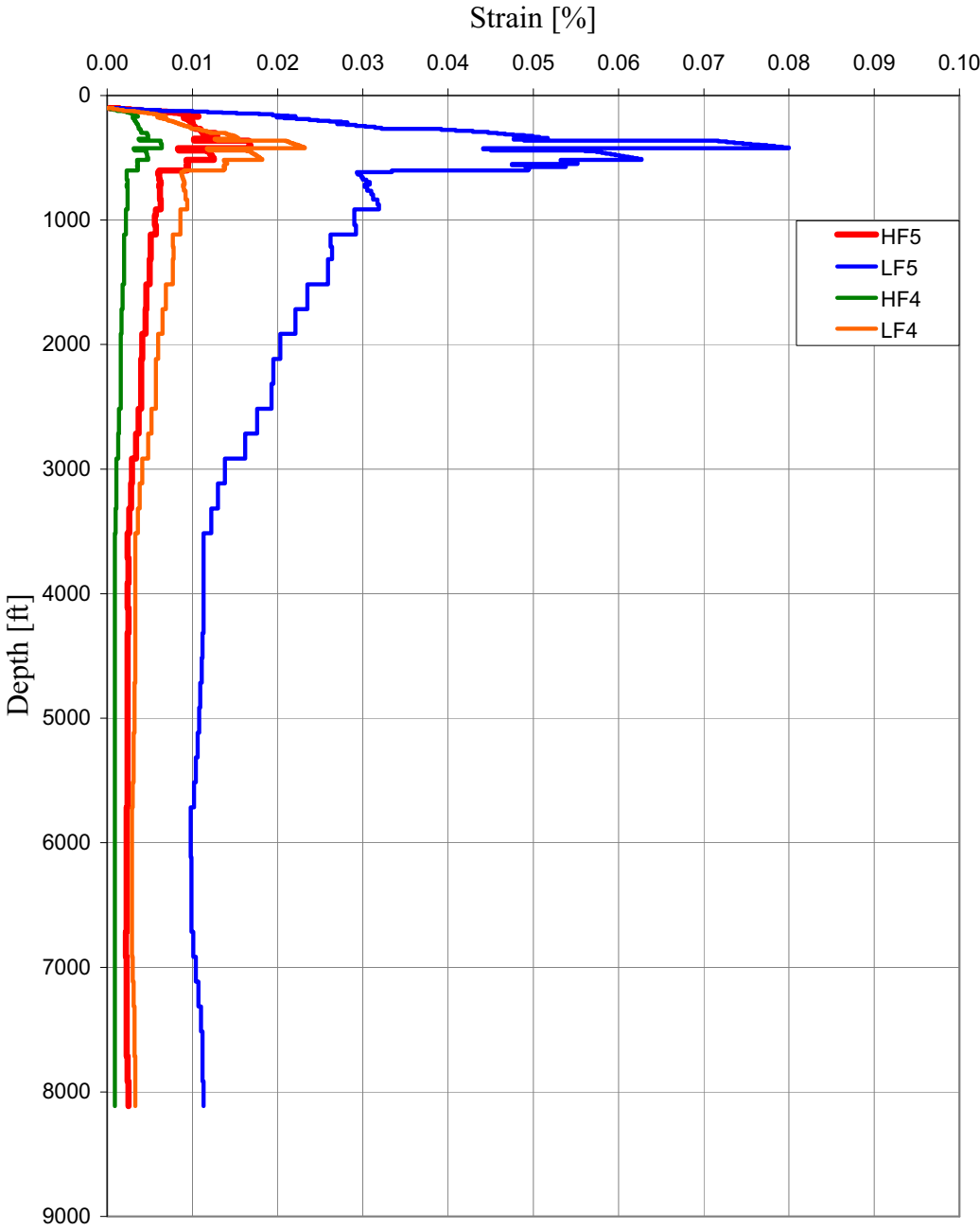


Figure 2.5.2-76 Log-Mean Maximum Strain Profiles — Unit 1

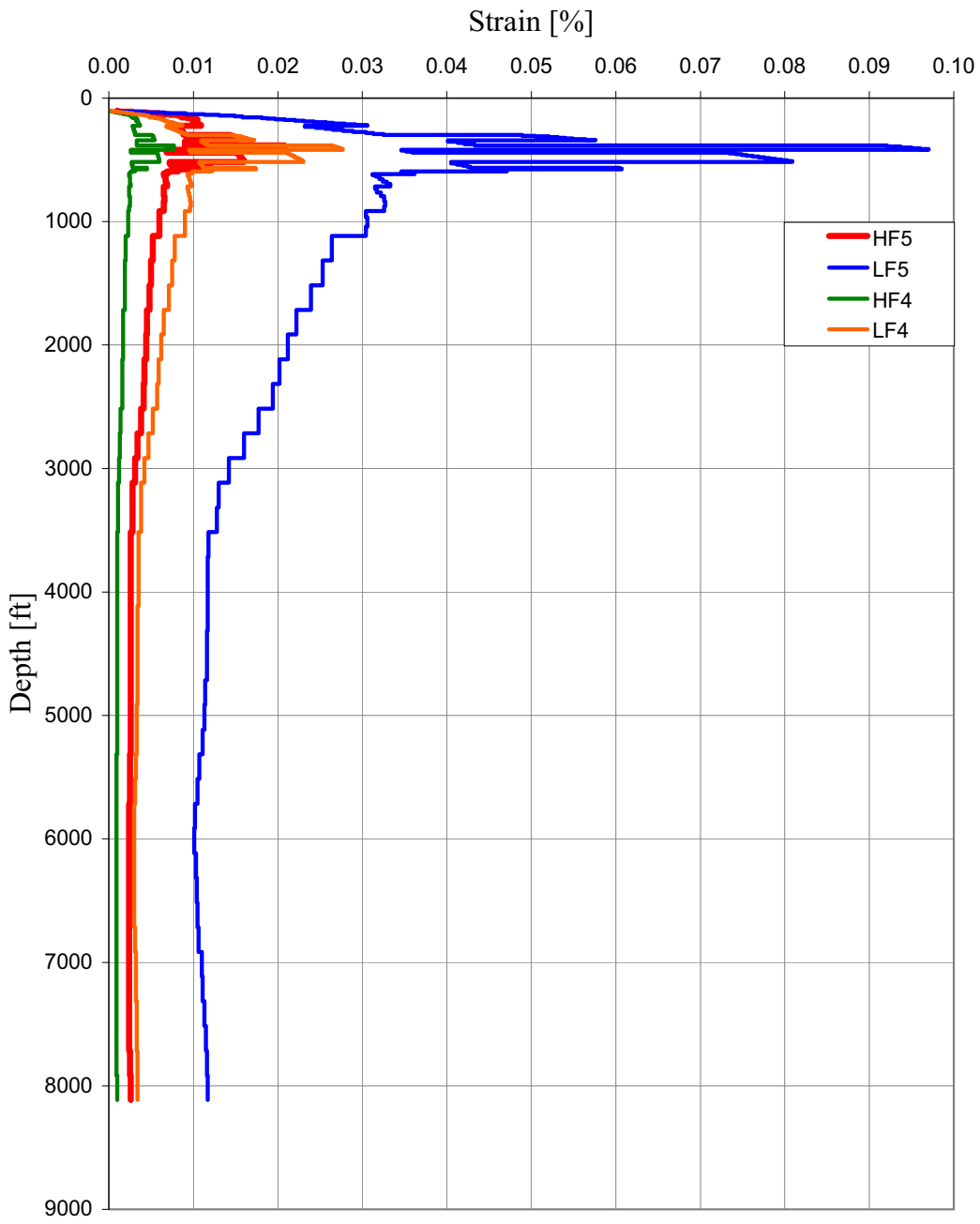


Figure 2.5.2-77 Log-Mean Maximum Strain Profiles — Unit 2

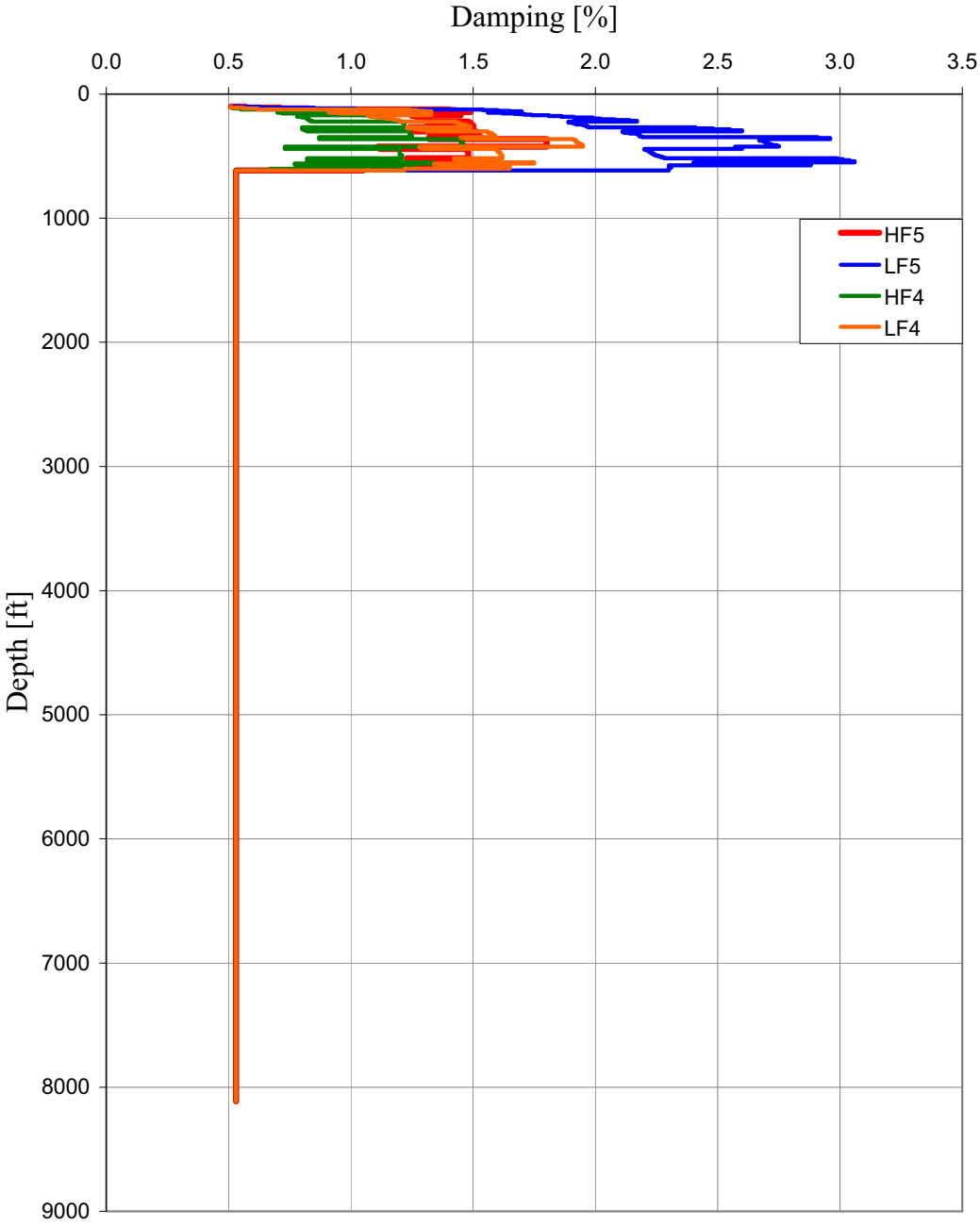


Figure 2.5.2-78 Log-Mean Profiles of Strain-Compatible Soil Damping — Unit 1

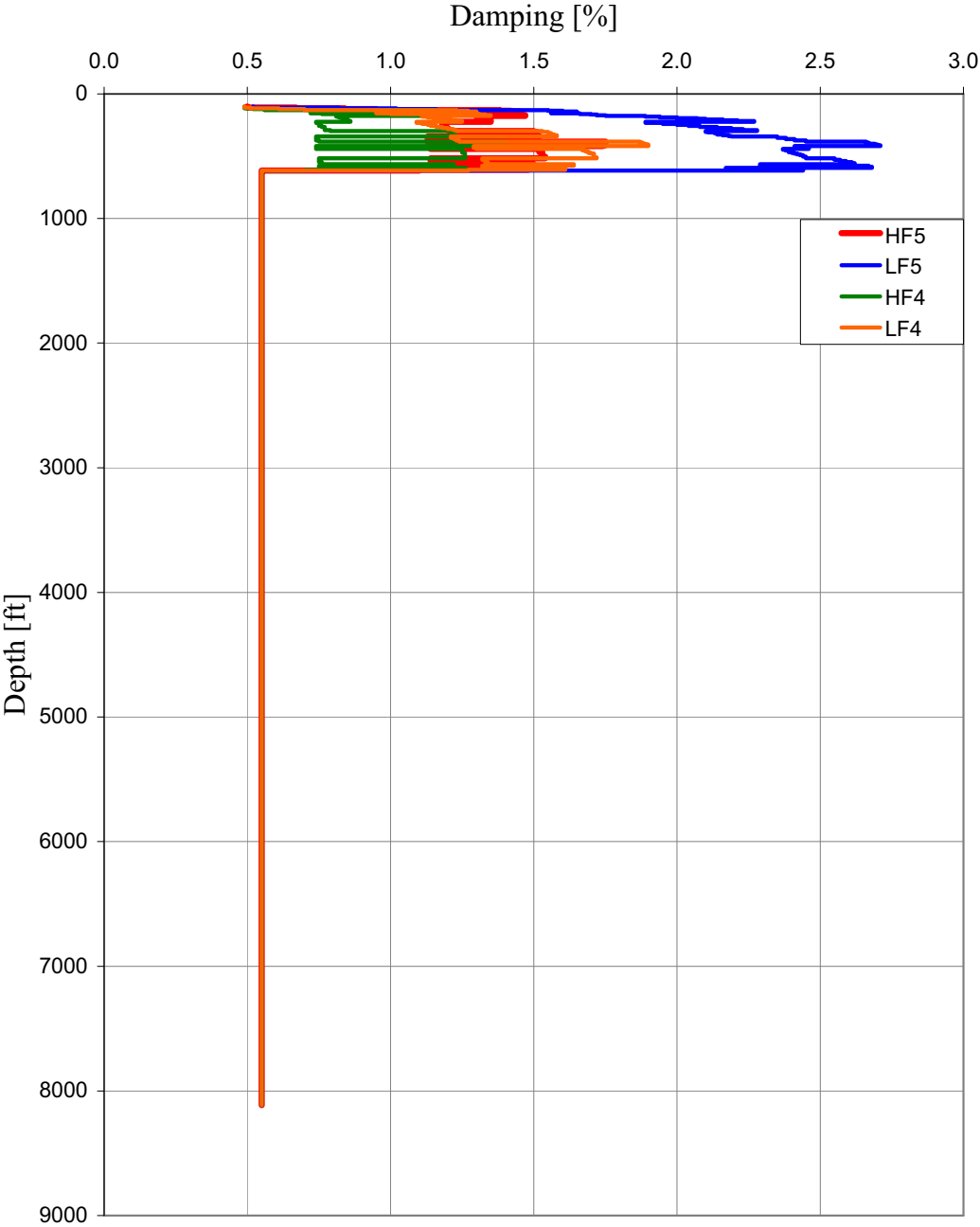
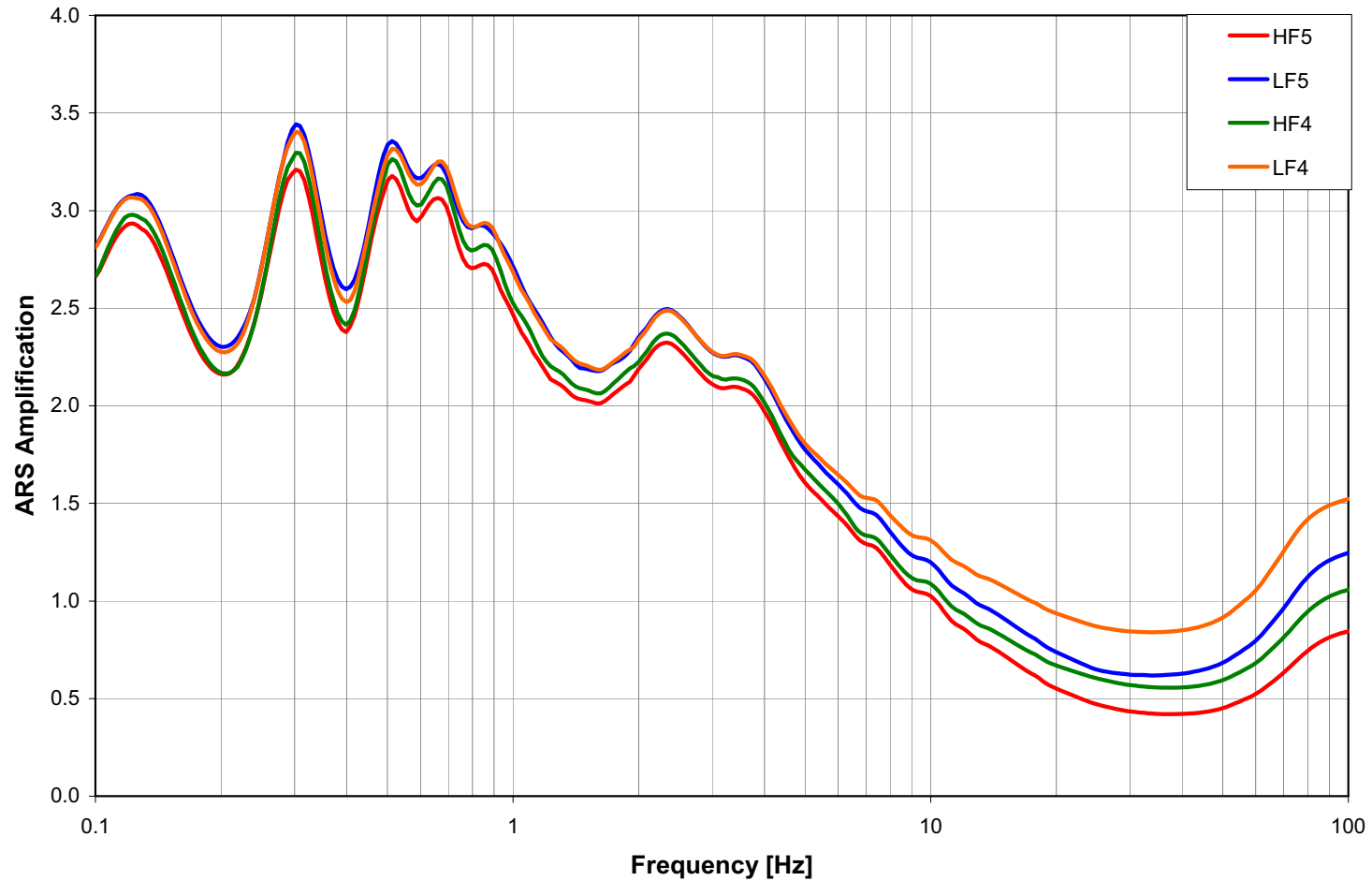


Figure 2.5.2-79 Log-Mean Profiles of Strain-Compatible Soil Damping — Unit 2



**Figure 2.5.2-80 Comparison of the Envelopes of the Unit 1 and Unit 2 Log-Mean Soil Amplification Factors at the GMRS Horizon 1 for LF and HF,  $10^{-4}$  and  $10^{-5}$  Input Motion**

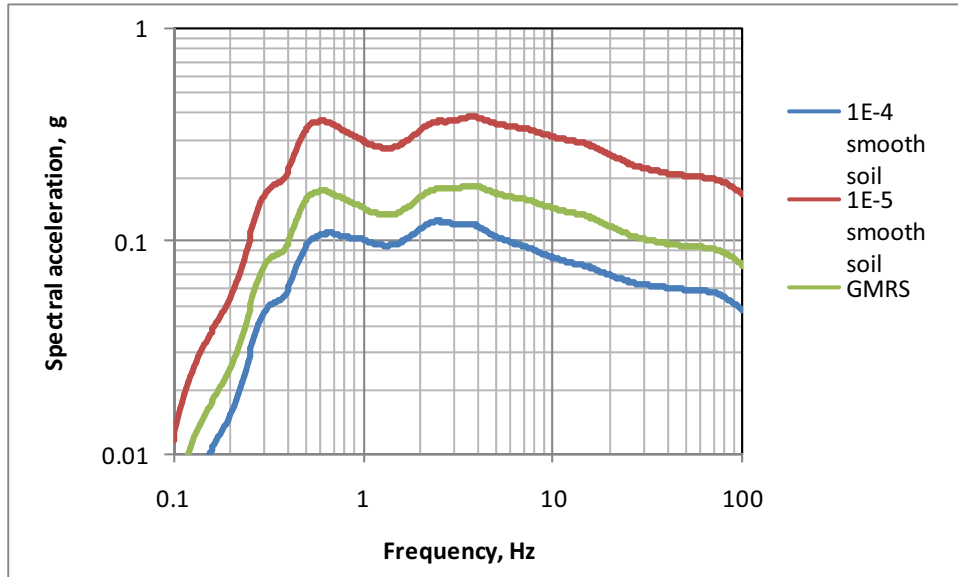


Figure 2.5.2-81 Smooth Horizontal  $10^{-4}$  and  $10^{-5}$  UHRS and GMRS

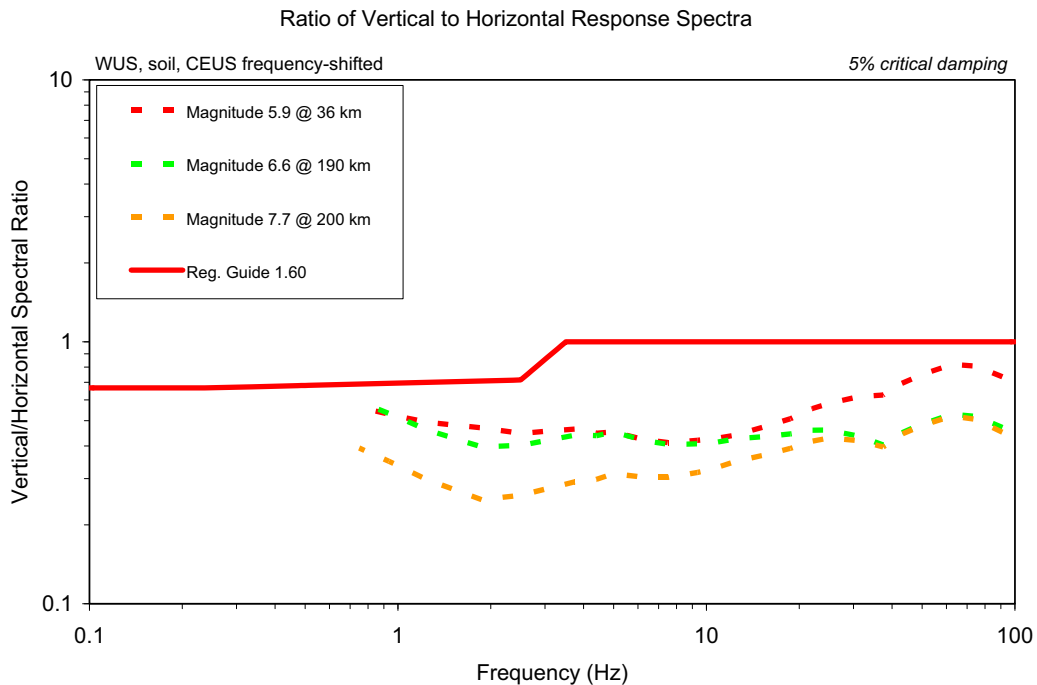
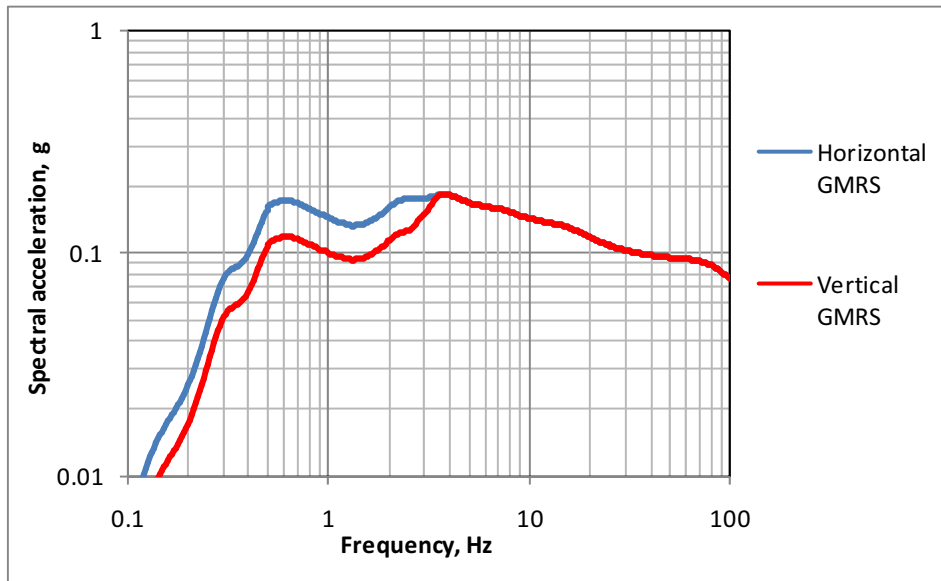


Figure 2.5.2-82 WUS Soil V/H Ratios (Reference 2.5.2-113) for Magnitudes 5.9, 6.6, and 7.7 at Distances of 36, 190, and 200 Kilometers, Respectively, with Frequencies Shifted by a Factor of 62.5/16.7 to Approximate a WUS-to-CEUS Transformation



**Figure 2.5.2-83 Smooth Horizontal and Vertical GMRS**

**Appendix 2.5.2-A**

**Computer Program: P-SHAKE**

**(1 page)**

## 2.5.2-A Computer Program: P-SHAKE

### 2.5.2-A-1 Description

P-SHAKE is a Bechtel proprietary modified version of SHAKE, and is a separate program (whereas SHAKE is a computer program developed at the University of California, Berkeley, by P. Schnabel and H.B. Seed in 1972 [[Reference 2.5.2-101](#)], and is the most widely used program for free-field seismic site response analysis). P-SHAKE generates the same design earthquake-induced strain-compatible soil properties and site response motions as SHAKE does, and the input files of the two programs for the most part are compatible. P-SHAKE, however, is built on different program logic that allows the site response analysis to be performed with an acceleration response spectrum as input instead of an acceleration time history as used by SHAKE.

### 2.5.2-A-2 Validation

P-SHAKE was developed by Bechtel and meets ASME NQA-1 requirements for safety-related applications. The program validation documents are located in Bechtel's Computer Services Library.

### 2.5.2-A-3 Extent of Application

P-SHAKE is used to provide site-specific earthquake-induced design ground motions and the associated strain-compatible soil properties.